NASA Contractor Report 172354

Design and Fabrication of the NASA Decoupler Pylon for the F-16 Aircraft

J. D. Clayton, R. L. Haller, and J. M. Hassler, Jr.

GENERAL DYNAMICS
Fort Worth Division
Fort Worth, Texas 76101

Contract NAS1 — 16879
January 1985

NASA
National Aeronautics and
Space Administration

Langley Research Center
Hampton, Virginia 23665

[redacted]

TABLE OF CONTENTS

PRECEDING PAGE BLANK NOT FILMED

PRECEDING PAGE BLANK NOT FILMED

TABLE OF CONTENTS (Continued)

TABLE OF CONTENTS (Continued)

SUMMARY

The NASA Langley Research Center (LaRC) has been developing a pylon, called the Decoupler Pylon, for the purpose of suppressing wing/store flutter.

As part of the on-going development of the Decoupler Pylon, NASA-LaRC awarded General Dynamics a contract for the design, fabrication, ground testing, and delivery of two Decoupler Pylons plus spares for a flight test demonstration program on the F-16 airplane. An aircraft modification kit to adapt the Decoupler Pylons to the F-16 for the flight test demonstration was also to be delivered. This report documents the accomplishment of this contract.

Basic design criteria were developed during the analysis study pertaining to pylon pitch stiffness, alignment system requirements, and damping requirements. These criteria were applied to the design of the pylon for the F-16 airplane. The store pitch excursions were limited to $\pm$ 3 degrees due to the limited clearance between the GBU-8 tail fins and the F-16 trailing edge control surfaces. A design was developed utilizing an electrical motor for the pylon alignment system. The design uses a four pin, two link pivot design which results in a remote pivot at the center of gravity of the store when the store is in the aligned position. The pitch spring was fabricated from a tapered constant stress cantilevered beam. The pylon design has the same external lines as the existing production pylon. The pylon is designed to use a MAU-12 ejection rack which is the same as the one used with the production pylon.

A detailed design of a decoupler pylon for the F-16 was completed. The drawings were released to the shop and the pylons were fabricated, assembled and ground tested. Spares

were fabricated and an F-16 modification kit assembled. The pylons were designed to be used at F-16 wing stations 3 and 7 (span station 120). The pylons were tailored for use with the GBU-8 weapon. The detailed design was supported with a series of analyses. These analyses included flutter analyses, aeroservoelastic analyses, response to abrupt maneuvers, loads analyses and stress analyses. The ground tests on the completed pylons included instrumentation calibration, damper tests, alignment system operational tests, influence coefficient measurements, ground vibration tests, structural proof tests and store ejection tests.

INTRODUCTION

Wing/Store Flutter Problem

Fighter aircraft are required to carry a very large number of external store combinations. There is a high probability that at least a small subset of the stores configurations will cause wing/store flutter speeds that are within the desired operational capability of the airplane. The probability is further increased by the practice of adding new store configurations to the inventory of the airplane long after it has become operational. If wing/store flutter problems occur, the solution usually requires increased structural stiffness, increased weight, and/or a speed reduction which reduces the operational envelope of the airplane. Flutter suppression with active controls is an option that has been investigated in recent years. The concept consists of feeding back signals from suitably located sensors, through a set of control laws and filters, to command movement of a control surface which suppresses the flutter mode. A study has been conducted which confirmed the feasibility of suppressing F-16 wing/store flutter by means of active controls (ref. 1).

The NASA Langley Research Center has investigated the use of a decoupler pylon as a passive means of suppressing wing/store flutter (references 2 through 7). The concept consists of reducing the pylon pitch stiffness with a soft spring until the store/pylon pitch frequency is less than the fundamental wing bending frequency thereby decoupling the wing from store pitch effects and increasing the flutter speed. The purpose of the work reported herein was to set the requirements for the decoupler pylon detailed design.

Decoupler Pylon Flutter Model Tests

The effectiveness of the decoupler pylon in suppressing flutter has been demonstrated during wind tunnel tests of three separate flutter models (ref. 7). Each model demonstrated that when the decoupler pylon was employed, the model could be tested to a dynamic pressure substantially higher than the dynamic pressure at which the model would flutter with a conventional pylon.

The first model that was tested was a semi-span wing with rectangular planform. The soft spring was implemented by means of a pneumatic system. A feedback system controlled the flow in the pneumatic system such that store pitch misalignment relative to the wing caused by aerodynamic drag loads was automatically corrected. A dash-pot damper was also employed to stabilize the feedback system.

The second model that was tested with the decoupler pylon was the F-16 1/4 scale flutter model. This model is shown suspended in the NASA/LRC Transonic Dynamics Tunnel in Figure 1. The decoupler pylons were attached at wing span station 120 (full scale) and were used to carry a GBU-8 weapon. The external store configuration shown in Figure 2 was tested with the decoupler pylons to a dynamic pressure that was 100 percent above the dynamic pressure at which the model fluttered with the production pylons. The decoupler pylons were implemented with mechanical springs. No automatic self-aligning system was developed for these pylons. However, pitch alignment corrections were made manually, as required, by controlling the pressurized air supply to the pneumatic dashpot dampers connected between the wing and the store at a point aft of the pylon pivot location.

The third model was a 0.30 scale, semi-span model of the YF-17. The decoupler pylon was essentially the same as employed on the F-16 model. It was located below the wing at the wing tip and supported an AIM-7S missile. Large increases in dynamic pressure above the flutter dynamic pressure were also demonstrated on this model by means of the decoupler pylon.

Feasibility Study for Application of NASA Decoupler Pylon to the F-16

As a result of the highly successful wind tunnel tests of the decoupler pylon on the F-16 flutter model, a feasibility study for application of the decoupler pylon to the F-16 was conducted. The results of this feasibility study are reported in reference 8.

The decoupler pylon was assumed to be self-aligning. The characteristics of the decoupler pylon to be investigated were the pitch stiffness, pitch damping and the pitch alignment system. Each characteristic was assumed to be independent of the other two. The alignment system was a servomechanism which produced a moment assumed to be proportional to the time integral of the store pitch deflection relative to the wing.

A single store configuration was considered, as shown in Figure 2. This store configuration, called configuration 33 in reference 1, consisted of an AIM-9 at the wing tip, GBU-8 at wing span station 120, and a 370 gallon fuel tank with the center bay empty at span station 71. This store configuration will be referred to as the GBU-8 configuration herein. The critical flutter mode for this configuration was antisymmetric with a flutter frequency of approximately 5 Hz. In the feasibility study the decoupler pylon was used to support the GBU-8 store.

A single flight condition was considered, namely, Mach 0.9 at sea level. Three GBU-8 center of gravity (c.g.) locations were considered. These consisted of the current c.g. location on the production pylon and a forward and aft shift from the location in an amount equal to ±10% of the local wing chord. These c.g. locations were referred to as nominal, forward, and aft locations in the text. This variation converted to a ±24.086 cm (±9.4828 in.) shift in the c.g. This requirement was primarily intended to demonstrate that the decoupler pylon was effective in suppressing flutter over a wide range of c.g. variations. For some of the dynamic load conditions a more realistic c.g. variation of ±7.62 cm (±3 in.) was also considered and was designated as a ±7.62 cm c.g. shift.

Two values of pylon spring stiffness were investigated. The original objective was to select two stiffness values that yielded a ratio of store pitch frequency to wing bending frequency of 0.5 and 0.8. Subsequently, the spring stiffness that yielded a flutter speed of 1.2 limit speed (without the flight control system activated) was selected as the upper spring stiffness. The lower spring stiffness was selected as the product of the upper spring stiffness and the square of the ratio of 0.5 to 0.8.

The following types of analyses were conducted:

Natural Modes of Vibration	Gust Response Analyses
Flutter	Response to Abrupt Maneuvers
Stability of Decoupler Pylon	Taxi
Aeroservoelastic Analyses	Store Ejection
Static Aeroelastic Analyses	

The same mathematical models of the F-16 structure, aerodynamics, and control system which were used in the feasibility study for F-16 wing/store flutter suppression with active controls (ref. 8), were used in this decoupler pylon study. Based on the results of these two studies, a comparison was made of the advantages and disadvantages between the decoupler pylon and the active control system approach to suppressing wing/store flutter.

Conceptual Design of Decoupler Pylon

The results of the analyses discussed above were used as the basis of a conceptual design study of the decoupler pylon for the F-16. The results of the design study are reported in reference 8.

Both pneumatic and hydraulic systems were considered as means of implementing the pylon spring, damping, and alignment requirements. Mechanical springs and viscous dampers were considered. The potential interference problems between the decoupler pylon and the deflected leading edge flap and flaperon control surfaces due to store pitch excursions were considered in the design. Preliminary design load and stress analyses were conducted. A preliminary analysis was conducted to determine the store separation characteristics when the GBU-8 store was ejected from the decoupler pylon.

The conceptual design study resulted in the preliminary design which is shown on Figure 3. This design had certain deficiencies which were addressed at the beginning of the detailed design phase of the project. These design deficiencies were overcome with the design which is discussed in detail herein.

The design featured a hydraulic alignment system, Belleville washers for the spring, and a dual beam arrangement. In this design a Belleville washer stack housed inside a push-pull mechanism was required to provide the correct spring rate in the limited space available. A dual beam system was incorporated in the design. The actuator force is transferred through the spring and damper mechanism to the store. With this system, the high stiffness inherent with the hydraulic actuator could be offset by connecting a spring in series with the actuator. The dual beam design accomplishes this.

The feasibility study and the conceptual design study (ref. 8) provided the basis for the detailed design and fabrication of a ship set of decoupler pylons for ground and flight tests on the F-16 airplane. The pylon requirements were determined from the feasibility study. Two design deficiencies were identified from the conceptual design study. These are (1) the decoupler pylon would have to be 15.24 cm (6 in.) deeper than the production pylon and (2) high alignment power was required. The pylon pitch stiffness requirement and the two design deficiencies discussed above were overcome with the current design.

STORE CONFIGURATION SELECTION

The F-16 production weapons pylon is designed to attach to the wing at wing span stations 71 and 120. The weapons pylon is carried interchangeably at either wing station. Therefore, the pylon is designed for the maximum loads expected to be experienced at either wing station. Flutter analyses, wind tunnel flutter model tests and flight flutter tests were conducted on a large number of external store carriage combinations. From these analyses and tests only two store configurations which have experienced flutter inside the aircraft operating envelope have been encountered. One of these configurations is identified as GBU-8 configuration and consists of a 1/2 full 370 gallon tank on span station 71, a GBU-8 on span station 120 and an AIM-9 on the wing tip. The 370 gallon tank has the center bay empty. This configuration flutters in the wind tunnel and encounters a limited amplitude oscillation in flight. The flutter mode is antisymmetric in both cases. A second store configuration which has encountered flutter in flight is defined as the B-61 store configuration. This store configuration has the B-61 weapon at span station 120 and the AIM-9 launcher at the wing tip. This configuration flutters in the wind tunnel and encounters a limited amplitude oscillation in flight. The flutter mode is antisymmetric in the wind tunnel and also in flight.

Extensive flutter analyses of the GBU-8 configuration have been conducted during the decoupler pylon feasibility study (ref 8). These analyses predict a flutter instability at a velocity very close to where the limited amplitude flutter is first detectable on the airplane. The analysis predicts a divergent instability and the characteristic of the unstable root has small damping changes with large increases in velocity. This characteristic has some similarity to the limited amplitude flutter encountered on the airplane. With this extensive analysis and test experience, the decision was made to design the decoupler pylon for the GBU-8 weapon.

A series of analyses were conducted on GBU-8 configuration to determine if the predicted flutter condition could be made more severe by moving the GBU-8 center of gravity or adding ballast masses to the GBU-8 weapon. The goal was to make the analysis velocity versus damping curve have a steeper slope, which would indicate a more catastrophic type of flutter condition. If a modified configuration which exhibited this type of characteristic in the analysis could be found, then it would be a good possibility that the airplane flutter characteristics could also be changed by this configuration change. Figure 4 shows the effect upon the unstable flutter root of moving the GBU-8 center of gravity forward and aft. The c.g. was moved 24.13 cm (9.5 in.) forward and the same amount aft. Moving the c.g. forward increases the flutter speed and does not significantly change the slope of the root. Moving the c.g. aft causes the unstable root to become lowly damped and stable. Therefore, the GBU-8 c.g. variations do not cause the change in the flutter characteristics desired.

The effect of increasing the inertia of the weapon upon the slope of the flutter root was investigated. It was determined by examination of the GBU-8 weapon that there was adequate space inside the store to locate 22.68 kg (50 lb) of ballast mass in both the forward and aft ends of the store. A flutter analysis was conducted with the addition of this 45.36 kg (100 lb) of mass in the GBU-8. The two 22.68 kg masses were located equidistant from the store c.g. which resulted in increased store pitch inertia with no shift in the c.g. The results of these two analyses are shown on Figure 5. The increased GBU-8 mass (pitch inertia) raises the flutter speed and does not significantly change the slope of the unstable root. Therefore, this store configuration does not create the desired effect.

A further search of simple changes which could be made to make the flutter mode slope steeper was undertaken by examining mass change in the AIM-9 on the wing tip. It was determined that space was available in the forward and aft part of the AIM-9 weapon for 11.34 kg (25 lb). Two 11.34 kg weights were located equidistant from the AIM-9 c.g. which resulted in increased pitch inertia and no c.g. shift. A flutter analysis was conducted with this additional 22.68 kg of mass in the AIM-9's. The results of the analysis are shown in Figure 6. The increased AIM-9 mass and pitch inertia raises the flutter speed and reduces the slope of the unstable root. Therefore, this configuration change does not provide the desired effect.

The flutter solutions discussed above were made with the k-solution method. The P-k solution method gives a better estimation of the system damping. Therefore, the flutter analysis of GBU-8 configuration was repeated using the P-k solution method. The damping was set to zero in each mode shape, and therefore, the P-k solution results can be compared directly with the k solution. These results are shown on Figure 7 and are compared with the k-solution results. The two solution methods predict the same damping values at the same velocities.

The P-k solution method was used to determine the effect of individual mode damping, upon the characteristics of the flutter root. The P-k analysis shown on Figure 7 was conducted with zero damping in each mode. The analysis was repeated with 0.05 damping in the first antisymmetric flexible mode. Another analysis was conducted with 0.05 damping in the second antisymmetric flexible mode. These results are shown on Figure 8. The addition of damping in the first flexible mode has a small effect upon the flutter speed. The addition of damping in the second flexible mode increases the flutter speed by 79.74 m/s (155 kt). The case with additional damping in mode one has less slope than the base case. The case with damping added to the second flexible mode has approximately the same slope as the case with zero damping.

The effect of the flight control system upon the flutter speed was also determined. This analysis was conducted with both the roll and yaw loops closed. Control system gains for a Mach number of 0.9 and sea level were used. The results of this case are shown on Figure 9. The flight control system has the effect of raising the flutter speed and decreasing the slope of the unstable root. The decrease in the slope of the unstable root makes the results with the flight control system compare more favorably with analysis and airplane flight experience.

The GBU-8 configuration analysis variations examined here indicate that there is not an easy way to make the configuration have a more severe flutter condition. The analyses also indicate that the Flight Control System has the effect of creating a condition more closely related to the limited amplitude oscillation which is encountered in flight. Based upon this series of analyses, it is concluded that the flight test demonstration of the decoupler pylon be conducted with GBU-8 configuration without any modifications.

The results of the flutter analyses which were performed to determine the flight test store configuration are summarized in Table 1.

DESIGN

The conceptual design study resulted in the decision to use a hydraulic actuator to perform the alignment function. There does not exist on the F-16 airplane sufficient pneumatic power to actuate the alignment system. The hydraulic system also had certain disadvantages. These were: (1) hydraulic power lines would be required out to the pylon location. These power lines did not exist and would have to be added. (2) The pylon alignment system needs its power at the same time that the aircraft control systems need maximum power, which is during high g maneuvers. These hydraulic system disadvantages clearly indicate the requirement for a pylon design that has a minimum alignment force requirement.

The conceptual design pylon with a hydraulic alignment system requires a pylon which is 15.24 cm (6 in.) deeper than the current production pylon. This increased depth was required to provide additional space for the movable pylon mechanism.

Remote Pivot Concept

At the beginning of the contract reported herein a fresh look at the pylon design which kept in mind the problem areas discussed above was undertaken. This review of the conceptual design configuration resulted in a new design which eliminated each of the above problems. This design uses a four pin, two link design which results in a remote pivot which is at the center of gravity of the store. The Belleville washer springs which were used for the pitch spring in the conceptual design were replaced with a tapered constant stress cantilevered beam spring. The remote pivot and the beam spring resulted in a design which would fit inside the existing production pylon external lines and have greatly reduced store excursions. The requirement for hydraulics to the pylon was also eliminated. The decoupler pylon with a remote pivot is shown in Figure 10.

The remote pivot concept creates a unique nonlinear spring problem which has been addressed. When the store is aligned in a pitch direction, the apex of the four bar linkage and the store c.g. are coincident. As the store pitches it rotates about its c.g. but the apex of the links moves from the store c.g. These effects result in geometry changes in the pylon and the effective spring length with respect to the pivot point is changed. These geometric effects were examined early in the design to determine if they would have a significant effect upon the pitch spring rate as a function of the alignment angle. Computer aided design technolgy was used to compute the location of each of the components for the store misaligned by ± 3 degrees. The 3 degree value was used because the decision was made to have the spring bottom out against stops at ± 3 degrees. These geometric relationships were used to compute the effective spring rate with respect to the store c.g. These geometric relationships and the reactions in the links due to the spring force are illustrated on Figure 11. The perpendicular distance from the spring line of action to the store c.g. changes from 111.76 cm (44 inches) with the store aligned to 103.76 cm (40.85 inches) for 3 degrees of nose down rotation of the store. The perpendicular distance from the spring line of action to the store c.g. is 118.47 cm (46.64 inches) for the store 3 degrees nose up. The beam spring, which is designed for a linear spring rate on a 111.76 cm (44 inch) arm, is compared to the effective spring rate which is due to a change in length on Figure 11. The effective spring is more flexible in the nose up position by 15%. In the nose down position, the effective spring is 6% stiffer. These changes in the spring rate are considered small and were not included in the dynamic analysis.

Self-Aligning System

The pylon misalignment angle is created by the airplane maneuvers and the store pitching moment that results from these maneuvers. The design criteria for maneuver loads which was used during the conceptual design phase of the pylon (ref. 8) was based upon MIL-A-8591E. The decision was made at the beginning of the detailed design, to use F-16 rational maneuver loads in the design. These loads are based upon analysis and F-16 flight test experience. The MIL-A-8591E loads criteria states that store center of gravity variations of ±7.62 cm (±3 in.) should be included in the loads analysis. The Air Force has specified that the GBU-8 weapon shall have no more than ± 1.27 cm (±0.5 in.) of center of gravity variations. This value was used in the design criteria.

The remote pivot design and the F-16 rational maneuver loads reduced the store misalignment angle during maneuvering by a large factor. The conceptual design pylon (Figure 3) and the MIL-A-8591E loads criteria results in a maximum misalignment angle of 8.8 degrees. The remote pivot and the F-16 rational loads criteria results in a maximum misalignment angle of 1.96 degrees. This very significant reduction in the misalignment angle results in reduced alignment power requirements. These reduced power requirements opened the possibility of using an electrical alignment device. Electrical power existed at the pylon station and this reduces the requirements for wing modifications to accommodate the pylons.

The design concept chosen for controlling the self-aligning system is a simple limit switch actuated system. Cams are provided that actuate switches when the pylon is out of deadband region, in pitch, ±0.5 degree. When a switch is actuated, the alignment motor will drive the pylon back toward zero degrees. The switches open at approximately ±.25 degree to deactivate the alignment system.

Two more limit switches are provided, one that is actuated at 3 degrees nose up and one at 3 degrees nose down. These switches cause lights to be illuminated on the instrument panel and alert the pilot that maximum misalignment has occurred. The electrical circuit for the alignment system is shown on Figure 12.

Two additional limit switches located at the aft end of the spring are provided that will stop the alignment motor should the limit of the drive mechanism be reached.

The catalogs were examined to determine what types of aircraft quality electric motors were available which could be used to drive the pylon alignment system. EEMCO Manufacturing builds such a unit which has 1.6 Hp. Preliminary analyses indicated that a 1.2 Hp motor was required for the alignment function. Therefore, a drive gear box was designed which used the EEMCO Electric Motor. The motor and gear box are shown on Figure 13. The gear box drives a screw with a recirculating ball nut (Saginaw). The ball nut is attached to the end of the pitch spring. Moving the ball nut up and down introduces pitch moment into the store through the beam spring.

Pitch Damper

The decoupler feasibility study (ref. 8) indicated the desirability of a pitch damper in conjunction with an integral feedback alignment system. The damping coefficient was determined from the feasibility study analysis. Assuming integral feedback in the alignment system and the remote pivot design the required damping coefficient was computed.

To achieve this damping coefficient a hydraulic damper was designed. The damping coefficient is achieved by pushing hydraulic fluid through an orifice. The orifice is located on the piston. Standard aircraft quality hydraulic oil is used in the chamber. The orifice is removable and exchangeable to achieve the desired damping coefficient. The orifices are standard off-the-shelf units that come with a range of orifice sizes. The interchangeable orifices provide the damper with a wide range of damping coefficients. The damper is shown in Figure 14. The design is equipped with a drain to fill and remove the fluid when disassembly is required. The design includes features which provide ease of assembly and disassembly for orifice change.

Electrical System

A master power control switch is provided in the crew station that enables (1) DC power only (2) both AC and DC power and (3) all power off. With DC power only applied, the alignment system is deactivated and the indication system is active. With AC and DC power on, the alignment and indication system are both active. With both AC and DC power off, all pylon systems are inactive.

F-16 number 2 has only an emergency jettison system, not a full up Stores Management System (SMS). Therefore, only emergency jettison wiring is provided in the pylons. The airplane number 2 emergency jettison system is shown on Figure 15.

Thus, when the pilot elects to jettison the stores, all stores will be released as there is no selective jettison capability on the aircraft. The pylon for the fuel tank would also be jettisoned, but the decoupler pylon would not.

FABRICATION OF PYLONS

The decoupler pylons were fabricated using materials, processes for materials and parts, and manufacturing methods that are standard and common in the aircraft industry. The machining tolerances, inspection methods and procedures, and surface finishes were those conventional for the materials and parts as used. The ground tests described in a later section of this report revealed that the alignment of the link pins with respect to each other is critical to free movement of the lower pylon. This is necessary to assure that there is no tendency for out-of-plane rotation of one pin with respect to the other and thus induce binding.

The materials used for the major components are shown in Figure 16. The drawing/part numbers for the decoupler pylon are shown in Table A1 of Appendix A. A pictorial representation of the drawing build-up is shown in Figure A1 of Appendix A. A brief summary follows, for each of the major parts, defining the material used, inspections performed, and applied finishes.

Upper Support Fitting (Strongback) - 676S040

The upper support fitting (strongback) is 2121-T851 aluminum. The part was machined from six inch bar stock. Aluminum bronze bushings were pressed into the holes for the link attachment joints and the alignment system attachment joint. The part was penetrant inspected and painted. The surfaces were chromic acid anodized, primed with an epoxy primer, and painted with two coats of urethane.

Lower Pylon Side Plates - 676S030

The lower pylon side plates are PH15-7MO(TH1050) stainless steel. The part was machined from 3/4 inch plate stock. Aluminum bronze bushings were pressed into the holes for the link attachment joints. Holes were added to the side plates for pin attachments to the MAU-12-D/A bomb rack and for access as required for operation of the rack. The side plates were heat treated to 190 ksi ultimate tensile strength. The parts were penetrant inspected and painted. The plates were passivated, primed with epoxy primer, and painted with two coats of urethane.

Links And Pins - 676S032, 676S033, 676S034

The forward and aft links that attach the lower pylon to the upper pylon are D6AC steel heat treated to 220-240 ksi ultimate tensile strength. The parts were machined from 3 inch bar stock. The links were magnetic particle inspected and painted. The surfaces were cadmium plated and primed with epoxy primer.

The attachment pins, 676S033, are D6AC steel heat treated to 260-280 ksi ultimate tensile strength. The parts were machined from 1 1/2 inch diameter bar stock with the finish diameter accomplished by grinding. The pins were nital etched after grinding and magnetic particle inspected. Lubrication fittings were incorporated in the ends of the pins and holes provided to lubricate the joints.

Spring And Pins - 676S036, 676S037

The spring, 676S036, that provides the pitch moment stiffness for the lower pylon is PH13-8Mo(H950) stainless steel heat treated to 220 ksi ultimate tensile strength. The part was machined from 2 inch bar stock. Aluminum bronze bushings were installed in the holes provided for attachment of the screw jack fitting. The spring was penetrant inspected, passivated, primed and painted with urethane.

The pins, 676S037, attaching the spring to the lower pylon are D6AC steel heat treated to 260-280 ksi ultimate tensile strength. The pins were made from 1 1/4 inch diameter bar stock with the finish diameter accomplished by grinding. The pins were nital etched after grinding, penetrant inspected, and solid film lubricant applied.

Damper Assembly - 676M010

The major components of the damper assembly are the outer cylinder and the piston. The damper assembly is shown on Figure 14.

The damper cylinder, 676M011, is 2124-T851 aluminum. The part was machined from 3 inch plate stock. Aluminum bronze bushings were installed in holes provided for attachment to the forward support link. The part was penetrant inspected. The interior surface of the cylinder was hard anodized. The exterior surface was anodized, primed with epoxy primer, and painted with two coats of urethane.

The piston, 676M012, is PH13-8Mo(H1000) stainless steel. The part was machined from 2 inch diameter bar stock. The heat treat of the piston is 200 ksi ultimate tensile strength. The part was penetrant inspected and the seal rubbing surfaces were chrome plated.

Alignment Assembly - 676M040

The major structural components of the alignment assembly are the 676041 alignment screw, 676M045 gears, and 676M043 gear case parts. The 676041 alignment screw is a 17-4PH stainless steel purchased part which has been nitrided (case hardened) by a malcomizing treatment. A minimum amount of machining was required on each end to accommodate the gears and lower support plate.

The 676M045 gears in the alignment gear train are purchased parts from the Boston Gear Co. The parts are AlS11117 steel gears which have been case hardened to withstand gear operations.

The 676M043 gear cases are 2124-T851 aluminum parts that have been machined from bar stock, penetrant inspected, and painted. The parts were chromic acid anodized, primed with epoxy primer, and painted with two coats of urethane.

External Skins - 676S043

The pylon skins and fairings are 2024-T81 and 2024-T62 aluminum respectively. The parts were cut and formed as necessary to the required contour. Parts were penetrant inspected, chem filmed, primed, and painted with urethane.

PYLON ANALYSES

The detailed design tasks were supported with a complete set of analysis tasks. These supporting analyses included dynamic analyses and loads and stress analyses. The analysis task utilized existing F-16 aircraft structural and aerodynamic data. This data was made available to this project from the F-16 data bases.

Dynamic Analysis

Structural Representation. - A finite element representation of the structure was employed. The structural model was composed of 730 beam and plate type elements with 946 independent degrees of freedom. The stiffness matrix of each element was assembled into a stiffness matrix for the entire unsupported structure. Only one side of the plane of symmetry was represented. Boundary conditions were employed along the plane of symmetry to restrict the simulation to symmetric (antisymmetric) loads and deflections. A minimum number of coordinates necessary to remove the rigid body symmetric (antisymmetric) modes were fixed. The matrix was then inverted to obtain the symmetric (antisymmetric) flexibility matrix for the supported case. The idealization of the structure is shown by the solid lines in Figure 17. The dashed lines show the external lines of the airplane.

The free-free natural modes of vibration were computed by a method which effectively released the fixed points in the flexibility matrix. Both symmetric and antisymmetric modes of vibration were computed. The natural modes computed with the production pylons had previously been computed and compared with modes measured during ground vibration tests. The finite element model had previously been modified to achieve good correlation between computed and measured data.

The weight and inertia characteristics of the external stores considered in this study are shown in Table 2. The weight data shown in the table does not include the pylon or launcher. The pitch and yaw inertia are the same for each store. The roll inertia of the tank is the value for the empty tank. That is, the roll inertia of the fuel is assumed to be zero.

The finite element simulation of the weapon pylon and its attachment to the wing at station 120 is shown on Figure 18. The pylon vertical load and pitching moment are reacted by the wing at the forward and aft attach points at wing station 120. The pylon rolling moment is distributed to the wing by an "H" frame. The roll moment is reacted by vertical loads applied to node points close to wing station 120. These nodes are located at wing stations 102, 140, and two stations on either side of 120. The yaw loads are reacted by a torque tube located between the wing and the lower portion of the pylon.

A side view of the weapon pylon geometry is shown in Figure 19. The upper part of the figure shows the representation used for the production pylon in the study described in reference 8. Also shown on the upper part of the figure is the location of the pylon pivot (in airplane scale) that was simulated during the wind tunnel tests of the F-16 1/4 scale flutter model. The lower part of Figure 19 shows the geometry of the finite element representation of the current decoupler pylon design. The pylon has a remote pivot which is located at the c.g. of the weapon, when the weapon is in the aligned position.

After a detailed layout drawing of the pylon design was made, pylon yaw and roll stiffnesses were computed. These stiffnesses are shown on Table 3 and compared with the production pylon values. The stiffness data shown in Table 3 was incorporated into the airplane simulation to compute the complete airplane symmetric and antisymmetric modes of vibration. This stiffness data was updated after the ground tests and this revised stiffness data is shown in the section titled PYLON GROUND TESTS.

A preliminary estimate of the decoupler pylon weight was made from the layout drawing. This weight includes the MAU-12 rack, and does not include the alignment device and the damper. This weight of 1164 N (261.79 lb) is approximately the same as the production pylon. Therefore, a weight of 1356.6 N (305 lb) was used in the complete airplane simulation to compute modes of vibration prior to the ground tests. The pylon was weighed after final assembly and this weight is 1575.6 N (354.22 lb). This weight was used to conduct the final flutter analysis.

<u>Aerodynamic Representation</u>. - The doublet lattice method was used to compute the oscillatory aerodynamic pressure distributions. The particular version of the method that was employed is described in reference 9. The method has been programmed and the AFFDL designation of the computer program is H7WC.

The aerodynamic panel arrangement is shown in Figure 20. The wing is represented by nine spanwise strips from span station 41.5 to 180. Each strip is divided into nine chordwise panels. The flaperon is represented by the last three chordwise panels of each strip extending from span station 41.5 to 140. The tip missile is represented by a single strip extending from span station 180 to 189.335 which is divided into eight chordwise panels. No aerodynamic forces were applied to the under wing stores, i.e., the GBU-8 and the 370 gallon tank.

The horizontal tail is represented by four spanwise strips divided into four chordwise panels per strip. The vertical tail is represented by seven spanwise strips with seven chordwise panels each. The rudder is represented by the aft three chordwise panels of the strip between waterline 136.0 and 217.5. The ventrals are represented by three panels.

The fuselage is represented by both interference panels and a slender body. Eleven interference panels and fourteen slender body segments are located along the fuselage centerline in a streamwise direction. The region between the fuselage representation and the wing and the horizontal tail shelf is represented by a single strip of lifting surface panels.

A comparison of stability derivatives derived from wind tunnel data with stability derivatives computed with the doublet lattice aerodynamic representation is shown in reference 1.

Method for Determining Pylon Dynamic Characteristics. - A series of analyses to determine the pylon spring rate, damping, and alignment system gain as a function of airplane velocity was conducted. These analyses utilized the equations of motion which were described in Reference 8 and are repeated in this document in Appendix B.

Symmetric and Antisymmetric Natural Modes of Vibration. The natural modes of vibration were computed with the finite element simulation shown on Figure 17 and the production and decoupler pylon simulations shown on Figure 19.

The first three analytical symmetric modes of vibration with the GBU-8 on the production pylon are shown in Figure

21. The first mode is identified as wing bending with a frequency of 3.869 Hz. The second mode is identified as GBU-8 pitch (also characterized by wing torsional motion) at a frequency of 5.343 Hz. The third mode is identified as tip missile pitch (also characterized by wing tip torsional motion) at a frequency of 6.135 Hz. The frequencies of the first three modes shown on Figure 21 are tabulated in Table 4 along with the frequencies of the next seven higher modes. These mode frequencies are listed under the heading "Production Pylon Analysis" in Table 4.

The symmetric natural frequencies that were measured during ground vibration tests of the airplane are also tabulated in Table 4. The good correlation that exists between the computed and measured frequencies is shown.

The column of natural frequencies under the "Decoupler Zero Pitch Feasibility Study" (Table 4) was computed during the feasibility study (ref.8) and have a single pylon pivot located 25.4 cm (10 in.) below the wing plane. The column of natural frequencies under the heading "Decoupler Zero Pitch Current Design" (Table 4) was computed by using the decoupler pylon simulation shown on Figure 19 and identified as current design simulation. Comparing the columns it can be seen that the most significant difference that occurs when the pylon and store are free to pitch is the elimination of the mode identified as "Sta. 120 GBU-8-Pitch."

The first three symmetric natural modes for the case in which the GBU-8 is carried by the current design decoupler pylon with zero pitch stiffness are shown on Figure 22.

After completing the ground vibration tests and the influence coefficient measurements of the completed pylon hardware on a fixture, the measured data was used to develop the final pylon stiffness finite element simulation.

This pylon stiffness data was used to compute cantilevered pylon natural frequencies and mode shapes. These mode frequencies are compared with the test results on Table 5. The revised pylon finite element simulation was incorporated into the complete airplane simulation and symmetric natural frequencies and modes were computed. These natural frequencies are shown on Table 4. The increased lateral and yaw flexibilities result in a large number of low frequency modes.

The first three symmetric natural modes for the case in which the pylon simulation reflects the test data are shown on Figure 23.

Antisymmetric natural modes of vibration were computed with the GBU-8 carried on the production pylon as represented by the simulation shown in Figure 19. The first three antisymmetric modes of vibration are shown on Figure 24. The first mode is identified as the GBU-8 pitch mode (also characterized by wing torsional motion) with a frequency of 5.112 Hz. The second mode is identified as the tip missile pitch mode (also characterized by wing tip torsional motion) with a frequency of 5.418 Hz. The third mode is identified as the GBU-8 yaw mode with a frequency of 7.118 Hz. The frequencies of the first three modes shown on Figure 24 are tabulated in Table 6 along with the frequencies of the next seven higher antisymmetric modes.

The antisymmetric natural frequencies that were measured during ground vibration tests of the airplane are also tabulated in Table 6. The good correlation that exists between the computed and measured frequencies is shown.

The column of natural frequencies under the heading "Decoupler Zero Pitch Feasibility Study" (Table 6) were computed during the feasibility study and have a single pylon pivot located 25.4 cm (10 in.) below the wing plane. The column of natural frequencies under the heading "Decoupler Zero Pitch Current Design" (Table 6) was computed by using the decoupler pylon simulation shown on Figure 19 and identified as current design simulation. Comparing the columns it can be seen that the feasibility study simulation and the current design simulation eliminates the GBU-8 pitch mode. The first three antisymmetric modes of vibration with a zero decoupler pitch spring are shown on Figure 25. The first mode is the missile pitch. The second mode is the tank pitch mode and the third mode is the GBU-8 yaw mode.

The first 16 modes which were computed with the current design simulation and the zero pitch spring together with rigid body lateral translation, roll and yaw were coupled with the store pitch mode to obtain a set of modes identified as "Decoupler Spring Coupled Current Design" modes in Table 6. These modes were obtained by substituting Equation B5 into Equation B3 (Appendix B) and solving for the coupled modes of vibration. A spring rate of 3502 N/cm (2000 lb/in) with the spring located 111.76 cm (44.0 inches) from a vertical axis through the c.g. of the store was used in these modes. This spring rate reflects the final detailed design value.

The first three antisymmetric natural modes for the cases in which the GBU-8 is carried by the decoupler pylon with a pylon spring of 3502 N/cm (2000 lb/in) are shown in Figure 26. The first mode is the GBU-8 pitch mode. The second mode is the tip missile pitch mode. The third mode is the GBU-8 yaw mode.

The ground test data was incorporated into the complete airplane simulation and antisymmetric natural frequencies and modes were computed. These natural frequencies are shown on

Table 6. The increased lateral and yaw flexibilities result in a larger number of low frequency modes.

The first three antisymmetric natural modes for the case in which the pylon simulation matches the test data are shown on Figure 27. The three lowest frequency modes are primary GBU-8 store modes.

Flutter Analysis. - The equations of motion for a flutter analysis with the decoupler pylon, with a non-zero pitch spring, are expressed by equation B13 (Appendix B) with C and G set equal to zero along with the forcing function on the right side of the equation. All subsequent analyses herein assume a value of 0.01 for the structural damping g_r. The spring coupling terms produced by the decoupler pylon spring prevent the equations from being solved by the conventional flutter analysis method.

The method used herein is to treat the decoupler pylon spring as a feedback loop in a feedback mechanism. The loop can be broken to compute the open-loop frequency response function. The equations of motion for computing the generalized coordinate response to an input deflection to the pylon spring are shown in equation B9. The ratio of store pitch (relative to the wing) to the input pitch angle applied to the spring is computed by equation B10. If the real and imaginary parts of equation B10 are plotted with frequency as the independent variable, the (+1,0) point is the critical point for determining stability because equation B10 is the expression for positive feedback. If the right hand side of equation B10 is multiplied by a minus-one, the (-1,0) point becomes the critical point for determining stability because the feedback has to be multiplied by a second minus-one before summing with the input (negative feedback). The latter option was used throughout this study.

For a system with negative feedback, the transfer function for the closed loop is

$$\frac{x_o(s)}{x_i(s)} = \frac{G}{1+GH} \qquad (1)$$

where

- x_i is the input signal as a function of the Laplace variable, s.
- x_o is the output signal.
- G is the Laplace transform of the forward loop.
- H is the Laplace transform of the feedback loop.
- s is $i\omega$

The Nyquist criteria provides a means of determining the stability of the closed loop system from a plot of the open-loop Frequency Response Function (FRF), $G(i\omega)\ H(i\omega)$. If there are values of s on the right hand side of the Laplace plane that cause the function 1+GH to become zero (right-hand side zero) then the system is unstable. The system is stable if all zeros are on the left hand side. If the function GH is plotted over the frequency range from minus infinity to plus infinity, the number of clockwise (CW) enclosures of the (-1,0) point is equal to the difference between the number of right hand zeros (Z) and right hand poles (P) (values of s that cause 1+GH to become infinite).

$$N = Z - P \qquad (2)$$

Hence, stability of the closed loop system can be deduced by determining N from the plot of GH and determining P by some other means. The feedback system H has no right hand side poles for the systems considered in this report. The unaugmented system is stable when the forward loop, G, has no right hand side poles. If the system has right hand side poles it is unstable.

Hence, for the case in which G is stable it can be deduced that 1+GH has no right hand side poles and P in equation 2 is zero. In that case, the number of CW enclosures of the (-1,0) point is equal to the number of right hand side zeros. Restated, if there are no CW enclosures of the (-1,0) point, the closed loop system is stable. Otherwise, it has one instability for each CW enclosure.

For the case in which G is unstable there will be a pair of complex conjugate poles for each non-zero frequency instability. For example, if P is two then for the closed loop system to be stable (Z=0) there must be two counterclockwise enclosures of the (-1,0) point to satisfy equation 2. One will occur for negative frequencies and one will occur for positive frequencies.

The open loop FRF is computed at a fixed velocity and a fixed arbitrary spring rate to determine the negative axis crossing. The spring rate is adjusted to make the negative axis crossing magnitude equal to -1.0. This spring rate and velocity determine a point on the velocity versus spring rate curve. By computing the FRF at additional velocity values and adjusting the spring rate, a complete flutter boundary can be developed. This type of analysis was used during the feasibility study (ref. 8) and was used in the analyses presented here.

A curve of spring rate versus flutter velocity has been developed for the current design pylon using the concepts presented above. A curve of required spring rate for a fixed damping value and zero alignment gain is shown on Figure 28 for the current design. The spring rates shown on the curve have units of kN/cm (lb/in) at a location 111.76 cm (44.0 in.) from the weapon c.g. A damping value of 383.5 N sec/cm (219 lb sec/in.) located 54.1 cm (21.3 inches) from the pivot was used in the analysis. This damping value is equivalent to 140 N sec/cm (80 lb sec/in) at 89.4 cm (35.21 in.) from the weapon c.g., which was the nominal value used during the feasibility study (ref. 8). The flutter speed for this damping value obtained during the feasibility study is also shown on Figure 28. The production pylon flutter speed is also shown on Figure 28 at an estimated spring rate value. The current design pylon analysis was computed for a damping value of zero. This data is also shown on Figure 28.

These results indicate that the spring rate that results in maximum flutter speed is approximately 7004 N/cm (4000 lb/in) at 111.76 cm (44.0 inches) from the pivot. A spring rate of 3502 N/cm (2000 lb/in.) has been chosen as the value to use in the design. This spring rate provides more than adequate increase in flutter speed and will probably be acceptable for lighter weapon carriage. This lower spring rate also results in lower loads in the alignment system linkage and drive train.

Conventional symmetric and antisymmetric flutter analyses were conducted using the natural modes and frequencies for the complete airplane computed with the pylon test stiffness data. The frequencies are listed in Tables 4 and 6. The unsteady aerodynamic data for the analysis was computed with the doublet lattice procedure for a Mach number of 0.9. The symmetric k solution flutter speed at an altitude of sea level is greater than 514.4 m/s (1000 kts). The antisymmetric analysis has a lowly damped root which crosses zero damping at 283 m/s (550 kts) and reaches a maximum damping value of 0.019 at 418 m/s (813 kts). This root has a frequency of 5.2 Hz.

A nonlinear flutter analysis of the airplane with the decoupler pylon was also conducted. The basic flutter analysis is based on a linear system with a constant spring rate. In the event that the store deflection with respect to the wing exceeds 3 degrees, the pylon will impact the pylon internal stops. This results in an increase in the effective pitch spring rate creating a nonlinear system.

A method for solving the nonlinear wing/store flutter problem is presented in reference 4. The analysis is based on the "Describing Function" or equivalent linearization method. The basis of the describing function method is to assume a sinusoidal displacement and then compute the load developed in the nonlinear spring. The spring load is then expanded into a Fourier series. The spring constant (K_e) of the equivalent linear spring is then determined by obtaining the ratio of the fundamental load term to the displacement amplitude. Higher order harmonics of the load series are assumed to be negligible.

$$\theta = \bar{\theta} + \theta_1 \sin \omega t \tag{3a}$$

$$M = \bar{M} + \sum_{n=1}^{\infty} M_n \sin n\omega t \tag{3b}$$

$$K_e = M_1/\theta_1 \tag{3c}$$

where

θ = store pitch angle

$\bar{\theta}$ = static store pitch angle due to preload

$\bar{M}$ = static preload moment

M = elastic restoring moment about store pitch axis

K_e = equivalent linear spring constant of nonlinear pitch spring

K = spring rate of linear soft spring

δ = describing function = K_e/K

M_o = static preload required to deflect store against hard spring

N = ratio of hard spring constant to soft spring constant

θ_1 = amplitude of sinusoidal store oscillation

The relationships of this method are illustrated in Figure 29 which is reproduced from reference 4.

Once the equivalent rate (K_e) has been calculated, the describing function (δ) may then be found for a given value of $\bar{M}/M_o$ and θ_1/θ_o. These results are then coupled with the linear flutter data to generate a nonlinear flutter boundary for a given ratio of the hard to soft spring rates (N).

Figures 30, 31, and 32 present the results of the nonlinear flutter analysis. These figures represent spring rate ratios of 6,10 and 20, respectively. The actual spring rates of the decoupler pylon were measured during the structural and operational pylon testing which established the spring rate ratio. These ratios measured during the influence coefficient tests are 15.6 nose up against the stop and 10.3 nose down against the stop. As seen in the figures, increasing the static preload moment ($\bar{M}$) results in a lower flutter speed than the linear system. The actual flight conditions for the GBU-8 store on the F-16 result in a maximum $\bar{M}/M_o$ ratio of 0.54 which will have a negligible effect on the aircraft flutter velocity as seen in the figures. Increases in the ratio of $\bar{M}/M_o$ for values greater than one and smaller values of the θ_1/θ_o ratio decreases the flutter speed. The flutter speed is reduced at a faster rate for the large values of N.

Stability of Decoupler Pylon. - The critical value of alignment gain was computed for symmetric and antisymmetric motion for two decoupler pitch spring rates. These spring rates were 3502 N/cm (2000 lb/in.) and 7005 N/cm (4000 lb/in). The alignment gain was evaluated for two damping values for the 3502 N/cm spring. All analyses described in this section were computed with the flight control system engaged. The analyses were conducted for sea level air density and Mach number of 0.9.

The degrees of freedom employed in all antisymmetric analyses consisted of rigid body lateral translation, rigid body yaw, rigid body roll, the first 16 antisymmetric modes of vibration (with a zero stiffness decoupler pitch spring), and the store pitch mode. The pylon spring and damping loops and the flight control system loops were closed and the alignment loop was open as expressed by Equation B12 (Appendix B). The system was driven by the forces produced by an input deflection to the alignment system.

The critical alignment gain can be determined from the FRF between the store pitch response angle and the input angle. These critical gain values were computed for fixed velocities. These gain calculations were made at two damping values for the 3502 N/cm (2000 lb/in.) spring and one damping value for the 7005 N/cm (4000 lb/in.) spring. The results of these analyses are presented in Figure 33, which is a plot of critical alignment gain versus velocity. The effect of pylon damping on the critical alignment gain for the 3502 N/cm spring is shown. The alignment gain values are for an alignment system location which is 111.76 cm (44.0 inches) from the weapon c.g. in a fore and aft direction.

MIL-F-9490D (USAF) specifies a gain margin of 6dB for the aircraft flight control system at the airplane limit speed. This criteria has been applied to the alignment system critical gain values for the design spring rate (3502 N/cm). Therefore the gain values presented on Figure 33 would be reduced to one-half the predicted value to meet this criteria. The alignment system gain of 16.11 KN sec/cm (9200 lb sec/in) with a damping value of 383.5 N sec/cm (219 lb sec/in) will provide the 6 dB gain margin at limit velocity. With a damping value of 175 N sec/cm (100 lb sec/in) and a value of alignment gain of 5604 N sec/cm (3200 lb sec/in) the system will meet the 6 dB gain margin. The alignment gain margins are approximately constant as a function of velocity. These requirements are based upon having a servo controlled alignment system. The decoupler pylon has an electrical drive motor and gear box with an on-off switch.

The electrical alignment system has a dead band region which is set by the on-off switches. Therefore, with small misalignment angles the alignment device is inactive, and the alignment device does not act continuously.

The degrees of freedom employed in the symmetric analyses consisted of rigid body vertical translation, rigid body pitch, the first 17 symmetric modes of vibration (with a zero stiffness decoupler pitch spring), and the store pitch mode. The critical alignment gain was obtained in the same manner as previously described for the antisymmetric analyses. The critical gain is plotted versus velocity on Figure 34. Since the symmetric flutter speeds (without the alignment system) are very high, the alignment gain does not reduce to zero over the speed range plotted. It can also be seen that the values of the alignment system gain, which was selected on the basis of the antisymmetric analyses, are satisfactory for the symmetric analyses.

Aeroservoelastic Analysis. - The coupling effects between the decoupler pylon mechanism and the F-16 Flight Control System (FCS) were studied. The decoupler pylon design should not introduce any FCS instabilities. Variations in decoupler spring rate and damping values have been evaluated as a function of velocity using the antisymmetric airplane modes of vibration and the lateral Flight Control System.

The antisymmetric FCS is a dual channel system. The separate channels are identified as yaw and roll. The yaw channel processes input from the airplane lateral accelerometer, yaw rate gyro and roll rate gyro. The processed signal from these sensors commands the rudder. The block diagram for this channel is shown on Figure 35. The roll channel responds to a single input, the airplane roll rate gyro, and commands the aileron which is a combination of differential flaperons and differential horizontal tails. The block diagram for this channel is shown on Figure 36. The values of the variable gains identified on Figures 35 and 36 are shown on Table 7 for Mach numbers of 0.6, 0.9, and 1.2. The antisymmetric analysis with the early estimates of the pylon lateral stiffnesses and the nominal decoupler pitch spring was conducted with the spring and damper on the left hand side of equation B13 (Appendix B). The FCS yaw loop was also closed and the stability boundary was determined from the open loop roll channel. The analyses were conducted for several velocities to obtain the velocity at which the roll loop has critical gain. These velocities have been plotted versus decoupler spring rate on Figure 37. A curve is shown for a damping value of 383.5 N sec/cm (219 lb sec/in). This curve was extended to a spring rate-velocity combination which was above the unaugmented flutter speed. The analysis at this point indicated that the FCS did not increase the unaugmented flutter speed. The analysis was repeated at spring rate of 3502 N/cm and a damping value of 175.1

N sec/cm (100 lb sec/in). This combination results in a slight increase in speed. With this combination of spring and damper the allowable alignment gain is reduced (Figure 33). The FCS degrades the flutter speed, which is the same conclusion which was arrived at during the feasibility study (ref. 8).

An analysis of the symmetric FCS was also conducted. The symmetric FCS is a single channel system. The pitch channel processes input from the airplane vertical accelerometer, pitch rate gyro and the airplane angle of attack. The processed signal from these sensors commands the symmetric horizontal tails. The block diagram for this channel is shown on Figure 38. The analysis of the symmetric modes and the open loop pitch channel indicates no adverse coupling between the pitch channel and the flexible airplane with the decoupler pylon. The system is stable with large margins up to a velocity of 305.5 m/s (594 kts) at an altitude of sea level.

Symmetric and antisymmetric aeroservoelastic analyses were conducted with the pylon simulation based upon the ground test data. The symmetric analysis was conducted with the pitch loop open. At M=0.9 and at an altitude of sea level the pitch loop has a large gain and phase margin. The antisymmetric analysis was conducted with the yaw loop closed and the roll loop open. The analysis was conducted with the unsteady aerodynamic terms computed for a Mach number of 0.9. By conducting the analysis with the yaw loop closed, the stability of the yaw loop is indicated and the stability and gain and phase margin of the roll loop are indicated. The results of these analyses are summarized on Table 8. The airplane is stable and has sufficient gain and phase margin at speeds up to 271.6 m/s (528 kts). At 305.5 m/s (594 kts) the yaw loop drives the airplane unstable and the roll loop does not stabilize the instability. At the lower velocities the roll loop has more than adequate gain and phase margins. At 305.5 m/s a 90° phase lead in the roll loop and a factor of 3 increase in the roll loop are required to stabilize the instability created by the yaw loop. The instability caused by the yaw loop is at 5.3 Hz and is most likely aggravated by the two low frequency GBU-8 lateral modes at 4.901 and 5.211 Hz (Table 6).

Response To Abrupt Maneuvers. - The decoupler pylon alignment system performance was evaluated by conducting a series of time history response to abrupt maneuvers analyses. Two symmetric maneuver conditions were selected from the F-16 flight test experiences which result in large GBU-8 pitching moment about the store c.g. The two maneuver conditions are a 3 g pushover and a 6 g pull up. A rudder kick maneuver was also used to evaluate the alignment system performance. The airplane angle of attack, vertical load factor, and pitch acceleration for the two symmetric maneuvers are shown on Figure 39. These two maneuver time histories were computed from F-16 rational loads data.

Analyses were conducted to evaluate the alignment system performance using the F-16 maneuver conditions and to derive the optimum combination of the alignment motor on-off switching system. Variables included variations in store c.g. location, misalignment angle at the beginning of the maneuver and angle at which the alignment motor comes on and goes off. The store c.g. was varied $\pm$ 1.27 cm ($\pm$0.5 inches) from the nominal value. Misalignment angles of zero and $\pm$0.4 degrees were used. The alignment motor was turned on in every case when the misalignment angle exceeded $\pm$0.5 degrees. The alignment motor turn off angle was set at zero degrees, 0.25 degrees and 0.5 degrees.

The analysis included the alignment drive system performance which includes the screw jack, gear box and the motor performance. The screw jack resisting torque was computed from the following equation:

$$T = \frac{d_m W}{2} \; \frac{\pi f_s d_m + \ell \cos\theta_n}{\pi d_m \cos\theta_n - f_s \ell} \tag{4}$$

where

T is torque

W is reaction load against screw

d_m is the screw thread diameter = 2.2098 cm (0.87 in)

θ_n is the thread angle = 3 degrees

n is the number of threads per inch = 4

f_s is the coefficient of friction of the recirculating balls = 0.02

ℓ = np where p is the screw pitch = 0.25

The above equation, the gear box gear ratio and gear inertia and the motor performance curve were used to compute the time required to return the store from a misalignment angle. The system was assumed to be 95% efficient. The motor manufacturer, EEMCO, provided the motor inertia value and the time required to engage the motor brake after the power to the motor is turned off. This time is 0.15 seconds. The motor brake braking torque was also obtained from EEMCO. This value is 2.54 N m (22.5 in.lbs). The motor torque versus RPM and motor efficiency which were obtained from EEMCO are shown on Figure 40.

Time history analyses were conducted for the combinations of variables discussed above to determine the optimum combination of the alignment system on-off switches which will minimize the misalignment angle. The combination of variables which produced the maximum misalignment angle was determined from the analysis for the symmetric maneuvers. For the symmetric pushover maneuver, the aft store c.g. and an initial misalignment of -0.4 degrees results in maximum misalignment without the alignment system activated. For the symmetric pullup maneuver, the aft store c.g. and an initial misalignment of +0.4 degrees results in maximum misalignment without the alignment system activated. The misalignment angles versus time for these conditions are shown on Figure 41. The maximum misalignment angle, with the motor off, for the symmetric pushover is -2.0 degrees. The maximum misalignment angle with the motor off, for the symmetric pullup is +2.75 degrees. These two cases have also been evaluated for motor on at ±0.5 degrees, motor off at ±0.5 degrees and motor on at ±0.5 degrees, motor off at ±0.25 degrees. These misalignment angles versus time are also shown on Figure 41. In both maneuver cases the alignment system significantly reduces the maximum misalignment angle. The maximum misalignment angle is the same for both switch off angles. The motor off at ±0.25 degrees results in no store oscillations which makes this switch configuration superior to the motor off at ±0.5 degrees case.

A complete set of misalignment angle versus time cases for the switches on at ±0.5 degrees and the switches off at ±0.25 degrees are presented in Appendix C. The data presented in Appendix C shows the effect upon the misalignment angle of having the alignment system operational, the effect of variation in store c.g. and response for variations in starting misalignment. The store c.g. was varied ±1.27 cm (±0.5 inches) from nominal value. The analysis was conducted for beginning misalignment angles of zero and ±0.4 degrees.

A rudder kick maneuver at 0.9 Mach and at an altitude of sea level was also used to evaluate the pylon alignment system. This type of maneuver creates a nose up store pitching moment. The misalignment angle versus time for the rudder kick maneuver is shown in Appendix D for the neutral, aft and forward store c.g. locations. The maximum misalignment angle for all three c.g. locations is 1.41 degrees with the alignment system off and an initial misalignment of +0.4 degrees. With the alignment system operating and the switches set to come on at ±0.5 degrees and go off at ±0.25 degrees, the maximum misalignment angle is -0.78 degrees.

The analytical data presented above was used as the basis for selecting the ground test conditions for evaluating the alignment system. An input store pitching moment time history which closely resembles the moment created by the rudder kick was used in the ground tests. The alignment system on-off switches were set to a nominal value of on at ±0.5 degrees and off at ±0.25 degrees.

Flutter Detection Device Criteria. - The F-16 airplane has been flight tested with production pylons and the GBU-8 weapon (GBU-8 configuration). Limited amplitude flutter oscillations on this airplane store configuration is experienced in flight. Flight test instrumentation includes an accelerometer on the nose of the GBU-8 weapon measuring vertical motion and on the forward part of the wing tip launcher measuring vertical motion. The flutter frequency is 5.0 Hz. These two accelerometers read approximately the same amplitude during the flutter oscillation. The maximum amplitude which has been observed at these locations is ±1.15 g's during 1g flight without airplane excitation in smooth air. During flight flutter testing of this configuration the 5.0 Hz flutter mode was excited through the airplane control system. The maximum response observed during excitation is ±2.8 g's.

Based upon this flight test experience a flutter detection device criteria has been developed. The detection device should monitor the accelerometer mounted on the wing tip launcher forward location in the vertical direction. The device should have a filter band from 4 to 10 Hz. The device should be designed to count peaks greater than ± 3.5 g's and when the count is greater than 3 per second it should activate.

Store Separation Analysis. - Analyses to determine the airplane and pylon response to ejection of the GBU-8 store from the decoupler pylon and from the F-16 weapons pylon have been conducted. The analyses were conducted utilizing a time domain simulation of the airplane and pylon and the continuous systems modeling program. The continuous systems modeling program is a discrete time domain simulation of linear or nonlinear system. Although the program has the capability for simulating the transient aerodynamics and the flight control system, the ejection analysis was conducted without aerodynamic forces on the airplane. The ejection analysis was conducted at a load factor of one g, and the maneuver loads were added to the ejection load. Symmetric pull up maneuvers, symmetrical pushover maneuvers and a rudder maneuver were each added to the ejection loads. These maneuvers give maximum total applied loads and moments on the store.

The airplane and pylon were represented in the analysis by rigid vertical translation and pitch degrees of freedom and five symmetric free-free normal modes. The rotation of the lower portion of the decoupler pylon was represented as a discrete coordinate coupled to the other degrees of freedom. The equations of motion are generated in the time domain and given in the feasibility study (reference 8).

The ejection condition excitation consisted of the application of a step function force and moment representing the change in inertial loading of the pylon by removal of the store and the simultaneous application of a force time history of 68 milliseconds duration representing the ejector rack thruster output. Small changes were made in the ejection force after this analysis was complete. The changes were the result of the store ejection tests which were conducted on the assembled pylon as part of the ground test.

Figure 42 illustrates the basics of the ejection analysis simulation. Table 9 contains a summary of the results obtained for the F-16 production weapon pylon as well as the decoupler pylon. Comparing the one g data indicates that the loads created by ejection forces are only slightly higher on the decoupler pylon. The pylon to wing attachment loads during ejection are less than the pylon design loads used to design the decoupler. These design loads are discussed in detail in the loads and stress analysis section of this document.

Loads and Stress Analysis

Loads Criteria. - The decoupler pylon is designed structurally to carry all of the stores currently certified on the F-16 weapons pylon (16S500). The store carriages for which the F-16 weapons pylon and the decoupler pylon have been designed are shown on Tables 10 and 11 under the "BL 120" column and the "BL 71" column (excluding tank carriage, which uses a 16S400 pylon). To support the flight test program planned for the decoupler pylons, a minimum structural margin of safety of +0.25 was maintained for loads resulting from carriage of the GBU-8 store. A minimum margin of safety of zero was maintained for all other stores currently carried on the weapons pylon, except the (4) CBU-58 carriage which is not fully certified.

The decoupler pylons are to be mounted at wing stations 3 and 7 (BL 120) and flight tested on F-16A No. 2. The flight test program is to consist of carriage of the GBU-8 stores (only) on the pylons. The pylon alignment springs have been tailored for the GBU-8 store and the minimum margin of safety of +0.25 described above will provide structural clearance for flight testing, with the GBU-8 store mounted on the pylons, to design limit loads.

The stress analysis was made with the assumption that the linkage apex remains aligned. The maximum GBU-8 store rotation is less than 2° and thus will remain aligned. Additional studies and analyses would be required (relative to spring stiffnesses and store rotation) for flight testing of stores other than the GBU-8.

Critical Load Conditions. - The decoupler pylon is designed to both GBU-8 and non-GBU-8 load conditions. There were 256 GBU-8 load conditions and 74 non-GBU-8 load which were considered in the analysis. These load conditions in their original form are defined with respect to the wing-pylon attachment points. A computer program was developed which took these interface loads and distributed them to the pylon internal members.

The computer program performed the following functions:

1. Transferred wing reference point loads to the pylon linkage apex.

2. Distributed loads from linkage apex to linkage pins.

3. Applied upper linkage pin loads to strongback and determined wing reactions and critical load locations.

4. Applied lower linkage pin loads to side plates and determined critical load locations.

The linkage apex loads are derived by transferring the wing reference point loads which were in the fuselage coordinate axis system, to the linkage apex of the decoupler pylon. The linkage apex shift which is a function of the store rotation was taken into account in the load transfer.

The internal load distributions were computed for three alignment positions.

1. Store aligned and spring unloaded.

2. Store $1/2^{\circ}$ nose down and spring unloaded.

3. Store $1/2^{\circ}$ nose up and spring unloaded.

A typical example of the loads which were used to design the pylon is presented on Table 12. Table 12 shows resulting pylon forces and moments and the force in the pitch spring. The X direction is fore and aft with positive X forward. The Y direction is lateral with positive Y outboard. The Z direction is vertical with positive Z up. The positive moments are wing tip up, nose up and nose outboard. The GBU-8 limit loads at the linkage apex with the store aligned and the spring in the neutral position are shown on Table 12. Similar sets of loads were developed for the other two misalignment angles ($1/2^{\circ}$ nose up and $1/2^{\circ}$ nose down) for the GBU-8 store carriage. In a similar manner the non-GBU-8 load conditions were computed for aligned $1/2^{\circ}$ nose up and $1/2^{\circ}$ nose down.

The forward and aft link loads are derived by applying the linkage apex loads to the four bar linkage to determine member loads. The computer program was used to distribute the axial, shear and moment at the lower side plates to the link and the link to upper strongback. The assumption was made that 40 percent of the load was carried by the forward link and 70 percent of the load was carried by the aft link. This assumption increased the total load by 10 percent above the load shown in Table 12. These internal loads were then used to size the individual members.

Stress Analysis. - Each of the load conditions shown on Table 12 was distributed to the internal members to determine the member loads. These member loads were then examined to find the critical load conditions. The stress level was computed and compared with the member allowable to determine margins of safety. The margins of safety on the pylon links and link joints are shown on Table 13. The margins of safety on these components are all positive. The lowest margin of safety is in the aft upper link lug and is only 2%. The non-GBU-8 load conditions have lower margins than the GBU-8 load conditions.

The upper pylon strongback was examined at seven cross sections in the fore and aft direction. The stresses at these sections were computed from the loads and reactions on the component. The margins of safety at each cross section are shown on Table 14. The cross sections run from the forward end of the part to the aft end. The lowest margins occur on the non-GBU-8 load conditions. A stress check was also made on the forward pylon to wing sway brace attachment. The margins of safety on this part are high.

The lower pylon side plates were examined at five locations. The stresses at these locations were computed from the load and reactions on the component. The margins of safety at each location are shown on Table 15. The margins of safety are large for these locations on the side plates.

The strength and the stiffness requirement was used to design the pylon pitch spring. The stiffness was set by flutter requirements. The strength criteria was to design a spring which has less than allowable stress when the spring deflection was 6 degrees. The 6 degree requirement is the result of having the alignment system driven to full over (3 degrees) and applying a moment at the store c.g. which would deflect the store 3 degrees in the opposite direction. This criteria was also used to design the spring retaining pins. The spring margins of safety are shown on Table 16. The margins of safety are adequate for the spring assembly.

The design criteria which was used on the spring was also applied to the alignment ball screw nut assembly. The margins of safety for this design criteria are shown on Table 17. The margins of safety are adequate for the ball screw nut assembly.

The same design criteria which was used on the spring was applied to the alignment system gear box. The thrust load created by the motor was also used as an additional design requirement. The margins of safety on the alignment gear box are shown on Table 18. The upper gear box bearing retainer has the lowest margin.

The pylon damper is designed to carry the loads created by the damping force and is also designed to carry the loads when the store bottoms out against the stops. The design loads were computed with the assumption that the alignment system failed with the spring in the neutral position and the pylon was deflected to 3 degrees to bottom out the pylon. With this criteria the damper component margins of safety were computed. These margins of safety are shown on Table 19. The damper rod end bolt has the lowest margin and this low margin occurs with the damper bottomed out.

PYLON GROUND TESTS

A series of ground tests were conducted on the assembled pylon and its components. These tests were accomplished to assure that the pylon functioned properly and possessed the requisite structural integrity to assure a safe and productive flight test program. Several different types of tests were accomplished. A summary of these tests and their objectives are presented in Table 20. Both pylons were used in the tests and some of the test objectives were accomplished on each pylon, while other objectives were met with component tests. All test objectives were met.

Further details concerning instrumentation, environment, load application, manner of support, test article configuration, and other pertinent items are presented in this section. The functionally complete pylon was mounted in two separate fixtures. The first of these two fixtures was used to conduct four tests (1) proof loads test (2) influence coefficient tests (3) alignment system operational tests and (4) ground vibration tests. In the second fixture the store ejection tests were conducted. Both of these fixtures are existing fixtures at the General Dynamics/Fort Worth Division Test Laboratory and have been used in previous F-16 pylon tests.

Two types of dummy stores were required for the pylon tests. One of these stores was required to have the correct dynamic characteristics (mass, mass moment of inertia and center of gravity). This dummy store was used to conduct the alignment system performance tests, the ground vibration tests and the store ejection tests. The other dummy store was required to have lugs for the application of large loads (proof test/influence coefficient test).

Damper Component Tests

Damping characteristics of the damper for various damper orifice sizes were determined from component tests. The tests were conducted at three temperature conditions at sea level altitude. The cylinder was supported in a vertical position with the piston at both extremes of its travel.

The damper installed in the test fixture is shown in Figure 43. The test fixture with the damper in its temperature chamber is shown in Figure 44. A machined clevis connected the rod end of the piston shaft to the sliding frame of the test fixture. The valve end of the piston shaft was connected to a displacement transducer by drilling a hole in the valve cap and tying a wire between the transducer and valve cap. The sliding frame was held up by the electrically controlled jaws of the impact test machine. When activated, the jaws released the frame, allowing the weights to extend the piston. As the piston extended, the wire connecting the valve cap to the displacement transducer pulled the transducer cable, thus providing a displacement measurement. Instrumentation measured the position of the piston and weight as a function of time. A chart recorder was started a few seconds prior to weight release and provided a hard copy measurement of displacement versus time.

To test the damper in compression, the damper was turned 180° so that the rod end was up. The machined clevis was threaded onto the rod that extended from the block at the top of the frame. The displacement transducer was moved to the lower end of the test fixture. Weight release and velocity measurement were identical to the tension set-up.

Before recording data, damper No. 1 was tested in tension to determine how much force was required to move the piston. Initially, 827 N (186 lb.) at 70^{O}F was needed to produce steady piston movement. In both directions, the damper would bind with the piston at its extreme limits of travel. The damper was cycled in an attempt to relieve the internal friction. After about 30 cycles, the load required to move the piston was reduced to 177.9 N (40 lbs). However, binding was still evident at extreme limits of travel.

Damper No. 1 was tested at room temperature in both tension and compression with an orifice of 0.14 cm (0.055 inch) diameter. To insure steady movement after weight release, it was necessary to extend the piston 1.9 to 2.54 cm (0.75 to 1.0 inch). This initial extension prevented the binding that would have otherwise occurred. After evaluation of the data, the orifice was changed to 0.1143 cm (0.045 inch) diameter and the room temperature tests were repeated.

The test was continued by testing damper No. 1 in tension at -65^{O}F. An environmental chamber made of styrofoam was placed around the damper (Figure 44). Liquid nitrogen was used to cool the chamber. Three thermocouples were used for temperature measurement. One measured free air temperature. The other two measured the cylinder body temperature. The two thermocouples measuring body temperature were taped to the cylinder, one at each end. It took approximately two hours to cool the cylinder to -65^{O}F. There was significant dissipation of the temperature differential through the rod and rod end which were at room temperature. With the damper cylinder at -65^{O}F the load was increased to 823 N (185 lb) and no movement was recorded. The difference in the thermal coefficient between the aluminum cylinder and the steel piston resulted in a locked system. The damper was returned to the shop for evaluation and rework. The binding and freeze up were determined to be due to lack of adequate clearance between the piston and cylinder wall and also a slight non-concentricity between the piston and cylinder.

Damper No. 2 was then put into the test fixture and tested in both tension and compression. This test was conducted with an orifice size of .1143 cm (0.045 inch) diameter. This unit did not have the same problem of binding at its limits of travel which was experienced on unit No. 1. The No. 2 unit was tested at room temperature, $-65^{\circ}F$ and $+160^{\circ}F$. An electric warm air blower was used to heat the styrofoam chamber for the test at $+160^{\circ}F$. In both the low and high temperature tests, 20 minutes of soak time was allowed before the weight was released.

After rework, the No. 1 unit was returned to the lab to continue the test. The binding and freeze up problems had been corrected, and the No. 1 unit was tested in tension at room temperature, $-65^{\circ}F$, and $+160^{\circ}F$. Since the data from these tests showed results that compared favorably to damper No. 2, further testing of damper No.1 in compression was considered unnecessary.

A limited test was conducted on damper No. 3 to determine if its characteristics were similar to the No. 1 and 2 units. The No. 3 unit had a very limited amount of binding at its limit of travel. The problem was not as severe as that of Unit No. 1 prior to rework. Unit No. 3 was tested at room temperature and $-65^{\circ}F$ with an orifice size of .1143 cm (0.045 inch) diameter. Based upon the results of these tests, the other tests of the damper unit were considered unnecessary. A summary of all the damper test conditions is shown on Table 21.

A summary of the damper test results is shown in Figure 45. The test results in Figure 45 show that at the low temperature extreme the damping rate is increased significantly. These results are for an orifice size of .1143 cm (0.045 inch) diameter. The damping rate which was used in the decoupler pylon analysis reported in the dynamic analysis section was 383.5 N sec/cm (219 lb sec/in.). This analysis value represents an average value over the operating temperature range.

Spring Calibration

Two instrumented alignment springs (one each per pylon) were calibrated so that spring load can be measured in flight. The spring calibration served a secondary purpose of determining the degree of linearity of the spring and a spring rate comparison between the two. The locations and related information on the strain gage bridges are shown on Figure 46. The component calibration of the individual spring bridges was accomplished by supporting the springs in a test fixture as cantilevered beams. The springs were supported by using the forward attachment provisions and vertical loads were applied at the ball nut attachment points on the aft end of the springs. The maximum calibration load applied was ±11.12 KN (±2500 lbs).

The sequence which was employed for unit load testing included exercise cycles to improve the linearity of the data collected. The load was increased by 20% increments of the maximum load and the data was recorded at each increment. Each spring was loaded to maximum load in both directions two separate times with the data recorded in each test run. The tests were conducted at room temperature. The strain gage reading, load cell reading and a deflection measurement were made and printed out during each test.

The load versus deflection measurement on the two springs is shown on Figure 47 and 48. This data indicates that the deflections and loads on both springs are providing linear response of the springs.

This data clearly shows that both springs have a linear spring rate and it is approximately 3502 N/cm (2000 lb/in) which was the design value. The strain gage measurements are plotted versus load on Figures 49 and 50. This data indicates that the gages on both springs are providing linear response of the springs.

Alignment System Operational Tests

A complete pylon with an attached dummy GBU-8 was tested with simulated applied loads and the active alignment system. The purpose of this test was to determine the operational characteristics of the alignment system under realistic load conditions. The complete pylon and a dummy GBU-8 with the correct dynamic characteristics were attached to the test fixture. Pitching moment about the store c.g. as a function of time was applied in combination with side and yaw loads. The loading conditions are summarized on Table 22. The time history of the applied pitching moment is shown on Figure 51.

The following instrumentation readouts were recorded as a function of time.

Pylon Pitch Angle Sensor.
Spring Strain Gages.
Accelerometers on Dummy Store Nose and Tail.
Applied - voltage - to - motor indicator.

Each test condition was started with the store at zero degrees of misalignment. All the tests were conducted at room temperature. The pitching moment time history was based upon a variation of a rudder kick flight maneuver which gives the highest store pitching moment in combination with side loads and yawing moments. The pitching moment (Figure 51) was varied with time while the side load and yawing moment were applied as constant values. The alignment motor on-off control cams were set prior to beginning the test and were determined to be satisfactory during the course of the test and therefore were not varied. Analyses had previously indicated that an on-off switch arrangement which consisted of turning the motor on when misalignment exceeded ± 0.5 degrees and turning the motor off when the misalignment became less than ± 0.25 degrees was the best combination. These values were the ones which were set prior to the test. The alignment system operational tests were conducted on both pylons. A summary of the alignment system tests is given in Table 22.

The alignment system on both pylons performed as expected and realigned the pylon when the pitch angle exceeded approximately ± 0.5 degrees. During tests AL4 (Table 22) on pylon No. 1 and AL3 and AL4 on pylon No. 2 the store pitch angle did not exceed 0.5 degrees and therefore the motor did not operate. The combination of yawing moment and/or side force created friction in the pivot joints which prevented the pitch angle from exceeding 0.5 degrees. The applied pitching moment and the misalignment angle as a function of the time for each of the test conditions are shown in Appendix E. Times at which the motor came on and went off are also shown. Each test condition that is identified in Appendix E is defined on Table 22.

The tests conducted indicated that the on-off switch settings described above would provide the alignment performance desired. Therefore the alignment switch settings were not changed as a result of the test conducted.

Influence Coefficient Tests

Influence coefficient tests were conducted on the assembled pylon in the test fixture. This data was then compared with the computed stiffness and used to modify the computed data. The structurally complete pylon was mounted in the test fixture. Loads were applied in the required directions by means of the existing dummy store with loading lugs. Pitch, yaw, roll, vertical, drag and side loads were applied separately and incrementally to the store. Deflections of the store relative to the test fixture were measured for each load level and for each type of loading. Two exercise cycles were run prior to each data run. For each type of load, the following sequence of loading was followed.

Step	Percent of Maximum Test Load	Instrumentation Readout Requirement
1	0	Zero and Record
2	20	Record
3	40	"
4	60	"
5	80	"
6	100	"
7	80	"
8	60	"
9	40	"
10	20	"
11	0	Record and Zero

The loading was then repeated in the opposite direction using the same test sequence shown above. At each load level the following instrumentation was recorded and printed:

1. Ram Load Cells.
2. Deflection Transducers.
3. Proof Test Strain Gages.
4. Pylon Pitch Angle Indicator.
5. Flight Test Load Strain Gages.

The alignment system was not activated during the load application. The test conditions and loadings are given in Table 23.

The deflection data was plotted versus load to determine the slope which is the flexibility. The cross coupling terms were also determined from the test data. The hand plotted data, using the measured deflections as a function of the loading, indicated that the pylon was primarily a linear system with only a small degree of nonlinearity. The flexibility influence coefficients determined from the measured data are shown on Table 24. The measured data was used to tune the finite element mathematical model of the pylon. The final tuned finite element flexibility values are also shown on Table 24. For every loading condition the deflection in the direction of the load was one order of magnitude above the cross coupling values.

The alignment system was used to drive the store to the stop, a pitching moment was applied, and deflections were measured. These tests provided a measure of the pylon pitch stiffness with the store bottomed against the stop. The deflection per pitching moment load for the store in the nose up direction is 1.44×10^{-9} rad/(N cm)(1.625×10^{-8} rad/(in.lb)). The deflection per pitching moment load for the store in the nose down direction is 2.17×10^{-9} rad/(N cm) (2.458×10^{-8}

rad/(in.lb)). These values indicate that the pylon against the stop is 15.6 times stiffer in the nose up direction and 10.3 times stiffer in the nose down direction. (Pitch stiffness values against the stop which were 6, 10 and 20 times stiffer were used in the non-linear flutter analysis.)

Ground Vibration Tests

Ground vibration tests were conducted at room temperature on a complete pylon with a dummy GBU-8 store. The dummy store had the correct mass and inertia characteristics. This test provided pylon natural frequencies, mode shapes and damping in each of the modes. The pylon and store were mounted in the stiff test fixture which has a fundamental natural frequency above the pylon fundamental frequencies. Excitation was provided by two electromagnetic shakers attached to the store. The shakers were mounted to shake the store vertically and in pitch. The shakers were also mounted laterally to excite the store in its lateral and yaw modes.

Frequency sweeps were made to locate the natural frequencies. At each natural frequency, acceleration was measured at points on the store and pylon to define the mode shapes. At each natural frequency the modal damping was determined from the decaying sinusoidal response.

Based upon the analysis information the pylon pitch frequency was expected to be 3.6 Hz. In the initial tests on the number 1 pylon an excitation force in excess of 444.8 N (100 lbs) in shakers at the nose and tail of the weapon was required to excite this pylon pitch mode. This mode could only be excited at this force level with the damper removed. The mode could not be excited with the damper engaged because of the output limitations on the shakers. The frequencies of the modes obtained with the number 1 pylon in this configuration are shown on Table 25. All modes except the pitch mode could be excited with low shaker force levels. The second pitch mode at 6.7 Hz is a mode which can be described as the upper pylon strongback bending which results in a mode which has a large amount of pitch motion. This mode is increased in frequency with the addition of the skin which stiffens the upper strongback. In order to determine the source of the resistance to pitch excitation a pitching breakout friction test was conducted. From this test it was determined that the breakout force required was 759 N m (6720 in.lbs) in the nose up direction and 900 N m (7968 in.lbs) in the nose down direction. These breakout pitching moments are shown in Table 26. From this test it was determined that the pylon lugs were experiencing high frictional forces in their attachment pins. The source of this friction is binding of the pins due to an adverse tolerance buildup on the adjacent parts. In order to reduce the binding the inside diameter of the bushing was increased by .01 cm (.004 inches). The breakout moments were obtained with this increased clearance in the bushing. These moments are shown in Table 26.

At this point in time the number 2 pylon was assembled and ready for ground test. The No. 2 unit was placed in the fixture and the No. 1 unit was partly disassembled to examine the linkages for sources of binding. The results of vibration tests and breakout friction tests on No. 2 are shown in Tables 25 and 26 and are identified as No. 2 with tight linkage fit. The damper configuration was changed for this test. The fluid was removed from the damper so that only air was forced through the orifice. The shaker force required to excite the pylon pitch mode (3.6 Hz) was approximately 356 N (80 lbs).

The link pins which were installed in the No. 1 unit were cadmium plated. When these pins were removed the cadmium plating was severely damaged. Part of the damage was the result of pressing the pins in and out. Detailed measurements were made of the link and lugs. The measurements were made at the outside of each hole to determine how far from being parallel the pins were when installed. These measurements are summarized in Table 27. Based upon these measurements the decision was made to machine a new set of link pins which were .01 cm (.004 inches) undersize. The clearance with these pins is shown on Table 28. These undersize pins were placed in the No. 2 pylon. Breakout friction was measured and a limited vibration test was conducted. These results are shown on Tables 25 and 26. The test condition is defined as No. 2 with loose linkage. Approximately 267 N (60 lbs) of shaker force at the front and back of the store was required to excite the pitch mode in this configuration. These loose fit pins allowed enough free play in the pins so that the binding was a minimum. However, the effect of the small amount of non-parallel in the pins can still cause binding. The original pins were manufactured within the tolerance called for on the drawings and enough differences between the parts could exist even with the part within tolerance, to cause the non-parallel effect to be significant. When the store rotates in pitch these small amounts of non-parallel pins can result in fore and att and vertical motion of the pins and binding occurs. If larger clearances are allowed such that no binding will occur, then excessive free play will result. Excessive free play could cause an adverse coupling between the airplane and the store yaw and roll degrees of freedom.

Based upon these tests of pylon No. 2 the decision was made to use undersize pins without cadmium plating. This design change required another type of pin retainer, since the pins were no longer press fitted into the links. The retainer design is shown on Figure 52. The free play of the loose fit pins was considered excessive and therefore a set of medium size pins with retainers were fabricated. The clearance with these pins is shown on Table 28. These pins were installed in the No. 2 pylon and breakout friction tests were repeated. These test results are shown on Table 26 and are identified as No. 2 with medium linkage fit.

The No. 1 pylon was fitted with a set of medium fit pins with retainers and the vibration tests and breakout friction test repeated. The damper was also reconfigured for this test. The o-rings were removed from the piston and the orifice was removed. The scrapers were removed and the end seal o-rings were replaced with teflon rings. This damper configuration provided minimum friction in the damper and still provides the pylon with its ± 3 degree stops. The alignment system ground tests have shown that the damping coefficient in the damper is not needed for stability. The test results of this pylon configuration are shown on Table 25 and 26. The shaker force required to excite the store pitch mode was approximately 267 N (60 lbs) at the forward and aft store locations. The increased free play in the pins resulted in a lower lateral bending frequency and also a lower yaw mode frequency.

The vibration test data was used to supplement the influence coefficient test data to improve the finite element simulation of the pylon. The improved pylon simulation was used to compute natural frequencies and mode shapes of the cantilevered pylon. These computed natural frequencies and mode shapes were compared with the test results and modified as required to improve the correlation. The final pylon flexibilities required to provide the best match to test data are shown on Table 24.

Structural Proof Tests

The pylon has been designed to maintain at least +25% margin of safety with respect to ultimate load for GBU-8 carriage. However, to provide increased confidence in the structural integrity of the pylon design, one pylon was proof tested to 110% of limit load for the most critical GBU-8 design condition. The pylon was supported in the test fixture, the dummy store with loading lugs was mounted on the MAU-12 rack in the pylon. For each condition the following loading sequence was followed:

Step	Percent Limit Loads	Instrumentation Readout Requirement
1	0	Zero and Record
2	20	Record
3	40	"
4	0	"
5	0	Rezero and Record
6	20	"
7	40	"
8	60	"
9	80	"
10	100	"
11	110	"
12	100	"
13	80	"
14	60	"
15	40	"
16	10	Do not Record
17	20	Record
18	0	Record

Readouts of the following instrumentation were recorded and printed out at each point noted on the above loading sequence listing:

- Ram Load Cells
- Deflection Transducers
- Proof Test Strain Gages (35 reading locations)
- Pylon pitch angle indicator
- Flight Test Load Measurement strain gages (one reading on the pitch spring)

The proof test load conditions are shown in Table 29. Condition 1575-2.3R was selected because it provides the highest GBU-8 loads on the aft strongback, the spring and the alignment system. Condition 1595-1.2R produces the maximum loads on the forward and aft links, the sideplates, and the forward portion of the strongback. Table 29 gives the limit loads which were applied at the store c.g. The pylon alignment system was inactive for the tests and the motor brake was set. The tests were conducted at room temperature.

The stress levels at 100% of limit load on all the strain gages were low. This verified the pylon structural integrity. The original assumption in the stress analysis was that the pin-jointed four bar linkage was statically determinant and the entire pitching moment load would be reacted through the spring. With this assumption the computed stress in the spring is compared with the spring gage for load condition 1575-2.3R.

Computed Force, P, in the screw = M_y/arm length =

$$\frac{12508 \text{ N m}}{1.1176 \text{ m}} = 11192 \text{ N} \left(\frac{110687 \text{ in-lb}}{44 \text{ in.}} = 2516 \text{ lb}\right)$$

Computed Moment, M, at gage =

0.381 m(11192 N) = 4264 N m

(15.0 in.(2516 lb) = 37740 in-lb)

Thickness, t, at gage = 0.03068 m (1.208 in.)

Width, W, at gage = 0.0762 m (3.0 in.)

Computed Bending Stress, f_B, at gage =

$$\frac{6(4264 \text{ N m})}{0.0762 \text{ m } (.03068 \text{ m})^2} = 3.567 \times 10^8 \text{ N/m}^2$$

$$\left(\frac{6\ (37740 \text{ in.-lb})}{3.0 \text{ in } (1.208 \text{ in.})^2} = 51725 \text{ lb/in.}^2\right)$$

Measured f_B at gage = 1.694×10^8 N/m^2 (24570 lb/in.^{2})

This lower measured value of bending stress in the spring indicates that some level of binding in the linkage occurs due to the large yaw moment applied to the store in load condition 1575-2.3R. This binding changes the four bar linkage to some level of fixed linkage, and the remaining pitching moment is reacted by in-plane shears in the links. The distribution of this shear load between the two links was not measurable with the existing strain gages. On the other hand the stresses in the links that were measured for condition 1595-1.2R can be used to compare analysis to test. This load condition creates primarily axial loads in the links without binding the joints, and can be used to determine the axial load distribution between the two links. This load distribution is 28% forward and 72% aft and confirms that the 40% forward and 70% aft load distribution assumption used in the stress analysis is reasonable.

Store Ejection Tests

Ground ejection tests were conducted from one pylon to determine the MAU-12-C/A orifice sizes necessary to assure safe jettison of a GBU-8 in airplane flight test. The pylon was mounted in a test fixture simulating the attachment to the airplane. A dummy GBU-8 store with the same mass and inertia properties as the flight test store was attached to an operational MAU-12-C/A rack attached to the pylon. The pylon alignment system was active.

Time histories of each ejection event were recorded using accelerometers, position transducers, and high speed movie cameras. The outputs from strain gages on the pylon were also recorded. All ejections were made at room temperature.

Five drops were made using four orifice combinations for determining store ejection velocities and pitch rate from the pylon. The forward orifice was increased from 0.206 cm (0.081 in) diameter to 0.28 cm (0.110 inch) diameter in order to match the ejection velocity that was used in the flight certification of the GBU-8 from the F-16. The orifice combination which has a forward orifice size of 0.28 cm (0.110 in.) and an aft orifice size of 0.206 cm (0.081 in.) provided an ejection velocity of 3.14 m/s (10.3 ft/s) and a pitch rate of 3.3 degrees/sec nose down. These ejection parameters will provide equal or slightly improved separation characteristics for the GBU-8 because of the small nose down pitch rate. The flow field on the GBU-8 from the decoupler pylon should be virtually the same as from the production pylon.

In light of the above information, the GBU-8 can be cleared to be released singly or in pairs from the decoupler pylon to 283 m/s (550 KCAS) to 0.9 Mach at load factors from +0.5 to +4.0. All normal store release parameters still apply, i.e., zero roll rate, $\pm 5^{\circ}$ roll angle, 0 to 45° climb angle, 0 to 60° dive angle. This clearance applies with or without the 370 gallon fuel tank at Stations 4 and 6.

SAFETY SYSTEM

Hazard analyses were performed for the NASA decoupler pylons. A Preliminary Hazard Analysis (PHA) was prepared to achieve early visibility of hazards to personnel and equipment. Finally an Operating and Support Hazard Analysis (O&SHA) was performed to examine the instructions for errors, inadequacies, and omissions that could result in personnel injury or equipment damage. These hazard analyses are given in Appendix F along with the hazard classifications and probabilities.

FLIGHT TEST DEMONSTRATION

The completed ship set of decoupler pylons were delivered to NASA Dryden for a flight test demonstration program. Electric wiring for both instrumentation and the pylon alignment system are required. The signals from the instrumentation are sent to an onboard tape recorder and selected signals will be telemetered to the test ground station. The particular signals which are transmitted to the ground station will be selected to provide the test engineer with maximum knowledge about the status of the test. The pylon alignment control switch will be installed in the pilot station. This switch will provide the pilot with a capability for turning the alignment system on and off. Flight test maneuvers will be performed with the alignment system on and off to provide information on the alignment system performance. The alignment system electrical circuit was described in the section titled Electrical System. Warning lights will be installed in the pilot station to notify the pilot that the store is against a stop. The store should only go to the stops when a malfunction in the alignment system has occurred. The plan is to fit and install the pylons on an instrumented F-16 for ground and flight tests. The flight test program will be directed toward a flutter demonstration with some maneuver loads testing and one store ejection.

The pylons will be installed and the initial tests will be on the GBU-8 configuration. Additional flight tests on the B-61 store configuration are also planned. Ground vibration tests of the GBU-8 configuration are planned prior to the first flight.

Flight Test Instrumentation

A flight test instrumentation list was prepared to meet the test objectives. This list is based upon previous flutter, loads and store ejections test experience on the F-16. This instrumentation list is shown on Table 30.

The flight test instrumentation on the pylon and store consists of strain gages installed on the pylon pitch springs, pylon pitch angular measurements, and accelerometers. The strain gages on the spring are located 38.1 cm (15 inches) forward of the aft end of the spring. The calibration of these gages was discussed in the section titled Spring Calibration. The wiring harnesses from these gages to the airplane system were designed and fabricated by the contractor. These harnesses assume that the F-16 airplane number 2 instrumentation package will be used. Harnesses for both the left and right hand pylons were fabricated.

The accelerometer locations on the flight test GBU-8 stores were defined by GD/FW. These locations were chosen based upon previous flight test experience with GBU-8 configuration. The installation drawings were made by the contractor. The wiring harnesses for accelerometer to the aircraft recording system were also designed. The accelerometers will be installed on each store by NASA. The wiring harnesses were fabricated by the contractor and these harnesses will be installed by NASA.

The flight test program will include one planned store ejection from the decoupler pylons. During the weapon release, first motion will be recorded. The contractor developed camera installation locations for ejection from Stations 3 and 7. These installations have been successfully used in previous store ejection tests. These installations were provided to NASA for their consideration in the store ejection flight test plan.

Aircraft Modification

The design concept used on the decoupler pylon resulted in a design which requires minimum modifications to the basic airframe. The pylons fit the F-16 attachment points provided at Stations 3 and 7. The decoupler pylon power requirements are electrical and the electrical power provided by the airplane at Stations 3 and 7 is adequate for the pylons. Therefore the aircraft modification to accommodate the decoupler pylons is minimal.

The aircraft modification will include fitting the pylons to the airplane, installing the pylons and installing the instrumentation system. The pylons were delivered with the upper skins not trimmed to the under wing contour. These skins will be trimmed to fit the wing contour.

CONCLUDING REMARKS

A ship set of decoupler pylons were designed, analyzed and fabricated for a flight test evaluation. These pylons were ground tested on fixtures by the contractor prior to delivery to NASA.

The decoupler pylon incorporates a design with a four bar linkage which results in a remote pivot location which is at the c.g. of the GBU-8 weapon when the weapon is aligned. This remote pivot design results in reduced misalignment forces during maneuvers. This very significant reduction in the misalignment angle results in reduced alignment power requirements. These reduced power requirements provided for using an electrical alignment device. Electrical power existed at the pylon station and this reduces the requirements for wing modifications to accommodate the pylons. The electrical alignment system consists of an electric motor driving a gear box. The system is equipped with on-off switches to activate the motor when the store misaligns. The switches have a dead band near zero misalignment, and therefore when the misalignment angle is less than ± 0.5 degrees the alignment system is not activated.

The pylon is equipped with a hydraulic damper. The damper has a removal orifice which can be changed to increase or decrease the damping coefficient. The damper is also used as stops to restrict the pitch excursions to ± 3 degrees. The ground tests plus analysis indicate that the damper will not be needed in flight and will be used only as stops.

The pylon pitch spring rate which will maximize the flutter speed when carrying the GBU-8 weapon is 3502 N/cm (2000 lb/in.) measured 111.76 cm (44 inches) from the pylon pivot location. This spring rate was determined by analysis and the analysis indicates that this spring rate will provide the airplane with a flutter speed outside of the airplane operations limit. Aeroservoelastic analyses were also conducted on the airplane with the decoupler pylon loaded with the GBU-8. These analyses indicate that the flight control system reduces the airplane flutter speed with respect to the unaugmented flutter speed. This reduction is not large enough to require a restriction in the airplane operating limits.

The correct spring rate in the pylon is provided with a constant stress cantilevered beam. The design provides for removal and replacement of the spring with a stiffer or more flexible spring. Ground tests of both springs and the assembled pylons indicated that the spring has the desired spring rate.

The ground vibration tests of the assembled pylon indicated that a large excitation force was required to excite the store pitch mode. It was determined that bearing friction in the pivot pins and binding of the linkage were causing this problem. The pivot joint friction was reduced to some extent by introducing free play in the joints. These loose fitting pivot joints resulted in lateral and yaw free play in the pylons. Large increases in the lateral and yaw free play might reduce the flutter speed, therefore the pivot joint free play could not be increased by a large amount. The linkage friction which still existed, will have the effect of delaying the separation of the GBU-8 pitch mode frequency from the tip missile pitch frequency until the breakout pitch moment is reached.

REFERENCES

1. Peloubet, R. P. Jr. and Haller, R. L., Feasibility Study for F-16 Flutter Suppression System, AFFDL-TR-78-113, September 1978.
2. Reed, Wilmer H., III; Foughner, Jerome T., Jr. and Runyan, Harry L.; Decoupler Pylon: A Simple Effective Wing/Store Flutter Suppressor, AIAA J. Aircraft, Vol. 17, No. 3, March 1980, pp. 206-211.
3. Runyan, Harry L.; Effect of a Flexibly Mounted Store on the Flutter Speed of a Wing, NASA CR-159245, April 1980.
4. Desmarais, Robert N.; and Reed, Wilmer H., III; Wing/Store Flutter with Nonlinear Pylon Stiffness, AIAA J. Aircraft, Vol. 18, No. 11, November 1981, pp. 984-987.
5. Reed, Wilmer H. III, Cazier, Frank W., Jr.; and Foughner, Jerome T., Jr.; Passive Control of Wing/Store Flutter, Presented at the Fifth JTGG/MD Aircraft Stores Compatibility Symposium in St. Louis, Mo., September 1980.
6. Cazier, F. W. Jr.; and Foughner, Jerome T., Jr.; NASA Decoupler Pylon Programs for Wing/Store Flutter Suppression, NASA CP2162, Part 1, Vol. 1, pp 207-218.
7. Reed, Wilmer, H., III, Cazier, F. W., Jr.; and Foughner, Jerome T., Jr.; Passive Control of Wing/Store Flutter, NASA TM 81865, December 1980.
8. Peloubet, R. P., Jr.; Haller, R. L.; and McQuien, L. J.; Feasibility Study and Conceptual Design for Application of NASA Decoupler Pylon to the F-16, NASA CR 165834, May 1982.
9. Giesing, J. P.; Kalman, T. P., and Rodden, W. P.; Subsonic Unsteady Aerodynamics for General Configurations, Part I, Vol. I, Direct Application of the Nonplanar Doublet Lattice Method, AFFDL-TR-71-5, November 1971.

TABLE 1.- PRODUCTION PYLON ANTISYMMETRIC FLUTTER ANALYSIS WITH WEIGHT VARIATIONS

$M = 0.9$, ALT = S.L.

VARIATION	FLUTTER VELOCITY V_f m/s (Kts) TAS $g = 0$	FLUTTER FREQUENCY f_f Hz
BASIC	172 (335)	5.27
GBU-8 C.G. 24.08 cm (9.48 in.) FWD	234 (455)	5.14
GBU-8 C.G. 24.08 cm (9.48 in.) AFT	720 (1400)	
GBU-8 WITH 45.36 Kg (100 lb) OF MASS	216 (420)	5.18
AIM-9 WITH 22.68 Kg (50 lb) OF MASS	244 (475)	4.76

TABLE 2.- WEIGHT AND INERTIAL CHARACTERISTICS OF EXTERNAL STORES

	UNITS SI (ENGLISH)	½ FULL 370 GAL. TANK CBE	GBU-8/B
WEIGHT	kN (lb)	6.47 (1454.4)	10.08 (2265)
CENTER OF GRAVITY AFT OF FWD HOOK	cm (in.)	11.1 (4.36)	37.5 (14.76)
I_{pitch} & I_{yaw} ABOUT C.G.	kN·m^2 (lb-in.^{2})	18.8 (6.54×10^6)	6.97 (2.428×10^6)
I_{roll} ABOUT C.G.	kN·m^2 (lb-in.^{2})	.092 (32×10^3)	.270 (94×10^3)

TABLE 3.- SUMMARY OF WEAPON PYLON STIFFNESS

	YAW STIFFNESS N-M/RAD (IN-lb/RAD)	ROLL STIFFNESS N-M/RAD (IN-lb/RAD)
PRODUCTION PYLON		
UPPER		1.921×10^6 (17.0×10^6)
LOWER		2.80×10^6 (24.83×10^6)
COMPOSITE	2.80×10^6 (24.83×10^6)	1.14×10^6 (10.09×10^6)
MAU-12 RACK	4.62×10^6 (40.85×10^6)	1.27×10^6 (11.25×10^6)
DECOUPLER PYLON		
UPPER	2.01×10^6 (17.76×10^6)	1.84×10^6 (16.33×10^6)
JOINT (FWD)	21.29×10^6 (188.4×10^6)	17.44×10^6 (154.3×10^6)
JOINT (AFT)	138.1×10^6 (1222.0×10^6)	8.06×10^6 (71.29×10^6)
LOWER	64.47×10^6 (570.5×10^6)	5.95×10^6 (52.63×10^6)
COMPOSITE	1.92×10^6 (17.02×10^6)	1.33×10^6 (11.81×10^6)

TABLE 4.- COMPLETE AIRPLANE SYMMETRIC MODE FREQUENCIES (HZ)

MODE DESCRIPTION	PRODUCTION PYLON		DECOUPLER ZERO PITCH FEASIBILITY STUDY	DECOUPLER ZERO PITCH CURRENT DESIGN	DECOUPLER BASED ON TEST DATA
	GVT	ANALYSIS			
WING BENDING	4.07	3.869	3.860	3.881	3.694
STA. 120 GBU-8 PITCH	5.35	5.343			3.259
TIP MISSILE PITCH	6.31	6.135	6.074	6.047	5.955
STA. 120 GBU-8 YAW	8.12	7.409	7.407	6.556	5.309
TANK YAW	7.61	7.843	7.897	7.882	7.923
TANK PITCH	7.81	8.014	7.071	6.743	7.381
STA. 120 GBU-8 YAW	10.20	9.806	9.815	10.952	
TANK YAW	14.02	14.453	14.161	14.693	14.175
FUSELAGE VERT. BEND.	10.81	11.859	11.783	11.986	11.757
WING 2ND BENDING	12.28	10.774	9.253	8.796	9.98
STA. 120 GBU-8 LATERAL					5.123
WING TORSION					6.603

TABLE 5.- NATURAL FREQUENCIES FOR CANTILEVERED STORE AND PYLON

MODE	NATURAL FREQUENCY - HZ GROUND TEST	FINITE ELEMENT
FIRST STORE PITCH	3.6	3.667
SECOND STORE PITCH	5.5	5.494
*STORE LATERAL	5.7	5.223
STORE YAW	6.7	6.644

* THERE IS SOME YAW MOTION COUPLED IN THE LATERAL MODE.

TABLE 6.- COMPLETE AIRPLANE ANTISYMMETRIC MODE FREQUENCIES (HZ)

MODE DESCRIPTION	PRODUCTION PYLON		DECOUPLER ZERO PITCH FEASIBILITY STUDY	DECOUPLER ZERO PITCH CURRENT DESIGN	DECOUPLER SPRING COUPLED CURRENT DESIGN	DECOUPLER BASED ON TEST DATA
	GVT	ANALYSIS				
STA. 120 GBU-8 PITCH	5.13	5.112			3.448	3.216
TIP MISSILE PITCH	5.44	5.418	5.405	5.412	5.413	5.543
STA. 120 GBU-8 YAW	7.09	7.118	7.284	6.498	6.394	5.211
TANK PITCH	7.91	7.883	6.488	6.151	6.614	7.113
TANK YAW	7.97	7.979	7.976	7.978	7.978	7.981
STA. 120 GBU-8 YAW	8.96	8.356	8.258	8.187	8.193	6.201
WING BENDING	10.20	10.485	9.924	9.644	9.846	8.721
TANK YAW	13.48	12.748	12.54			
VERTICAL TAIL BEND.		11.990	11.517	11.607	11.619	11.735
FUSELAGE SIDE BEND.		14.61	13.50	13.126	13.158	
VERT. TAIL BEND.				12.090	12.104	12.882
GBU-8 LATERAL						4.901

TABLE 7.-FLIGHT CONTROL SYSTEM GAIN SCHEDULES

MACH	0.6	0.9	1.2
ALTITUDE	S.L.	S.L.	S.L.
V_{CAL} M S^{-1}(Kts)	204(397)	306(595)	408(793)
α_{TRIM}	1.5	1.0	1.0
F2	.50	.322	-.536
F3	.728	.3395	.0835
F7	.0934	.5446	1.0
F8	.50	.50	.50
F10	.25	.25	.50
$G\alpha/_{57.3}$	.02618	.01745	.01745
G_{ARI}	-.00659	-.4151	-.8250

TABLE 8.- LATERAL AIRPLANE AEROSERVOELASTIC STABILITY ANALYSIS (Using Ground Test Data) ALT=S.L., M=0.9.

VELOCITY M S^{-1} (Kts)	YAW LOOP STABILITY	ROLL LOOP GAIN AND PHASE MARGINS GAIN CROSSOVER	PHASE MARGIN
203(396)	STABLE	0.14	+100°
237(462)	STABLE	0.20	+97°
271(528)	STABLE	0.30	+35°
305(594)	UNSTABLE	-	-

TABLE 9.- SUMMARY OF RESPONSE TO GBU-8 EJECTION LOADS
INCREMENTAL MAXIMUM AND MINIMUM VALUES

	F_V KN(LBS)	M_P N M(IN-LBS)	θ_P (DEG)	Z CM(IN)	θ (DEG)	F_{SPRING} N(LBS)	F_{DAMPER} N(LBS)	$\ddot{\theta}_m$ (RAD/SEC^2)	$\ddot{Z}_m$ (g's)
DECOUPLER PYLON									
SYMMETRICAL PUSHOVER	.80(181) -32.6(-7338)	7719(68313) -8951(-79214)	.187 -.028	.14(.056) -.19(-.074)	.4021 -.0038	442(99.4) 0	398(89.5) -38(-8.56)	53.8 -40.1	+4.04 -5.34
SYMMETRICAL PULLUP	103.3(23224) 55(12364)	27571(243990) 14871(131600)	.330 -.561	5.3(2.086) .49(-.193)	.0125 -.2133	0 -2396(-538.6)	124(27.8) -2112(-474.8)	150.1 -193.2	+15.24 -15.94
RUDDER KICK	54.7(12312) 11.4(2566)	9193(81358) -3016(-26687)	.225 -.383	2.74(1.077) -1.06(-.416)	.0078 -.5925	0 -6539(-1470)	77(17.3) -5868(-1319)	103.5 -122.1	+7.96 -10.23
ONE G	48.2(10842) 5.3(1196)	14552(128780) 2410(21325)	.234 -.275	2.33(.916) -1.14(-.448)	.0073 -.0076	57(12.9) -48(-10.9)	72(16.2) -75(-16.9)	93.7 -106.9	+7.10 -9.39
PRODUCTION PYLON									
ONE G	47.6(10696) 4.47(1005)	12395(109690) 2323(20556)	.228 -.264	2.29(.903) -.87(-.341)	- -	- -	- -	73.0 -105.5	+9.18 -7.20

F_V - Force at pylon to wing attachment - Station 349.67
M_P - Moment at pylon to wing attachment - Station 349.67
θ_P - Pitch angle of ejector rack
z_P - Vertical displacement of ejector rack
θ - Relative angle between ejector rack and wing
F_{SPRING} - Alignment system spring force
F_{DAMPER} - Alignment system damper force
$\ddot{\theta}_m$ - Wing tip missile pitch acceleration
$\ddot{z}_m$ - Wing tip missile vertical acceleration

ORIGINAL PAGE IS
OF POOR QUALITY

TABLE 10.- F-16 STORE CARRIAGE, RELEASE, JETTISON REQUIREMENTS

STORE	CARRIAGE: Max Speed (KIAS)	CARRIAGE: Max Mach	CARRIAGE: Load[3] Factor (g)	CARRIAGE: Max Bank[11] Angle Change (Deg)	RELEASE[1]: Mode	RELEASE[1]: Max[4] Speed (KIAS)	RELEASE[1]: Max[4] Mach	RELEASE[1]: Max(α/Min Spd[4] Deg/KIAS	RELEASE[1]: Load[4] Factor Min	RELEASE[1]: Load[4] Factor Max	RELEASE[1]: Delivery[4] Angle Climb	RELEASE[1]: Delivery[4] Angle Dive	SELECTIVE JETTISON[2]: Max Speed (KIAS)	SELECTIVE JETTISON[2]: Max Mach	SELECTIVE JETTISON[2]: Load Factor Min	SELECTIVE JETTISON[2]: Load Factor Max
AIM-9J	A/C	A/C	A/C	360	Firing[5]	A/C	A/C	A/C/A/C	0.0	6.5	ALL	ALL	N/R	N/R	N/R	N/R
ACMI	700	1.6	8.5	360	N/R	N/R	N/R	N/R	N/R	N/R	N/R	N/R	N/R	N/R	N/R	N/R
MK-82	-	0.9	5.5	180	Ejecting	550	0.9	10/300	0.5	4.0	45°	60°	500	0.8	0.8	1.5
MK-82R	-	0.9	5.5	180	Ejecting	500	0.9	10/300	0.7	2.0	15°	30°	500	0.8	0.8	1.5
MK-36	-	0.9	5.5	180	Ejecting	500	0.9	10/300	0.7	2.0	15°	30°	500	0.8	0.8	1.5
MK-84	-	0.9	5.5	180	Ejecting	550	0.9	10/300	0.5	4.0	45°	60°	SAR	SAR	SAR	SAR
BLU-27B/B(UF)	-	0.9	5.5	180	Ejecting	500	0.9	10/300	0.5	2.0	15°	30°	500	0.8	0.8	1.5
BLU-52	-	-	-	180	Ejecting	-	-	10/300	-	-	-	-	-	-	-	-
MATRA-250	-	-	-	180	Ejecting	-	-	10/300	-	-	-	-	-	-	-	-
MXU-648/A	-	-	-	180	N/R	-	-	10/300	-	-	-	-	N/R	N/R	N/R	N/R
AGM-65A,B	-	0.9	7.33	180	Firing	550	0.9	10/300	0.5	1.2	15°	60°	500	0.8	0.8	1.5
GBU-10B,A/B,C/B	-	0.9	5.5	180	Ejecting	550	0.9	10/300	0.5	1.2	15°	60°	SAR	SAR	SAR	SAR
GBU-12B/B	-	0.9	5.5	180	Ejecting	550	0.9	10/300	0.5	1.2	15°	60°	SAR	SAR	SAR	SAR
GBU-8/B	-	0.9	5.5	180	Ejecting	550	0.9	10/300	0.5	1.2	15°	60°	SAR	SAR	SAR	SAR
CBU-52B/B	-	0.9	5.5	180	Ejecting	550	0.9	10/300	0.5	4.0	45°	60°	500	0.8	0.8	1.5
CBU-58/B,A/B	-	0.9	5.5	180	Ejecting	550	0.9	10/300	0.5	4.0	45°	60°	500	0.8	0.8	1.5
CBU-71/B,A/B	-	0.9	5.5	180	Ejecting	550	0.9	10/300	0.5	4.0	45°	60°	500	0.8	0.8	1.5
BL755 MK-2	-	0.9	5.5	180	Ejecting	550	0.9	10/300	0.5	4.0	45°	60°	500	0.8	0.8	1.5
M129E2	-	-	-	180	Ejecting	-	-	10/300	-		-	-	-	-	-	-
SUU-25C/A,E/A (Loaded)	-	0.9	5.5	180	Dispensing Flares	550	0.9	10/300	0.8	1.2	15°	15°	400	0.8	0.8	1.5
SUU-25C/A,E/A (Empty)	-	0.9	5.5	180	Ejecting Empty	400	0.8	10/300	0.8	1.2	15°	15°	400	0.8	0.8	1.5
MK-20 MOD 3,4	-	0.9	5.5	180	Ejecting	550	0.9	10/300	0.7	4.0	15°	45°	500	0.8	0.8	1.5
LAU-3/A,C/A,D/A (Loaded)	500	0.9	5.5	180	Firing 2.75"FFAR	400	0.8	10/300	0.5	2.0	15°	60°	400	0.8	0.8	1.5
LAU-3/A,C/A,D/A (Empty)	450	0.9	5.5	180	Ejecting Empty	450	0.8	10/300	0.8	1.5	15°	15°	400	0.8	0.8	1.5
LAU-68A/A (Loaded)	-	-	-	180	Firing 2.75"FFAR	-	-	10/300	-	-	-	-	-	-	-	-
LAU-68A/A, (Empty)	-	-	-	180	Ejecting (Empty)	-	-	10/300	-	-	-	-	-	-	-	-
LAU-68B/A (Loaded)	-	-	-	180	Firing 2.75" FFAR	-	-	10/300	-	-	-	-	-	-	-	-
LAU-68B/A (Empty)	-	-	-	180	Ejecting (Empty)	-	-	10/300	-	-	-	-	-	-	-	-
LAU-5003(Loaded)	-	-	-	180	Firing 2.75" FFAR	-	-	10/300	-	-	-	-	-	-	-	-
LAU-5003(Empty)	-	-	-	180	Ejecting (Empty)	-	-	10/300	-	-	-	-	-	-	-	-
SUU-20A/A,B/A	-	0.9	7.33	180									500	0.8	0.8	1.5
w/BDU-33A/B					Dispensing BDU-33B/B	550	0.9	10/300	0.5	4.0	45°	60°				
w/MK-106					Dispensing MK-106	550	0.9	10/300	0.7	2.0	15°	30°				
w/2.75" FFAR					Firing 2.75" FFAR	400	0.8	10/300	0.5	2.0	15°	60°				
B43 A/C	A/C	A/C	5.5	180	Ejecting	550	0.95	10/300	0.8	4.0	45°	20°	SAR[9]	SAR	SAR	SAR
B57 A/C	A/C	A/C	5.5	180	Ejecting	550	0.95	10/300	0.8	4.0	45°	20°	SAR[9]	SAR	SAR	SAR
B61 A/C	A/C	A/C	5.5	180	Ejecting	550	0.95	10/300	0.8	4.0	45°	20°	SAR[9]	SAR	SAR	SAR
370 Gal Tank	600	1.6[6]	6.5	180[10]	Ejecting[7]	600	1.6[6]	10/300	0.7	2.0	15°	15°	600[7]	1.6[6]	0.7	2.0
600 Gal Tank	500	0.9	4.0[8]	TBD	N/R	N/R	N/R	10/300	N/R	N/R	N/R	N/R	350[7]	0.85	0.7	2.0
300 Gal Tank	600	1.6[6]	6.5	180[12]	Ejecting[7]	600	1.6[6]	10/300	0.7	2.0	15°	15°	600[7]	1.6[6]	0.7	2.0
ECM Pod	A/C	A/C	A/C	360	N/R	N/R	N/R	10/300	N/R	N/R	N/R	N/R	N/R	N/R	N/R	N/R
BRU Rack	550	1.5	A/C	180	Ejecting (Empty)	500	0.8	10/300	0.7	2.0	15°	15°	500	0.8	0.7	2.0

A/C - SAME AS AIRCRAFT CAPABILITY/LIMIT   N/R - NOT REQUIRED   SAR - SAME AS RELEASE

[1] Release refers to the separation of store from pylon or rack, except for 370 gallon tanks where it refers to separation of tank plus plyon from wing.

[2] Jettison refers to selective separation of store plus rack from pylon when stores are are carried on rack (full racks only - limits not applicable for hung weapons). Design goals.

[3] Limit for most restrictive load of store or store cluster.

[4] Aircraft design requirement as limited by GPAE S&R weapon capabilities.

[5] Firing load factor of 0.0 to 4.0g is intended as initial clearance.

[6] Requirement of 1.4 Mach, goal of 1.6.

[7] All fuel quantities.

[8] Function of fuel quantity. Min load factor of 4.0 with full tank; max load factor of 7.33 empty.

[9] Jettison only in accordance with Air Force Procedures.

[10] For fuel quantities less than 69% full, limit is 360 degrees.

[11] The limits are for maximum lateral command rolls checked to stop at the specified bank angle change.

[12] Full tank; 360°/sec permissible with partial fuel quantities.

TABLE 11.- F-16 INITIAL TAKEOFF STORE LOADINGS AND STORE CERTIFICATION CONFIGURATIONS

LOADING	TIP	BL 157	BL 120	BL 71	CENTERLINE	BL 71	BL 120	BL 157	TIP
1	AIM-9J	—	—	370TK	—	370TK	—	—	AIM-9J
2	AIM-9J	AIM-9J	—	370TK	ALQ-119-12	370TK	—	AIM-9J	AIM-9J
3	AIM-9J	—	ALQ-119-14	370TK	—	370TK	ALQ-119-14	—	AIM-9J
4	AIM-9J	—	ALQ-119-12	(6)MK-82	300TK	(6)MK-82		—	AIM-9J
5	AIM-9J	—	(3)MK-82	370TK	ALQ-119-12	370TK	(3)MK-82	—	AIM-9J
6	AIM-9J	—	(3)MK-82R	370TK	ALQ-119-12	370TK	(3)MK-82R	—	AIM-9J
7	AIM-9J	—	(1)MK-36	(4)MK-36	300TK	(4)MK-36	(1)MK-36	—	AIM-9J
8	AIM-9J	—	MK-84	370TK	ALQ-119-12	370TK	MK-84	—	AIM-9J
10	AIM-9J	—	(3)AGM-65	370TK	ALQ-119-12	370TK	(3)AGM-65	—	AIM-9J
11	AIM-9J	—	GBU-10A/B	370TK	ALQ-119-12	370TK	GBU-10A/B	—	AIM-9J
12	AIM-9J	—	GBU-8/B	370TK	ALQ-119-12	370TK	GBU-8/B	—	AIM-9J
14	AIM-9J	—	ALQ-119-12	(4)CBU-58/B	300TK	(4)CBU-58/B	(2)CBU-58/B	—	AIM-9J
15	AIM-9J	—	SUU-25C/A	370TK	ALQ-119-12	370TK	SUU-25C/A	—	AIM-9J
16	AIM-9J	—	(3)MK-20 Mod4	370TK	ALQ-119-12	370TK	(3)MK-20 Mod4	—	AIM-9J
18	AIM-9J	—	ALQ-119-12	370TK	B-57	370TK	—	—	AIM-9J
19	AIM-9J	—	ALQ-119-12	370TK	B-61	370TK	—	—	AIM-9J
20	Launcher	—	SUU-20B/A	370TK	—	370TK	SUU-20B/A	—	Launcher
21	Launcher	—	SUU-20B/A	370TK	—	370TK	SUU-20B/A	—	Launcher
22	Launcher	—	—	370TK	300TK	370TK	—	—	Launcher

LOADING	TIP	B.L. 157	B.L. 120	B.L. 71	CENTERLINE	B.L. 71	B.L. 120	B.L. 157	TIP
					AIR-TO-AIR				
29	AIM-9L	-	-	370 TK	-	370 TK	-	-	AIM-9L
30	AIM-9L	AIM-9L	-	370 TK	ALQ-119-12	370 TK	-	AIM-9L	AIM-9L
31	AIM-9L	-	ALQ-119-14	370 TK	-	370 TK	ALQ-119-14	-	AIM-9L
32	AIM-9L	-	ALQ-119-14	-	300 TK	-	-	-	AIM-9L
					AIR-TO-GROUND				
33	AIM-9L	-	ALQ-119-12	(6)MK-82	300 TK	(6)MK-82	-	-	AIM-9L
34	AIM-9L	-	(3) MK-82	370 TK	ALQ-119-12	370 TK	(3)MK-82	-	AIM-9L
35	AIM-9L	-	(3) MK-82R	370 TK	ALQ-119-12	370 TK	(3)MK-82R	-	AIM-9L
36	AIM-9L	-	(1) MK-82R	(4)MK-82R[6]	300 TK	(4)MK-82R[6]	(1)MK-82R	-	AIM-9L
37	AIM-9L	-	(1) MK-84	370 TK	ALQ-119-12	370 TK	(1)MK-84	-	AIM-9L
38	AIM-9L	-	(3) AGM-65	370 TK	ALQ-119-12	370 TK	(3)AGM-65	-	AIM-9L
39	AIM-9L	-	(1) GBU-10A/B	370 TK	ALQ-119-12	370 TK	(1)GBU10A/B	-	AIM-9L
40	AIM-9L	-	(1) GBU8/B	370 TK	ALQ-119-12	370 TK	(1)GBU-8/B	-	AIM-9L
41	AIM-9L	-	ALQ-119-12	(4)CBU-58/B[6]	300 TK	(4)CBU-58/B[6]	(2)CBU-58/B[6]	-	AIM-9L
42	AIM-9L	-	(1)SUU-25C/A[3]	370 TK	ALQ-119-12	370 TK	(1)SUU-25C/A[3]	-	AIM-9L
43	AIM-9L	-	(3)MK-20 MOD4	370 TK	ALQ-119-12	370 TK	(3)MK-20 MOD 4	-	AIM-9L
44	AIM-9L	-	ALQ-119-12	370 TK	B-57[6]	370 TK	-	-	AIM-9L
45	AIM-9L	-	ALQ-119-12	370 TK	B-61[6]	370 TK	-	-	AIM-9L

LOADING	TIP	B.L. 157	B.L. 120	B.L. 71	CENTERLINE	B.L. 71	B.L. 120	B.L. 157	TIP
					AIR-TO-AIR				
46	AIM 9J	AIM 9J	-	370 TK	ALQ-131	370 TK	-	AIM 9J	AIM 9J
47	AIM 9J	-	ALQ-131	370 TK	-	370 TK	ALQ-131	-	AIM 9J
48	AIM 9J	-	ALQ-131	-	300 TK	-	-	-	AIM 9J
					AIR-TO-GROUND				
49	AIM 9J	-	(3) MK 82	370 TK	ALQ 131	370 TK	(3) MK 82	-	AIM 9J
50	AIM 9J	-	(3) MK 82R	370 TK	ALQ 131	370 TK	(3) MK 82R	-	AIM 9J
51	AIM 9J	-	(1) MK 84	370 TK	ALQ 131	370 TK	(1) MK-84	-	AIM 9J
52	AIM 9J	-	(3) AGM 65	370 TK	ALQ 131	370 TK	(3) AGM-65	-	AIM 9J
53	AIM 9J	-	(1) GBU 10A/B	370 TK	ALQ 131	370 TK	(1) GBU-10A/B	-	AIM 9J
54	AIM 9J	-	(1) GBU-8/B	370 TK	ALQ 131	370 TK	(1) GBU-8/B	-	AIM 9J
55	AIM 9J	-	(1) SUU-25C/A	370 TK	ALQ-131	370 TK	(1) SUU-25C/A	-	AIM 9J
56	AIM 9J	-	(3) MK-20 MOD 4	370 TK	ALQ-131	370 TK	(3) MK-20 MOD 4	-	AIM 9J
57	AIM 9J	-	ALQ 131	370 TK	B57	370 TK	-	-	AIM 9J
58	AIM 9J	-	ALQ 131	370 TK	B61	370 TK	-	-	AIM 9J
59	AIM 9J	-	(3) MK-82	(3) MK-82	300 TK	(3) MK-82	ALQ-131	-	AIM 9J
					AIR-TO-AIR				
60	AIM 9L	AIM 9L	-	370 TK	ALQ-131	370 TK	-	AIM 9L	AIM 9L
61	AIM 9L	-	ALQ-131	370 TK	- -	370 TK	ALQ-131	-	AIM 9L
62	AIM 9L	-	ALQ-131	-	300 TK	-	-	-	AIM 9L
					AIR-TO-GROUND				
63	AIM 9L	-	(3) MK-82	370 TK	ALQ-131	370 TK	(3) MK-82	-	AIM 9L
64	AIM 9L	-	(3) MK-82R	370 TK	ALQ-131	370 TK	(3) MK-82R	-	AIM 9L
65	AIM 9L	-	(1) MK-84	370 TK	ALQ-131	370 TK	(1) MK-84	-	AIM 9L
66	AIM 9L	-	(3) AGM 65	370 TK	ALQ-131	370 TK	(3) AGM-65	-	AIM 9L
67	AIM 9L	-	(1) GBU-10A/B	370 TK	ALQ 131	370 TK	(1) GBU-10A/B	-	AIM 9L
68	AIM 9L	-	(1) GBU 8/B	370 TK	ALQ 131	370 TK	(1) GBU-8/B	-	AIM 9L
69	AIM 9L	-	(1) SUU 25C/A	370 TK	ALQ-131	370 TK	(1) SUU-25C/A	-	AIM 9L
70	AIM 9L	-	(3) MK 20 MOD 4	370 TK	ALQ 131	370 TK	(3) MK-20 MOD 4	-	AIM 9L
71	AIM 9L	-	ALQ 131	370 TK	B57	370 TK	-	-	AIM 9L
72	AIM 9L	-	ALQ 131	370 TK	B61	370 TK	-	-	AIM 9L
73	AIM 9L	-	(3) MK-82	(3) MK-82	300 TK	(3) MK-82	ALQ-131	-	AIM 9L

TABLE 12.- DESIGN LOAD CONDITIONS (GBU-8 CARRIAGE, STORE ALIGNED)

PX, PY, PZ N(LBS) MX, MZ, MY N-M (IN-LBS)
POSITIVE AFT, O/B, UP POSITIVE WTIP UP, NOSE UP, NOSE O/B

COND	PX	PY	PZ	MX	MZ	PSPRING	MY
1458-1.3L	368.(83.)	18335.(4122.)	-28415.(-6388.)	-1118.(-9898.)	-310.(-2740.)	-1371.(-308.)	1532.(13559.)
1458-1.3R	42.(9.)	12761.(2869.)	-74038.(-16645.)	-1494.(-13217.)	-1735.(-15357.)	-2926.(-658.)	3271.(28947.)
1439-3.1L	1752.(394.)	1014.(228.)	-10257.(-2306.)	-282.(-2497.)	224.(1978.)	-426.(-96.)	477.(4219.)
1439-3.1R	1743.(392.)	983.(221.)	-10418.(-2342.)	-285.(-2523.)	222.(1963.)	-426.(-96.)	476.(4212.)
1439-3.2L	1264.(284.)	881.(198.)	-11779.(-2648.)	-277.(-2449.)	216.(1915.)	-732.(-165.)	818.(7243.)
1439-3.2R	1256.(282.)	1068.(240.)	-11939.(-2684.)	-279.(-2473.)	218.(1929.)	-732.(-164.)	818.(7237.)
1439-3.3L	4388.(986.)	-1850.(-416.)	30305.(6813.)	384.(3399.)	-1380.(-12211.)	-122.(-28.)	137.(1211.)
1439-3.3R	4468.(1004.)	-2126.(-478.)	30535.(6865.)	405.(3584.)	-1355.(-11992.)	-103.(-23.)	115.(1020.)
1439-3.4L	3978.(894.)	-2024.(-455.)	30840.(6933.)	401.(3545.)	-1428.(-12638.)	-497.(-112.)	556.(4919.)
1439-3.4R	3986.(896.)	-2055.(-462.)	30995.(6968.)	412.(3648.)	-1424.(-12604.)	-484.(-109.)	541.(4783.)
1439-3.5L	4158.(935.)	-2180.(-490.)	31464.(7074.)	394.(3485.)	-1430.(-12653.)	-397.(-89.)	443.(3925.)
1439-3.5R	4159.(935.)	-1877.(-422.)	31454.(7072.)	414.(3665.)	-1411.(-12484.)	-364.(-82.)	407.(3604.)
1439-3.6L	1206.(271.)	747.(168.)	-10056.(-2261.)	-246.(-2173.)	181.(1598.)	-839.(-189.)	938.(8302.)
1439-3.6R	1194.(268.)	921.(207.)	-10297.(-2315.)	-251.(-2222.)	180.(1591.)	-838.(-188.)	937.(8293.)
1442-3.1L	-1772.(-398.)	6463.(1453.)	-57843.(-13004.)	-1051.(-9298.)	-1226.(-10848.)	-1464.(-329.)	1636.(14480.)
1442-3.1R	-1860.(-418.)	6485.(1458.)	-58229.(-13091.)	-1068.(-9455.)	-1277.(-11305.)	-1492.(-335.)	1667.(14756.)
1442-3.2L	-1852.(-416.)	6512.(1464.)	-58333.(-13114.)	-1048.(-9278.)	-1219.(-10787.)	-1482.(-333.)	1657.(14664.)
1442-3.2R	-1857.(-418.)	6392.(1437.)	-58401.(-13130.)	-1066.(-9436.)	-1259.(-11142.)	-1516.(-341.)	1695.(14999.)
1442-3.3L	2715.(610.)	1170.(263.)	-12010.(-2700.)	-338.(-2991.)	296.(2616.)	336.(76.)	-375.(-3322.)
1442-3.3R	2636.(593.)	1419.(319.)	-12165.(-2735.)	-351.(-3104.)	273.(2420.)	330.(74.)	-369.(-3267.)
1442-3.4L	1735.(390.)	1054.(237.)	-10934.(-2458.)	-276.(-2438.)	219.(1939.)	-408.(-92.)	456.(4033.)
1442-3.4R	1739.(391.)	903.(203.)	-10849.(-2439.)	-284.(-2511.)	209.(1846.)	-418.(-94.)	467.(4131.)
1442-3.5L	2352.(529.)	1005.(226.)	-10053.(-2260.)	-285.(-2523.)	234.(2067.)	29.(6.)	-32.(-283.)
1442-3.5R	2352.(529.)	1059.(238.)	-10048.(-2259.)	-296.(-2619.)	224.(1984.)	19.(4.)	-21.(-189.)
1442-3.6L	-1852.(-416.)	6512.(1464.)	-58333.(-13114.)	-1048.(-9278.)	-1219.(-10787.)	-1482.(-333.)	1657.(14664.)
1442-3.6R	-1857.(-418.)	6392.(1437.)	-58401.(-13130.)	-1066.(-9436.)	-1259.(-11142.)	-1516.(-341.)	1695.(14999.)
1444-1.1L	1734.(390.)	1708.(384.)	-6306.(-1418.)	-216.(-1907.)	-2253.(-19935.)	-2840.(-639.)	3175.(28095.)
1444-1.1R	3785.(851.)	5062.(1138.)	26740.(6012.)	68.(600.)	-299.(-2648.)	-588.(-132.)	657.(5814.)
1444-1.2L	1817.(408.)	33827.(7605.)	-5117.(-1151.)	-42.(-369.)	-1618.(-14323.)	-1944.(-437.)	2173.(19230.)
1444-1.2R	1937.(436.)	32697.(7351.)	-6269.(-1409.)	-966.(-8547.)	120.(1062.)	-1043.(-235.)	1166.(10321.)
1444-1.3L	3279.(737.)	17107.(3846.)	22414.(5039.)	322.(2851.)	-415.(-3677.)	-396.(-89.)	442.(3914.)
1444-1.3R	975.(219.)	10315.(2319.)	-25379.(-5706.)	-1025.(-9071.)	-1136.(-10057.)	-2938.(-661.)	3284.(29062.)
1445-1.1L	1317.(296.)	3647.(820.)	-27220.(-6120.)	-727.(-6435.)	-1468.(-12988.)	-3395.(-763.)	3795.(33587.)
1445-1.1R	1927.(433.)	8611.(1936.)	3445.(775.)	-355.(-3143.)	153.(1355.)	-665.(-149.)	743.(6575.)
1445-1.1L	934.(210.)	44471.(9998.)	-23970.(-5389.)	-446.(-3943.)	-1155.(-10224.)	-2314.(-520.)	2586.(22887.)
1445-1.2R	851.(191.)	44934.(10102.)	-24073.(-5412.)	-1330.(-11774.)	-34.(-297.)	-1249.(-281.)	1396.(12354.)
1445-1.3L	1892.(425.)	23828.(5357.)	7447.(1674.)	21.(190.)	6.(55.)	-415.(-93.)	464.(4109.)
1445-1.3R	447.(101.)	15626.(3513.)	-44812.(-10075.)	-1422.(-12587.)	-1253.(-11093.)	-3855.(-867.)	4309.(38132.)
1450-1.1L	221.(50.)	6814.(1532.)	-61652.(-13861.)	-1500.(-13278.)	-2710.(-23979.)	-5175.(-1164.)	5785.(51196.)
1450-1.1R	-926.(-208.)	12397.(2787.)	-35515.(-7984.)	-907.(-8024.)	-1252.(-11076.)	-760.(-171.)	849.(7515.)
1450-1.2L	-560.(-126.)	30887.(6944.)	-58059.(-13053.)	-1663.(-14713.)	-2251.(-19924.)	-4817.(-1083.)	5384.(47646.)
1450-1.2R	-1136.(-255.)	33707.(7578.)	-59464.(-13369.)	-1290.(-11420.)	-2047.(-18119.)	-295.(-66.)	330.(2922.)
1450-1.3L	-909.(-204.)	19602.(4407.)	-30433.(-6842.)	-1020.(-9024.)	-734.(-6493.)	-1446.(-325.)	1617.(14307.)
1450-1.3R	-298.(-67.)	14185.(3189.)	-73902.(-16615.)	-1396.(-12353.)	-2432.(-21520.)	-2657.(-597.)	2970.(26283.)
1453-2.1L	1711.(385.)	12090.(2718.)	-32635.(-7337.)	-2953.(-26130.)	-3487.(-30859.)	-6370.(-1432.)	7120.(63010.)
1453-2.1R	-1990.(-447.)	19398.(4361.)	-38837.(-8731.)	1028.(9100.)	1051.(9300.)	-1680.(-378.)	1878.(16619.)
1453-2.2L	-5975.(-1343.)	12606.(2834.)	-11749.(-2641.)	1615.(14289.)	-169.(-1495.)	-1630.(-366.)	1822.(16125.)
1453-2.2R	9637.(2167.)	-5765.(-1296.)	765.(172.)	-2708.(-23965.)	-3512.(-31080.)	-8107.(-1823.)	9062.(80197.)
1453-2.3L	1235.(278.)	9568.(2151.)	-13275.(-2985.)	1680.(14865.)	1777.(15729.)	-2169.(-488.)	2425.(21459.)
1453-2.3R	1351.(304.)	36.(8.)	-14394.(-3236.)	-3123.(-27637.)	-5574.(-49327.)	-9035.(-2031.)	10099.(89370.)
1453-2.4L	2926.(658.)	11903.(2676.)	-38482.(-8652.)	-3084.(-27291.)	-3741.(-33104.)	-7072.(-1590.)	7905.(69956.)
1453-2.4R	-3512.(-789.)	21608.(4858.)	-38774.(-8717.)	934.(8269.)	681.(6030.)	-1628.(-366.)	1820.(16105.)

TABLE 12.- (CONTINUED)

COND	PX	PY	PZ	MX.	MZ	PSPRING	MY
1456-1.1L	2103.(473.)	930.(209.)	-6718.(-1510.)	219.(1942.)	-4019.(-35563.)	-1432.(-322.)	1601.(14168.)
1456-1.1R	4934.(1109.)	3594.(808.)	26975.(6064.)	410.(3625.)	-1214.(-10741.)	-304.(-68.)	339.(3004.)
1456-1.2L	2527.(568.)	31430.(7066.)	-2463.(-554.)	438.(3874.)	-3665.(-32437.)	-738.(-166.)	825.(7300.)
1456-1.2R	2930.(659.)	30736.(6910.)	-5086.(-1143.)	-705.(-6242.)	-144.(-1274.)	-715.(-161.)	800.(7077.)
1456-1.3L	4870.(1095.)	15421.(3467.)	24932.(5605.)	813.(7199.)	-1790.(-15844.)	81.(18.)	-91.(-804.)
1456-1.3R	1193.(268.)	10769.(2421.)	-24234.(-5448.)	-616.(-5449.)	-1607.(-14225.)	-1702.(-383.)	1903.(16840.)
1457-1.1L	1528.(343.)	2242.(504.)	-28294.(-6361.)	-431.(-3817.)	-2193.(-19406.)	-2390.(-537.)	2671.(23641.)
1457-1.1R	3151.(708.)	6000.(1349.)	3302.(742.)	-181.(-1601.)	-83.(-735.)	-456.(-103.)	510.(4510.)
1457-1.2L	1943.(437.)	40561.(9119.)	-20858.(-4689.)	-81.(-718.)	-2729.(-24148.)	-1474.(-331.)	1648.(14583.)
1457-1.2R	1715.(386.)	41909.(9422.)	-20647.(-4642.)	-1205.(-10661.)	292.(2583.)	-929.(-209.)	1039.(9191.)
1457-1.3L	3592.(807.)	20434.(4594.)	9207.(2070.)	300.(2659.)	-692.(-6121.)	-166.(-37.)	186.(1645.)
1457-1.3R	474.(107.)	15079.(3390.)	-44196.(-9936.)	-1158.(-10247.)	-1078.(-9541.)	-2428.(-546.)	2713.(24013.)
1458-1.1L	440.(99.)	6432.(1446.)	-63227.(-14215.)	-1536.(-13591.)	-2046.(-18107.)	-4606.(-1035.)	5148.(45559.)
1458-1.1R	238.(53.)	11956.(2688.)	-35190.(-7911.)	-1054.(-9325.)	-474.(-4194.)	-647.(-145.)	723.(6395.)
1458-1.2L	-4.(-1.)	31870.(7165.)	-57264.(-12874.)	-1650.(-14606.)	-1981.(-17533.)	-4082.(-918.)	4563.(40377.)
1458-1.2R	-235.(-53.)	34178.(7684.)	-60786.(-13666.)	-1493.(-13217.)	-1312.(-11612.)	120.(27.)	-135.(-1192.)
1461-2.1L	1357.(305.)	17507.(3936.)	-34555.(-7769.)	-3635.(-32169.)	-4387.(-38819.)	-7465.(-1678.)	8344.(73845.)
1461-2.1R	-331.(-75.)	20639.(4640.)	-39646.(-8913.)	1364.(12067.)	940.(8320.)	-1270.(-286.)	1420.(12563.)
1461-2.2L	-6306.(-1418.)	11111.(2498.)	-11817.(-2657.)	2397.(21214.)	-1171.(-10361.)	-1255.(-282.)	1402.(12410.)
1461-2.2R	11608.(2610.)	-4519.(-1016.)	4841.(1088.)	-2990.(-26462.)	-5698.(-50425.)	-8915.(-2004.)	9965.(88189.)
1461-2.3L	1986.(447.)	8247.(1854.)	-13343.(-3000.)	2412.(21346.)	1254.(11101.)	-2047.(-460.)	2288.(20251.)
1461-2.3R	1900.(427.)	2669.(600.)	-15661.(-3521.)	-3628.(-32104.)	-7802.(-69046.)	-10303.(-2316.)	11517.(101922.)
1461-2.4L	3458.(778.)	15661.(3521.)	-40756.(-9163.)	-3724.(-32958.)	-4421.(-39120.)	-8073.(-1815.)	9024.(79861.)
1461-2.4R	-2675.(-602.)	23525.(5289.)	-39313.(-8838.)	1162.(10282.)	440.(3893.)	-1115.(-251.)	1246.(11030.)
1464-1.1L	1302.(293.)	827.(186.)	-6190.(-1392.)	186.(1650.)	-3146.(-27843.)	-840.(-189.)	939.(8309.)
1464-1.1R	3924.(882.)	3985.(896.)	26560.(5971.)	372.(3296.)	-1037.(-9174.)	-223.(-50.)	250.(2210.)
1464-1.2L	1587.(357.)	31376.(7054.)	-3936.(-885.)	314.(2781.)	-2514.(-22248.)	-365.(-82.)	408.(3608.)
1464-1.2R	2035.(458.)	31447.(7070.)	-2837.(-638.)	-648.(-5738.)	-171.(-1516.)	-650.(-146.)	727.(6430.)
1464-1.3L	3555.(799.)	17343.(3899.)	20869.(4692.)	616.(5447.)	-1240.(-10970.)	57.(13.)	-64.(-564.)
1464-1.3R	433.(97.)	12205.(2744.)	-23078.(-5188.)	-658.(-5824.)	-1353.(-11976.)	-1549.(-348.)	1732.(15328.)
1465-1.1L	888.(200.)	2091.(470.)	-26848.(-6036.)	-417.(-3689.)	-1503.(-13304.)	-1856.(-417.)	2075.(18359.)
1465-1.1R	1923.(432.)	6872.(1545.)	2930.(659.)	-195.(-1726.)	7.(62.)	-399.(-90.)	446.(3944.)
1465-1.2L	866.(195.)	43933.(9877.)	-20689.(-4651.)	-159.(-1404.)	-1659.(-14678.)	-861.(-194.)	962.(8515.)
1465-1.2R	1019.(229.)	45325.(10190.)	-20424.(-4592.)	-1110.(-9819.)	270.(2386.)	-760.(-171.)	850.(7518.)
1465-1.3L	2170.(488.)	24166.(5433.)	7134.(1604.)	167.(1479.)	-340.(-3007.)	-148.(-33.)	165.(1459.)
1465-1.3R	-53.(-12.)	17841.(4011.)	-41983.(-9439.)	-1135.(-10043.)	-1037.(-9175.)	-2368.(-532.)	2647.(23428.)
1466-1.1L	30.(7.)	7170.(1612.)	-61098.(-13736.)	-1482.(-13113.)	-2522.(-22316.)	-4116.(-925.)	4601.(40719.)
1466-1.1R	-1180.(-265.)	13126.(2951.)	-37491.(-8429.)	-1028.(-9097.)	-1739.(-15392.)	365.(82.)	-408.(-3614.)
1466-1.2L	-829.(-186.)	29566.(6647.)	-58311.(-13109.)	-1649.(-14594.)	-2292.(-20280.)	-3576.(-804.)	3997.(35372.)
1466-1.2R	-1314.(-295.)	31732.(7134.)	-60749.(-13658.)	-1432.(-12669.)	-2141.(-18946.)	1088.(245.)	-1216.(-10763.)
1466-1.3L	-1356.(-305.)	20225.(4547.)	-36620.(-8233.)	-1202.(-10640.)	-1273.(-11263.)	-804.(-181.)	899.(7954.)
1466-1.3R	-422.(-95.)	15097.(3394.)	-71631.(-16104.)	-1479.(-13086.)	-2552.(-22587.)	-1786.(-402.)	1996.(17667.)
1470-2.1L	1812.(407.)	16867.(3792.)	-34276.(-7706.)	-3028.(-26800.)	-4232.(-37449.)	-6280.(-1412.)	7020.(62122.)
1470-2.1R	-2843.(-639.)	21728.(4885.)	-42017.(-9446.)	990.(8763.)	756.(6688.)	-1609.(-362.)	1798.(15915.)
1470-2.2L	-6296.(-1415.)	10026.(2254.)	-6285.(-1413.)	2053.(18170.)	-928.(-8211.)	-1665.(-374.)	1861.(16469.)
1470-2.2R	10232.(2300.)	-5693.(-1280.)	6115.(1375.)	-2276.(-20146.)	-4675.(-41373.)	-7199.(-1618.)	8047.(71214.)
1470-2.3L	881.(198.)	7624.(1714.)	-14063.(-3162.)	1961.(17350.)	1481.(13105.)	-2521.(-567.)	2818.(24939.)
1470-2.3R	1103.(248.)	1868.(420.)	-16317.(-3668.)	-2982.(-26385.)	-6502.(-57539.)	-8795.(-1977.)	9831.(86999.)
1470-2.4L	2371.(533.)	17267.(3882.)	-39398.(-8858.)	-3151.(-27889.)	-4449.(-39374.)	-6630.(-1491.)	7411.(65584.)
1470-2.4R	-3843.(-864.)	24202.(5441.)	-42777.(-9617.)	862.(7627.)	527.(4663.)	-1576.(-354.)	1762.(15592.)
1562-3.1L	3974.(893.)	-338.(-76.)	-11310.(-2543.)	-14.(-122.)	-326.(-2886.)	-154.(-35.)	172.(1522.)
1562-3.1R	3952.(888.)	-98.(-22.)	-11705.(-2632.)	-39.(-343.)	-341.(-3016.)	-171.(-39.)	192.(1696.)
1562-3.2L	3673.(826.)	-285.(-64.)	-12829.(-2884.)	-11.(-98.)	-337.(-2979.)	-290.(-65.)	324.(2865.)
1562-3.2R	3739.(841.)	-187.(-42.)	-12825.(-2883.)	-34.(-298.)	-338.(-2992.)	-310.(-70.)	346.(3064.)
1562-3.3L	6778.(1524.)	-4150.(-933.)	29407.(6611.)	962.(8512.)	-2951.(-26118.)	1937.(436.)	-2166.(-19164.)
1562-3.3R	6867.(1544.)	-4421.(-994.)	29795.(6699.)	986.(8723.)	-2913.(-25778.)	1968.(442.)	-2200.(-19469.)
1562-3.4L	6305.(1417.)	-4492.(-1010.)	29954.(6734.)	1000.(8852.)	-3059.(-27072.)	1621.(364.)	-1811.(-16030.)

TABLE 12.- (CONTINUED)

COND	PX	PY	PZ	MX.	MZ	PSPRING	MY
1562-3.4R	6309.(1418.)	-4279.(-962.)	30028.(6751.)	1001.(8858.)	-3051.(-27003.)	1635.(368.)	-1828.(-16173.)
1562-3.5L	6393.(1437.)	-4186.(-941.)	31833.(7157.)	944.(8355.)	-2835.(-25088.)	1430.(321.)	-1598.(-14143.)
1562-3.5R	6407.(1440.)	-4252.(-956.)	32067.(7209.)	966.(8550.)	-2804.(-24817.)	1453.(327.)	-1624.(-14376.)
1562-3.6L	3482.(783.)	-587.(-132.)	-11252.(-2530.)	36.(318.)	-373.(-3299.)	-498.(-112.)	557.(4926.)
1562-3.6R	3468.(780.)	-267.(-60.)	-11485.(-2582.)	5.(41.)	-393.(-3478.)	-527.(-118.)	589.(5211.)
1565-3.1L	290.(65.)	6058.(1362.)	-61611.(-13851.)	-1229.(-10872.)	195.(1729.)	-1857.(-418.)	2076.(18374.)
1565-3.1R	385.(87.)	5845.(1314.)	-61045.(-13724.)	-1243.(-11000.)	182.(1609.)	-1889.(-425.)	2112.(18686.)
1565-3.2L	243.(55.)	5760.(1295.)	-62059.(-13952.)	-1215.(-10756.)	212.(1875.)	-1893.(-425.)	2116.(18722.)
1565-3.2R	225.(50.)	6085.(1368.)	-62372.(-14022.)	-1251.(-11070.)	179.(1585.)	-1931.(-434.)	2158.(19097.)
1565-3.3L	4956.(1114.)	383.(86.)	-14380.(-3233.)	-159.(-1411.)	-174.(-1543.)	588.(132.)	-658.(-5819.)
1565-3.3R	4814.(1082.)	471.(106.)	-14528.(-3266.)	-178.(-1574.)	-217.(-1920.)	570.(128.)	-638.(-5642.)
1565-3.4L	4028.(906.)	-320.(-72.)	-11120.(-2500.)	15.(134.)	-356.(-3151.)	-70.(-16.)	79.(695.)
1565-3.4R	4097.(921.)	-294.(-66.)	-11028.(-2479.)	-27.(-235.)	-379.(-3353.)	-117.(-26.)	131.(1160.)
1565-3.5L	4098.(921.)	-222.(-50.)	-10379.(-2333.)	-6.(-52.)	-343.(-3039.)	-63.(-14.)	70.(622.)
1565-3.5R	4173.(938.)	-320.(-72.)	-10215.(-2297.)	-23.(-206.)	-347.(-3070.)	-83.(-19.)	93.(820.)
1565-3.6L	243.(55.)	5760.(1295.)	-62059.(-13952.)	-1215.(-10756.)	212.(1875.)	-1893.(-425.)	2116.(18722.)
1565-3.6R	225.(50.)	6085.(1368.)	-62372.(-14022.)	-1251.(-11070.)	179.(1585.)	-1931.(-434.)	2158.(19097.)
1567-1.1L	3935.(885.)	1214.(273.)	-3361.(-756.)	135.(1196.)	-4707.(-41657.)	-1451.(-326.)	1622.(14350.)
1567-1.1R	6329.(1423.)	1646.(370.)	22714.(5107.)	461.(4076.)	-1030.(-9111.)	227.(51.)	-253.(-2243.)
1567-1.2L	4469.(1005.)	24050.(5407.)	-127.(-28.)	273.(2420.)	-5034.(-44546.)	-611.(-137.)	683.(6043.)
1567-1.2R	4701.(1057.)	23766.(5343.)	1412.(318.)	-276.(-2441.)	-125.(-1105.)	-265.(-59.)	296.(2617.)
1567-1.3L	6819.(1533.)	11022.(2478.)	21882.(4920.)	649.(5742.)	-1945.(-17212.)	721.(162.)	-806.(-7135.)
1567-1.3R	2853.(641.)	9181.(2064.)	-16232.(-3649.)	-282.(-2497.)	-1522.(-13472.)	-981.(-221.)	1097.(9707.)
1568-1.1L	3092.(695.)	3029.(681.)	-24900.(-5598.)	-503.(-4447.)	-3153.(-27899.)	-2873.(-646.)	3211.(28418.)
1568-1.1R	4714.(1060.)	4057.(912.)	-303.(-68.)	-133.(-1178.)	-188.(-1661.)	-349.(-78.)	390.(3452.)
1568-1.2L	3548.(798.)	31114.(6995.)	-19646.(-4417.)	-223.(-1973.)	-4161.(-36823.)	-1982.(-445.)	2215.(19602.)
1568-1.2R	3521.(792.)	31412.(7062.)	-18824.(-4232.)	-936.(-8283.)	342.(3023.)	-673.(-151.)	753.(6661.)
1568-1.3L	5300.(1192.)	16284.(3661.)	2951.(663.)	230.(2037.)	-825.(-7297.)	14.(3.)	-15.(-136.)
1568-1.3R	2074.(466.)	14078.(3165.)	-37919.(-8525.)	-953.(-8437.)	-669.(-5924.)	-1462.(-329.)	1634.(14459.)
1573-1.1L	1759.(395.)	7588.(1706.)	-60539.(-13610.)	-1590.(-14074.)	-2641.(-23371.)	-4743.(-1066.)	5302.(46921.)
1573-1.1R	2037.(458.)	9750.(2192.)	-38332.(-8618.)	-1097.(-9711.)	157.(1392.)	-1167.(-262.)	1304.(11543.)
1573-1.2L	1615.(363.)	26937.(6056.)	-55793.(-12543.)	-1745.(-15439.)	-2995.(-26505.)	-4756.(-1069.)	5316.(47043.)
1573-1.2R	1533.(345.)	27684.(6224.)	-57225.(-12865.)	-1449.(-12822.)	-174.(-1537.)	-1070.(-241.)	1196.(10588.)
1573-1.3L	2517.(566.)	14710.(3307.)	-32285.(-7258.)	-1108.(-9809.)	-459.(-4060.)	-1360.(-306.)	1520.(13451.)
1573-1.3R	1304.(293.)	12121.(2725.)	-68461.(-15391.)	-1400.(-12388.)	-759.(-6713.)	-2445.(-550.)	2734.(24191.)
1575-2.1L	4617.(1038.)	24224.(5446.)	-20483.(-4605.)	-3720.(-32924.)	-3612.(-31961.)	-6582.(-1480.)	7357.(65106.)
1575-1.1R	-676.(-152.)	28120.(6322.)	-55203.(-12411.)	1209.(10699.)	-1487.(-13155.)	-2491.(-560.)	2785.(24645.)
1575-2.2L	-5444.(-1224.)	14420.(3242.)	-21556.(-4846.)	2232.(19752.)	-1354.(-11982.)	-657.(-148.)	734.(6496.)
1575-2.2R	12722.(2860.)	-1735.(-390.)	-5703.(-1282.)	-4506.(-39879.)	8217.(72718.)	-10339.(-2324.)	11557.(102275.)
1575-2.3L	3739.(841.)	9154.(2058.)	-15314.(-3443.)	2609.(23087.)	904.(7998.)	-1300.(-292.)	1453.(12857.)
1575-2.3R	3476.(781.)	2291.(515.)	-11827.(-2659.)	-3957.(-35022.)	-9416.(-83325.)	-11085.(-2492.)	12391.(109653.)
1575-2.4L	5231.(1176.)	20834.(4684.)	-14312.(-3218.)	-3543.(-31356.)	-3561.(-31510.)	-6384.(-1435.)	7137.(63155.)
1575-2.4R	-804.(-181.)	25594.(5754.)	-53542.(-12037.)	1177.(10413.)	-2084.(-18439.)	-2850.(-641.)	3185.(28189.)
1578-3.1L	2597.(584.)	156.(35.)	-10482.(-2357.)	-83.(-738.)	-158.(-1399.)	-144.(-32.)	161.(1421.)
1578-3.1R	2592.(583.)	142.(32.)	-10562.(-2374.)	-85.(-754.)	-158.(-1400.)	-144.(-32.)	161.(1421.)
1578-3.2L	2235.(502.)	85.(19.)	-12170.(-2736.)	-70.(-623.)	-165.(-1464.)	-342.(-77.)	383.(3387.)
1578-3.2R	2234.(502.)	156.(35.)	-12166.(-2735.)	-84.(-744.)	-176.(-1558.)	-356.(-80.)	397.(3517.)
1578-3.3L	5296.(1191.)	-3305.(-743.)	28428.(6391.)	765.(6768.)	-2609.(-23092.)	1832.(412.)	-2048.(-18123.)
1578-3.3R	5305.(1193.)	-3354.(-754.)	28576.(6425.)	783.(6928.)	-2602.(-23031.)	1852.(416.)	-2071.(-18323.)
1578-3.4L	4920.(1106.)	-3563.(-801.)	29626.(6660.)	808.(7151.)	-2789.(-24680.)	1620.(364.)	-1811.(-16026.)
1578-3.4R	4920.(1106.)	-3354.(-754.)	29618.(6659.)	809.(7156.)	-2793.(-24717.)	1628.(366.)	-1820.(-16106.)
1578-3.5L	4788.(1076.)	-3407.(-766.)	30021.(6749.)	795.(7038.)	-2783.(-24626.)	1499.(337.)	-1676.(-14833.)
1578-3.5R	4863.(1093.)	-3465.(-779.)	30166.(6782.)	811.(7181.)	-2763.(-24449.)	1519.(342.)	-1698.(-15029.)
1578-3.6L	2083.(468.)	-40.(-9.)	-10078.(-2266.)	-36.(-321.)	-210.(-1856.)	-499.(-112.)	557.(4932.)
1578-3.6R	2141.(481.)	-80.(-18.)	-10241.(-2302.)	-40.(-356.)	-196.(-1739.)	-499.(-112.)	557.(4931.)
1581-3.1L	-1176.(-264.)	7086.(1593.)	-61170.(-13752.)	-1275.(-11280.)	-987.(-8471.)	-1898.(-810.)	1887.(16781.)

TABLE 12.- (CONTINUED)

COND	PX	PY	PZ	MX.	MZ	PSPRING	MY
1581-3.1R	-4102.(-248.)	7019.(1578.)	-61008.(-13716.)	-1295.(-11462.)	-977.(-8645.)	-1417.(-319.)	1584.(14016.)
1581-3.2L	-1213.(-273.)	7192.(1617.)	-61990.(-13937.)	-1276.(-11288.)	-963.(-8525.)	-1360.(-306.)	1520.(13449.)
1581-3.2R	-1068.(-240.)	6912.(1554.)	-61751.(-13883.)	-1294.(-11451.)	-971.(-8590.)	-1383.(-311.)	1546.(13681.)
1581-3.3L	3461.(778.)	658.(148.)	-14625.(-3288.)	-199.(-1761.)	-59.(-521.)	596.(134.)	-666.(-5897.)
1581-3.3R	3399.(764.)	618.(139.)	-14546.(-3270.)	-185.(-1636.)	-62.(-551.)	609.(137.)	-681.(-6025.)
1581-3.4L	2585.(581.)	138.(31.)	-10832.(-2435.)	-63.(-556.)	-181.(-1602.)	-96.(-22.)	107.(949.)
1581-3.4R	2659.(598.)	40.(9.)	-10671.(-2399.)	-79.(-697.)	-183.(-1621.)	-119.(-27.)	133.(1173.)
1581-3.5L	2698.(607.)	209.(47.)	-10614.(-2386.)	-77.(-685.)	-167.(-1479.)	-30.(-7.)	33.(295.)
1581-3.5R	2773.(623.)	80.(18.)	-10453.(-2350.)	-88.(-776.)	-164.(-1448.)	-44.(-10.)	49.(435.)
1581-3.6L	-1176.(-264.)	7086.(1593.)	-61170.(-13752.)	-1275.(-11280.)	-957.(-8471.)	-1393.(-313.)	1557.(13781.)
1581-3.6R	-1102.(-248.)	7019.(1578.)	-61008.(-13716.)	-1295.(-11462.)	-977.(-8645.)	-1417.(-319.)	1584.(14016.)
1583-1.1L	2367.(532.)	890.(200.)	-6241.(-1403.)	146.(1296.)	-3533.(-31267.)	-693.(-156.)	775.(6854.)
1583-1.1R	4962.(1116.)	3438.(773.)	24575.(5525.)	383.(3387.)	-804.(-7118.)	161.(36.)	-180.(-1592.)
1583-1.2L	2921.(657.)	29455.(6622.)	157.(35.)	271.(2402.)	-3253.(-28784.)	327.(73.)	-365.(-3230.)
1583-1.2R	3360.(755.)	29161.(6556.)	104.(23.)	-364.(-3220.)	-25.(-219.)	-244.(-55.)	273.(2416.)
1583-1.3L	5124.(1152.)	15034.(3380.)	23328.(5245.)	583.(5155.)	-1423.(-12595.)	674.(152.)	-754.(-6670.)
1583-1.3R	1540.(346.)	11200.(2518.)	-18832.(-4234.)	-437.(-3866.)	-1579.(-13973.)	-1239.(-279.)	1385.(12254.)
1584-1.1L	1816.(408.)	2019.(454.)	-26581.(-5976.)	-446.(-3946.)	-2103.(-18609.)	-1994.(-448.)	2229.(19725.)
1584-1.1R	3172.(713.)	5827.(1310.)	1436.(323.)	-155.(-1374.)	-58.(-513.)	-315.(-71.)	352.(3118.)
1584-1.2L	2209.(497.)	39458.(8871.)	-18242.(-4101.)	-181.(-1600.)	-2511.(-22221.)	-714.(-161.)	799.(7067.)
1584-1.2R	2221.(499.)	41429.(9314.)	-16932.(-3807.)	-882.(-7806.)	368.(3255.)	-524.(-118.)	586.(5183.)
1584-1.3L	3731.(839.)	20661.(4645.)	6510.(1464.)	142.(1261.)	-554.(-4899.)	-82.(-18.)	92.(813.)
1584-1.3R	703.(158.)	16484.(3706.)	-40390.(-9081.)	-1013.(-8962.)	-1123.(-9934.)	-2027.(-456.)	2266.(20054.)
1589-1.1L	756.(170.)	7001.(1574.)	-61685.(-13868.)	-1521.(-13456.)	-1970.(-17430.)	-3959.(-890.)	4426.(39166.)
1589-1.1R	221.(50.)	11916.(2679.)	-36534.(-8214.)	-1048.(-9277.)	-653.(-5780.)	-887.(-199.)	992.(8777.)
1589-1.2L	253.(57.)	30255.(6802.)	-58523.(-13157.)	-1714.(-15164.)	-1860.(-16464.)	-3545.(-797.)	3962.(35066.)
1589-1.2R	-150.(-34.)	33173.(7458.)	-59475.(-13371.)	-1460.(-12921.)	-1418.(-12546.)	3.(1.)	-3.(-31.)
1589-1.3L	185.(42.)	20012.(4499.)	-34417.(-7738.)	-1212.(-10726.)	-572.(-5063.)	-1484.(-334.)	1659.(14682.)
1589-1.3R	303.(68.)	15595.(3506.)	-71949.(-16176.)	-1494.(-13220.)	-1494.(-13220.)	-2575.(-579.)	2878.(25471.)
1591-2.1L	3171.(713.)	11983.(2694.)	-18082.(-4065.)	-3089.(-27334.)	-3845.(-34023.)	-6399.(-1439.)	7153.(63299.)
1591-2.1R	-1258.(-283.)	16324.(3670.)	-46061.(-10356.)	1522.(13473.)	791.(6998.)	-1491.(-335.)	1667.(14754.)
1591-2.2L	-5227.(-1175.)	11694.(2629.)	-19572.(-4400.)	2143.(18963.)	-543.(-4804.)	-1472.(-331.)	1645.(14560.)
1591-2.2R	10058.(2261.)	-4257.(-957.)	-1256.(-282.)	-2894.(-25612.)	-5575.(-49336.)	-8424.(-1894.)	9416.(83329.)
1591-2.3L	2373.(534.)	8714.(1959.)	-11795.(-2652.)	2281.(20185.)	1176.(10410.)	-1985.(-446.)	2219.(19639.)
1591-2.3R	2224.(500.)	-463.(-104.)	-11447.(-2573.)	-3121.(-27619.)	-7663.(-67815.)	-9101.(-2046.)	10173.(90024.)
1591-2.4L	2978.(670.)	13704.(3081.)	-23520.(-5288.)	-3240.(-28671.)	-4083.(-36131.)	-6763.(-1521.)	7560.(66904.)
1591-2.4R	-1499.(-337.)	18704.(4205.)	-47618.(-10706.)	1455.(12875.)	827.(7318.)	-1548.(-348.)	1730.(15312.)
1594-1.1L	1340.(301.)	2033.(457.)	-6502.(-1462.)	140.(1237.)	-2788.(-24673.)	-134.(-30.)	149.(1321.)
1594-1.1R	3858.(867.)	5444.(1224.)	24625.(5536.)	308.(2725.)	-692.(-6123.)	120.(27.)	-134.(-1186.)
1594-1.2L	1774.(399.)	29343.(6597.)	-863.(-194.)	198.(1755.)	-2227.(-19705.)	547.(123.)	-612.(-5412.)
1594-1.2R	2483.(558.)	29499.(6632.)	1920.(432.)	-360.(-3185.)	-112.(-990.)	-268.(-60.)	300.(2652.)
1594-1.3L	3776.(849.)	17743.(3989.)	20764.(4668.)	468.(4140.)	-1044.(-9238.)	636.(143.)	-711.(-6294.)
1594-1.3R	681.(153.)	13357.(3003.)	-17542.(-3944.)	-462.(-4092.)	-1263.(-11176.)	-996.(-224.)	1113.(9850.)
1595-1.1L	1008.(227.)	1850.(416.)	-26113.(-5871.)	-434.(-3838.)	-1370.(-12125.)	-1479.(-333.)	1653.(14632.)
1595-1.1R	1915.(430.)	6752.(1518.)	1441.(324.)	-157.(-1387.)	30.(265.)	-263.(-59.)	294.(2603.)
1595-1.2L	1031.(232.)	43759.(9838.)	-17740.(-3988.)	-223.(-1969.)	-1515.(-13408.)	-228.(-51.)	255.(2260.)
1595-1.2R	1399.(315.)	45939.(10328.)	-15662.(-3521.)	-795.(-7035.)	372.(3296.)	-389.(-87.)	434.(3845.)
1595-1.3L	2535.(570.)	25821.(5805.)	6936.(1559.)	68.(600.)	-318.(-2817.)	-49.(-11.)	55.(482.)
1595-1.3R	-37.(-8.)	20745.(4664.)	-37941.(-8530.)	-946.(-8372.)	-900.(-7963.)	-1690.(-380.)	1889.(16719.)
1597-1.1L	470.(106.)	8429.(1895.)	-59236.(-13317.)	-1577.(-13954.)	-2696.(-23856.)	-4042.(-909.)	4518.(39980.)
1597-1.1R	-1480.(-333.)	13842.(3112.)	-39998.(-8992.)	-1263.(-11177.)	-2446.(-21643.)	965.(217.)	-1078.(-9541.)
1597-1.2L	-683.(-153.)	25905.(5824.)	-60167.(-13527.)	-1593.(-14098.)	-2552.(-22586.)	-2493.(-561.)	2787.(24663.)
1597-1.2R	-1464.(-329.)	27400.(6160.)	-60702.(-13647.)	-1641.(-14519.)	-2390.(-21152.)	1071.(241.)	-1197.(-10594.)
1597-1.3L	-1473.(-331.)	19389.(4359.)	-46841.(-10531.)	-1438.(-12728.)	-2389.(-21144.)	453.(102.)	-506.(-4481.)
1597-1.3R	-274.(-62.)	16564.(3724.)	-66440.(-14937.)	-1623.(-14364.)	-2718.(-24050.)	-1858.(-418.)	2077.(18380.)

TABLE 12.- (CONCLUDED)

COND	PX	PY	PZ	MX.	MZ	PSPRING	MY
1599-2.1L	4229.(951.)	10528.(2367.)	-14363.(-3229.)	-2464.(-21809.)	-3325.(-29426.)	-5653.(-1271.)	6318.(55915.)
1599-2.1R	-4160.(-935.)	16146.(3630.)	-46226.(-10393.)	1139.(10081.)	465.(4116.)	-2039.(-458.)	2279.(20167.)
1599-2.2L	-5768.(-1297.)	10373.(2332.)	-18107.(-4071.)	1699.(15036.)	-379.(-3352.)	-1870.(-420.)	2091.(18500.)
1599-2.2R	8660.(1947.)	-4742.(-1066.)	-271.(-61.)	-2202.(-19491.)	-4119.(-36452.)	-6757.(-1519.)	7553.(66844.)
1599-2.3L	1316.(296.)	7802.(1754.)	-11477.(-2580.)	1835.(16236.)	1277.(11296.)	-2417.(-543.)	2702.(23914.)
1599-2.3R	1235.(278.)	-1170.(-263.)	-11745.(-2640.)	-2467.(-21830.)	-6148.(-54405.)	-7526.(-1692.)	8413.(74449.)
1599-2.4L	4077.(917.)	12388.(2785.)	-19696.(-4428.)	-2582.(-22845.)	-3502.(-30987.)	-5853.(-1316.)	6542.(57898.)
1599-2.4R	-4543.(-1021.)	18748.(4215.)	-48461.(-10895.)	1073.(9494.)	436.(3858.)	-2104.(-473.)	2352.(20813.)
1602-1.1L	788.(177.)	2224.(500.)	-3607.(-811.)	138.(1222.)	-2185.(-19334.)	194.(44.)	-217.(-1923.)
1602-1.1R	2973.(668.)	5502.(1237.)	22758.(5117.)	256.(2267.)	-675.(-5976.)	145.(33.)	-162.(-1432.)
1602-1.2L	1071.(241.)	24362.(5477.)	1052.(237.)	175.(1551.)	-1500.(-13273.)	518.(116.)	-579.(-5121.)
1602-1.2R	1762.(396.)	23374.(5255.)	2269.(510.)	-291.(-2573.)	-242.(-2145.)	-259.(-58.)	289.(2560.)
1602-1.3L	2530.(569.)	16555.(3722.)	15247.(3428.)	342.(3028.)	-770.(-6811.)	486.(109.)	-543.(-4810.)
1602-1.3R	398.(89.)	13090.(2943.)	-11345.(-2551.)	-407.(-3598.)	-1024.(-9058.)	-777.(-175.)	869.(7690.)
1603-1.1L	579.(130.)	2397.(539.)	-23324.(-5244.)	-444.(-3930.)	-850.(-7519.)	-1244.(-280.)	1391.(12310.)
1603-1.1R	887.(200.)	6792.(1527.)	-583.(-131.)	-172.(-1522.)	11.(99.)	-247.(-56.)	276.(2443.)
1603-1.2L	66.(15.)	40606.(9129.)	-15934.(-3582.)	-271.(-2400.)	-873.(-7722.)	-153.(-34.)	171.(1516.)
1603-1.2R	1072.(241.)	41255.(9275.)	-14454.(-3250.)	-662.(-5857.)	371.(3282.)	-274.(-62.)	306.(2712.)
1603-1.3L	1262.(284.)	26639.(5989.)	2443.(549.)	-6.(-56.)	-61.(-541.)	-29.(-6.)	32.(283.)
1603-1.3R	-138.(-31.)	22196.(4990.)	-30672.(-6896.)	-828.(-7323.)	-632.(-5592.)	-1364.(-307.)	1525.(13493.)
1605-1.1L	-578.(-130.)	9238.(2077.)	-55173.(-12404.)	-1194.(-10563.)	-2460.(-21771.)	-2602.(-585.)	2909.(25740.)
1605-1.1R	-2100.(-472.)	11173.(2512.)	-46033.(-10349.)	-1222.(-10812.)	-2661.(-23549.)	185.(42.)	-207.(-1833.)
1605-1.2L	-1678.(-377.)	16733.(3762.)	-57763.(-12986.)	-1109.(-9812.)	-2444.(-21631.)	-948.(-213.)	1059.(9375.)
1605-1.2R	-1772.(-398.)	16818.(3781.)	-57817.(-12998.)	-1357.(-12006.)	-3041.(-26909.)	-127.(-29.)	142.(1259.)
1605-1.3L	-2169.(-488.)	14287.(3212.)	-52177.(-11730.)	-1071.(-9481.)	-2320.(-20527.)	507.(114.)	-567.(-5019.)
1605-1.3R	-964.(-217.)	13148.(2956.)	-59413.(-13357.)	-1260.(-11155.)	-2681.(-23729.)	-1219.(-274.)	1362.(12056.)
1607-2.1L	3325.(748.)	11543.(2595.)	-13947.(-3135.)	-1893.(-16750.)	-2897.(-25635.)	-4031.(-906.)	4506.(39872.)
1607-2.1R	-4194.(-943.)	15777.(3547.)	-40521.(-9110.)	677.(5990.)	154.(1366.)	-1947.(-438.)	2176.(19261.)
1607-2.2L	-5090.(-1144.)	9425.(2119.)	-15436.(-3470.)	1237.(10951.)	-94.(-836.)	-1962.(-441.)	2193.(19408.)
1607-2.2R	6309.(1418.)	-3816.(-858.)	-6596.(-1483.)	-1824.(-16142.)	-3325.(-29423.)	-5783.(-1300.)	6464.(57207.)
1607-2.3L	521.(117.)	6414.(1442.)	-11950.(-2687.)	1363.(12064.)	1198.(10606.)	-2411.(-542.)	2695.(23850.)
1607-2.3R	497.(112.)	-525.(-118.)	-12504.(-2811.)	-1962.(-17360.)	-4875.(-43146.)	-6220.(-1398.)	6953.(61531.)
1607-2.4L	3816.(858.)	9448.(2124.)	-10597.(-2382.)	-1797.(-15907.)	-2546.(-22530.)	-4221.(-949.)	4718.(41755.)
1607-2.4R	-4413.(-992.)	13936.(3133.)	-39329.(-8842.)	714.(6322.)	124.(1095.)	-1957.(-440.)	2187.(19355.)
ARR LDG 120	-45711.(-10277.)	-11151.(-2507.)	-47179.(-10607.)	-155.(-1369.)	-701.(-6203.)	27242.(6124.)	-30451.(*******)
ARR LDG 4CF	-43662.(-9816.)	11076.(2490.)	20992.(4719.)	-333.(-2950.)	4473.(39580.)	-7613.(-1712.)	8510.(75311.)
ARR LDG 2GA	20562.(4623.)	-11076.(-2490.)	-31338.(-7045.)	333.(2950.)	-4473.(-39580.)	8079.(1816.)	-9031.(-79921.)

TABLE 13.- LINK JOINT MARGINS OF SAFETY

COMPONENT	GBU-8 LOADING	NON-GBU-8 LOADING
FWD LINK JOINT UPPER PIN	+1.28	+0.36
FWD LINK JOINT LOWER PIN	+1.80	+0.47
FWD LINK JOINT UPPER LUG	+1.22	+0.47
FWD LINK JOINT LOWER LUG	+1.36	+0.38
FWD LINK JOINT SIDE PLATE LUG	+1.68	+0.45
FWD LINK JOINT STRONG BACK LUG	+0.73	+0.06
FWD LINK JOINT STRONG BACK BUSHING	+1.84	+0.73
FWD LINK JOINT SIDE PLATE BUSHING	+1.95	+0.59
AFT LINK JOINT UPPER PIN	+0.88	+0.29
AFT LINK JOINT LOWER PIN	+1.09	+0.34
AFT LINK JOINT UPPER LUG	+0.49	+0.02
AFT LINK JOINT LOWER LUG	+0.69	+0.08
AFT LINK JOINT SIDE PLATE LUG	+0.97	+0.26
AFT LINK JOINT STRONG BACK LUG	+0.79	+0.23
AFT LINK JOINT STRONG BACK BUSHING	+3.07	+1.80
AFT LINK JOINT SIDE PLATE BUSHING	+0.77	+0.14

TABLE 14.- STRONGBACK MARGINS OF SAFETY

CROSS SECTION	GBU-8 LOADING	NON-GBU-8 LOADING
BETWEEN LINKS	+1.95	+0.45
BETWEEN LINKS AT SWAY BRACE	+1.97	+0.63
AT AFT LINK	+1.61	+0.27
BETWEEN FWD AND AFT WING ATTACHMENT POINTS	+0.68	+0.06
AFT OF AFT WING ATTACHMENT	+0.92	+0.35
FWD OF ALIGNMENT ATTACHMENT	+0.12	-
AT THE ALIGNMENT ATTACHMENT	HIGH	+0.06

TABLE 15.- SIDE PLATE MARGINS OF SAFETY

CROSS SECTION	GBU-8 LOADING	NON-GBU-8 LOADING
AT FWD LINK	+2.21	+0.51
AT AFT LINK	+3.97	+0.79
SPRING ATTACHMENT	+1.07	
AT FWD SPRING ATTACHMENT BOLT	+0.82	
DAMPER ATTACHMENT	+1.21	

TABLE 16.- SPRING MARGINS OF SAFETY

COMPONENT	MARGIN
SUPPORT PINS (SHEAR)	+1.00
FORWARD PIN BENDING	+0.07
AFT PIN BENDING	+0.23
FORWARD LUG	+0.59
AFT LUG	+1.14
BALL SCREW BUSHING	HIGH
BALL SCREW LUG (BEARING)	HIGH
BALL SCREW (TRANSVERSE)	+2.64

TABLE 17.- BALL SCREW NUT MARGINS OF SAFETY

COMPONENT	MARGIN
ATTACHMENT LUGS	+3.57
BUSHING	+1.32
NUT BASE	+0.09
PIN	+0.53
SAGINAW (TENSION)	+0.00
SAGINAW (COMPRESSION)	+2.21
THREADS	+0.26

TABLE 18.- ALIGNMENT GEAR BOX MARGINS OF SAFETY

COMPONENT	MARGIN
GEAR BOX THRUST BEARING	+0.67
BEARING RETAINER (TOP)	+0.03
HOUSING TO STRONG BACK LUG	HIGH
HOUSING TO STRONG BACK BUSHING	HIGH
HOUSING TO SCREW (LOWER BEARING)	HIGH
HOUSING TO SCREW (LOWER LUG)	HIGH
THRUST BEARING TO HOUSING FLANGE (UPPER)	+1.92
SHAFT NO. 1	HIGH
SHAFT NO. 2	HIGH
SHAFT NO. 3	HIGH
SHAFT NO. 4	+0.11

TABLE 19.- DAMPER MARGINS OF SAFETY

COMPONENT	MARGIN
ROD END LINK	+0.12
ROD END THREAD (SHEAR)	+3.01
ROD END THREAD (TENSION)	+0.79
ROD END BOLT (SHEAR)	+1.26
ROD END BOLT (BENDING)	+0.02
DAMPER PISTON THREAD (SHEAR)	+4.46
DAMPER PISTON THREAD (TENSION)	+0.78
CYLINDER END CAP	+0.08
CYLINDER CLEVIS LUGS	+0.04
CLEVIS PIN (SHEAR)	+1.01
CLEVIS PIN (BENDING)	+0.38
FORWARD LINK LUG TO DAMPER (TRANSVERSE LOAD)	+0.05
FORWARD LINK LUG TO DAMPER (BENDING)	+0.22
LOWER DAMPER MOUNT LUG	HIGH
LOWER DAMPER MOUNT LUG (BUSHING)	HIGH
LOWER DAMPER MOUNT LUG (TRANSVERSE LOAD)	+3.70
DAMPER MOUNT TO SIDE PLATE (VERTICAL LOAD)	+3.02
DAMPER MOUNT TO SIDE PLATE BOLT	+0.28
DAMPER MOUNT TO SIDE PLATE (SIDE LOAD)	+0.22

TABLE 20.- DECOUPLER PYLON GROUND TESTS

Test		Environments	Purpose of Test
Damper Component	Damper Cylinder	$-65^{o}F$, RT, $+160^{o}F$	Determine damping characteristics and confirm orifice design.
Pylon Alignment System Operation	Structurally and functionally complete pylon with dummy store (GBU-8)	R.T.*	Determine dynamic response of pylon alignment system to misalignment.
Pylon Proof	Structurally complete pylon	R.T.	Assure structural integrity by application of critical combinations of 110% of GBU-8 limit design loads.
Pylon Influence Coefficients	Structurally complete pylon	R.T.	Verify stiffness characteristics employed in analysis and determine free play.
Pylon Ground Vibration	Complete pylon with dummy store (GBU-8)	R.T.	Determine natural frequencies, mode shapes, and modal damping.
Store Ejection	Structurally and functionally complete pylon with ejectable dummy store (GBU-8)	R.T.	Select MAU-12-C/A orifices that will assure adequate flight ejection characteristics for GBU-8 store.
Flight Loads Instrumentation Calibration	Alignment springs for both pylons	R.T.	Obtain calibration constants to allow determination of flight loads.

*R.T. - Room Temperature

TABLE 21.- DAMPER PISTON VELOCITY - CM/SEC (IN/SEC)

		DAMPER 1 ORIFICE = .14cm(.055 in.)		DAMPER 1 BEFORE RE-WORK ORIFICE = .11cm(.045 in.)		DAMPER 1 AFTER RE-WORK ORIFICE = .11cm(.045 in.)		DAMPER 2 ORIFICE = .11cm(.045 in.)		DAMPER 3 ORIFICE = .11cm(.045 in.)	
TEMPERATURE °C (°F)	LOAD N (lbs)	TENSION	COMPRESSION	TENSION	COMPRESSION	TENSION	COMPRESSION	TENSION	COMPRESSION	TENSION	COMPRESSION
21(70)	267(60)	1.83(.722)	1.94(.763)	1.24(.490)	1.30(.513)	1.56(.615)	1.575(.62)	1.51(.595)	1.45(.57)	.99(.39)	NO DATA
21(70)	378(85)	2.59(1.02)	2.55(1.003)	1.88(.740)	1.77(.695)	1.99(.785)	2.0(.79)	1.94(.765)	1.86(.732)	1.61(.635)	TAKEN
21(70)	489(110)	3.04(1.195)	2.96(1.167)	2.15(.845)	2.13(.840)	2.34(.92)	-	2.3(.905)	2.26(.89)	2.08(.82)	
21(70)	600(135)	-	-	2.39(.940)	-	2.65(1.045)	-	2.74(1.08)	2.58(1.015)	2.41(.95)	
21(70)	712(160)	-	-	-	-	2.93(1.155)	-	2.92(1.15)	-	2.73(1.075)	
21(70)	823(185)	-	-	-	-	-	-	-	-	-	
-54(-65)	267(60)	NO DATA	NO DATA	NO	NO DATA	.10(.04)	NO DATA	.254(.10)	.157(.062)	-	
-54(-65)	378(85)	TAKEN	TAKEN	MOVEMENT	TAKEN	.19(.074)	TAKEN	.315(.124)	.236(.093)	.254(.1)	
-54(-65)	489(110)					.26(.102)		.394(.155)	.340(.134)	.414(.163)	
-54(-65)	600(135)					.30(.118)		-	.46(.18)	.584(.23)	
-54(-65)	712(160)			DAMPER		-		.737(.29)	-	.795(.313)	
-54(-65)	823(185)			FROZEN		.44(.175)		-	.572(.225)	.98(.385)	
-54(-65)	934(210)					.48(.188)		-	-	1.07(.42)	
71(160)	267(60)					1.62(.638)		1.63(.64)	1.69(.665)	NO DATA	
71(160)	378(85)					2.11(.830)		2.07(.815)	2.12(835)	TAKEN	
71(160)	489(110)			NO DATA		2.49(.980)		2.43(.955)	2.48(.975)		
71(160)	600(135)			TAKEN		2.79(1.10)		2.78(1.095)	2.80(1.105)		
71(160)	712(160)					3.09(1.215)		3.02(1.19)	-		
71(160)	823(185)					-		-	-		

C-2

C-2

TABLE 22.- ALIGNMENT SYSTEM OPERATION TEST LOADS

TEST NUMBER	PITCH MOMENT	YAW MOMENT N m (in lb)	SIDE LOAD KN (lbs)	REMARKS
AL1	Figure E1	0	0	Alignment System Inactive, locked
AL2	Figure E1	0	0	Alignment System Active
AL3	Figure E1	-7232 (-64000)	0	Alignment System Active
AL4	Figure E1	-7232 (-64000)	10.96(2465)	Alignment System Active
AL5	(-1) x Figure E1	0	0	Alignment System Active

NOTES:

1) All conditions started at 0^{o} misalignment
2) Store properties: wt = 10.07 KN (2265 lbs) c.g. at pylon station .86m(33.757 in), pylon waterline -.24m(-9.35 in.), $I_{yaw} = I_{pitch} = 734.7$ kgm^2 (542.2sl.ft^2)
3) Moment applied about the store c.g.
4) Yaw moment and side load were held constant at level shown.

TABLE 23.- DECOUPLER PYLON - INFLUENCE COEFFICIENT TEST CONDITIONS

CONDITION NO.	LOAD TYPE	V	S	PM	RM	YM	ALIGNMENT POSITION
IC 1	VERTICAL	22.2(5)					NEUTRAL
IC 2	SIDE		22.2(5)				NEUTRAL
IC 3	PITCH MOMENT			6.78(60)			NEUTRAL
IC 4	ROLL MOMENT				3.39(30)		NEUTRAL
IC 5	YAW MOMENT					6.78(60)	NEUTRAL
IC 6	PITCH MOMENT (2)			2.26(20)			NOSE UP AGAINST STOPS.
IC 7	PITCH MOMENT (3)			-2.26(-20)			NOSE DOWN AGAINST STOPS.

NOTES: (1) Forces in $\frac{N}{1000}$ $\left(\frac{lb}{1000}\right)$ Moments in $\frac{N \cdot M}{1000}$ $\left(\frac{in\text{-}lb}{1000}\right)$

(2) Nose up pitching moment only. No reversal.

(3) Nose down pitching moment only. No reversal.

TABLE 24.- DECOUPLER PYLON INFLUENCE COEFFICIENTS FOR CANTILEVERED PYLON AND GBU-8 STORE

LOAD DIRECTION	DEFLECTION DIRECTION	*INFLUENCE COEFFICIENT (DEFLECTION PER UNIT LOAD)			
		GROUND TEST		FINITE ELEMENT	
VERTICAL	VERTICAL	8.51×10^{-6}	(1.49×10^{-5})	8.39×10^{-6}	(1.47×10^{-5})
	SIDE	1.34×10^{-6}	(2.35×10^{-6})	**	**
	PITCH	5.99×10^{-8}	(2.66×10^{-7})	9.41×10^{-8}	(4.18×10^{-7})
	ROLL	7.25×10^{-8}	(3.22×10^{-7})	**	**
	YAW	1.65×10^{-8}	(7.35×10^{-8})	**	**
SIDE	SIDE	5.89×10^{-5}	(1.031×10^{-4})	5.68×10^{-5}	(9.95×10^{-5})
	PITCH	7.50×10^{-8}	(3.332×10^{-7})	**	**
	ROLL	1.36×10^{-6}	(6.056×10^{-6})	1.34×10^{-6}	(5.936×10^{-6})
	YAW	2.10×10^{-7}	(9.335×10^{-7})	2.10×10^{-7}	(9.336×10^{-7})
PITCH	PITCH	2.24×10^{-8}	(2.53×10^{-7})	2.48×10^{-8}	(2.80×10^{-7})
	ROLL	9.89×10^{-10}	(1.118×10^{-8})	**	**
	YAW	3.85×10^{-10}	(4.354×10^{-9})	**	**
ROLL	ROLL	4.15×10^{-8}	(4.69×10^{-7})	4.12×10^{-8}	(4.65×10^{-7})
	YAW	9.41×10^{-10}	(1.063×10^{-8})	1.12×10^{-12}	(1.265×10^{-11})
YAW	YAW	1.07×10^{-8}	(1.211×10^{-7})	1.07×10^{-8}	(1.212×10^{-7})

* ANGULAR DISPLACEMENT UNITS ARE RADIANS, LOADS ARE N(LB), MOMENTS ARE N m (IN.LB), LINEAR DISPLACEMENTS ARE CM(IN.).

** SIMULATION DOES NOT HAVE THIS COUPLING DEGREE OF FREEDOM.

TABLE 25.- GROUND VIBRATION TESTING OF DECOUPLER PYLON

CONFIGURATION	NATURAL FREQUENCY - H_z 1st PITCH MODE	2nd PITCH MODE	LATERAL BENDING MODE	YAW MODE	COUPLED PITCH & YAW
Pylon #1 with Tight Linkage Pins, Upper LH Skin Off -					
Damper Installed	*N.E.	6.7	5.7	6.7	5.5
Damper Removed	3.6	7.3	5.7	6.7	5.5
Pylon #1 with Tight Linkage Pins, Upper LH Skin On -					
Damper In	*N.E.	7.8	-	-	5.0
Damper Remov.	3.5	8.0	-	-	5.0
Damper in, No Fluid	3.5	8.0	-	-	5.0
Pylon #2 with Tight Linkage Pins, Upper LH Skin On -					
Damper in, No Fluid	3.61	8.0	-	-	4.5
Pylon #2 with Loose Linkage Pins, Upper LH Skin On,					
Damper in, No Fluid	*N.E.	7.8	-	-	4.5
Damper Out	3.56	7.8	-	-	4.5
Pylon #1 with Medium Linkage Fit Pins, Upper LH Skin On,					
Damper in, No Fluid	**3.6	**6.7	**4.1	**3.61	4.5
Damper Out	3.6	7.3	-	-	4.5

* N.E. - Not Excited Due to Load Limitations of the Test Equipment.
**Final Configuration

TABLE 26.- BREAKOUT FRICTION TESTING OF DECOUPLER PYLON

CONFIGURATION	NOSE UP MOMENT N·M (IN·LB)	NOSE DOWN MOMENT N·M (IN·LB)
PYLON #1 with Tight Linkage Fit and Damper Removed	759(6720)	900(7968)
PYLON #1 with Tight Linkage Fit Except Support Bushings Looser by .002 in. diameter		
- Damper Installed	850(7520)	795.5(7040)
- Damper Removed	488(4320)	578.5(5120)
PYLON #2 with Tight Linkage Fit		
- Damper Installed with No Fluid	643.5(5695)	544(4815)
PYLON #2 with Loose Linkage Fit		
- Damper Installed with No Fluid	428(3785)	311(2755)
- Damper Removed	276(2445)	279(2466)
PYLON #2 with Medium Linkage Fit		
- Damper Installed with No Fluid	390(3451)**	532(4712)**
- Damper Out	314(2781)	416(3682)
PYLON #1 with Medium Linkage Fit		
- Damper Installed Teflon Rings	617(5460)*	591(5227)*
- Damper Out	579(5125)	561.5(4969)

** Final Configuration Except for Damper Rework of O-Rings
 * Final Configuration

TABLE 27.- LINKAGE GEOMETRY MEASUREMENTS

	Difference in L.H. and R.H. Dimension - cm(in.)			
	Pylon No. 1		Pylon No. 2	
	Fore and Aft	Vertical	Fore and Aft	Vertical
Upper Support Fwd Holes	0(0)	0(0)	0(0)	0(0)
Upper Support Aft Holes	.0051(.002)	0(0)	.0102(.004)	.0102(.004)
Fwd Link Lower Holes	.0099(.0039)	.0208(.0082)	.0127(.005)	.0038(.0015)
Fwd Link Upper Holes	.0114(.0045)	.0229(.0090)	.0025(.001)	0(0)
Aft Link Lower Holes	.0020(.0008)	.0046(.0018)	0(0)	.0025(.001)
Aft Link Upper Holes	.0033(.0013)	.0036(.0014)	.0127(.005)	0(0)

TABLE 28.- LINK PIN CLEARANCES

Design Concept	* Pin Clearances - cm(in.)	
	Links	Support & Sideplate
Original Design with Pins Pressed in Links	-.0025(-.001)	.0051(.002)
Dummy Pins with Loose Fit	.0076(.003)	.0152(.006)
Intermediate Design with Medium Fit	.0041(.0016)	.0140(.0055)
Final Design with Loose Fit	.0076(.003)	.0140(.0055)

* Negative Sign Indicates Interference Fit

TABLE 29.- DECOUPLER PYLON STRUCTURAL PROOF TEST CONDITIONS

CONDITION	Limit Design Load at Store C.G.					
	P_x	P_y	P_z	M_x	M_y	M_z
1575-2.3R	3.47(781)	2.29(515)	-22.9(-5151)	-3957(-35021)	12508(110687)	-9427(-83428)
1595-1.2R	1.40(315)	45.94(10328)	-16.05(-3608)	-794(-7028)	516(4570)	138(1222)

NOTES:
1) Forces in KN (lbs) Moments in N m (in lb).
2) Store C.G. at pylon station .857m(33.737 in), pylon waterline -.237m(-9.35in).
3) Pylon in neutral position.

TABLE 30.- DECOUPLER PYLON PARAMETER LIST

PARMID	PARAMETER NAME	RANGE	MAX FREQ. (HZ)
PD010	Calibrated Airspeed	75 to 1000 Kts	2
PD020	True Airspeed	250 to 1500 Kts	2
PD013	Mach #	0 to 2.0	2
PD011	Altitude - Coarse	-1.5 to 78.5 K-Ft.	2
PD012	Altitude - Fine	10 K-Ft.	2
TA011C	Total Temp. - Coarse	-100 to 300 Deg. F	2
TA011F	Total Temp. - Fine	40 Deg. F	2
ALPHA	Angle of Attack	-5 to 40 Deg.	5
BETA	Angle of Sideslip	-22.5 to 22.5 Deg	5
GD011	Pitch Angle	-180 to 180 Deg.	10
GD012	Roll Angle.	-180 to 180 Deg.	20
GD016	Heading	0 to 360 Deg.	10
GD013	Pitch Rate	-60 to 60 Deg/Sec	16
GD014	Roll Rate	-300 to 300 Deg/Sec	20
GD015	Yaw Rate	-200 to 200 Deg/Sec	10
AB002	Long. Accel. C.G.	-1 to 1g	20
AB003	Lat. Accel. C.G.	-1 to 1g	20
AB006	Normal Accel. C.G.	-1 to 1g	20
AS031	L/H Wingtip Launcher Fwd	-5 to 5g	50
AS032	L/H Wingtip Launcher Aft	-5 to 5g	50
AS063	R/H Wingtip Launcher Fwd	-5 to 5g	50
AS064	R/H Wingtip Launcher Aft	-5 to 5g	50
AT009	L/H Horizontal Tail	-25 to 25g	50
AT010	R/H Horizontal Tail	-25 to 25g	50
AT012	Vrt. Fintip Fwd	-15 to 15g	50
AS051T	*L/H GBU-8 Vrt. Fwd	-5 to 5g	25
AS051J	*R/H GBU-8 Vrt. Fwd	-5 to 5g	25
AS052T	*L/H GBU-8 Lat. Fwd	-5 to 5g	25
AS052J	*R/H GBU-8 Lat. Fwd	-5 to 5g	25
AS029K	*L/H 370 Gal. Tank-Nose-Vrt.	-5 to 5g	25
AS030K	*L/H 370 Gal. Tank-Nose-Lat.	-2.5 to 2.5g	25
AS029K	*R/H 370 Gal. Tank-Nose-Vrt.	-5 to 5g	25
AS033R	*R/H 370 Gal. Tank-Nose-Lat.	-2.5 to 2.5g	25
AT013	Vrt. Fintip Aft	-15 to 15g	50
	Excitation Mode	Digital -2 Bits	10
	Excitation Signal	TBD	25
DW008	Leading Edge Flap Pos.	-5 to 30 Deg.	20
DW006	L/H Flapperon Pos	-20 to 20 Deg.	20
DW007	R/H Flapperon Pos.	-20 to 20 Deg.	20
DT004	L/H Horiz. Tail Pos.	-45 to 45 Deg.	20
DT005	R/H Horiz. Tail Pos.	-45 to 45 Deg.	20
DT006	Rudder Pos.	-45 to 45 Deg.	10
	*L/H Lower Pylon Align. Pos.	-5 to 5 Deg.	10
	*R/H Lower Pylon Align. Pos	-5 to 5 Deg.	10
	*L/H U/L Pylon Pos.	-8 to 8 In.	2
	*R/H U/L Pylon Pos.	-8 to 8 In.	2
EVENT	Pilot Event Marker	ON/OFF	2
TAPE	Tape Motion	ON/OFF	2
VDC10	Reg. 10 VDC Mon.	0 to 10 VDC	2
VDC28	Inst. 28 VDC Mon.	0 to 28 VDC	2
GD001	Fwd Fuselage Fuel Quan.	0 to 4000 lbs.	2
GD002	Aft Fuselage Fuel Quan.	0 to 3000 lbs.	2
GD004	L/H Wing Fuel Quan.	0 to 650 lbs.	2
GD005	R/H Wing Fuel Quan.	0 to 650 lbs.	2
GD006	L/H 370 Gal. Tank Fuel Quan.	0 to 4000 lbs.	2
GD007	R/H 370 Gal. Tank Fuel Quan.	0 to 4000 lbs.	2
GD003	Total Fuel Quan.	0 to 15000 lbs.	2
	*L/H Pylon Pitch Spring Bending Mom	$\pm$ 6000 In. lbs.	2
	*R/H Pylon Pitch Spring Bending Mom	$\pm$ 6000 In. lbs.	2

* - STORE AND PYLON INSTRUMENTATION

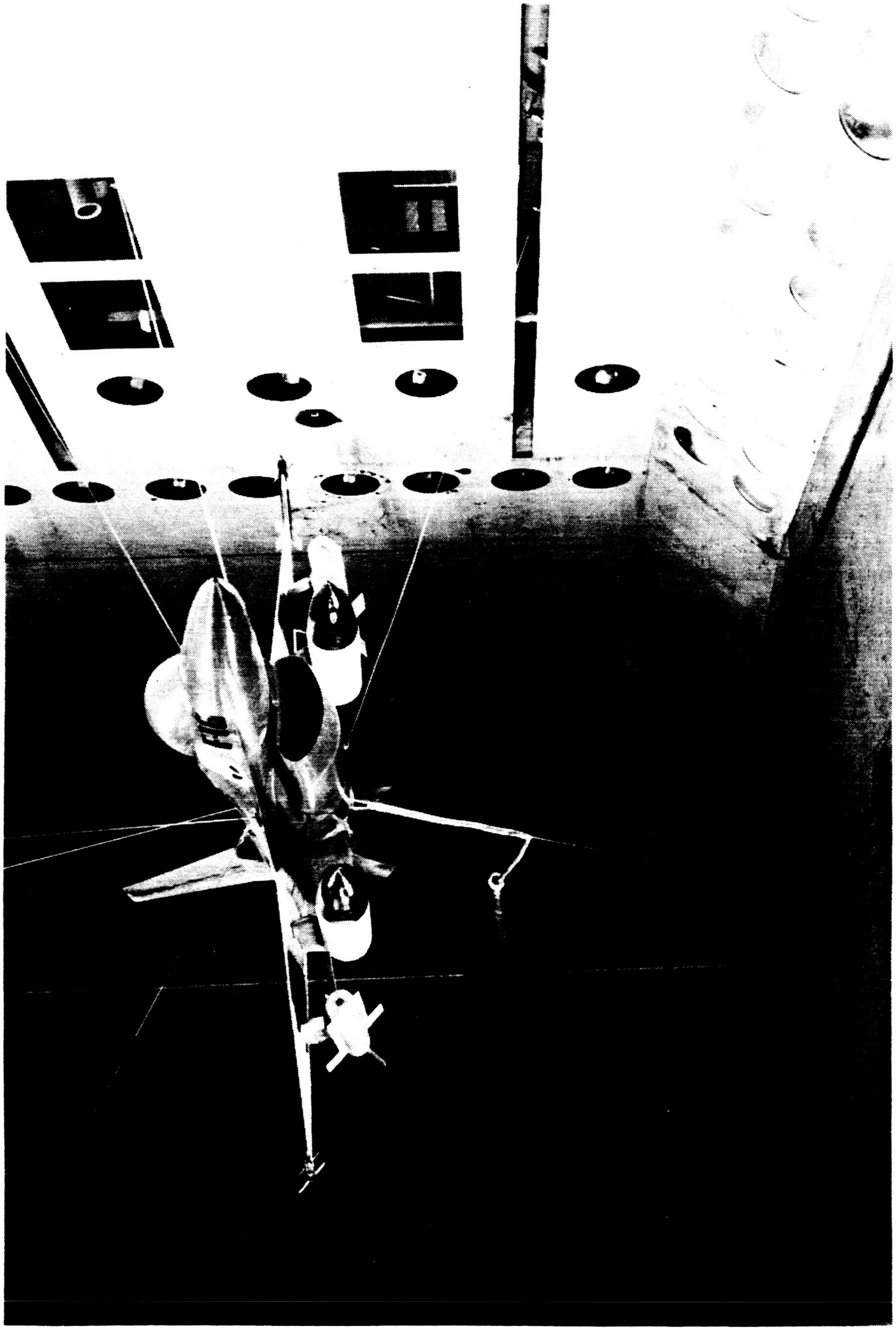

Figure 1.- F-16 Flutter Model.

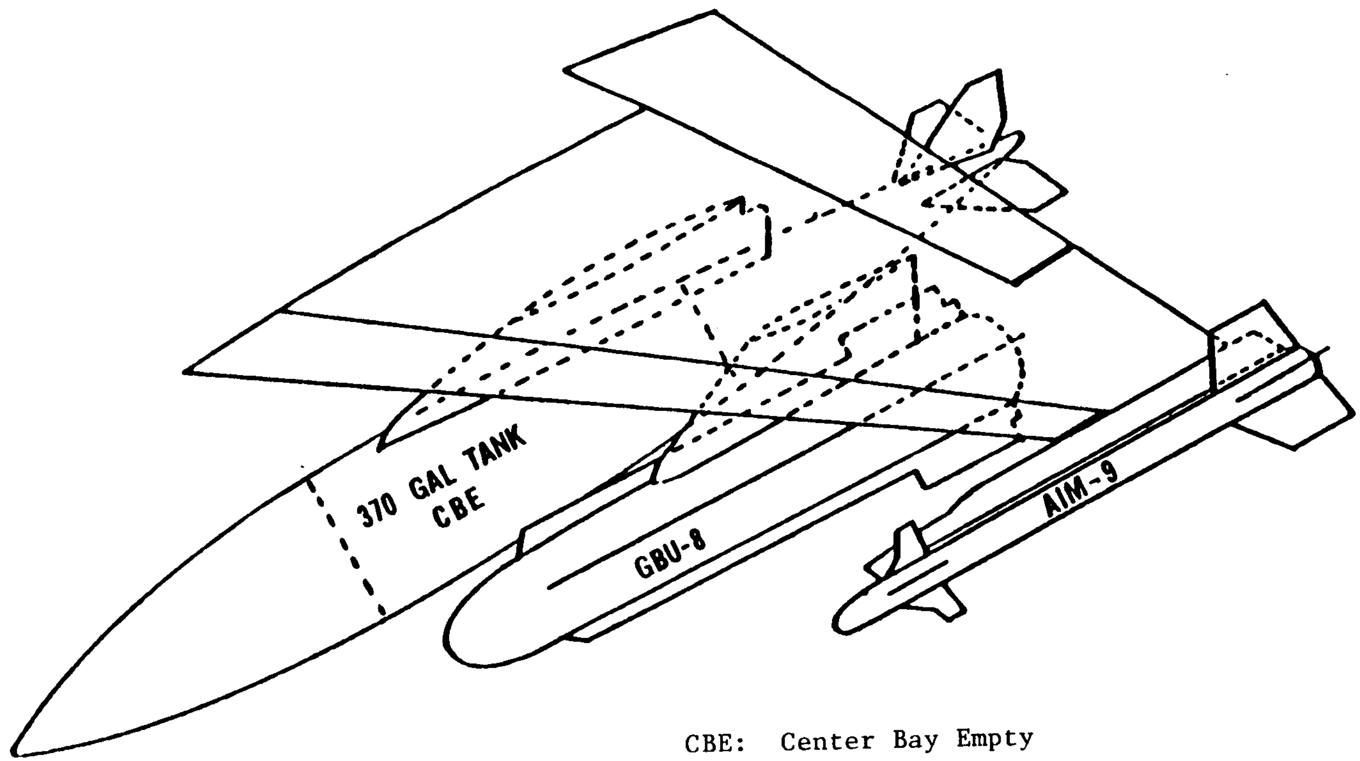

CBE: Center Bay Empty

Figure 2.- GBU-8 configuration.

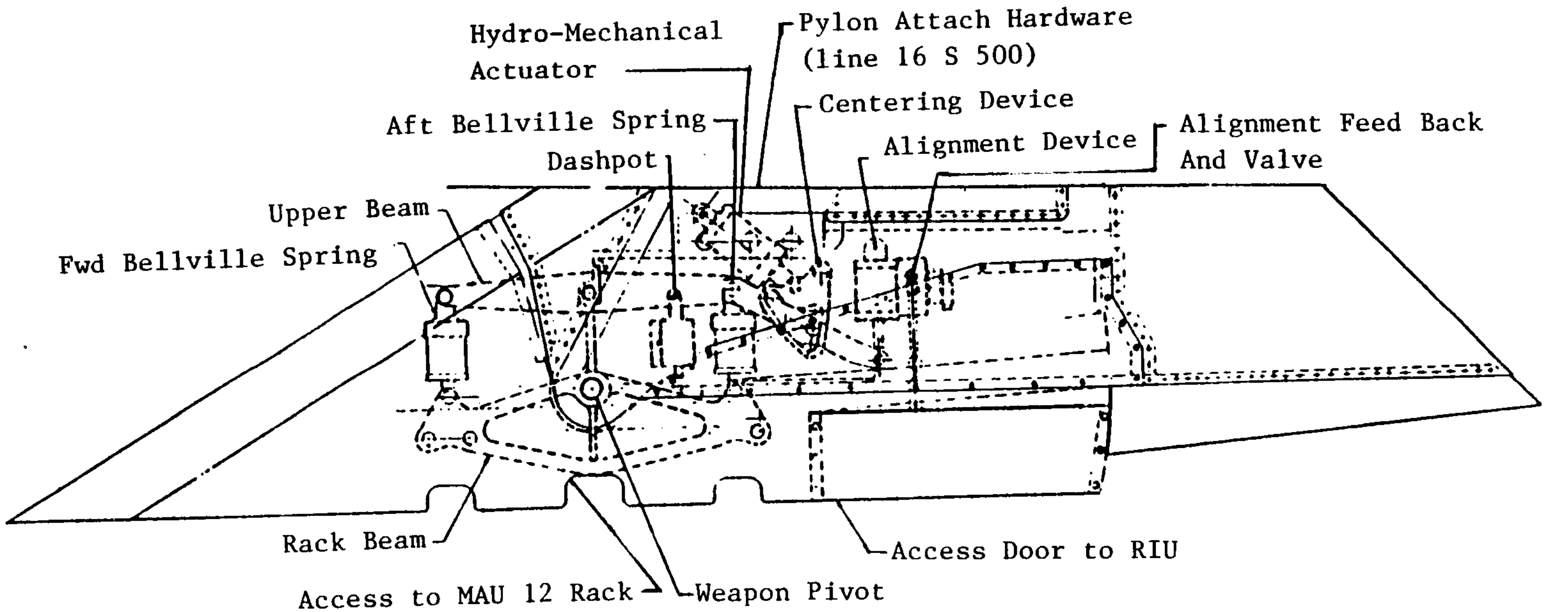

Figure 3.- Conceptual design configuration.

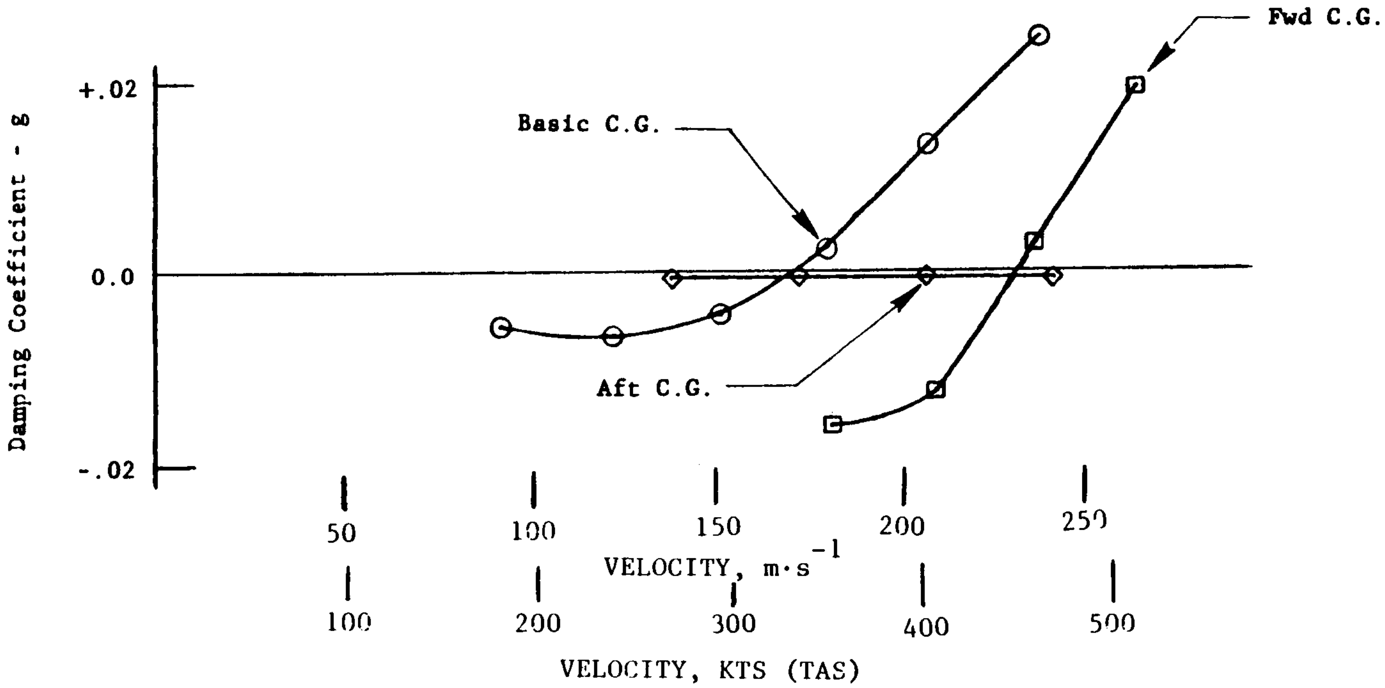

	V_f $m \cdot s^{-1}$ (KTS)	f_f Hz
BASIC C.G., g=0	172(335)	5.27
FWD C.G. , g=0	233(453)	5.20
AFT C.G. , g=0	-	-

Figure 4.- Effect of GBU-8 C.G. variation on flutter speed - production pylon.

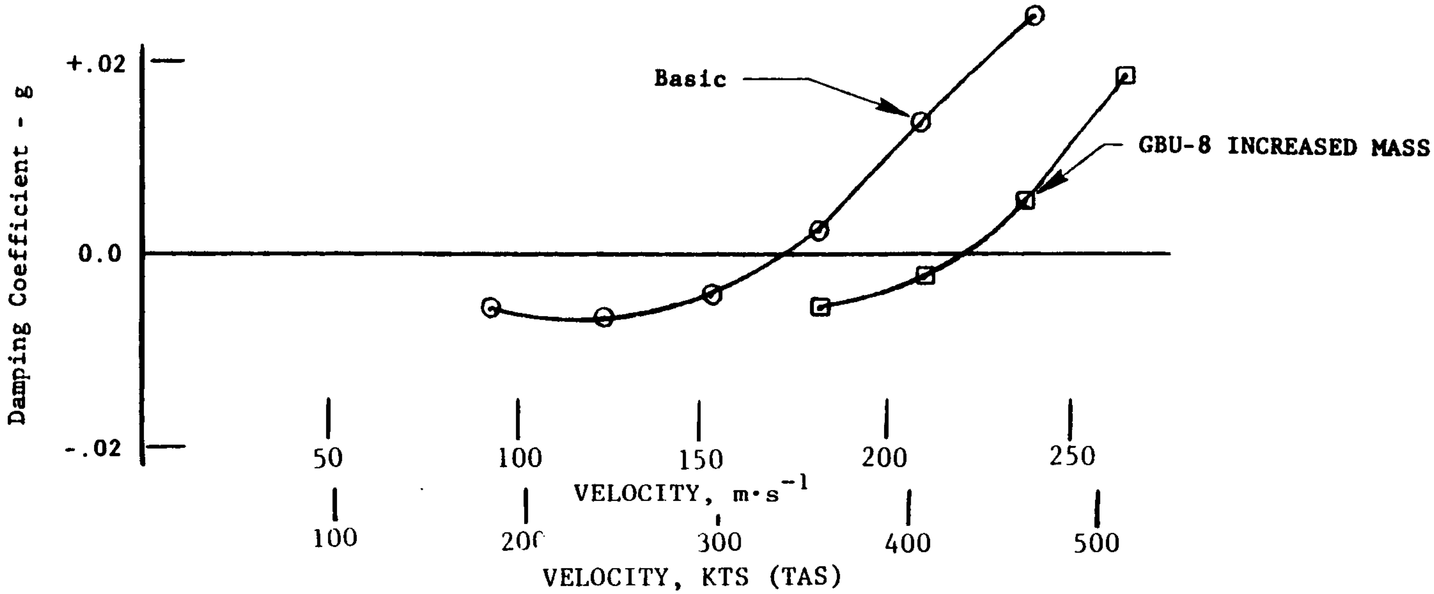

	V_f $m \cdot s^{-1}$ (KTS)	f_f Hz
BASIC g=0	172(335)	5.27
ADDITIONAL MASS g=0	216(420)	5.18

Figure 5.- Effect of additional 45.36 Kg (100 lb) mass in the GBU-8 on flutter speed - production pylon.

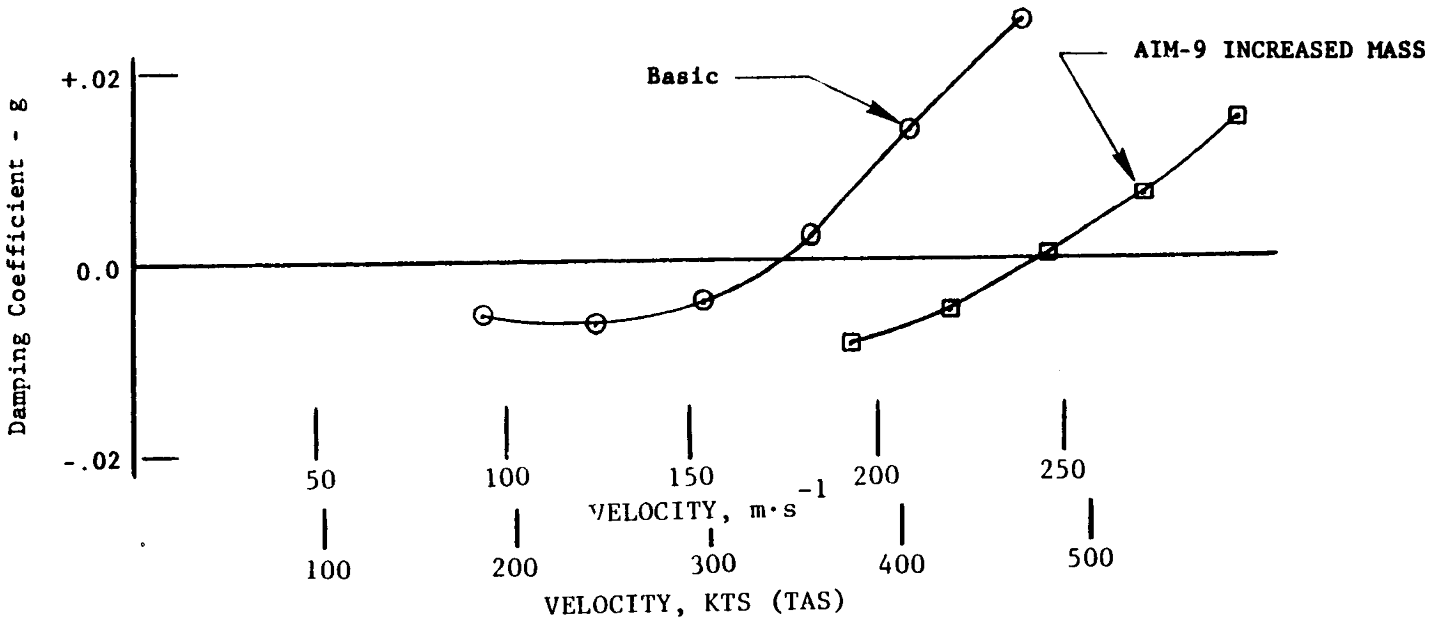

	V_f $m \cdot s^{-1}$ (KTS)	f_f Hz
BASIC g=0	172(335)	5.27
ADDITIONAL MASS g=0	244(475)	4.76

Figure 6.- Effect of additional 22.68 Kg (50 lb) mass in the AIM-9 on flutter speed - production pylon.

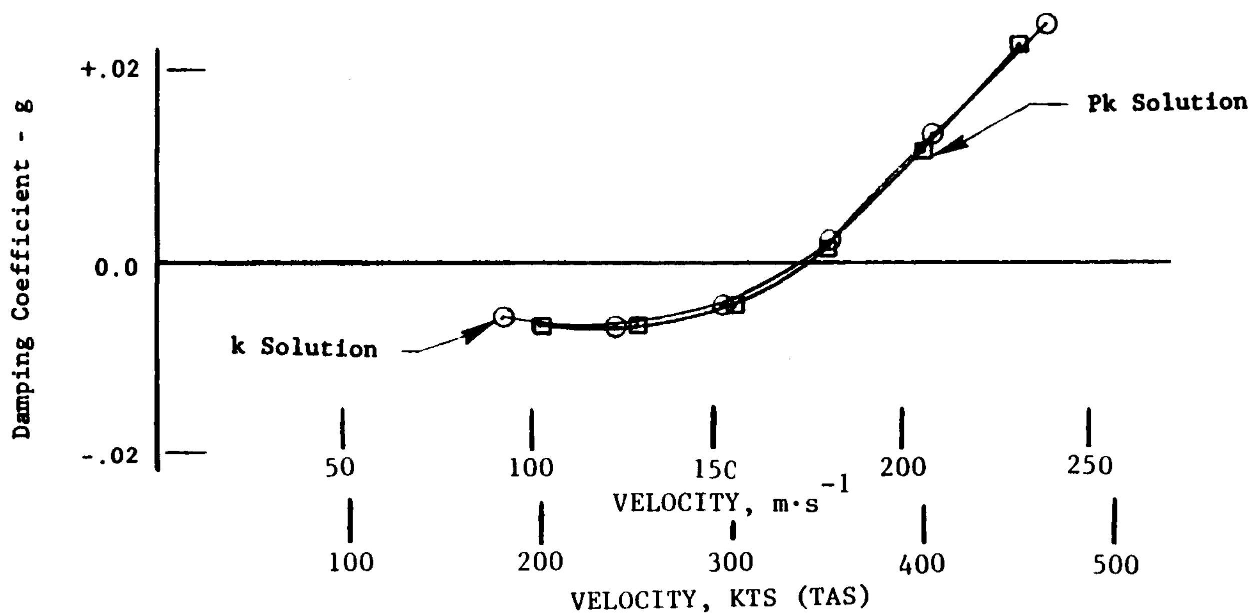

g=0 IN BOTH CASES

FLUTTER SPEED THE SAME

Figure 7.- K solution versus P-k solution - production pylon.

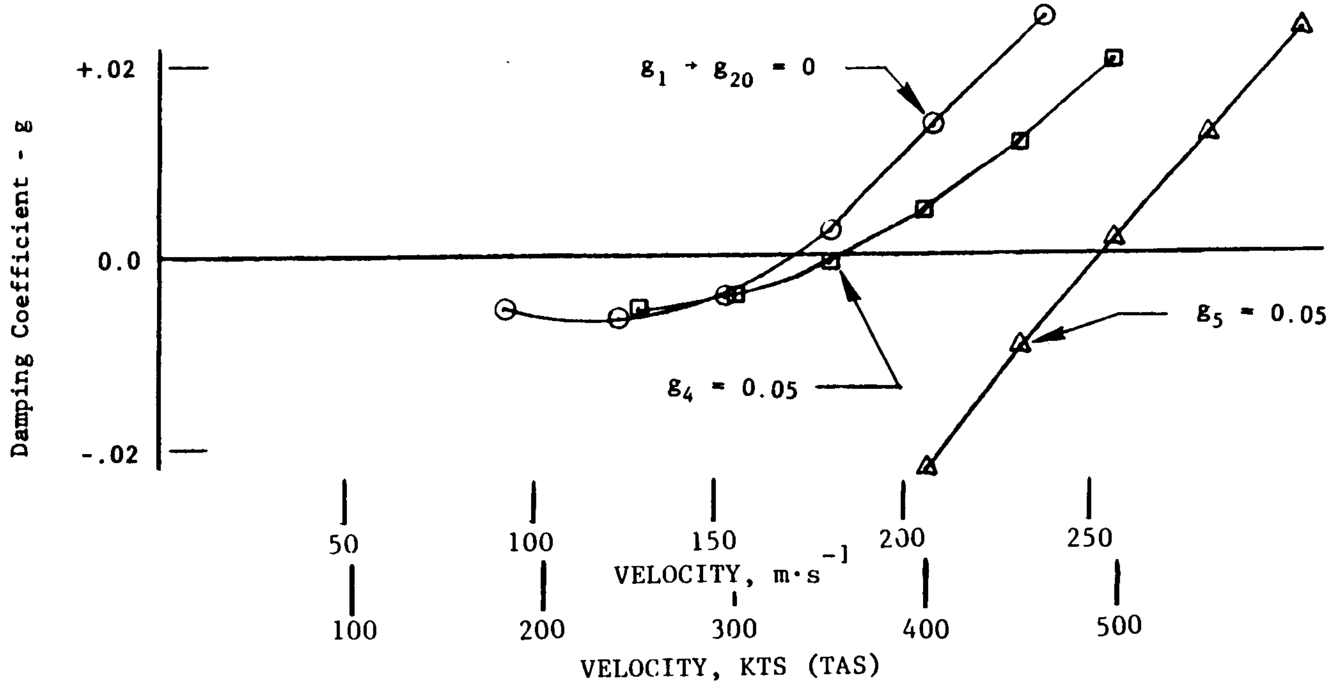

	V_f $m \cdot s^{-1}$ (KTS)	f_f Hz
$g_1 \rightarrow g_{20} = 0$	172(335)	5.27
g_4(FIRST FLEXIBLE MODE) = .05	185(360)	5.29
g_5(SECOND FLEXIBLE MODE) = .05	252(490)	5.17

Figure 8.- Effect of individual mode damping variation on flutter speed - production pylon.

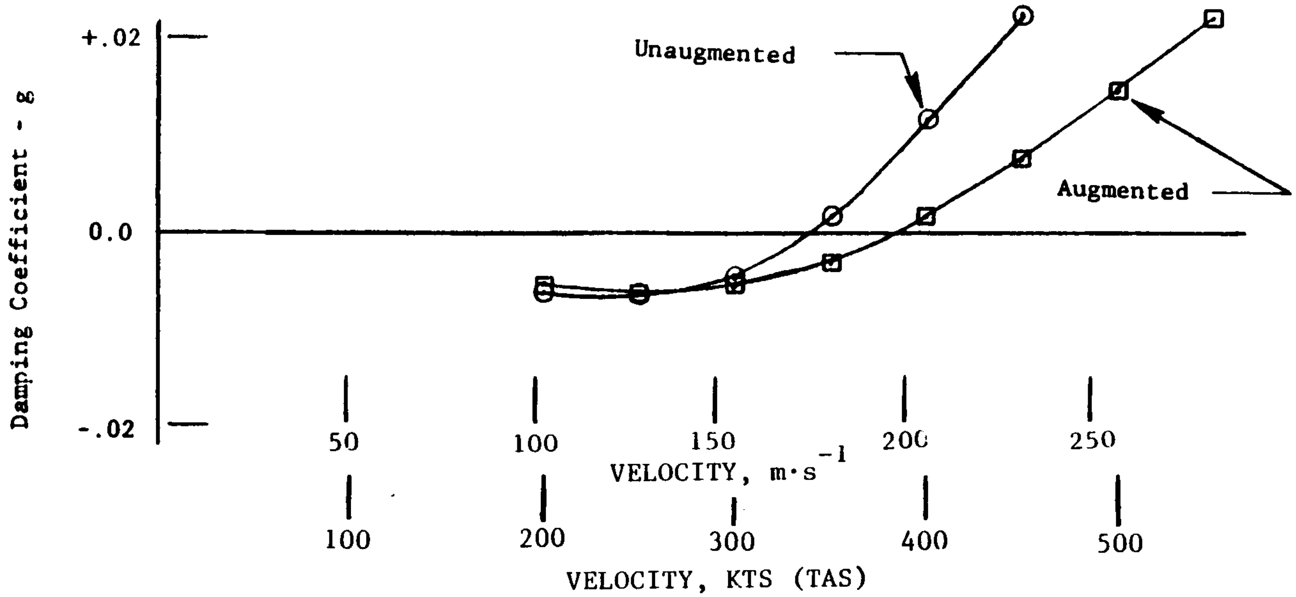

	V_f $m \cdot s^{-1}$ (KTS)	f_f Hz
UNAUGMENTED	172(335)	5.27
AUGMENTED	198(385)	5.28

Figure 9.- Effect of flight control system on flutter speed - production pylon.

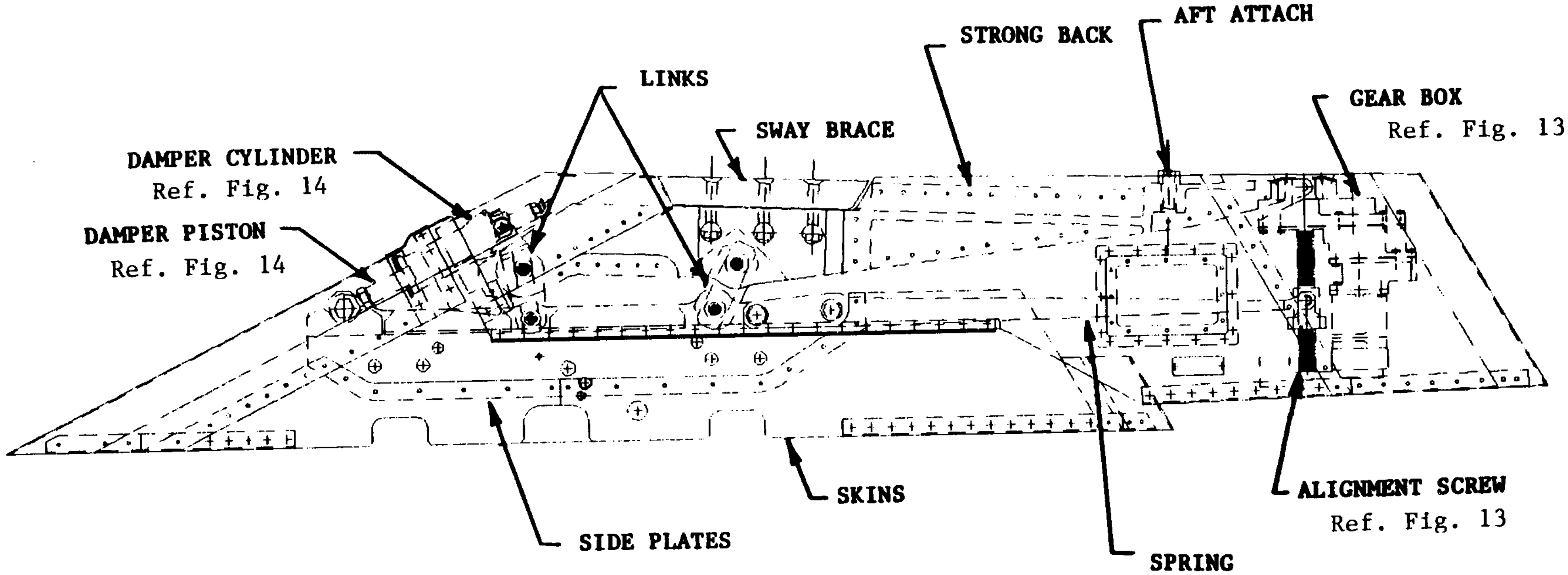

Figure 10.- Final decoupler pylon design configuration.

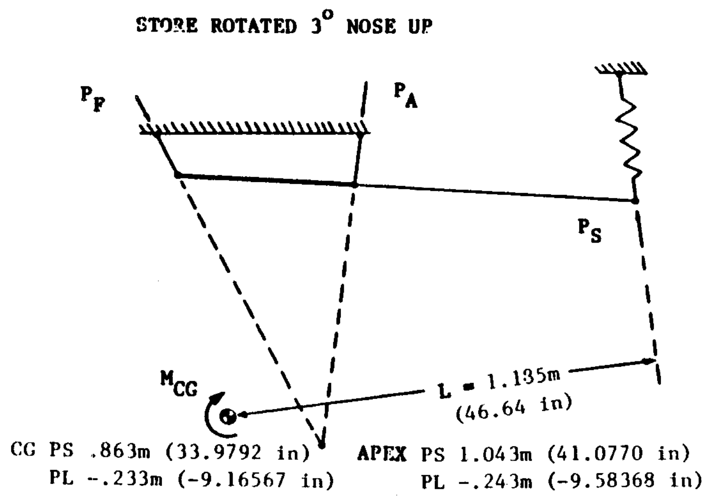

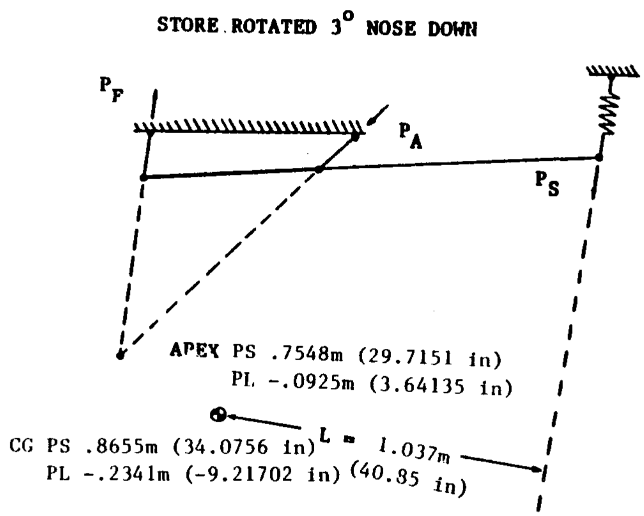

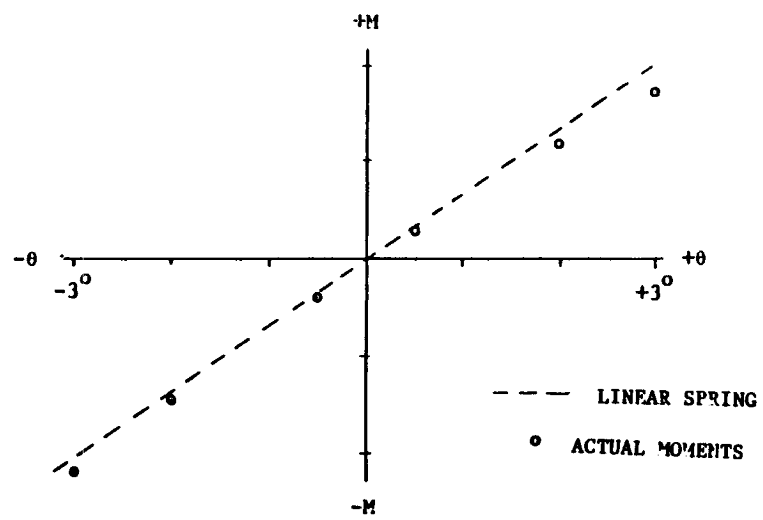

PS - Pylon Station

PL - Pylon Location, Vertical

θ	P_F	P_A	P_S	M_{CG}
+3°	-9.4 KN (-2121 lb)	-10.9 KN (-2452 lb)	19.4 KN (4365 lb)	19.5 KN·M (172,898 in-lb)
-3°	20.9 KN (4694 lb)	-.107 KN (-24 lb)	-20.9 KN (-4691 lb)	-24.2 KN·M (-214,576 in-lb)

Figure 11.- Pylon geometry effects upon spring rate.

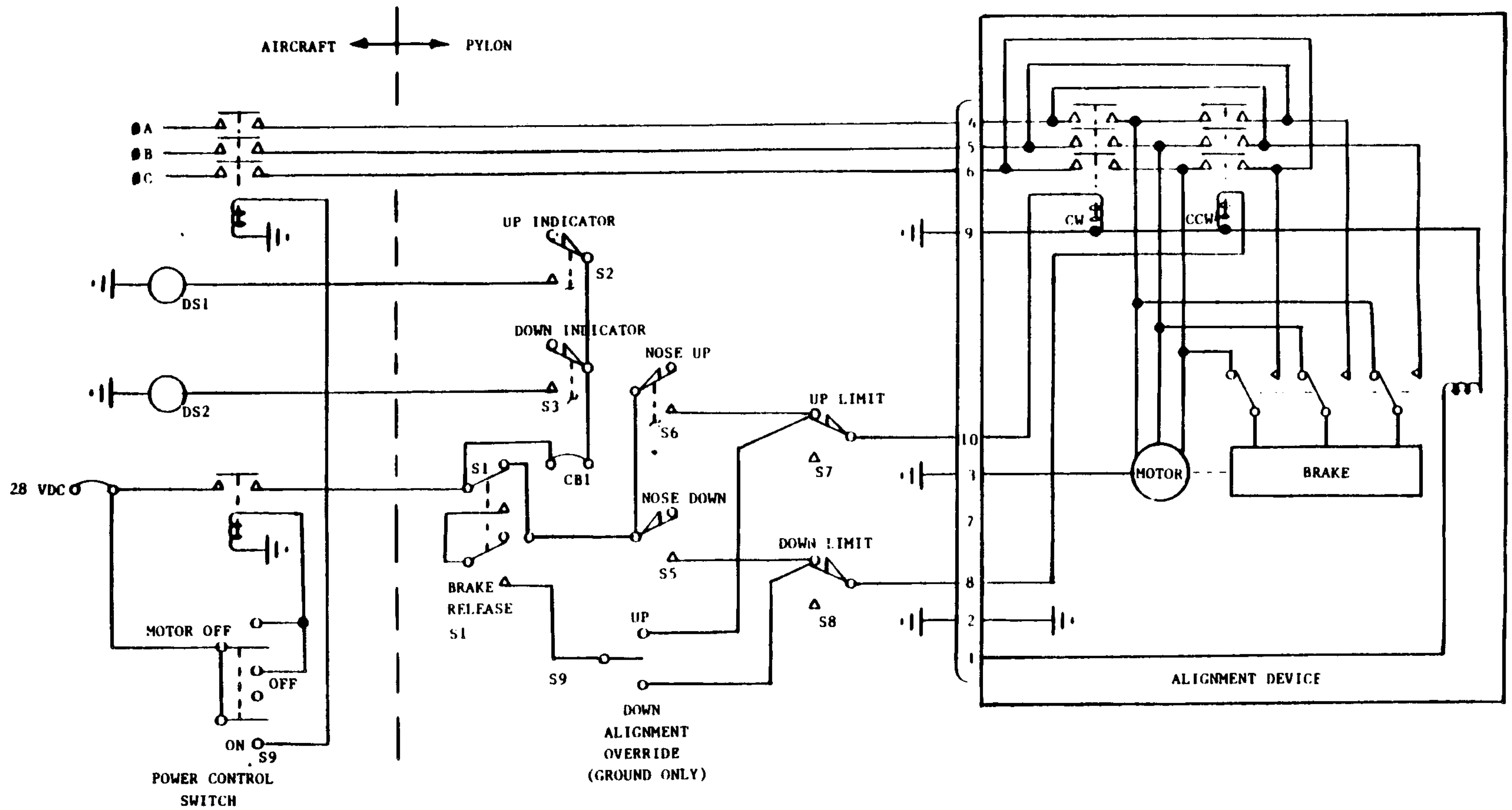

Note: Both S1 and S9 must be operated for override.

Figure 12.- Pylon alignment control.

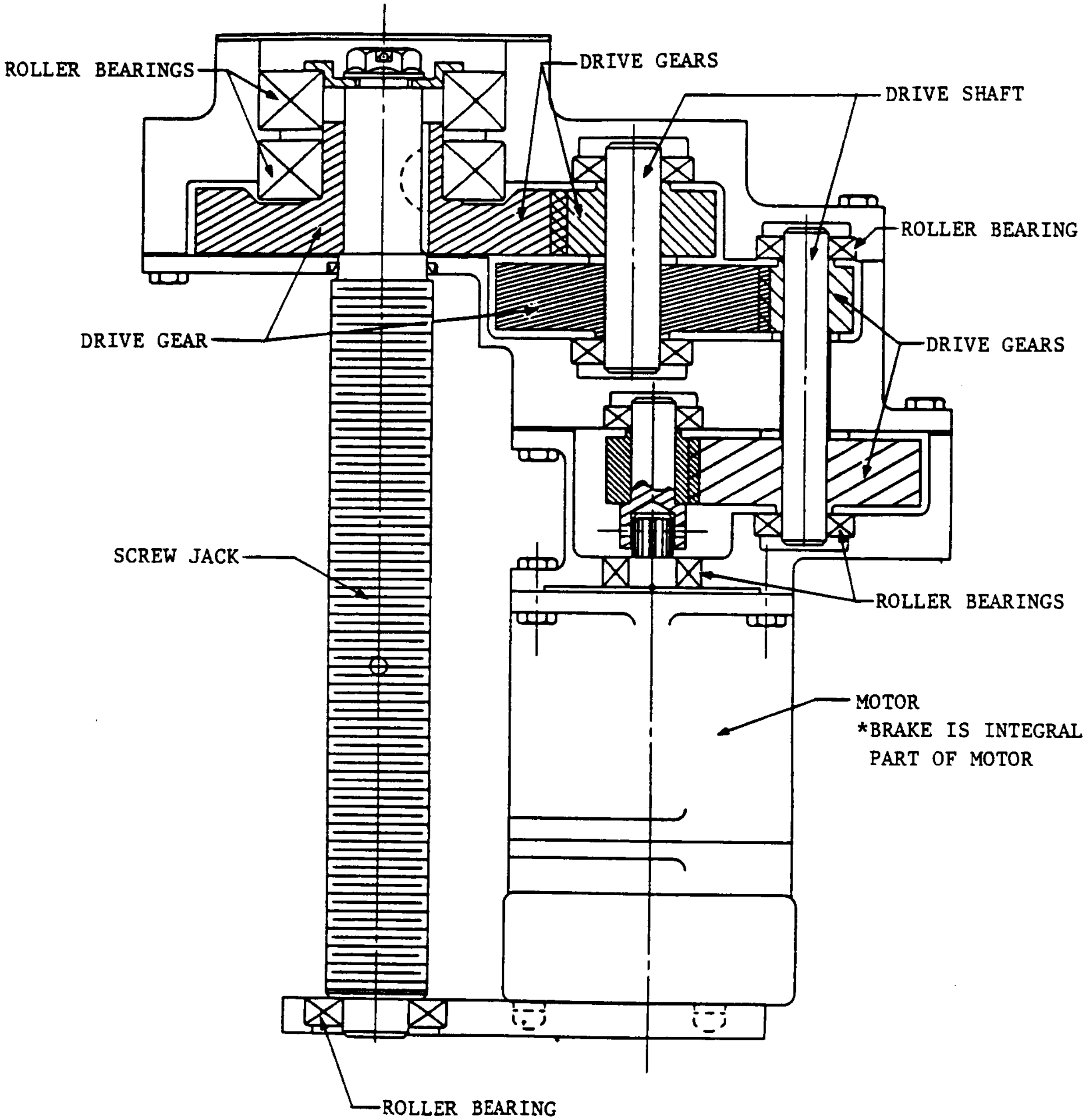

Figure 13.- Pylon alignment motor and gear train.

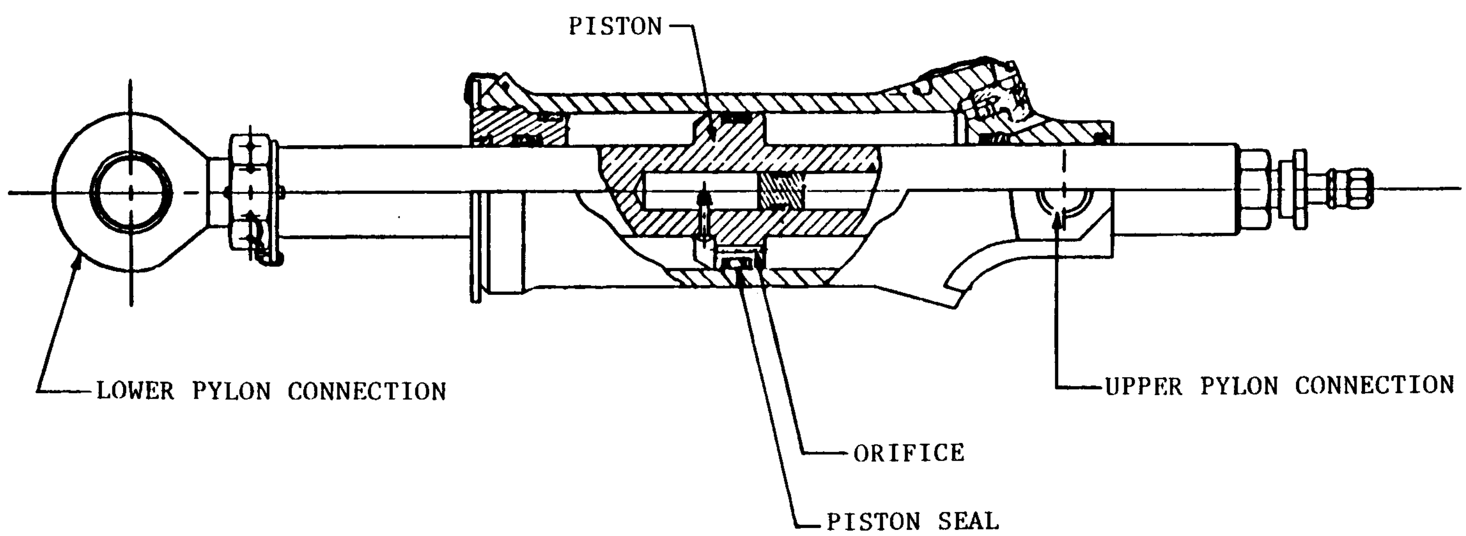

Figure 14.- Pylon hydraulic damper.

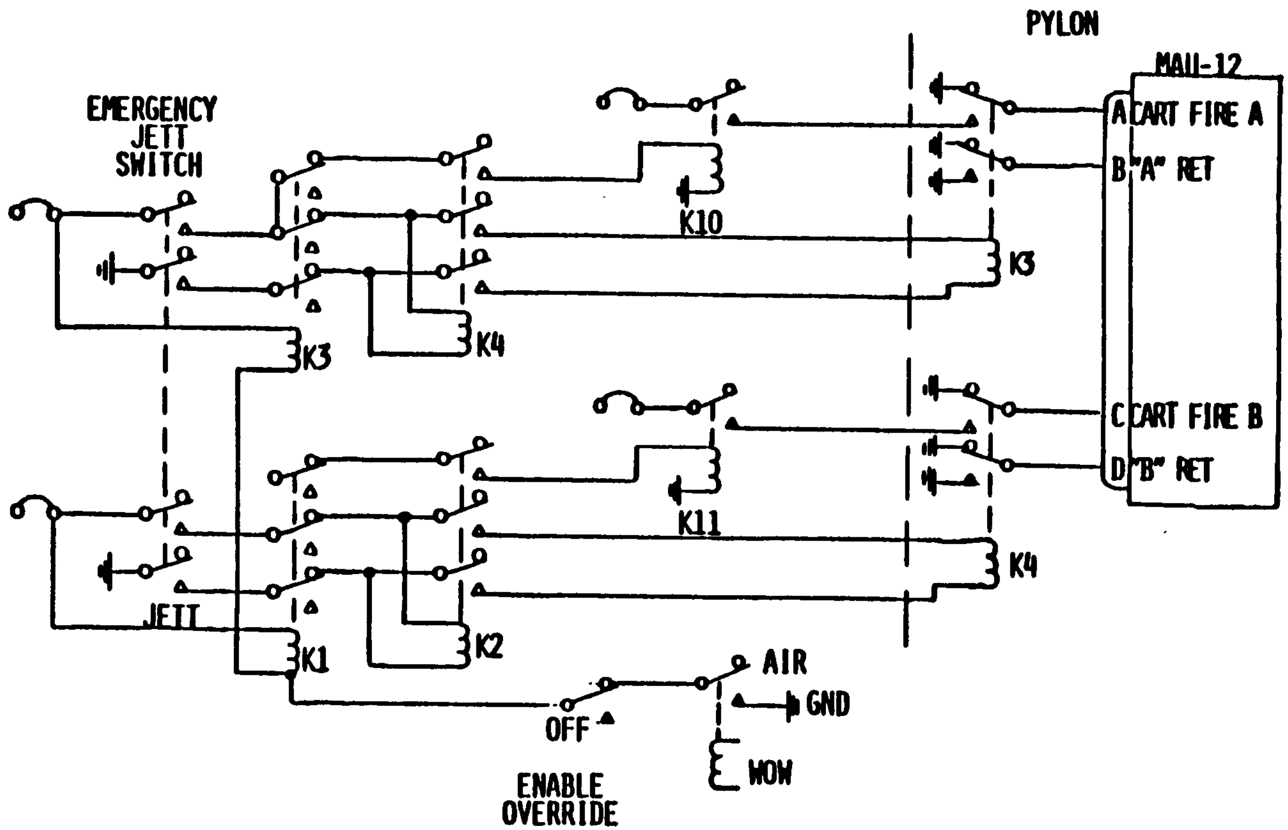

Note: F-16A NO. 2 HAS NO STORES MANAGEMENT SYSTEM, ONLY AN EMERGENCY JETTISON (RELAY) SYSTEM

Figure 15.- F-16A no. 2 Emergency Jettison system.

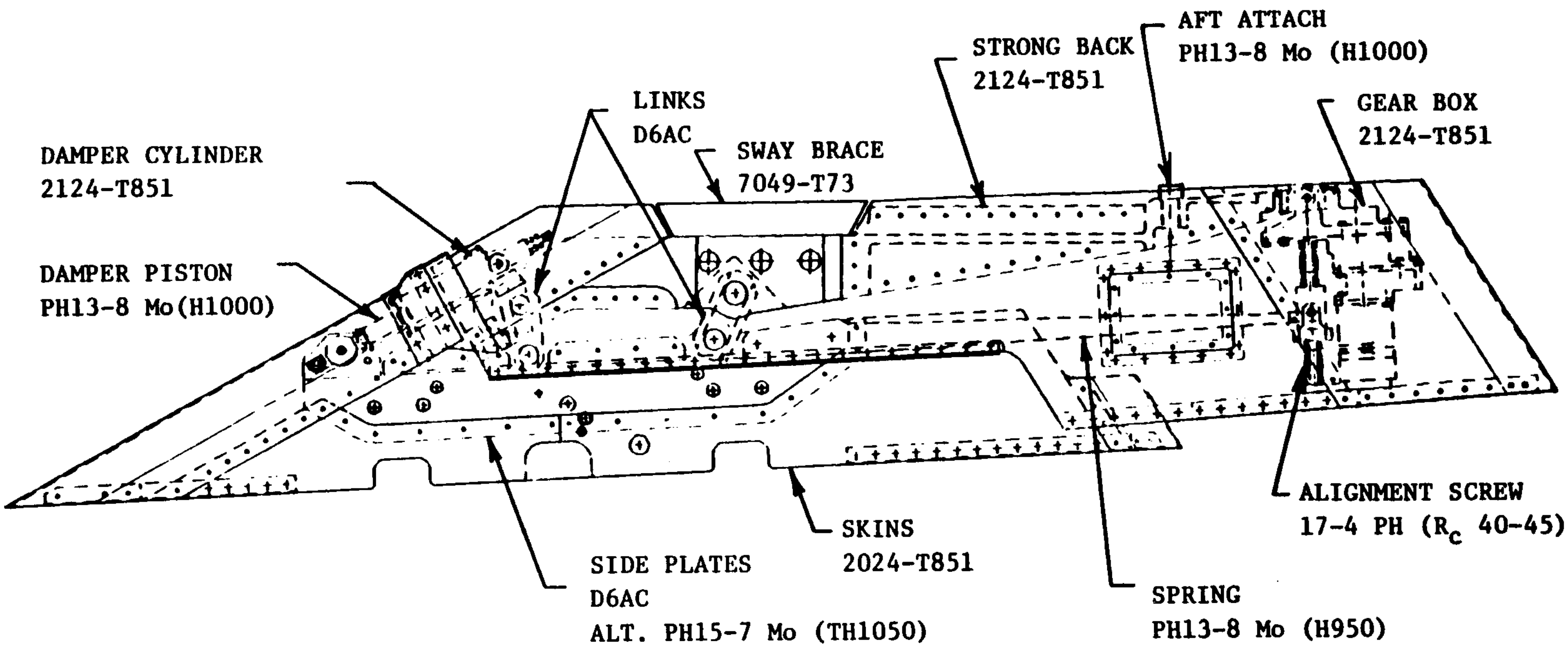

Figure 16.- Pylon material selection.

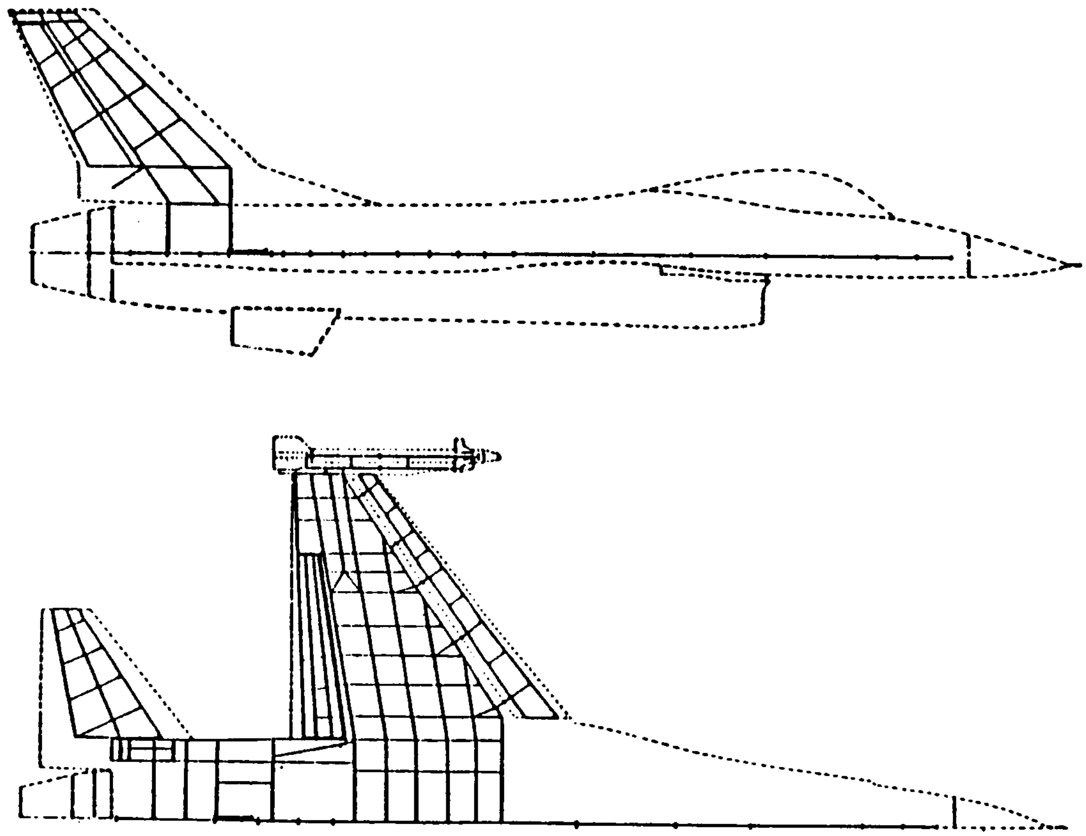

Figure 17.- Structural representation.

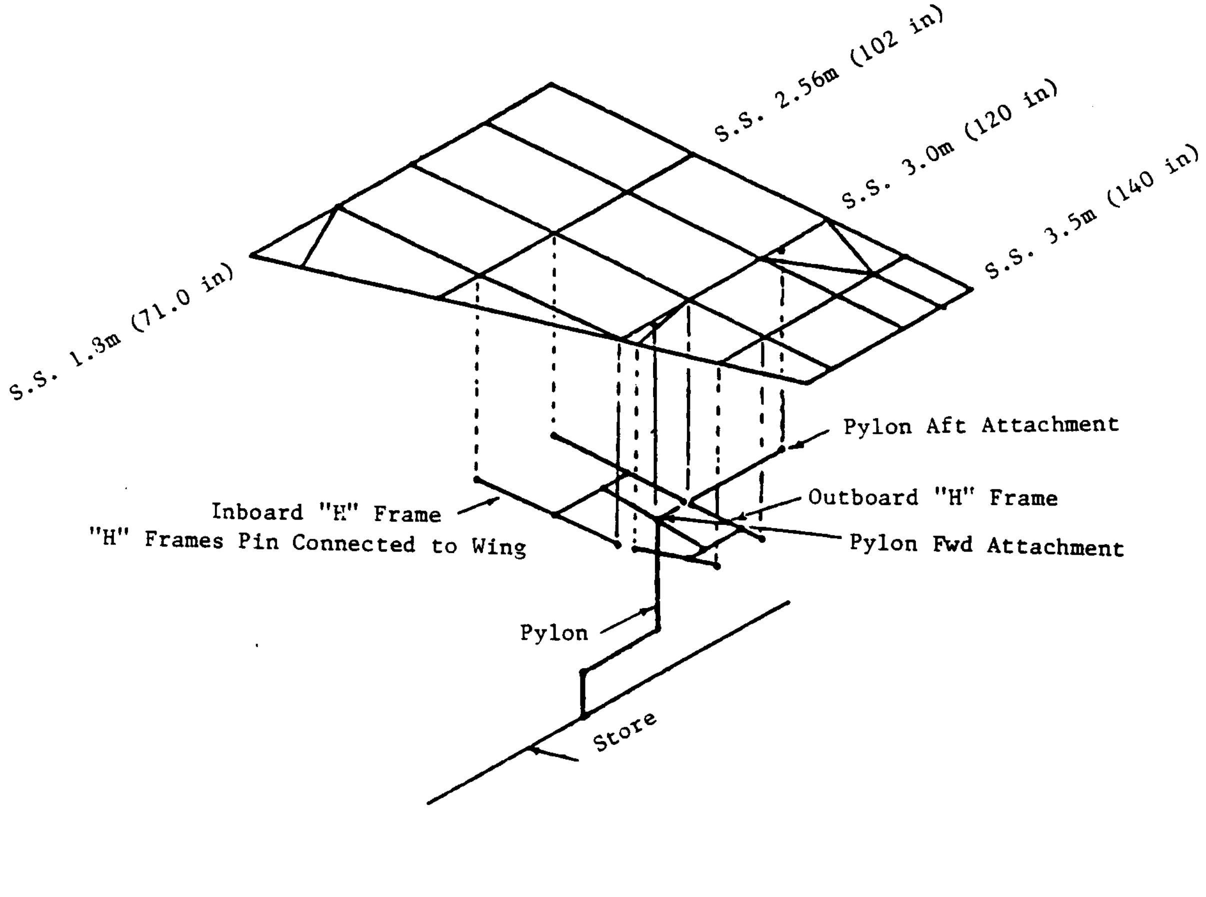

Figure 18.- F-16 wing-weapon-pylon attachment simulation.

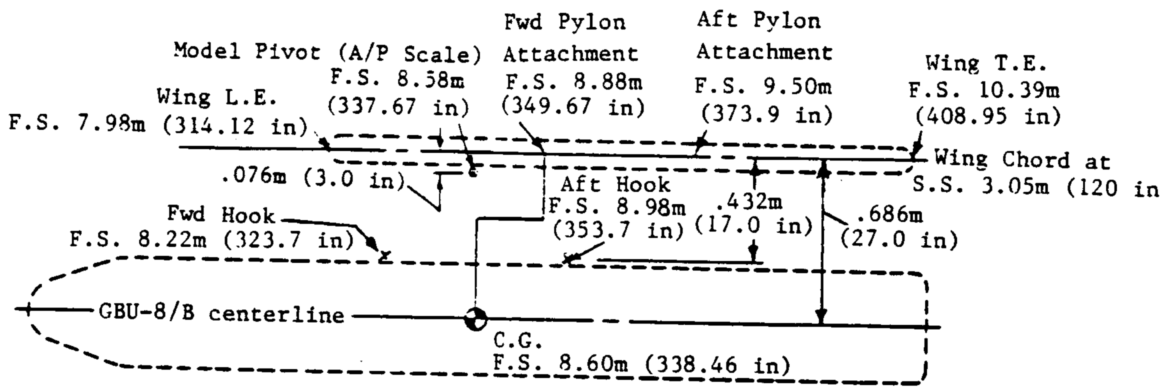

a.) Production pylon

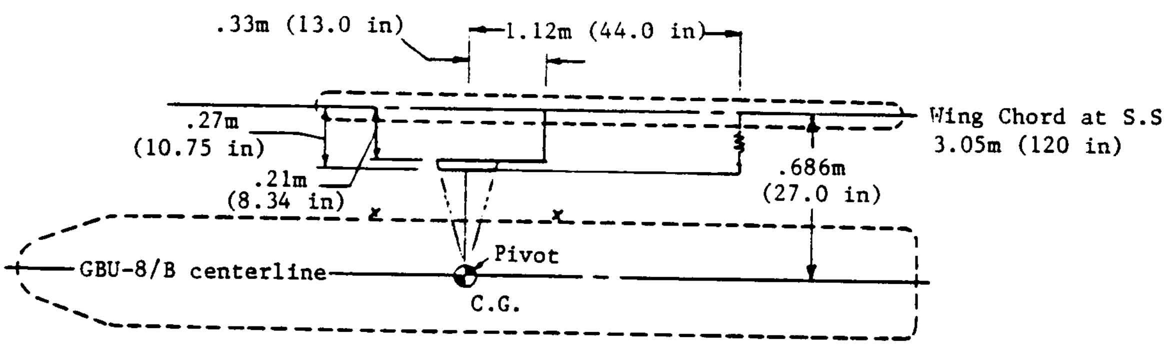

b.) Decoupler pylon, Current Design Simulation

Figure 19.- Structural representation of production pylon and decoupler pylon.

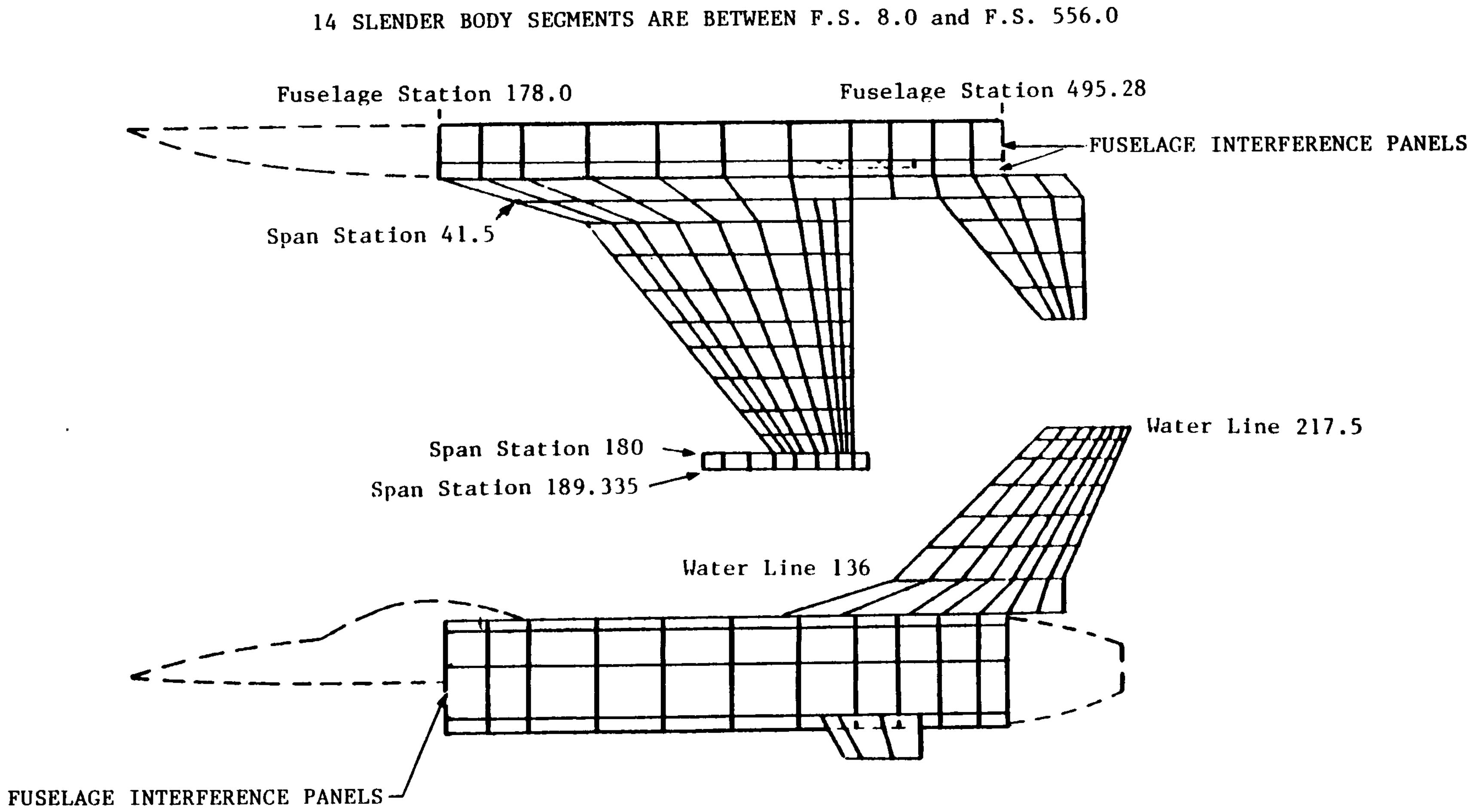

Figure 20.- Doublet lattice paneling for aerodynamic representation.

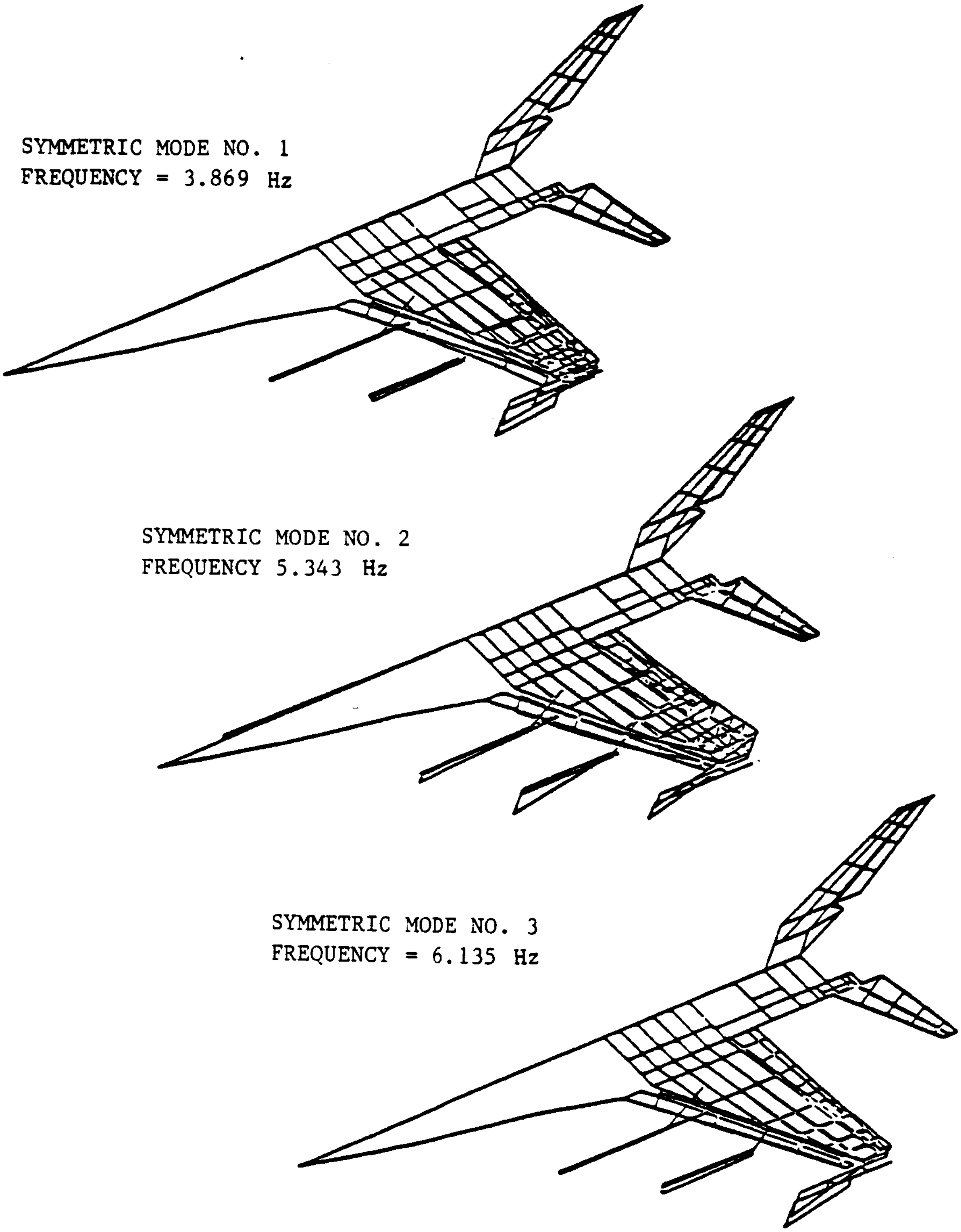

Figure 21.- First three analytical symmetric modes with production pylon.

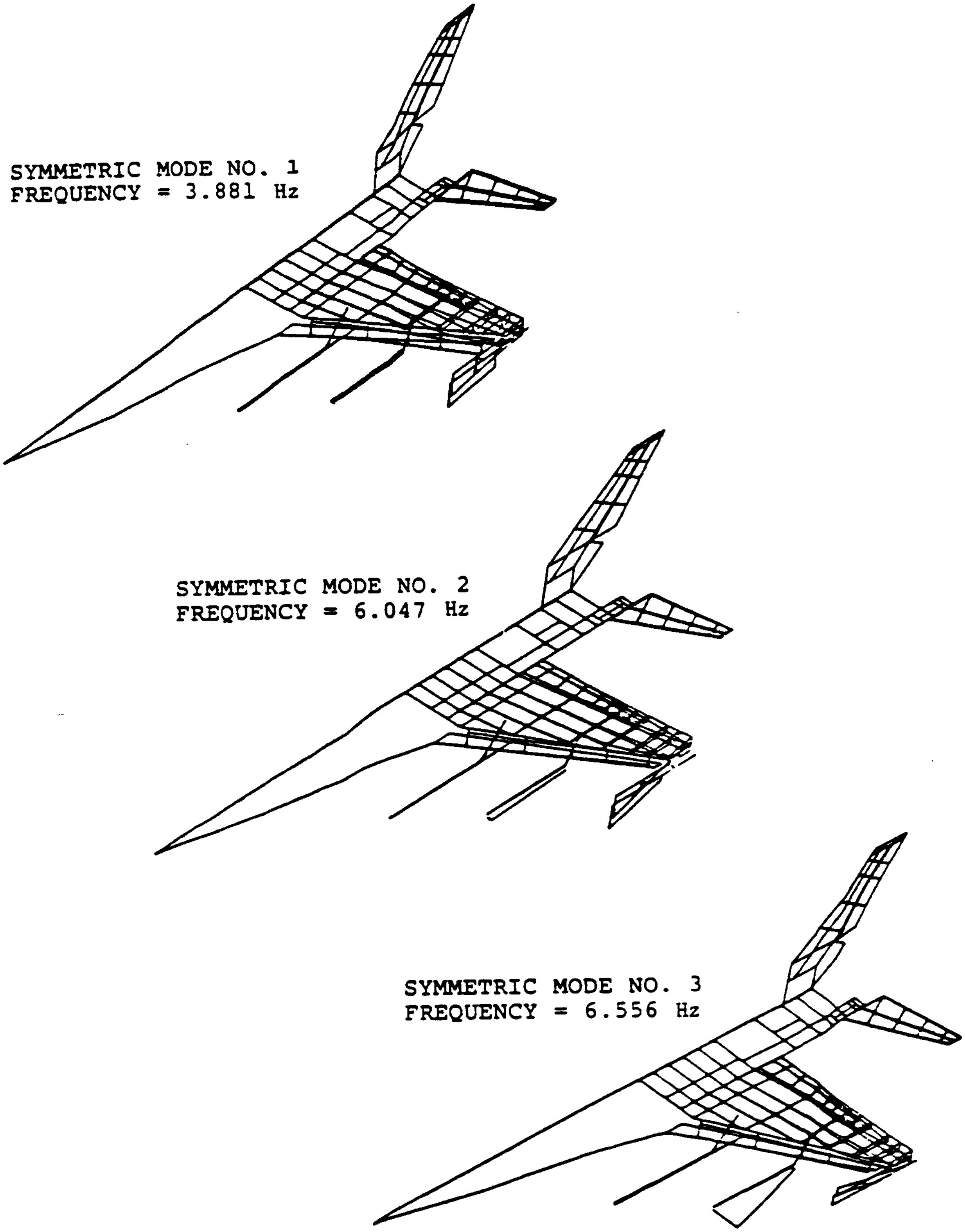

Figure 22.- First three analytical symmetric modes with zero pitch stiffness of current design decoupler pylon.

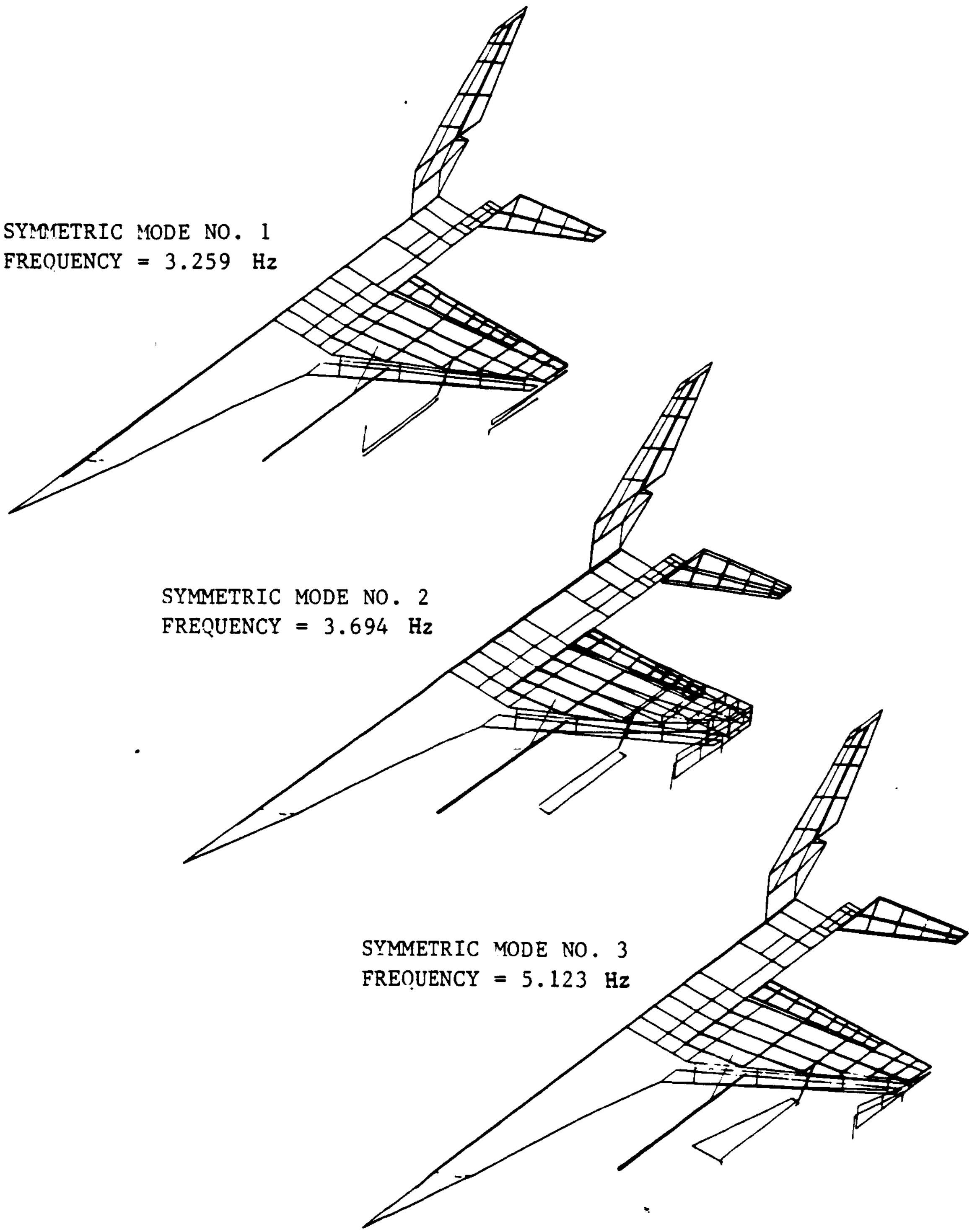

Figure 23.- First three analytical symmetric modes with decoupler pylon stiffness based on test data.

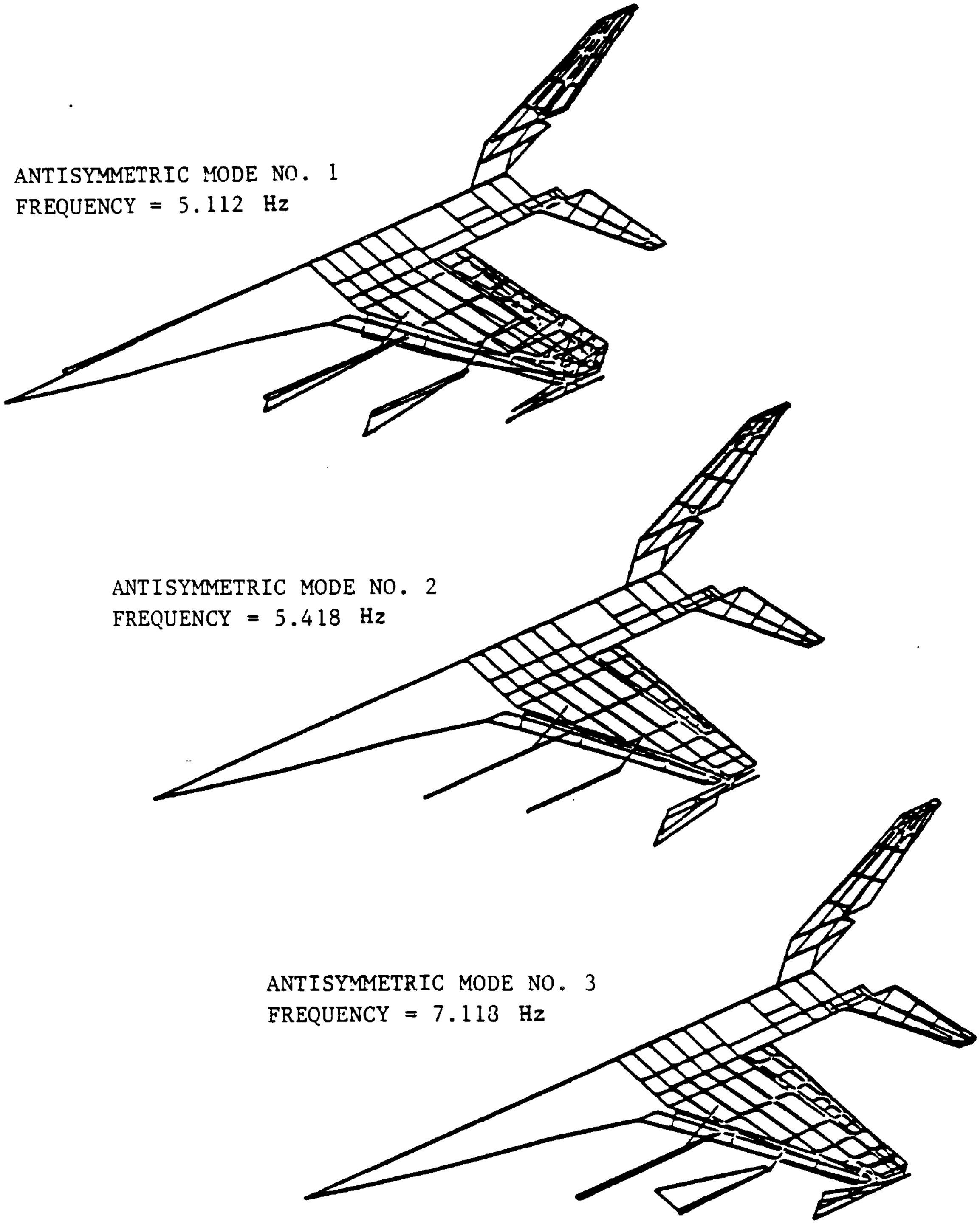

Figure 24.- First three analytical antisymmetric modes with production pylon.

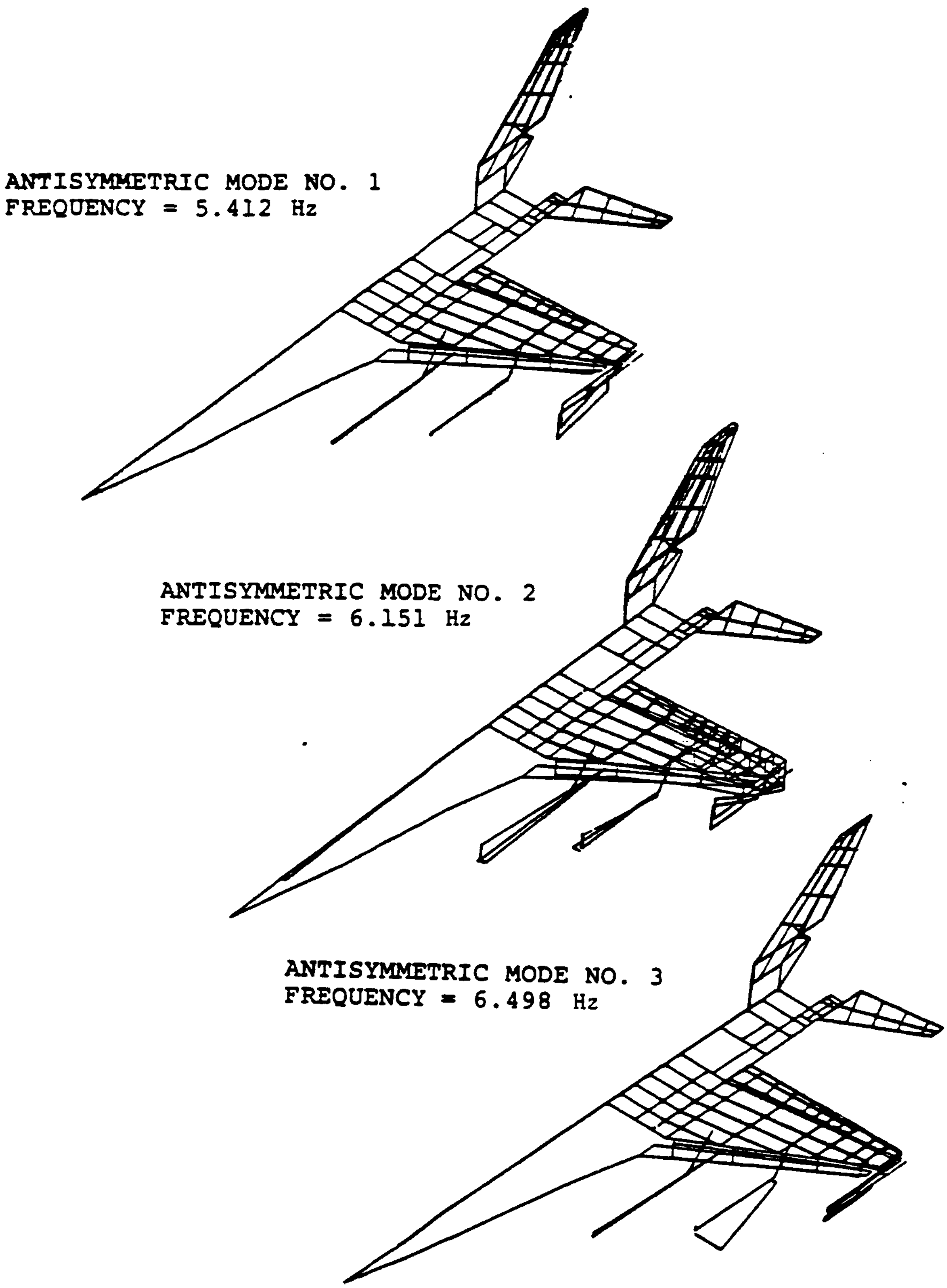

Figure 25.- First three analytical antisymmetric modes with zero pitch stiffness of current design decoupler pylon.

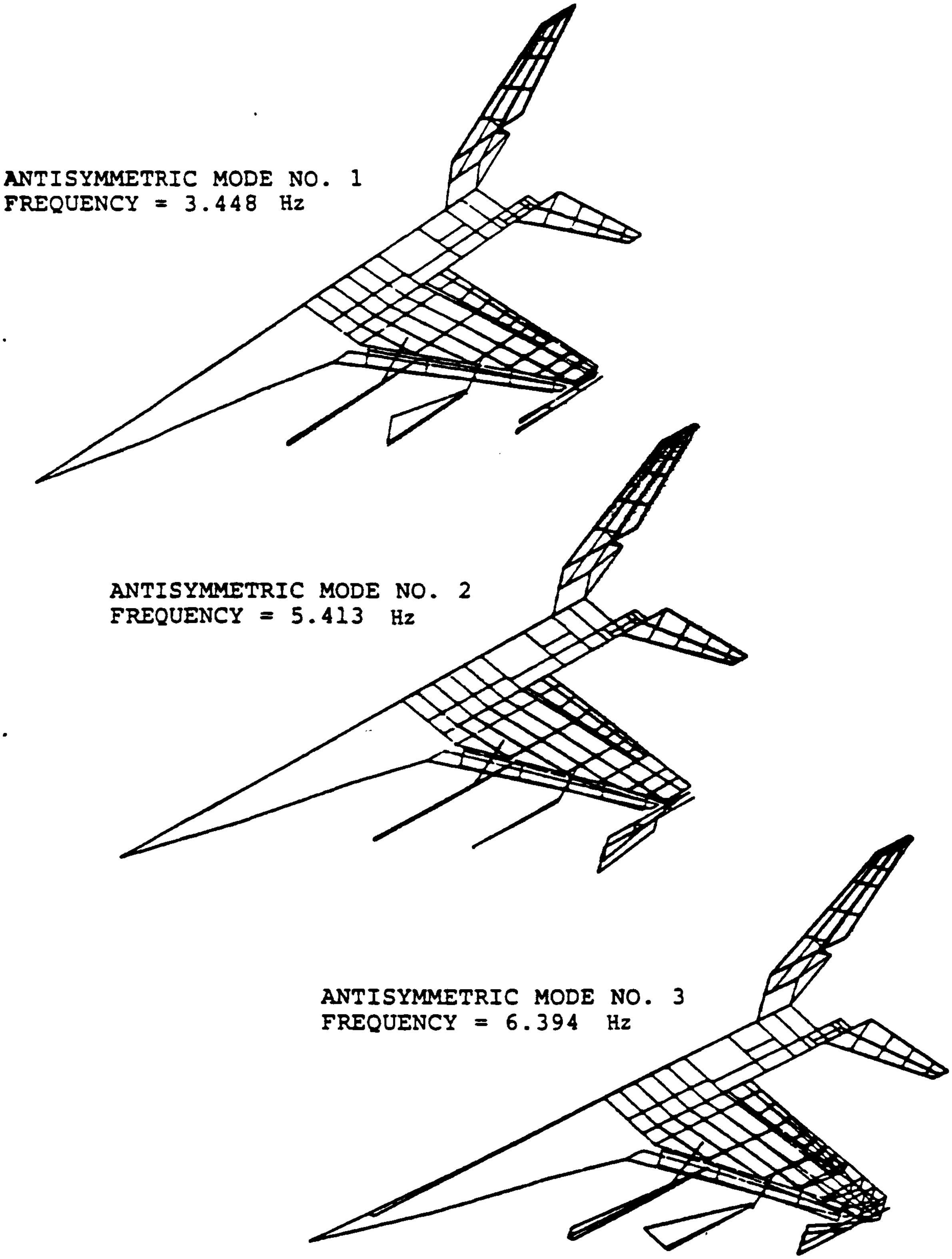

Figure 26.- First three analytical antisymmetric modes with decoupler pylon pitch stiffness equal to 3502 $N \cdot cm^{-1}$ (2000 $lb \cdot in^{-1}$).

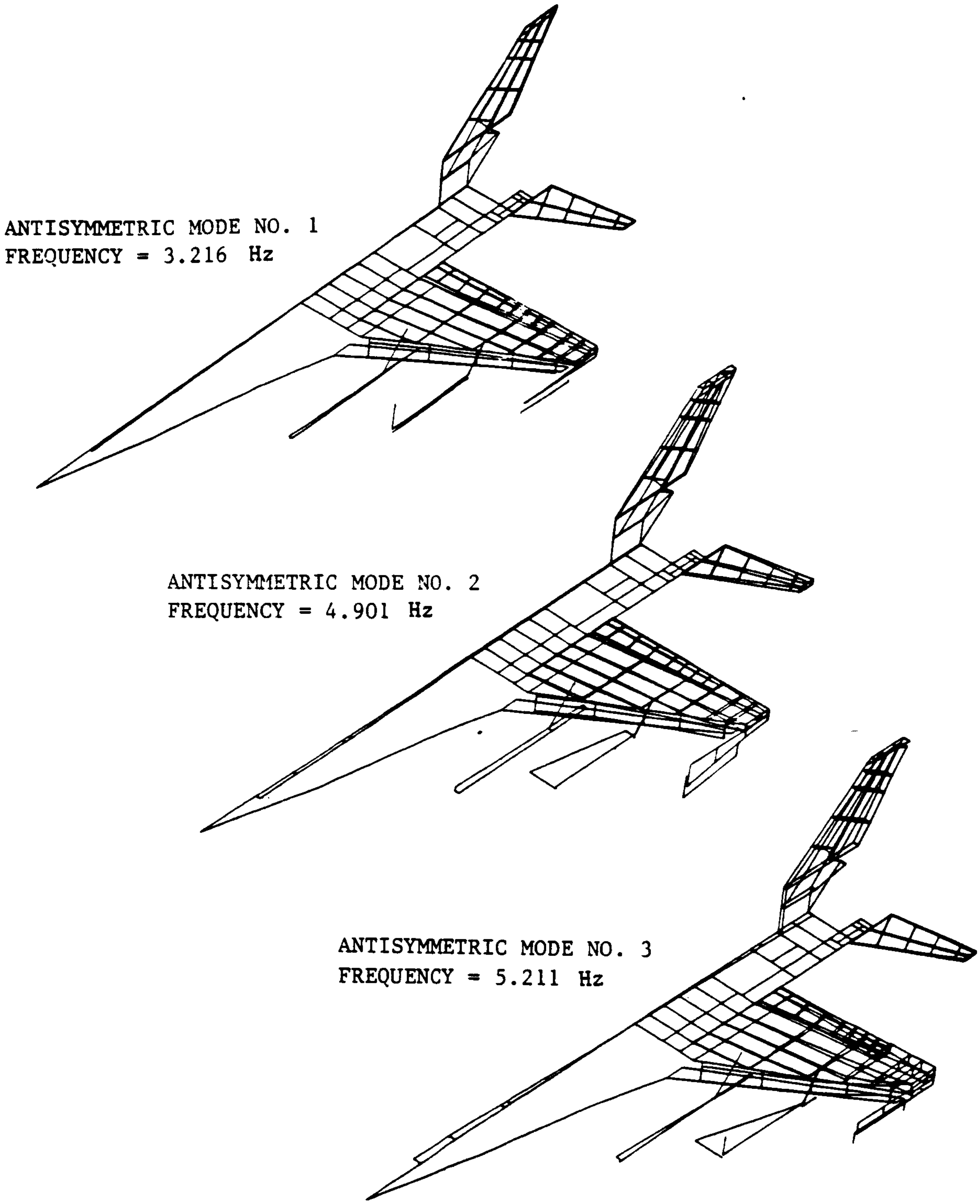

Figure 27.- First three analytical antisymmetric modes with decoupler pylon stiffness based on test data.

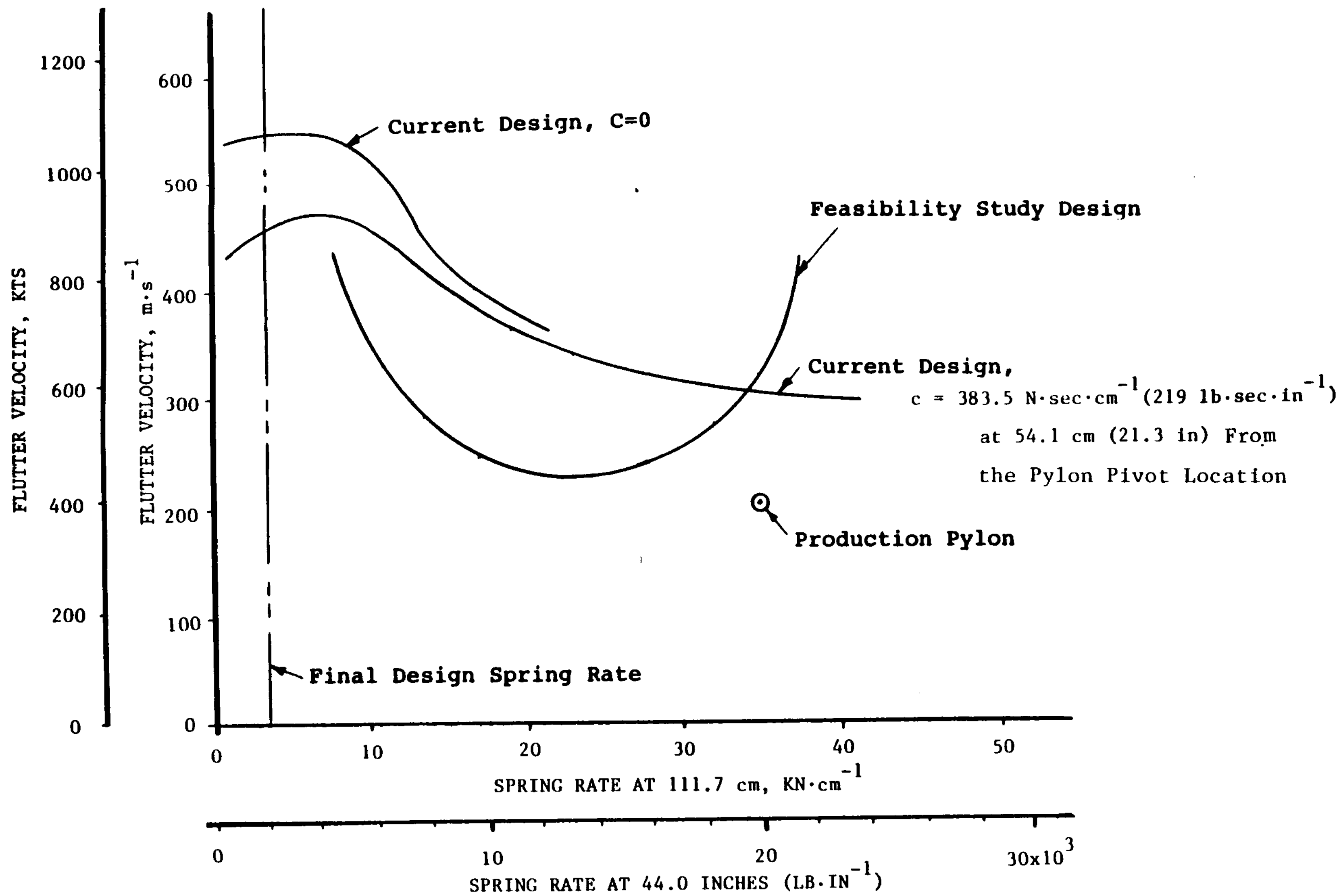

Figure 28.- Effect of pylon spring rate on antisymmetric airframe flutter speeds.

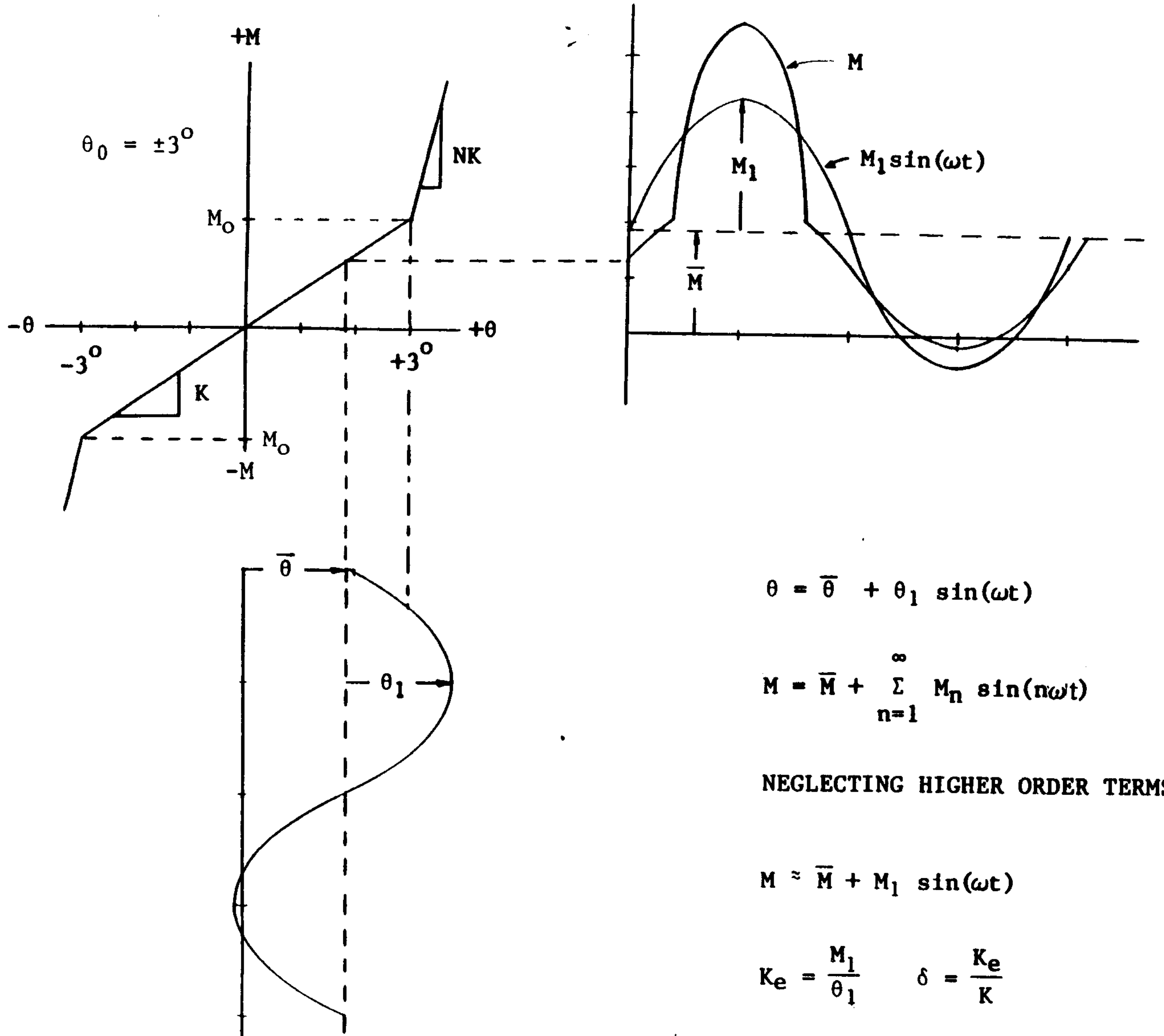

$$\theta = \overline{\theta} + \theta_1 \sin(\omega t)$$

$$M = \overline{M} + \sum_{n=1}^{\infty} M_n \sin(n\omega t)$$

NEGLECTING HIGHER ORDER TERMS

$$M \approx \overline{M} + M_1 \sin(\omega t)$$

$$K_e = \frac{M_1}{\theta_1} \qquad \delta = \frac{K_e}{K}$$

Figure 29.- Calculation of the describing function for a bilinear spring.

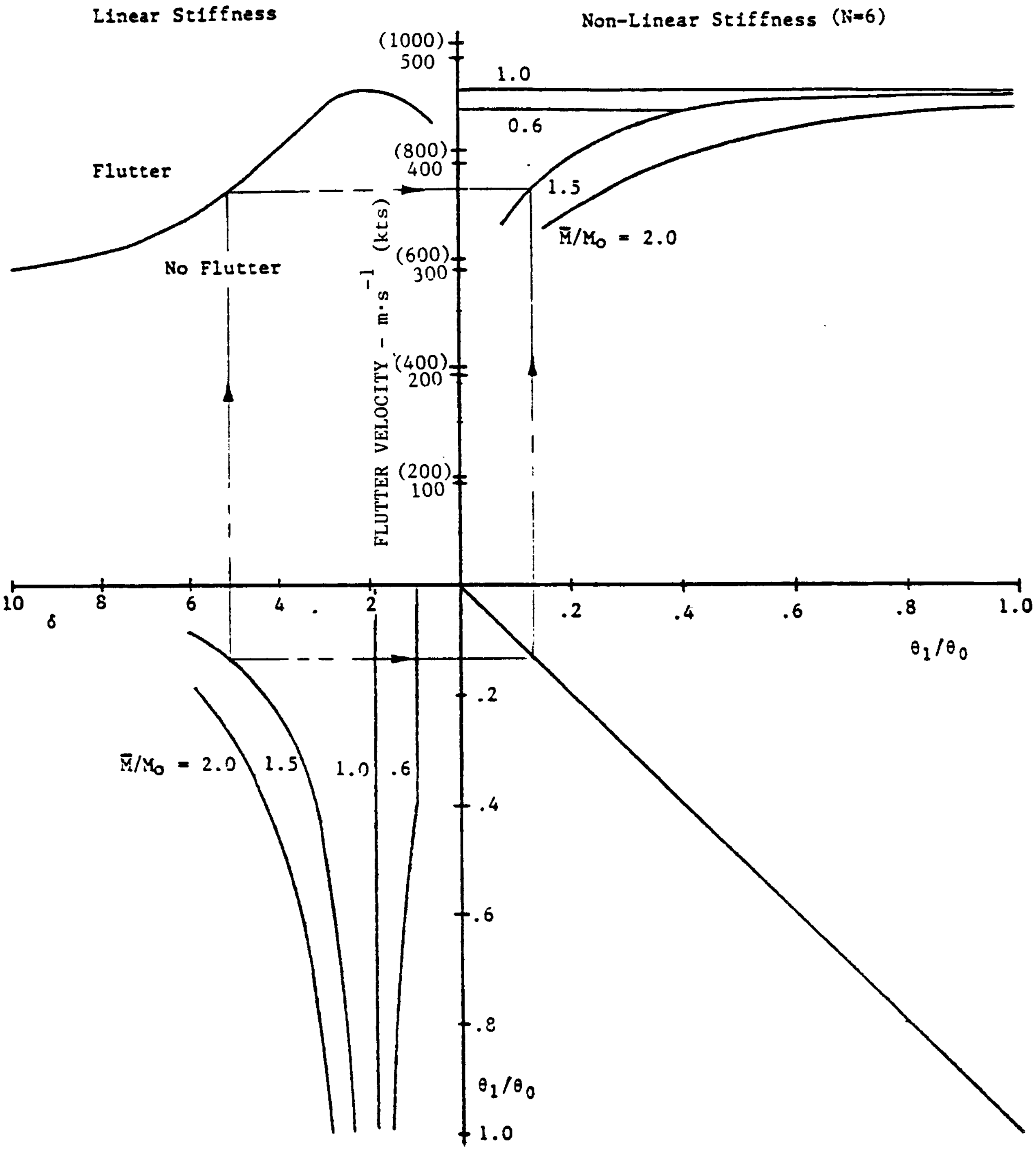

Figure 30.- Flutter boundary determination with non-linear pylon stiffness. Stiffness ratio (N)=6.

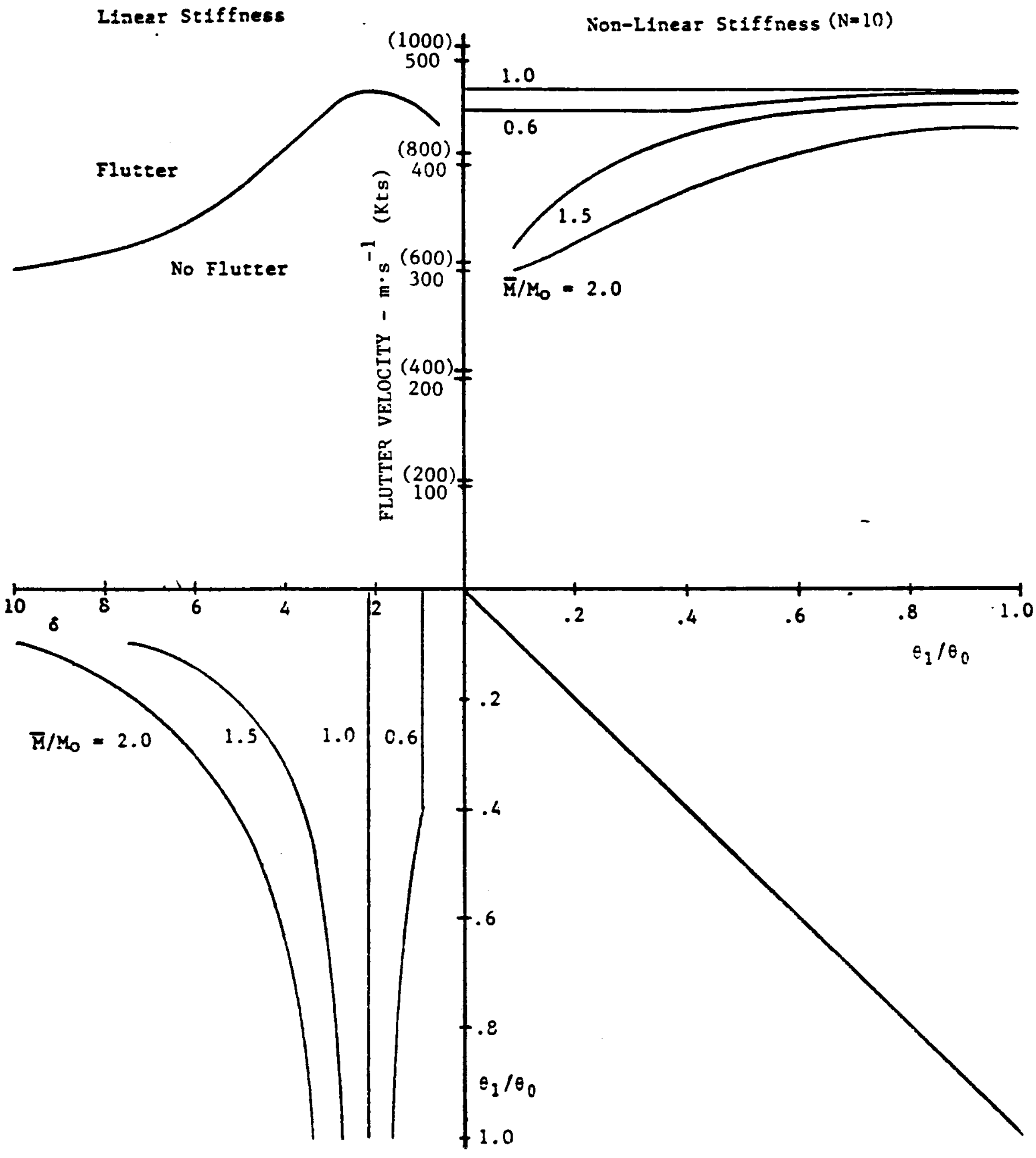

Figure 31.- Flutter boundary determination with non-linear pylon stiffness. Stiffness ratio (N)=10.

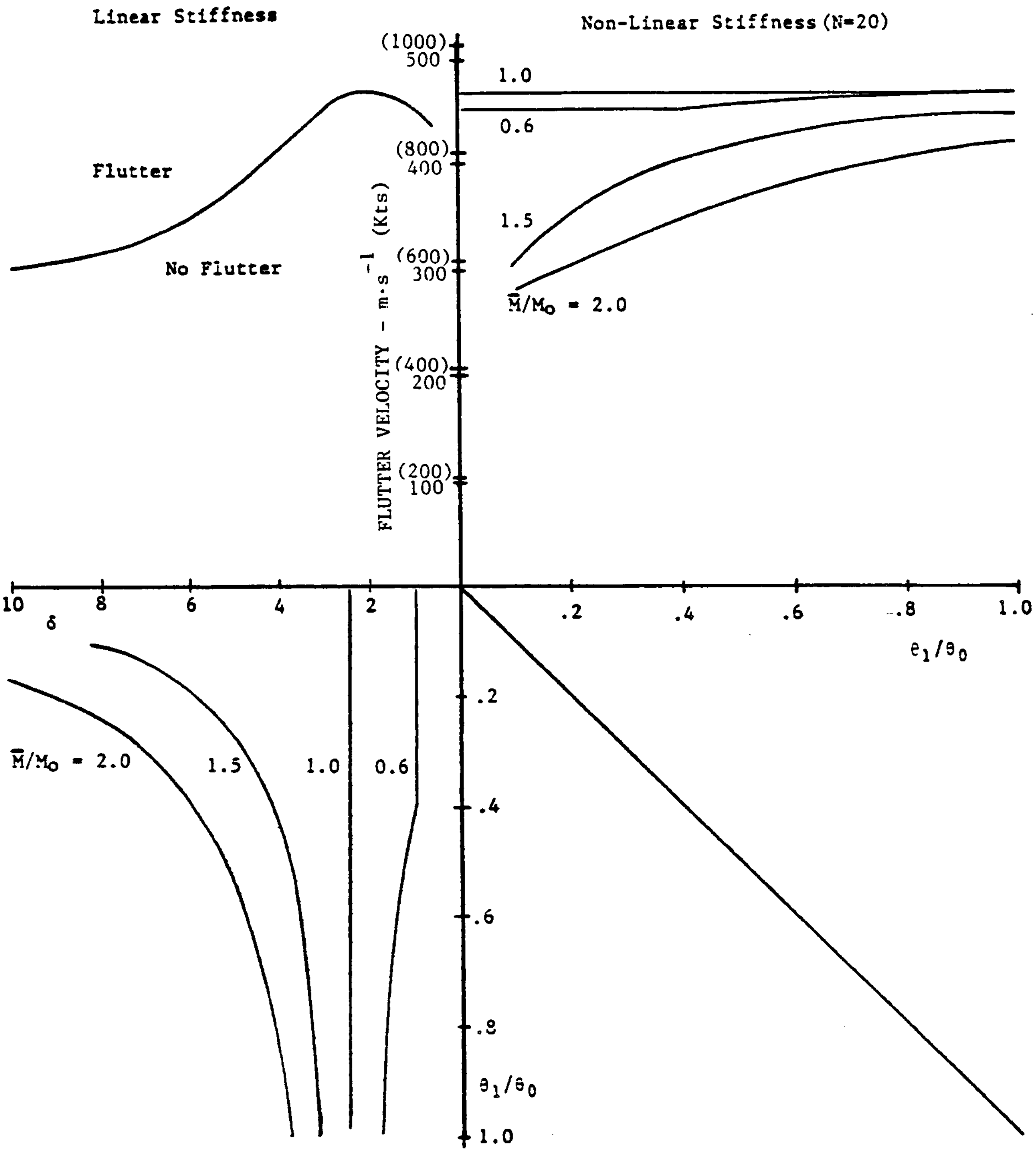

Figure 32.- Flutter boundary determination with non-linear pylon stiffness. Stiffness ratio (N)=20.

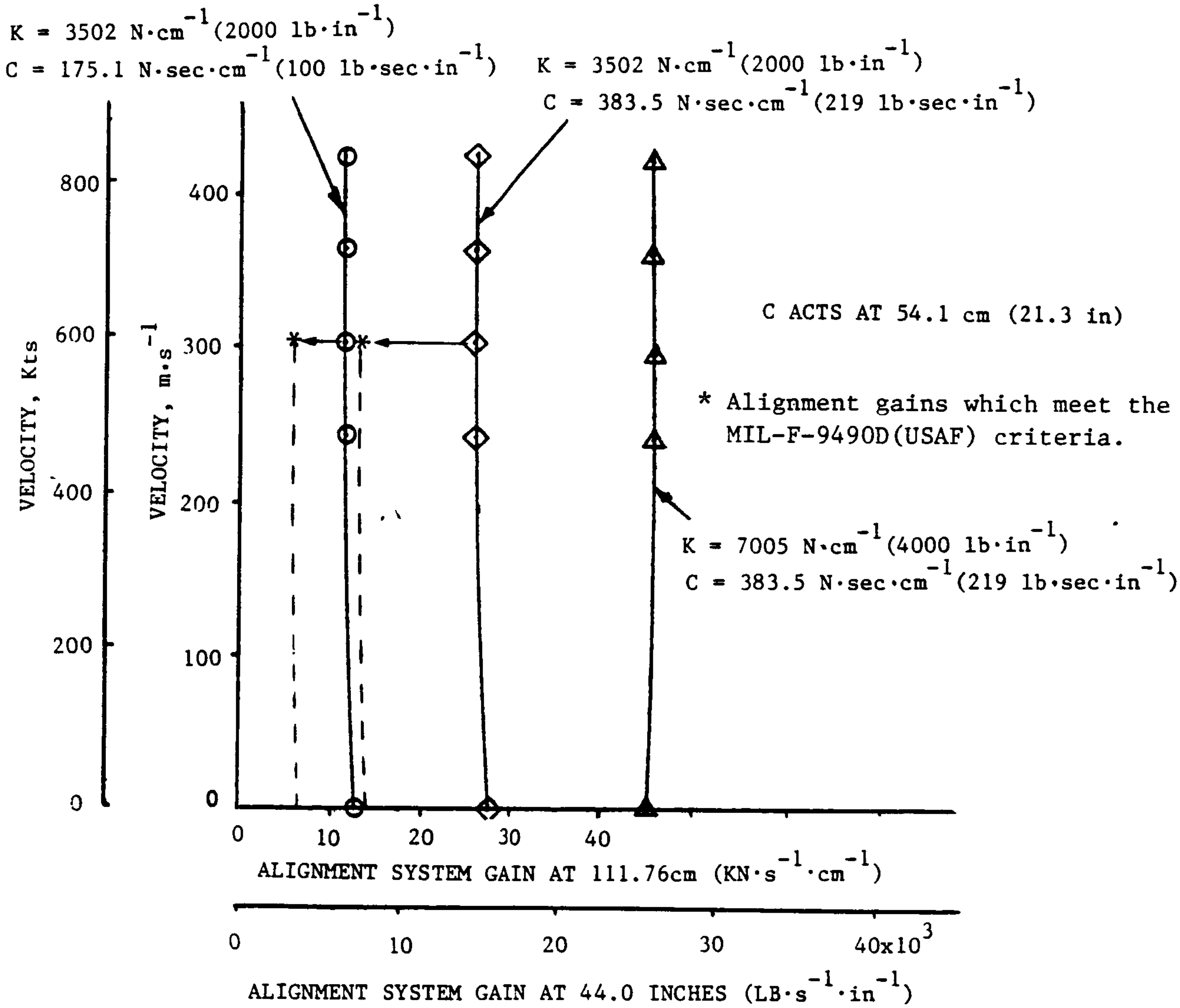

Figure 33.- Antisymmetric alignment gain versus airspeed.

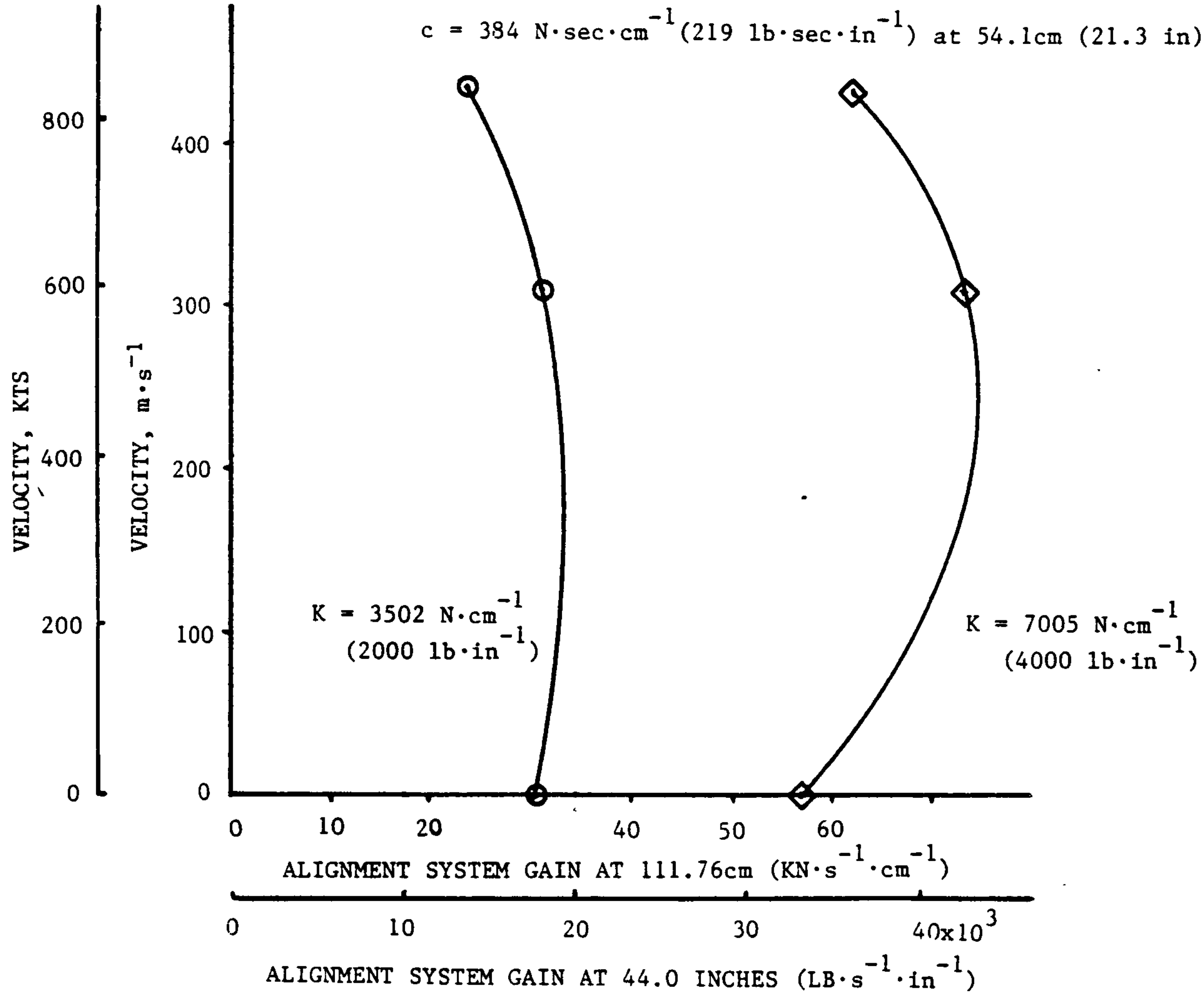

Figure 34.- Symmetric alignment gain versus airspeed.

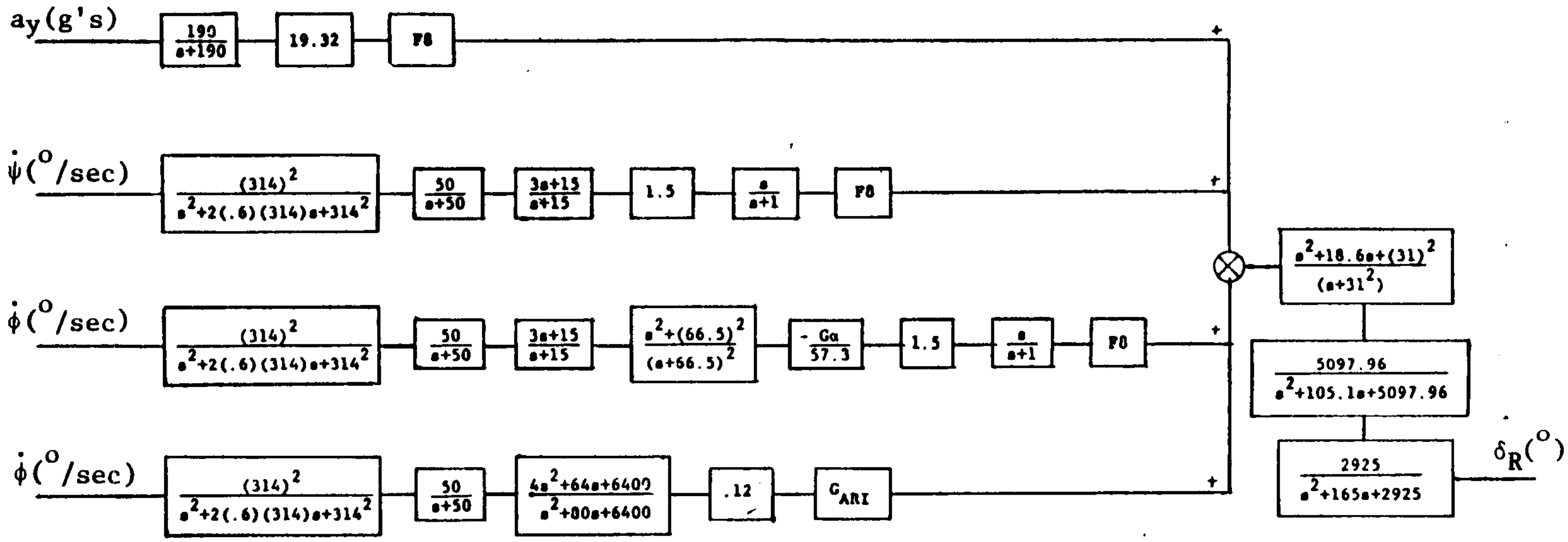

a_y - Lateral Acceleration
$\dot{\psi}$ - Yaw Rate
$\dot{\phi}$ - Roll Rate
δ_R - Rudder

Figure 35.- **F-16 antisymmetric flight control system block diagram (yaw channel).**

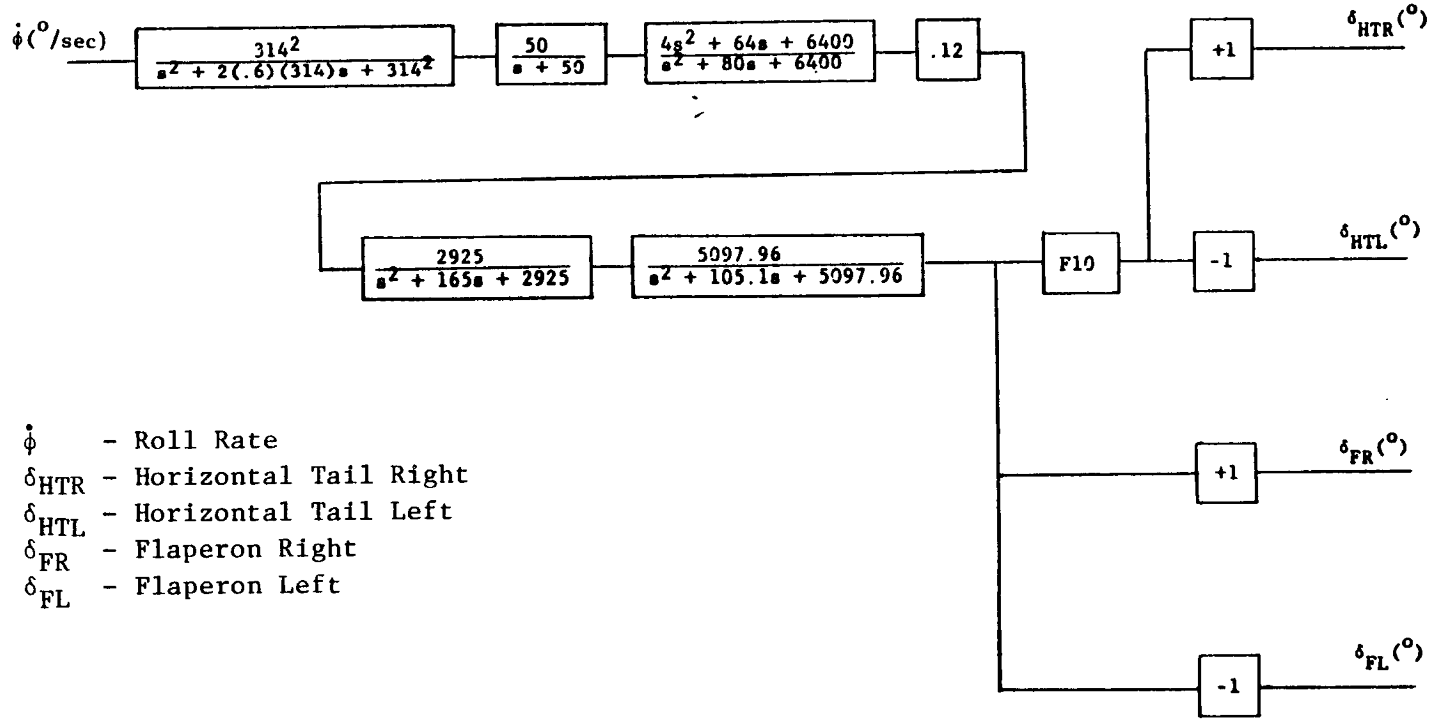

$\dot{\phi}$ - Roll Rate
δ_{HTR} - Horizontal Tail Right
δ_{HTL} - Horizontal Tail Left
δ_{FR} - Flaperon Right
δ_{FL} - Flaperon Left

Figure 36.- **F-16 Antisymmetric flight control system block diagram (roll channel).**

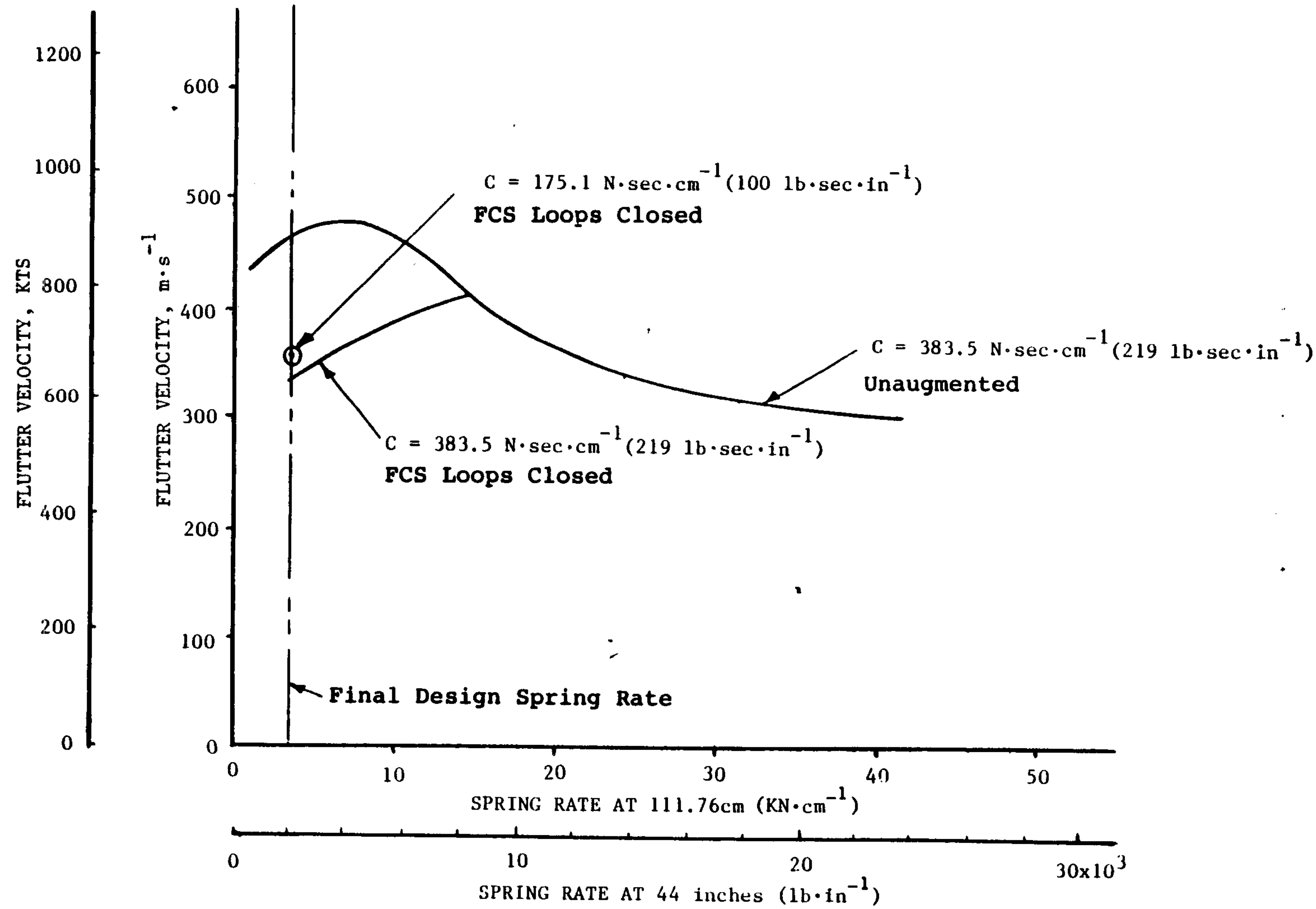

Figure 37.- Effect of flight control system on flutter speed.

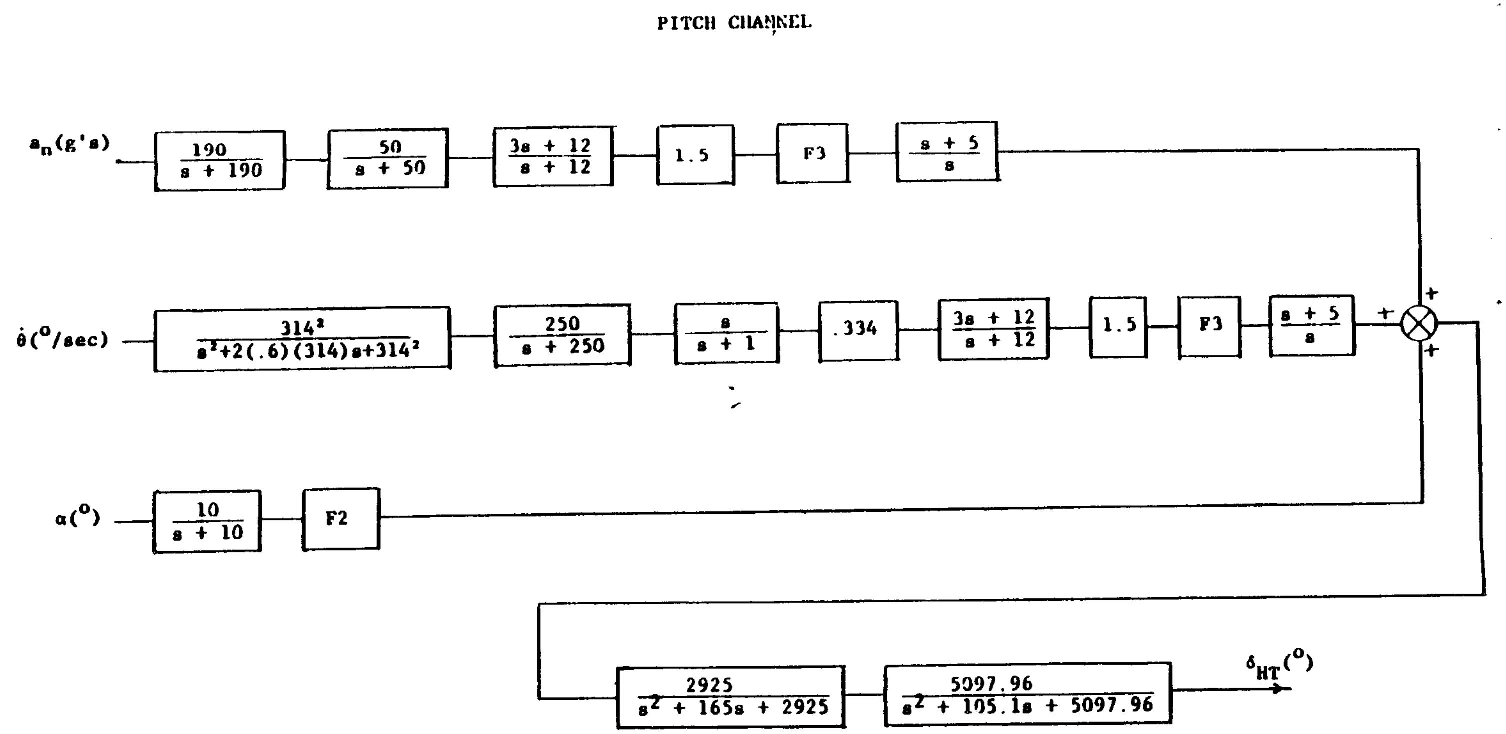

a_n - Normal Acceleration
$\dot{\theta}$ - Pitch Rate
α - Angle of Attack
δ_{HT} - Horizontal Tail

Figure 38.- **F-16 symmetric flight control system block diagram.**

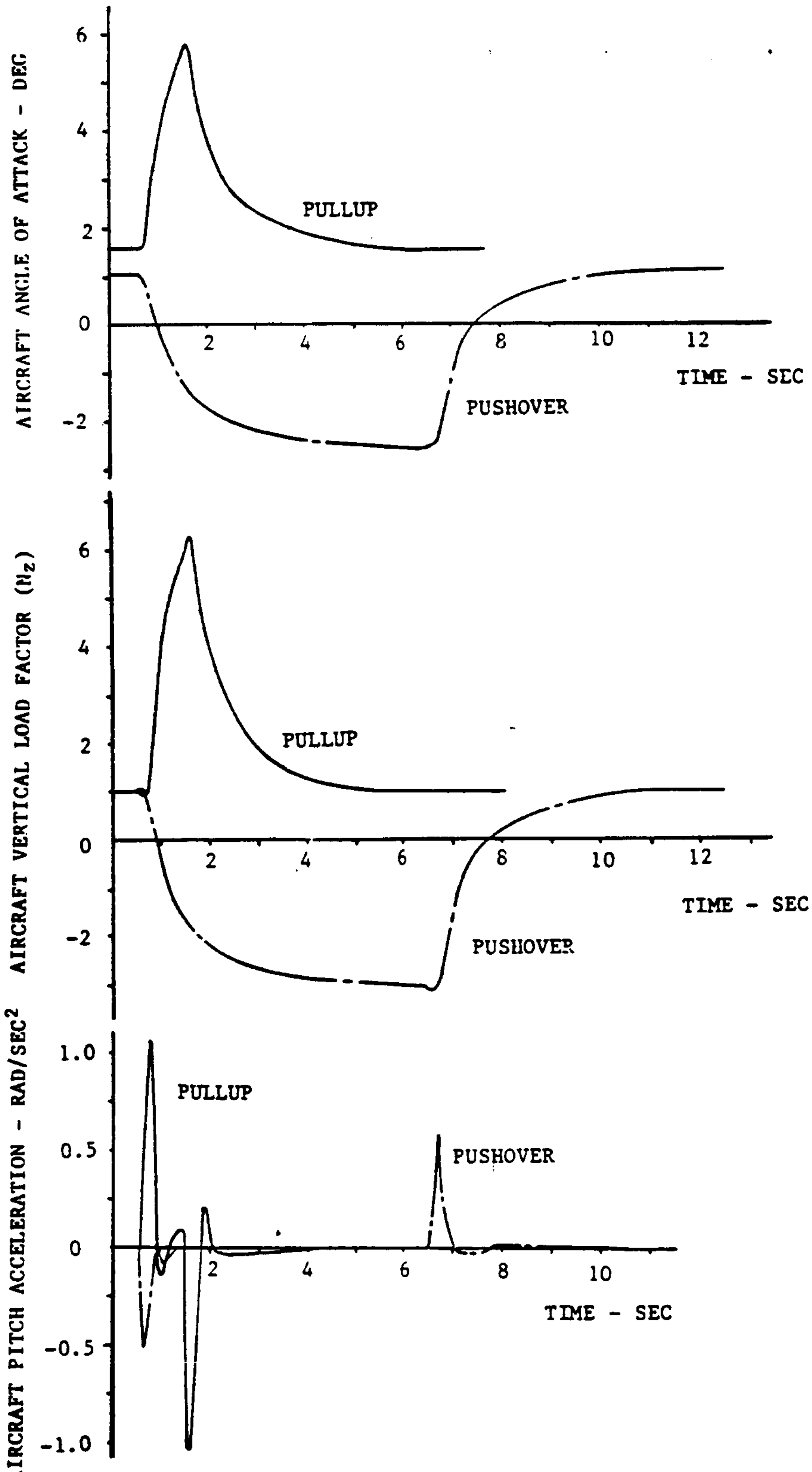

Figure 39.- Aircraft flight parameters for symmetric pullup pushover maneuvers, altitude = S.L., M=0.9.

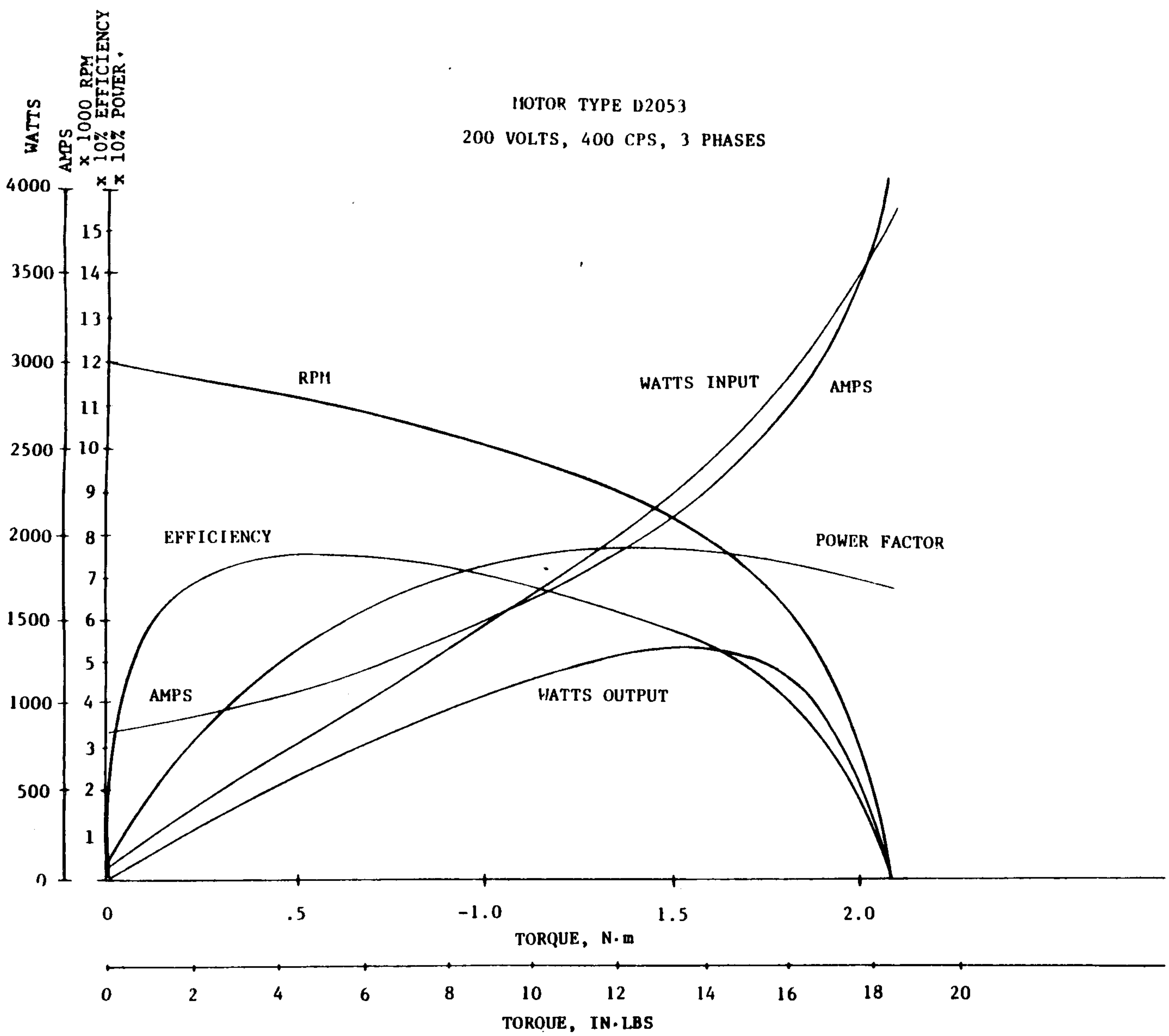

Figure 40.- Motor parameters.

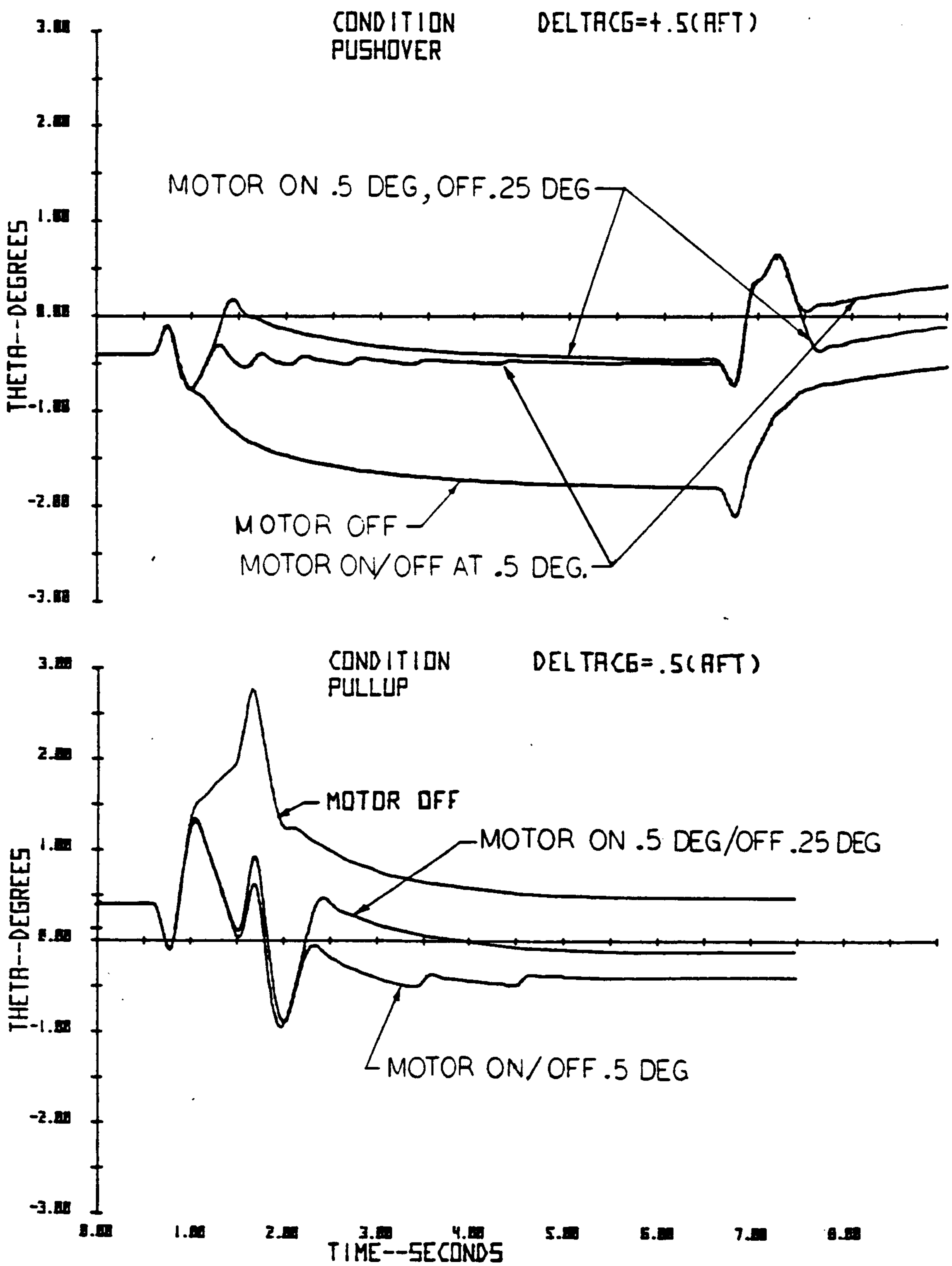

Figure 41.- Store alignment system performance for symmetrical pullup and pushover maneuvers.

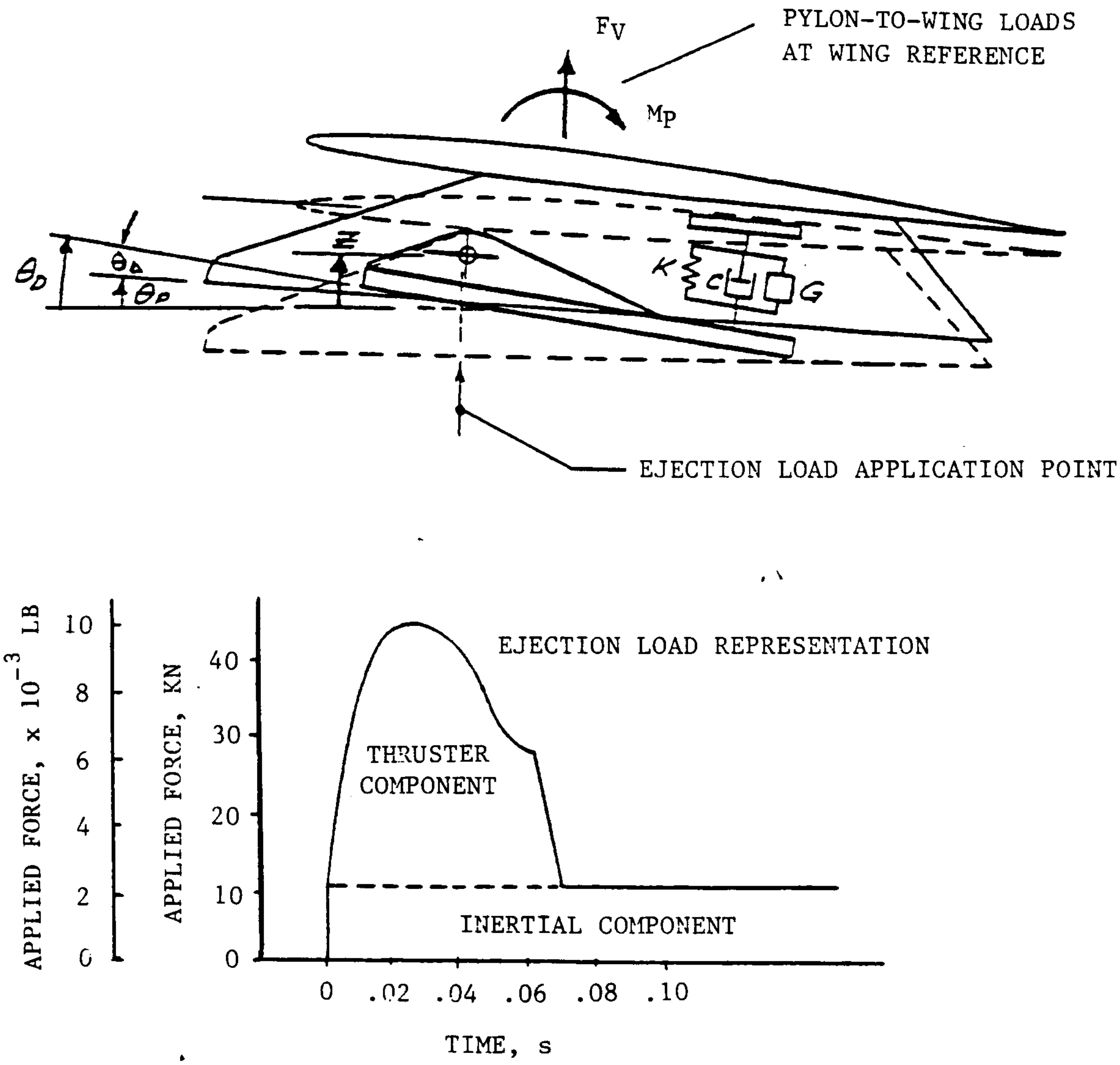

Figure 42.- Single store (GBU-8) ejection analysis representation.

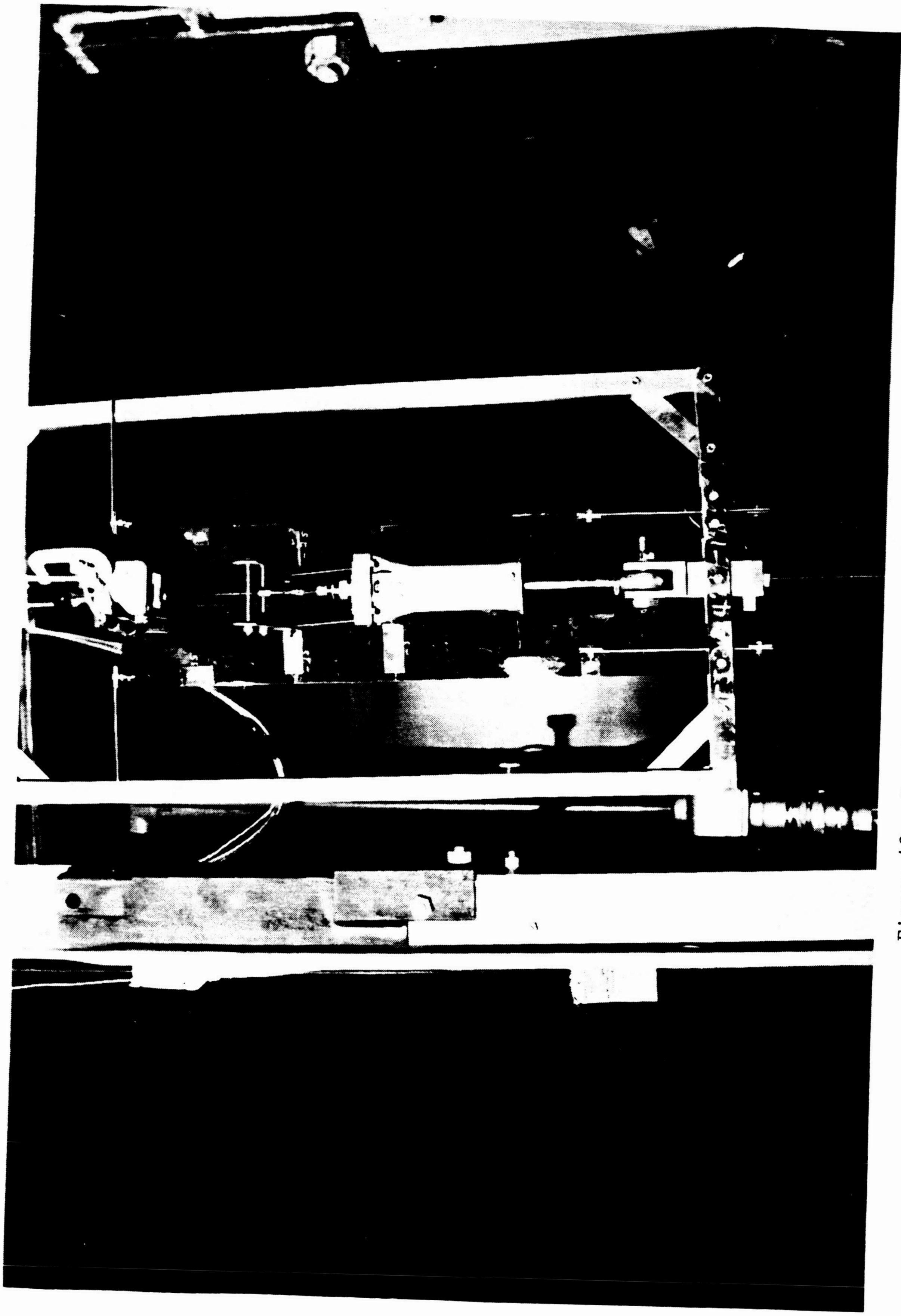

Figure 43.- Tension test set-up for damper.

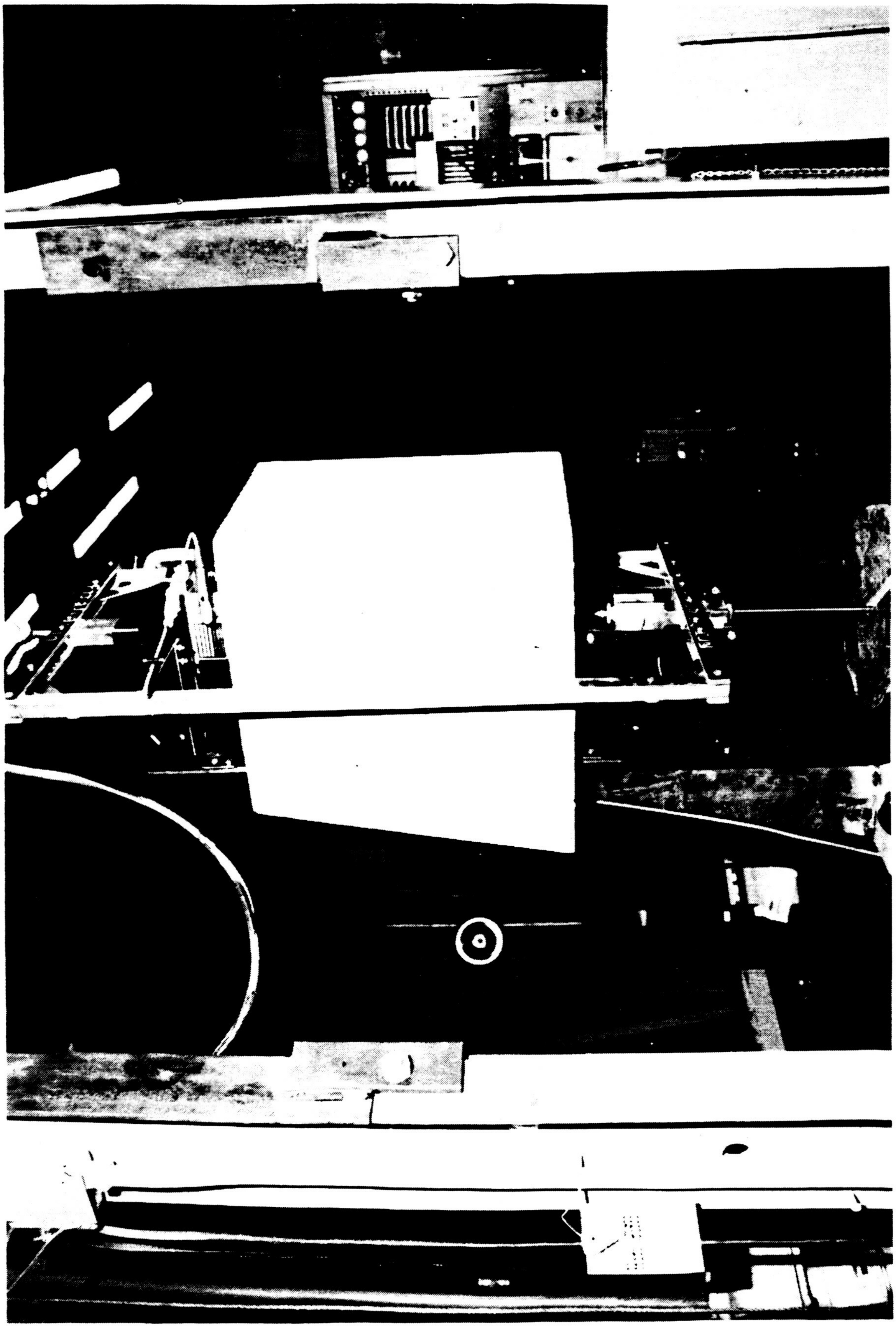

Figure 44.- Environmental chamber installation for damper test.

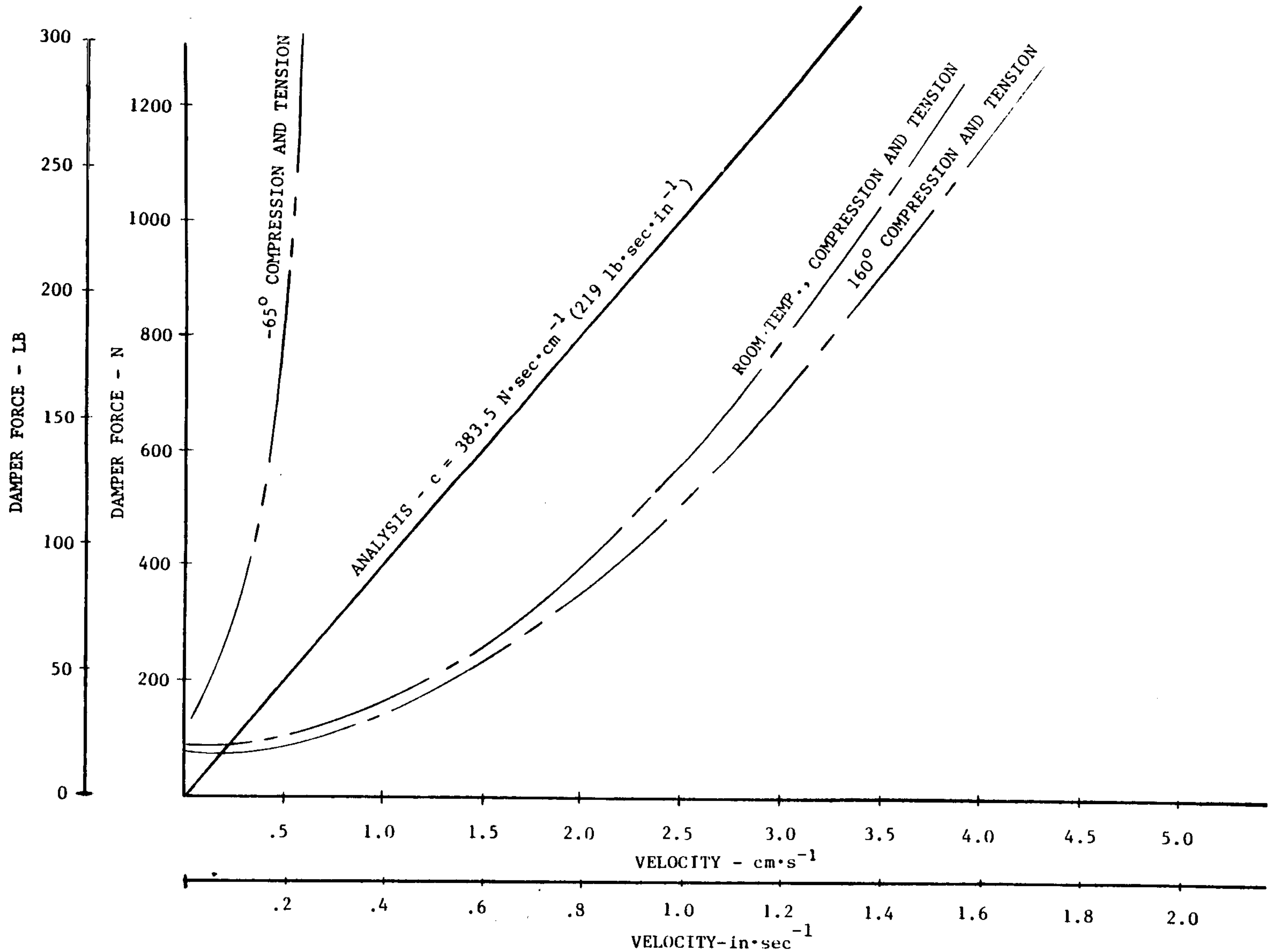

Figure 45.- Decoupler pylon damper test results.

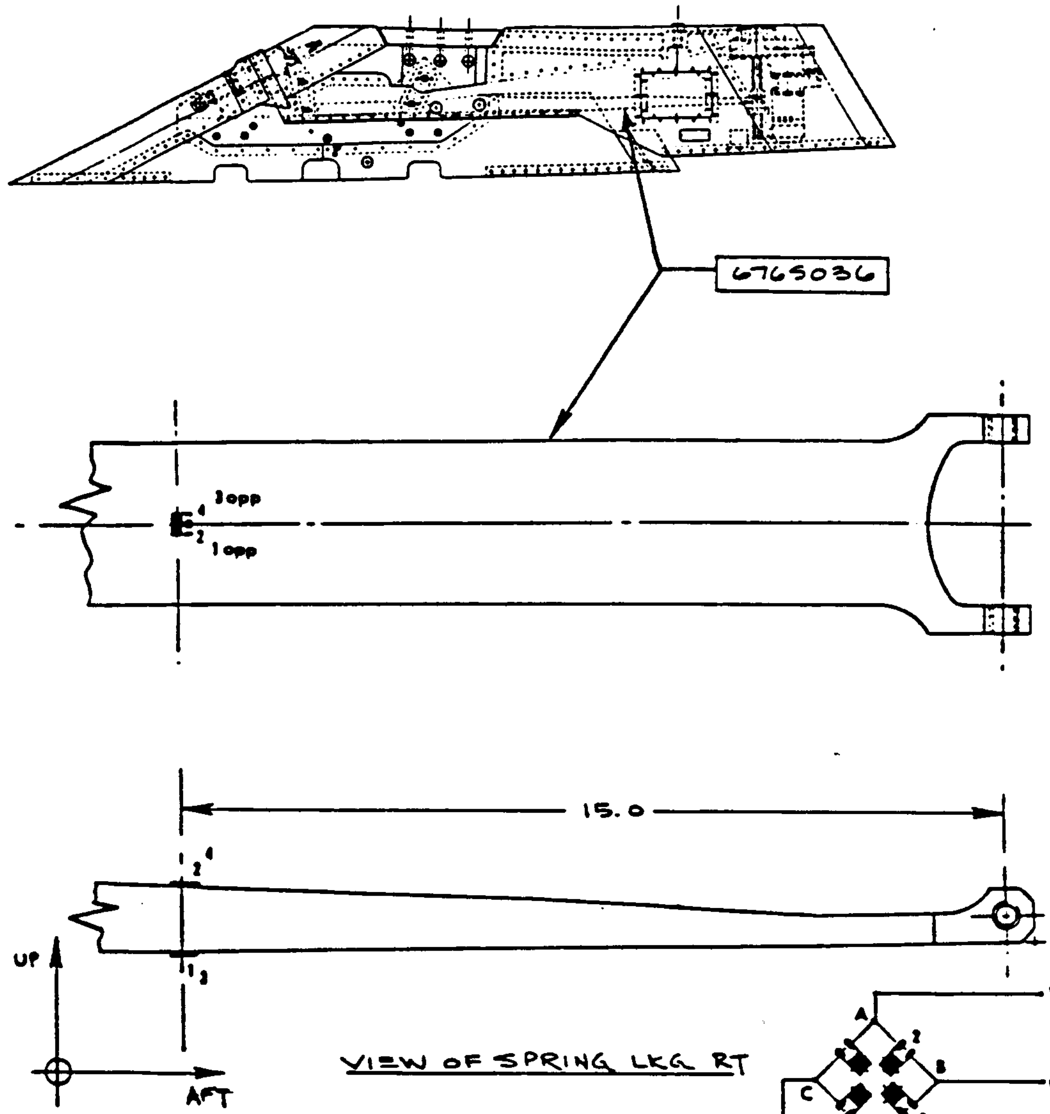

BRIDGE CODE No	GAGES	MEAS	LOCATION
SS248	1 – 4	F_Z	
SS 248J	MEAS. @ STA. 3		LH BL 120
SS 248T	MEAS. @ STA 7		RH BL 120

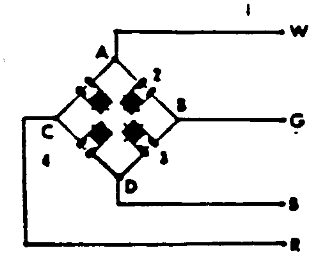

WIRING DIAGRAM

Figure 46.- NASA decoupler pylon loads measurement instrumentation spring (676S036) installation.

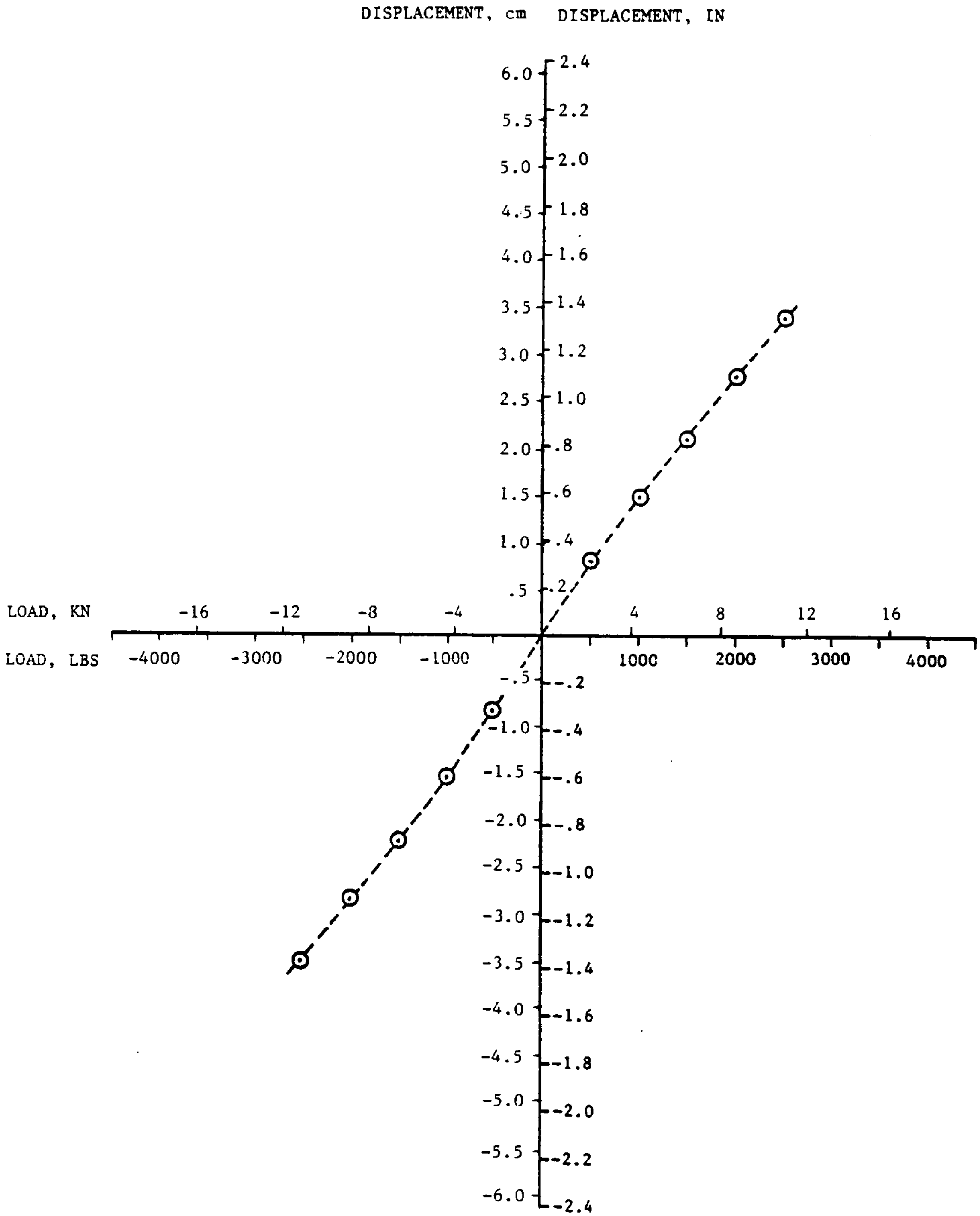

Figure 47.- Decoupler pylon spring no. 1, load vs. displacement.

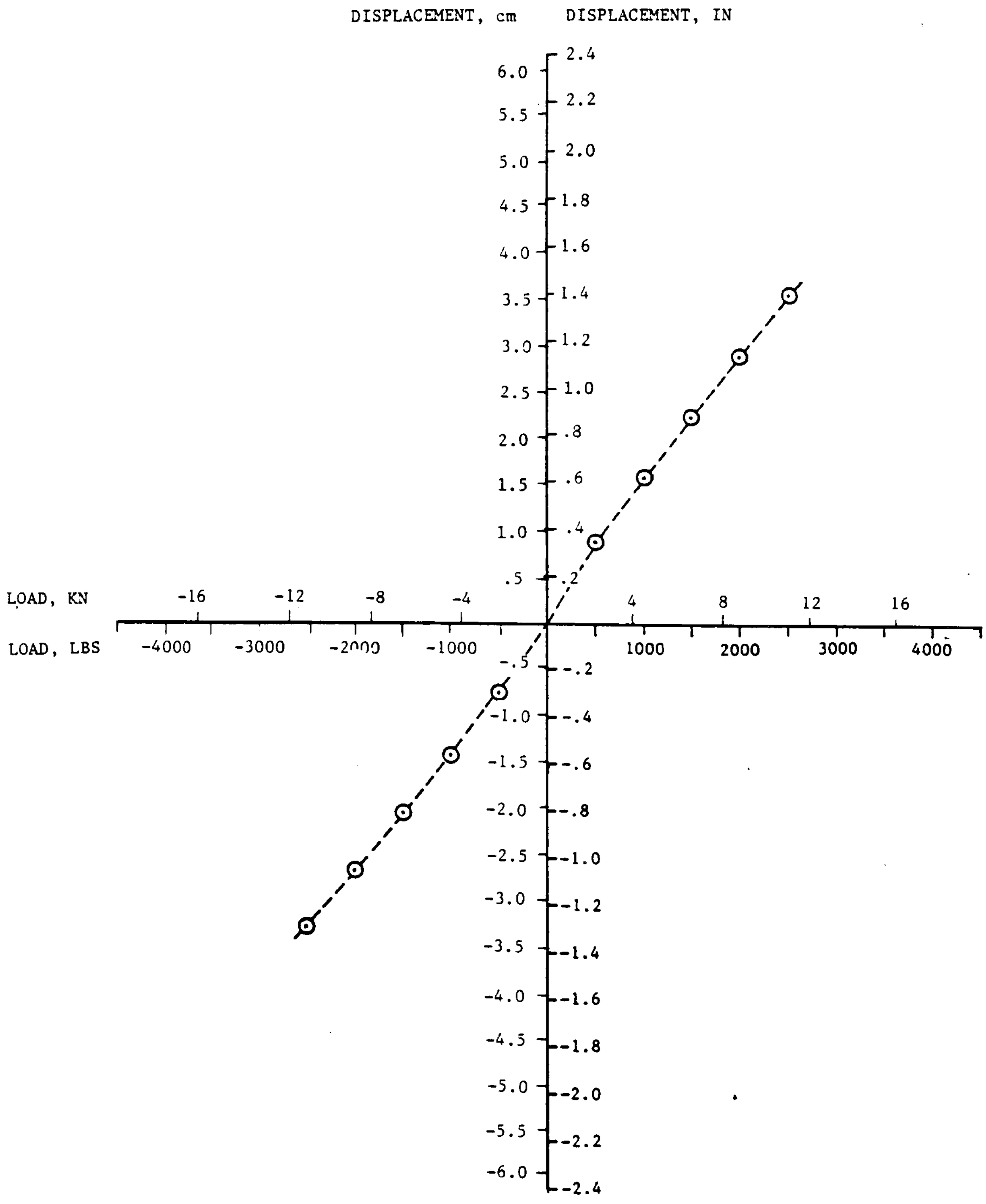

Figure 48.- Decoupler pylon spring no. 2, load vs. displacement.

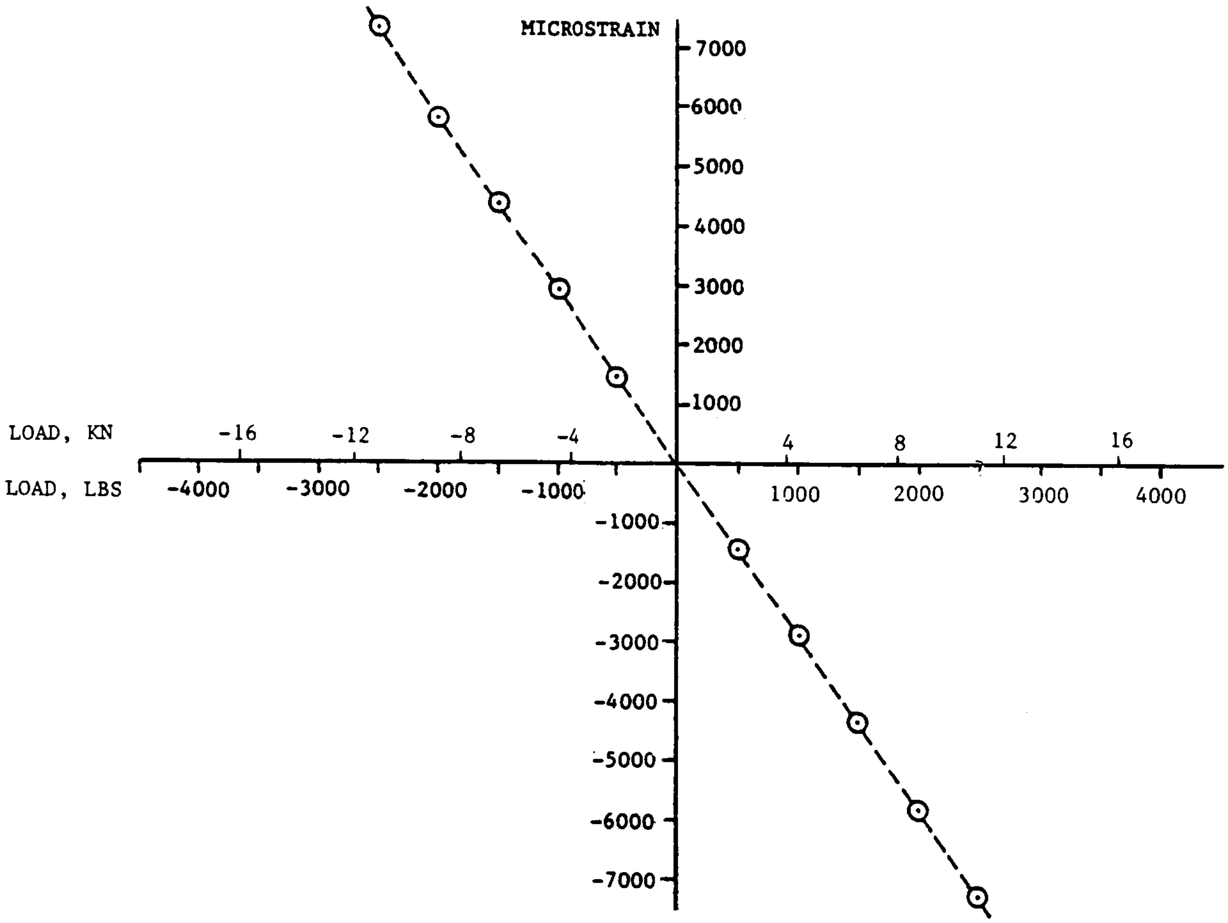

Figure 49.- Decoupler pylon spring no. 1, load vs. strain.

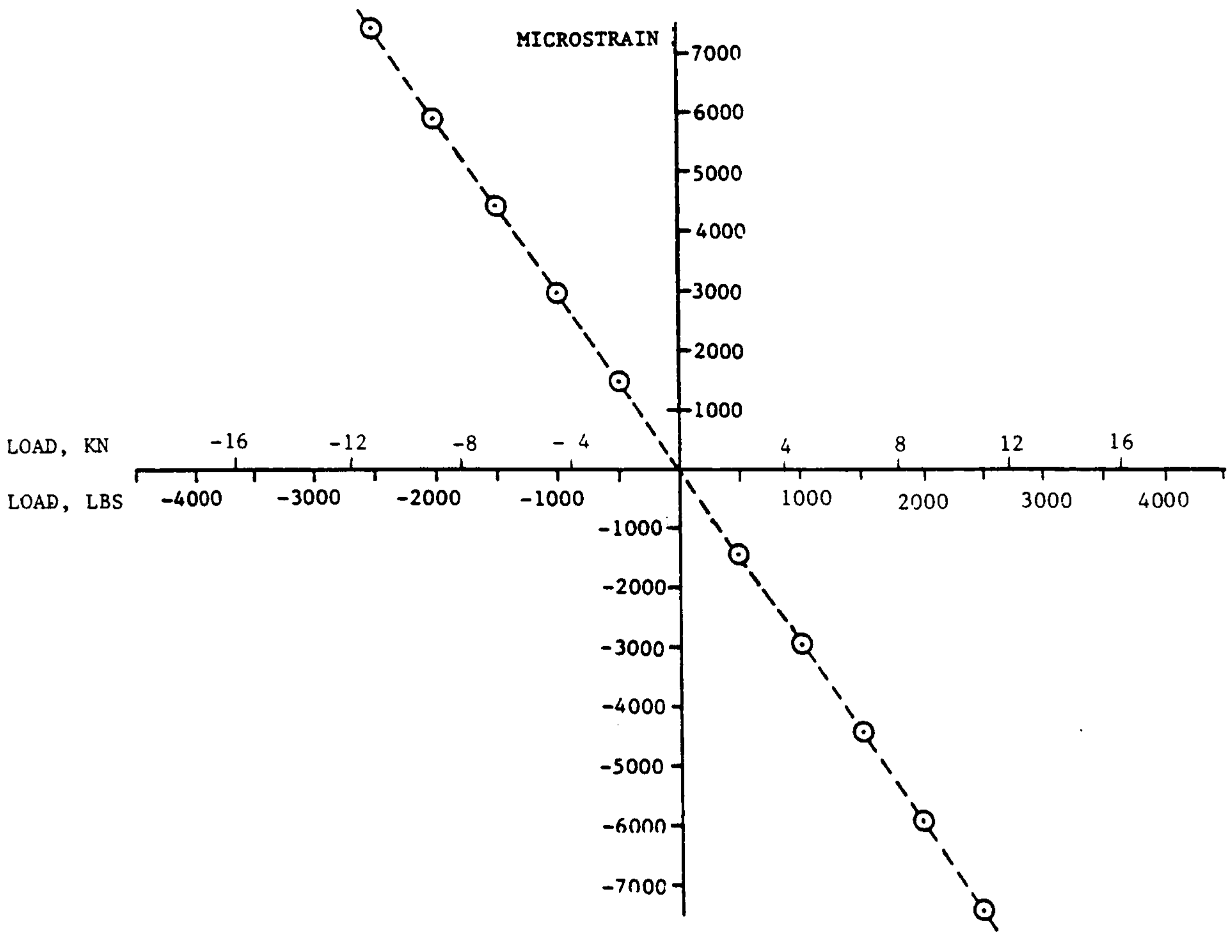

Figure 50.- Decoupler pylon spring no. 2, load vs. strain.

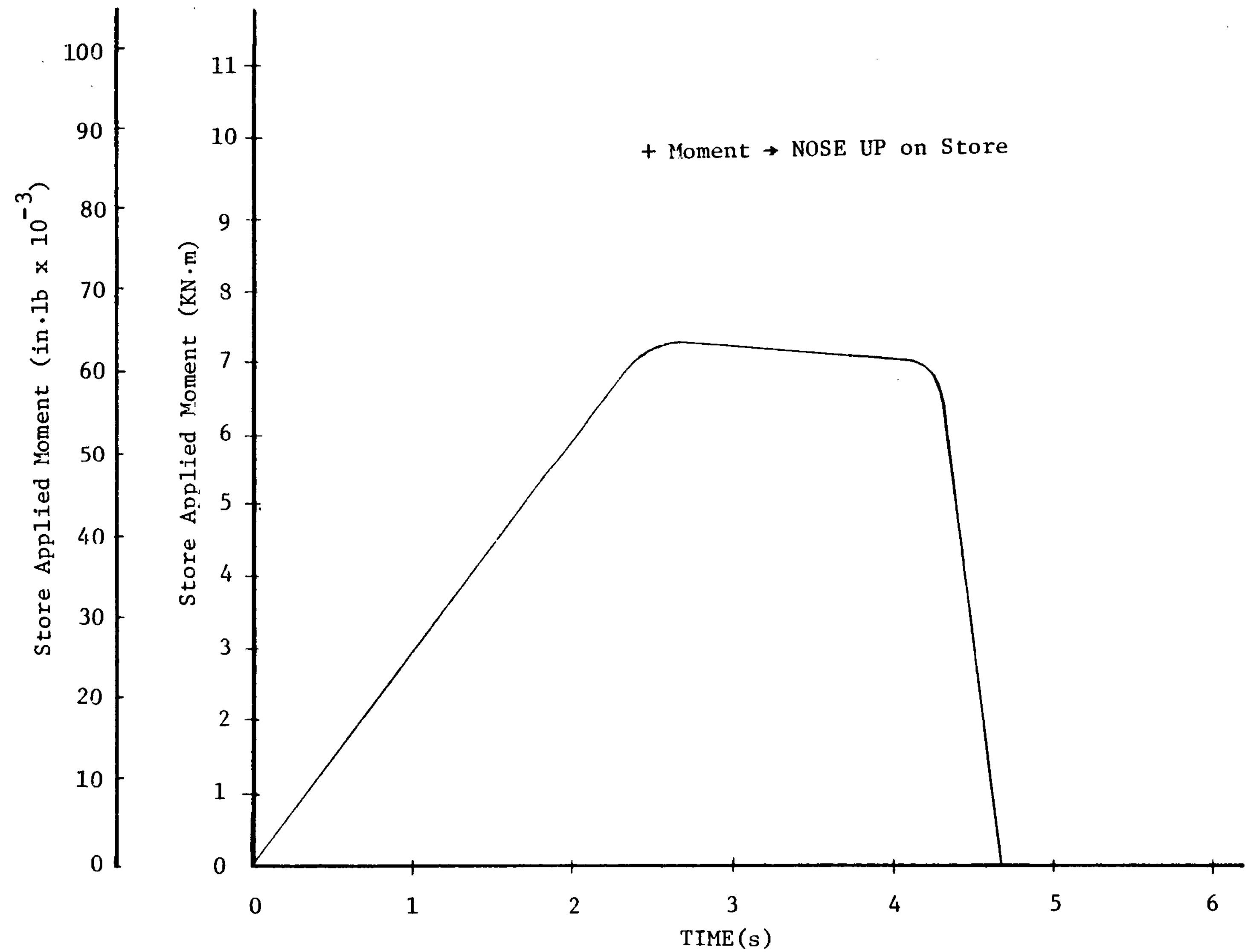

Figure 51.- Store applied pitching moment vs. time.

Dimensions In Inches

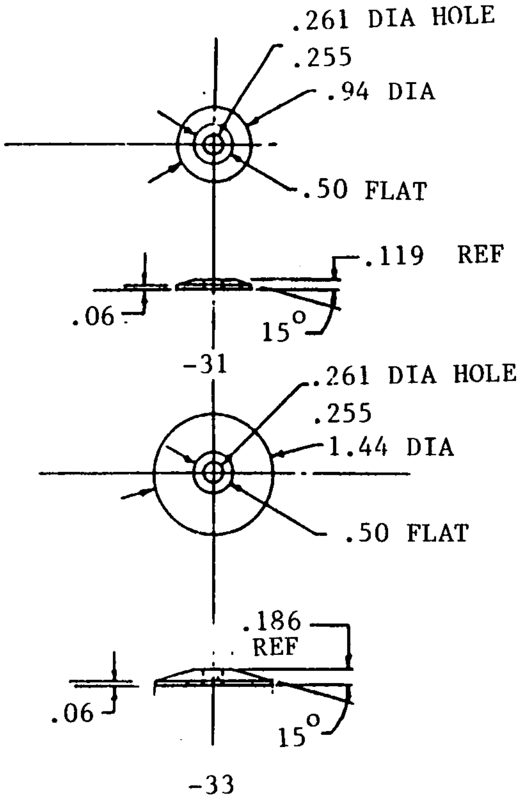

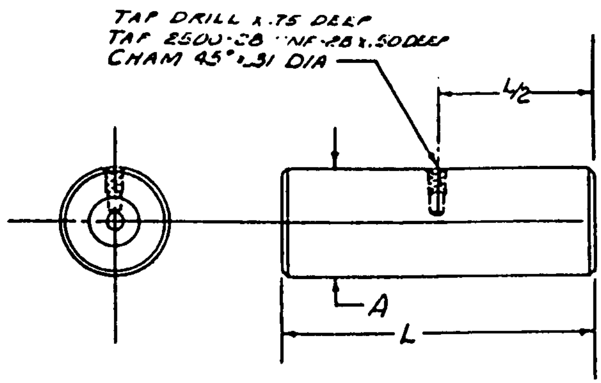

DASH NO.	L ±.03	A ±.0003	B ±.015
-23	4.81	1.1263	.46
-25	4.47	1.2483	.38
-27	5.97	1.3742	.75
-29	4.47	1.1233	.38

DASH	MAKE	MAT'L	FIN
-31	4	QQ-A-268	A402
-33	4	QQ-A-268	A402

676 5033 PIN MOD
26 MAR 83

Figure 52.- Modified pin retainer system.

APPENDIX A

Drawing Numbers and Parts

This appendix contains the final design drawing numbers and information on how these drawings are used in the pylon assembly. Each engineering change order which was issued during the course of the design and fabrication phases are also documented. A drawing tree which identifies the drawing numbers and their relationship with each other is also included.

TABLE A1.- NASA DECOUPLER PYLON CONFIGURED ARTICLES LIST

PAGE 1 OF 6

CONTRACT END ITEM NUMBER: DP67600

CEI DRAWING NUMBER: 676S001

CEI PART NUMBER: 676S001-1

CEI SERIAL NUMBER: 001 & 002

CONTRACT END ITEM NOMENCLATURE: NASA DECOUPLER PYLON

MANUFACTURER: GENERAL DYNAMICS/FORT WORTH DIVISION

CONTRACT MANAGEMENT PLAN:
676PP002, dated 25 February 1982
Revision A, dated 26 April 1983

CONFIGURATION MANAGEMENT PLAN:
676PP003, dated 15 April 1982
(Previously FZM-6973)

DESIGN AND PERFORMANCE SPECIFICATION:
676PS002, dated 18 June 1982
Revision A, dated 21 April 1983

INTERFACE REQUIREMENTS AND CONTROL DOCUMENT:
676PS001, dated 26 April 1982
Rev. A, 15 June 1982: Rev. B, 21 April 1983

ACCEPTANCE TEST PLAN:
676PR009, dated 15 December 1982

END ITEM DATA PACKAGE:

1. CLASS I CHANGES (NONE)
2. CLASS II CHANGES (ECNs)
3. FAILURE REPORTS (NONE)
4. DISCREPANCY REPORTS (NONE)
5. DRAWING LIST
6. CONFIGURED ARTICLES LIST
7. DRAWINGS
8. DESIGN/PERFORMANCE SPEC.
9. SPARE PARTS LIST (DWG. 676S300)
10. DD250 FORM
11. OPERATING & SUPPORT HAZARD ANALYSIS REPORT

INTENDED USE: DECOUPLER PYLON AIRCRAFT MODIFICATION

INDENTURE 1	2	3	4	5	6	DRAWING/PART NUMBER(S)	REV LTR	DRAWING DATE	LINE ITEM NOMENCLATURE
X						676Z001-1		09-07-83	NASA DECOUPLER PYLON
	X					676S100-1,-7	B	04-18-83	PYLON INSTALLATION
		X				676S001-1	C	04-18-83	PYLON ASSEMBLY
			X			676S002-1	A	03-09-83	SUPPORT ASSEMBLY
				X		676S040-1,-9,-11	C	12-09-82	SUPPORT HOGOUT
				X		676S043-1,-2,-15,-17, -19,-51,-52,-53	C	04-18-83	SKIN DETAILS
				X		676S050-7	A	03-09-83	MOUNT - SWITCH MOUNT DETAILS
			X			676S004-1	A	11-01-82	RACK BEAM ASSEMBLY
				X		676S030-1,-2,-9,-11	D	04-18-83	RACK SIDE PLATES - RACK BEAM
				X		676S031-7,-9	A	10-14-83	RACK BEAM INTERCOSTAL
				X		676S038-1	A	11-01-82	DAMPER MOUNT
				X		676S043-3,-5,-27,-37, -39,-40,-41,-43,-45,-46	C	04-18-83	SKIN DETAILS
			X			676M014-7,-9		10-25-82	DAMPER MOUNT DETAILS
			X			676M042-1	A	10-14-82	NUT ASSEMBLY - BALL SCREW
			X			676M048-7	A	11-01-82	MOUNTING PIN - ALIGNMENT SYSTEM

TABLE A1.- (CONTINUED)

INDENTURE 1	2	3	4	5	6	DRAWING/PART NUMBER(S)	REV LTR	DRAWING DATE	LINE ITEM NOMENCLATURE
			X			676S036-1		10-11-82	SPRING ASSEMBLY
			X			676S037-7,-9		10-11-82	SPRING DETAILS
			X			676M010-1	C	04-18-83	DAMPER ASSEMBLY
				X		676M011-7	A	12-18-82	CYLINDER
				X		676M012-7	D	01-17-83	DAMPER ASSEMBLY
				X		676M013-7,-9		09-01-82	GLAND AND DIAPHRAGM
			X			676M040-1	C	03-09-83	DRIVE ASSEMBLY - ALIGNMENT SYSTEM
				X		676M041-7	A	11-01-82	BALL SCREW - ALIGNMENT SYSTEM
				X		676M043-1,-3,-5,-13,-15	A	12-13-82	HOUSING ASSEMBLY - ALIGNMENT SYSTEM
				X		676M044-7,-9,-11	A	02-15-83	IDLER AND INPUT SHAFTS
				X		676M045-7,-9,-11,-13, -15,-17		09-17-82	GEARS (AMR REWORK)
				X		676M046-7		08-20-82	BEARING RETAINER - ALIGNMENT SYSTEM
				X		676M050-1		03-08-83	MOTOR ASSEMBLY
					X	676M049-1,-3,-4,-5,-9, -11		03-08-83	MOTOR DETAILS
			X			676S033-31,-33,-803, -805,-807,-809	D	04-18-83	LINK PINS
			X			676S034-7	A	02-15-83	AFT LINK
			X			676S032-3,-7	C	03-09-83	FWD LINK
				X		676S050-9,-11,-13	A	03-09-83	SWITCH MOUNT DETAILS - CAMS
				X		676S050-15	A	03-09-83	SWITCH MOUNT DETAILS - RETAINER
			X			676E001-1,-3,-7,-9, -11,-23	C	04-27-83	J+ RELAY INSTALLATION - ALIGNMENT SYS.
			X			676E003-1	A	04-27-83	HARNESS ROUTING
				X		676D002-50	B	03-01-83	EMERGENCY JETTISON - WIRING
				X		676D003-50	E	03-10-83	HARNESS - ALIGNMENT SYS. LIMIT SWITCH
			X			16S503-5	Y	01-05-83	SWAY BRACE ASSEMBLY
	X					676S200-1		03-09-83	AIRCRAFT MOD KIT

TABLE A1. - (CONTINUED)

INDENTURE 1	2	3	4	5	6	DRAWING/PART NUMBER(S)	REV LTR	DRAWING DATE	LINE ITEM NOMENCLATURE
		X				676E004-1,-7		09-13-82	EQUIPMENT INSTALLATION AND CIU MOD.
			X			676D003-52	E	03-10-83	JETTISON MATRIX
		X				676F001-1,-7,-9,-15		09-07-82	LIGHT PANEL INSTALLATION - COCKPIT
			X			676D003-51,-53,-54,-55, -56	E	03-10-83	LIGHT PANEL DETAILS - ALIGNMENT SYS.
		X				676IS001-1,-2		01-14-83	STRAIN GAGE INSTL. - SPRING
		X				16IS029-1,-3,-5,-801	B	01-13-83	ACCELEROMETER INSTL. - GBU-8
		X				676ID826-2		10-12-82	SIGNAL DIAGRAM (HARNESSES)
		X				16ID1501-2	T	11-22-82	REMOTE CONNECTOR SCHEDULE L/H
		X				16ID1502-2	P	11-22-82	REMOTE CONNECTOR SCHEDULE R/H
	X					676S300		09-07-83	SPARES LIST

TABLE A1. - (CONTINUED)

RFCC NO.	CLASS I	CLASS II	DRAWING NO.(S) AFFECTED	ECN NO.	COMMENTS
676-R-001		X	676D003	2A 658	CDR Action Item No. 676-24. Delete null position sensing on pylon. Provide pilot control of AC power to pylon.
676-R-002		X	676M012	2C 363	Added piston head dimensions for "Before and After" chrome plating.
676-R-003		X	676M042	4E 020	New part called out for unavailable part.
			676M044	4E 022	Change End Article quantity.
			676M045	4E 021	Change End Article quantity.
			676M046	4E 019	Correct finish callout.
			676S030	4E 025	Add LaRC No. and make drawing changes to accomodate skin.
			676S031	4E 023	Add LaRC No. and change End Article qty.
			676S032	4E 024	Add switch cams.
676-R-004		X	676M010	2C 364	Obtain greater flexibility of distance between ends of damper.
			676M012	4E 017	Provide changeable damping orifice.
			676S033	1C 588	Add lubrication provisions.
			676S040	4E 018	Accomodate fastener requirements.
676-R-005		X	676M040	2C 353	To more accurately define dimensions to assure non-leaking fit of Alignment Drive Assembly components.
			676M041	2C 352	To call out Saginaw Steering Gear Div. part number to ensure correct fit of next assembly.
			676S036	6E 345	To correct callout of next assembly.
			676S038	2C 354	To change dimensions callouts to eliminate interference of damper mount.
676-R-006		X	676M048	6E 346	To decrease overall length of mounting pin to clear thicker skin requirement.
			676S004	6E 347	To correct title block to call out correct sheet number.
			676S030	6E 329	To correct ECN number in "A" Change" block and to correct stock size of side plate.
			676S033	6E 328	To change length and diameter of fwd and aft link pins.
676-R-007		X	676S033	2C 359	To correct next assembly callout.
			676S040	2C 355	To add safety wire hole.
676-R-008		X	676M012	2C 358	To provide changeable damping orifice.
			676S030	6E 348	To provide for alternate material.
676-R-009		X	676D003	4B 186	Correct clearance deficiency on Alignment System wiring.

TABLE A1. - (CONTINUED)

RFCC NO.	CLASS I	CLASS II	DRAWING NO.(S) AFFECTED	ECN NO.	COMMENTS
676-R-010		X	676E001	2C 907	To change material callout.
676-R-011		X	676S030 676S032 676S033 676S040	6E 417 6E 349 6E 416 6E 419	To ream bushings for correct fit. To make holes compatible with both fwd. links. To make holes compatible with link pins To ream bushings for correct fit.
676-R-012		X	676M043 676M045 676S037	6E 421 6E 422 6E 420	To make part accomodate Alignment Assembly Motor. To specify commercial heat treat process. To call out dry film lube.
676-R-013		X	676M042 676M040 676M010 676M011	2E 020 2E 026 2E 027 2E 028	To correct next assembly callout. To accomodate motor changes. To add callout for variable orifice. To eliminate duplicate callout.
676-R-014		X	676S100 676M044 676S001 676S034 676S043	2E 031 2E 033 2E 030 2E 032 2E 029	To eliminate finish callout. To correct shaft bore To change finish callout. To provide clearance for full pylon rotation. To implement shop request to ease manufacturing and handling.
676-R-015		X	676D002 676D003 676M012	4B 193 4B 191 OE 490	To lengthen ground wires for shielding. To correct S7 & S8 switches on drawing. To remove Note 6 from drawing.
676-R-016		X	676D002 676D003	4B 197 4B 196	To make drawing agree with as-built hardware. To make drawing agree with as-built hardware.
676-R-017		X	676E001	4E 516	To make drawing/parts list agree with as-built hardware.
676-R-018		X	676D003	4B 199	To correct pin callouts which were reversed on Alignment Device and Limit switches.

TABLE A1. - (CONTINUED)

RFCC NO.	CLASS I	CLASS II	DRAWING NO.(S) AFFECTED	ECN NO.	COMMENTS
676-R-019		X	676S001	2E 084	To make engineering compatible with as-built hardware.
			676S002	2E 083	To make engineering compatible with as-built hardware.
			676S032	2E 085	To make engineering compatible with as-built hardware.
			676S043	2E 086	To make engineering compatible with as-built hardware.
			676S050	2E 080	To make engineering compatible with as-built hardware.
			676M040	2E 034	To make engineering compatible with as-built hardware.
676-R-020		X	676S100	OD 220	To provide for installation of nuclear lockout pin.
			676S033	OD 221	To increase clearance to reduce friction.
			676S001	OD 222	To increase pin clearance to reduce friction.
			676S030	OD 223	To add ½ inch hole in side plate to remove orifice.
			676S043	OD 224	To add ½ inch hole in upper skin for access to screw in lower skin. To cut radius in lower skin closure for rack removal.
			676M010	OD 225	To change seals and remove orifice in damper to reduce friction.
676-R-021		X	676E003	8E 865	To add current wiring harness callouts to Parts List.
676-R-022		X	676F001	6E 885	To replace switch callout and harness callout.
676-R-023		X	676E003	8E 875	Key not required on Vendor part.
			676E001	8E 876	To correct circuit breaker callout.
676-R-024		X	676S100	OD 227	To add NASA decals to pylons.

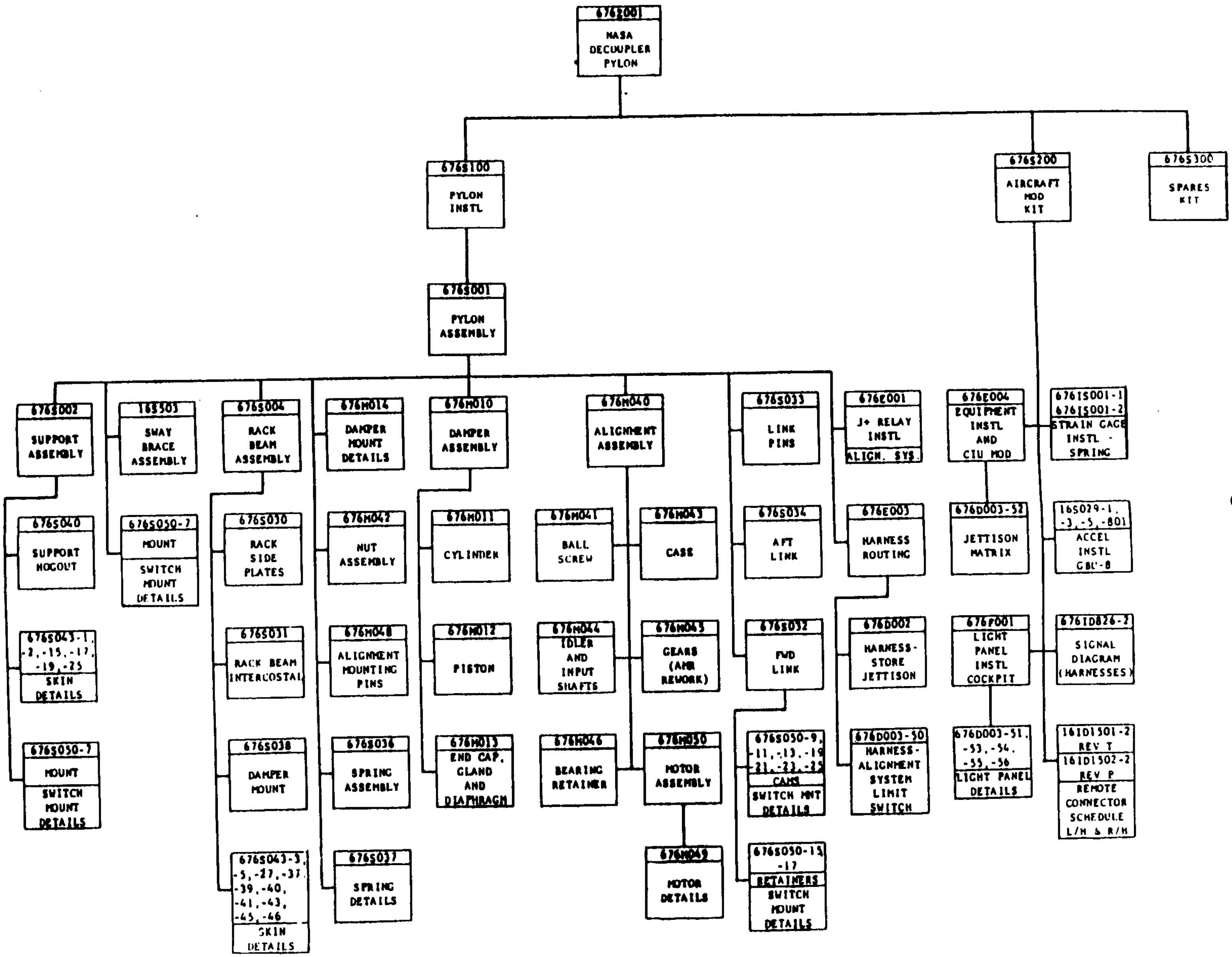

Figure A1.- NASA decoupler pylon drawing tree.

APPENDIX B

Equations of Motion

In the preliminary analyses conducted prior to the pylon ground tests, the natural modes of vibration were computed with the decoupler pylon pitch spring removed. Hence, the decoupler pylon and attached store introduced no pitch moment to the wing in the calculation of these modes of vibration. Also, the absolute pitch angle of the store was zero for each of these natural modes. The Lagrangian equations of motion were then applied to couple the natural modes computed in this manner with a single store pitch mode. In the store pitch mode, the entire airplane was constrained to zero deflection except for the lower part of the pylon and the attached store. All other degrees of freedom of the weapon motion were represented by the natural modes. The deflections in the store pitch mode were described entirely by the rigid body pitching motion about the pylon pivot.

The pitch deflection, θ, of the wing at the decoupler pylon station is defined by the difference in the vertical deflection of the wing at the spring damper alignment attachment x_2, and the vertical deflection of the pylon pivot x_1, divided by the distance between the two stations r.

$$\theta_s = \frac{h_s(x_2) - h_s(x_1)}{r} \qquad \text{(B1)}$$

where $h_s(x_1)$ and $h_s(x_2)$ are the vertical deflections in mode s at the decoupler pivot and at fuselage station x_2 at the decoupler pylon wing station.

The deflection in the element connecting the decoupler pylon to the wing, δ , can be expressed in terms of the generalized coordinates, q, as follows:

$$\delta = r\left(\sum_{s=1}^{N} \theta_s q_s - \theta_p q_p\right) = r\theta_\delta \qquad \text{(B2)}$$

where δ is positive in compression and θ_δ is the relative pitch angle between the wing and the store and is positive when the wing pitch angle (positive nose up) is greater than the store pitch angle (positive nose up). The subscripts s and p represent the N natural modes of the airplane and the store pitch mode, respectively.

Zero airspeed equations of motion. The equations of motion for zero airspeed and for the special case in which the element connecting the wing and decoupler pylon is represented by only a spring can be expressed as follows:

$k>0, C = G = 0$

$$\left[\begin{array}{c|c} M_{rr} & M_{rp} \\ \hline M_{pr} & M_{pp} \end{array}\right] \begin{Bmatrix} \ddot{q}_r \\ \ddot{q}_p \end{Bmatrix} + \left[\begin{array}{c|c} K_{rr} & 0 \\ \hline 0 & 0 \end{array}\right] \begin{Bmatrix} q_r \\ q_p \end{Bmatrix} = \begin{Bmatrix} Q_r \\ Q_p \end{Bmatrix} \qquad \text{(B3)}$$

The M_{rr} matrix is a diagonal generalized mass matrix computed for the N natural modes of vibration. The M_{pr} and M_{rp} row and column vectors contain the mass coupling terms between the natural modes and the store pitch mode.

The K_{rr} matrix is a diagonal generalized stiffness matrix for the N natural modes of vibration. The N+1 row and column are zero because the forces produced by the decoupler pylon spring are treated as externally applied loads.

The elements of the Q_r vector represent the generalized forces acting upon equations 1 through N in Equation B3, and Q_p is the generalized force acting upon the store pitch mode.

When the pylon spring is in compression it produces a nose down moment on the wing and a nose up moment on the pylon. The generalized force produced by the pylon spring force can be expressed as follows:

$$
\begin{aligned}
Q_r &= r(-r\theta_\delta k)\theta_r \\
Q_p &= r(+r\theta_\delta k)\theta_p
\end{aligned}
\tag{B4}
$$

Substituting the expression for θ_δ from equation B2 into equation B4 yields the following expression for the generalized forces.

$$
\begin{Bmatrix} Q_r \\ \cdot \\ \cdot \\ \cdot \\ \cdot \\ \hline Q_p \end{Bmatrix} = -r^2 k \left[\begin{array}{cccc|c} \theta_1^2 & \theta_1\theta_2 & \theta_1\theta_3 & \cdots & -\theta_1\theta_p \\ \theta_2\theta_1 & \theta_2^2 & \theta_2\theta_3 & \cdots & -\theta_2\theta_p \\ \theta_3\theta_1 & \theta_3\theta_2 & \theta_3^2 & \cdots & -\theta_3\theta_p \\ \vdots & \vdots & \vdots & & \vdots \\ \hline -\theta_p\theta_1 & -\theta_p\theta_2 & -\theta_p\theta_3 & \cdots & +\theta_p^2 \end{array}\right] \begin{Bmatrix} q_r \\ \cdot \\ \cdot \\ \cdot \\ \cdot \\ \cdot \\ \hline q_p \end{Bmatrix} \tag{B5}
$$

The generalized forces can be seen to be expressible as a stiffness matrix. When transferred to the left side of equation B3, they add a stiffness coupling term to every element of the stiffness matrix.

To include the effect of viscous damping C and of feedback gain G, replace k in equation B5 with $(k+i\omega C+G/i\omega)$ for harmonic motion.

Zero airspeed stability analysis. - To determine the value of G that would drive the system unstable at zero airspeed, for particular values of k and C, it is convenient to think of disconnecting the valve feedback linkage (breaking the loop) and commanding a valve deflection, δ_i.

The pylon is connected to the wing by the spring and damper elements. The force produced by the alignment device in response to the δ_i input deflection to the valve is applied to the wing and pylon. The equations of motion are expressed as follows:

$$\left[\begin{array}{c|c} M_{rr} & M_{rp} \\ \hline M_{pr} & M_{pp} \end{array}\right] \left\{\begin{array}{c} \ddot{q}_r \\ \hline \ddot{q}_p \end{array}\right\} + \left[\begin{array}{c|c} K_{rr} & 0 \\ \hline 0 & 0 \end{array}\right] \left\{\begin{array}{c} q_r \\ \hline q_p \end{array}\right\} + \qquad \text{(B6)}$$

$$r^2(k+i\omega C)\left[\begin{array}{cccc|c} \theta_1^2 & \theta_1\theta_2 & \theta_1\theta_3 & \cdots & -\theta_1\theta_p \\ \theta_2\theta_1 & \theta_2^2 & \theta_2\theta_3 & \cdots & -\theta_2\theta_p \\ \theta_3\theta_1 & \theta_3\theta_2 & \theta_3^2 & \cdots & -\theta_3\theta_p \\ \vdots & \vdots & \vdots & & \vdots \\ \hline -\theta_p\theta_1 & -\theta_p\theta_2 & -\theta_p\theta_3 & \cdots & \theta_p^2 \end{array}\right] \left\{\begin{array}{c} q_r \\ \cdot \\ \cdot \\ \cdot \\ \cdot \\ \hline q_p \end{array}\right\} = -r^2\left(\frac{G}{i\omega}\right) \left\{\begin{array}{c} +\theta_1 \\ +\theta_2 \\ +\theta_3 \\ \vdots \\ \hline -\theta_p \end{array}\right\} \left(\frac{\delta_i}{r}\right).$$

The relative pitch angle between the wing and the store, in response to the force produced by the input pitch angle command to the alignment device, can be computed. The ratio of the response pitch angle to the input command pitch angle is expressed by equation B7.

$$\frac{\theta_\delta}{(\delta_i/r)} = \sum_{s=1}^{N} \theta_s\left(\frac{q_s}{\delta_i/r}\right) - \theta_p\left(\frac{q_p}{\delta_i/r}\right) \qquad \text{(B7)}$$

The ratio expressed by equation B7 can be plotted and the Nyquist criteria applied to determine the stability of the system for a specific value of G and/or to determine the critical value of G.

<u>General open loop equations with aerodynamics.</u> - To obtain the equations of motion for a flight condition, the generalized aerodynamic terms are added to the left side of equation B6.

$$\left[\begin{array}{c|c} A_{rs} & A_{rp} \\ \hline A_{ps} & A_{pp} \end{array}\right] \left\{\begin{array}{c} q_s \\ \hline q_p \end{array}\right\} = \frac{-r^2}{-4\rho b_r^3\omega^2}\left(k + i\omega C + \frac{G}{i\omega}\right) \left\{\begin{array}{c} +\theta_s \\ \hline -\theta_p \end{array}\right\} \left(\frac{\delta_i}{r}\right) \quad \text{(B8)}$$

where

$$A_{rr} = 1 - \left(\frac{\omega_r}{\omega}\right)^2 (1+ig_r)\, \overline{M}_{rr} + \overline{Q}_{rr}$$

$$A_{rs} = \overline{Q}_{rs}$$

$$A_{ps} = A_{rp} = \overline{M}_{rp} \qquad ;\ r=s$$

$$A_{pp} = \overline{M}_{pp}$$

$$\overline{M}_{rs} = \frac{1}{4\rho b_r^3} \iint h_r h_s dm$$

$$\overline{Q}_{rs} = \frac{1}{-4\rho b_r^3\omega^2} \iint h_r \Delta p_s dS$$

and

g_r is the structural damping coefficient for the r^{th} generalized coordinate

b_r is a reference length

ω_r is the r^{th} natural mode frequency

ω is the exciting frequency

These equations have been divided by $(-4\rho b_r^3\omega^2)$ to put the left hand side into the standard format that is used for flutter analyses.

The right hand side consists of the forces produced by the k, C, and G elements due to a commanded δ_i deflection. This is equivalent to breaking the loop for all three elements simultaneously. Conceptually, the forces produced by the input deflection to the k, C, and G elements can be applied to the wing and the pylon. The response to these excitation forces can then be computed in the form of the store pitch angle relative to the wing, θ_δ. The frequency response function relating the feedback, θ_δ, to the input (δ_i) can then be computed.

Stability analysis to select pylon pitch stiffness. To determine the pylon pitch stiffness necessary to stabilize the system, C and G are set equal to zero in equation B8 with an arbitrarily selected value of k.

$$\left[\begin{array}{c|c} A_{rs} & A_{rp} \\ \hline A_{ps} & A_{pp} \end{array}\right] \left\{\begin{array}{c} q_s \\ \hline q_p \end{array}\right\} = \frac{r^2 k}{4\rho b_r^3 \omega^2} \left\{\begin{array}{c} +\theta_s \\ \hline -\theta_p \end{array}\right\} \left(\frac{\delta i}{r}\right) \qquad \text{(B9)}$$

At each selected airspeed, the generalized coordinate response per ($\delta_{i/r}$) can be computed and then weighted to determine the store pitch relative to the wing.

$$\frac{\theta_\delta}{(\delta_i/r)} = \sum_{s=1}^{N} \theta_s\left(\frac{q_s}{\delta_i/r}\right) - \theta_p\left(\frac{q_p}{\delta_i/r}\right) \qquad \text{(B10)}$$

The real and imaginary parts of equation B10 can be plotted with frequency as the independent variable. Since the magnitude of the plot is proportional to the selected value of k, the value of k that causes the system to pass through the minus-one point (negative feedback) can be determined. This is the value of k that produces neutral stability. The process can be repeated for several selected airspeeds to define a curve that relates the airspeed vs. the spring stiffness that causes instability. This analysis is equivalent to a flutter analysis which includes all stiffness and mass coupling terms between the N natural modes and the single store pitch mode.

Stability analysis to select pylon pitch damping. To determine the effect of pylon damping a value of C is selected, the damping loop is closed, and G is set equal to zero to obtain the following equation.

$$\left[\begin{bmatrix} A_{rs} & A_{rp} \\ A_{ps} & A_{pp} \end{bmatrix} - \frac{r^2(i\omega C)}{4\rho b_r^3\omega^2}\begin{bmatrix} \theta_r\theta_s & -\theta_r\theta_p \\ -\theta_p\theta_s & \theta_p^2 \end{bmatrix}\right]\begin{Bmatrix} q_r \\ q_p \end{Bmatrix} = \frac{r^2(k)}{4\rho b_r^3\omega^2}\begin{Bmatrix} \theta_r \\ -\theta_p \end{Bmatrix}\left(\frac{\delta i}{r}\right) \tag{B11}$$

Repeating the analysis procedure described in the preceding section for determining the pylon pitch stiffness to stabilize the system with zero damping, yields a similar relationship between airspeed and pylon stiffness for selected values of pylon damping.

<u>Stability analysis to select pylon alignment gain.</u> To determine the critical value of the alignment gain for selected values of pylon spring stiffness and damping, the loop is closed for the selected value of k and C and the system is driven with the forces produced by an input δ_i to the alignment element. Equation B10 reduces to the following equation

$$\left[\begin{bmatrix} A_{rs} & A_{rp} \\ A_{ps} & A_{pp} \end{bmatrix} - \frac{r^2(k+i\omega C)}{4\rho b_r^3\omega^2}\begin{bmatrix} \theta_r\theta_s & -\theta_r\theta_p \\ -\theta_p\theta_r & \theta_p^2 \end{bmatrix}\right]\begin{Bmatrix} q_s \\ q_p \end{Bmatrix} = \frac{r}{4\rho b_r^3\omega^2}\left(\frac{G}{i\omega}\right)\begin{Bmatrix} \theta_r \\ \theta_p \end{Bmatrix}\left(\frac{\delta i}{r}\right) \tag{B12}$$

An arbitrary value of G can be selected to compute the ratio of θ_δ to ($\delta i/r$) through the application of equation B10. Following the procedure for the previous two sections, the real and imaginary parts of the ratio can be plotted and subsequently scaled up or down to determine the value of G that causes the plot to pass through the minus-one point. By repeating this analysis for several selected airspeeds a plot of the critical value of G versus airspeed can be determined for any preselected value of k and C.

Equations with all decoupler pylon loops closed. - The equations of motion for the case in which the decoupler pylon spring, damper, and alignment loops are closed can be expressed as follows:

$$\left[\left[\begin{array}{c|c} A_{rs} & A_{rp} \\ \hline A_{ps} & A_{pp} \end{array}\right] - \frac{r^2\left(k+i\omega C + \frac{G}{i\omega}\right)}{4\rho b_r^3\omega^2}\left[\begin{array}{c|c} \theta_r\theta_s & -\theta_r\theta_p \\ \hline -\theta_p\theta_r & \theta_p^2 \end{array}\right]\right]\left\{\begin{array}{c} q_s \\ \hline q_p \end{array}\right\} = \left\{\begin{array}{c} Q_r \\ \hline Q_p \end{array}\right\} \quad \text{(B13)}$$

The right hand side of equation B13 represents the generalized external forces on the system, such as, the generalized forces produced by gusts, control surface deflection, taxi, or store ejection.

APPENDIX C

Predicted Alignment System Performance to Symmetric Maneuvers

Time history store pitch misalignment angles were computed and are shown for variations in starting misalignment angle, store c.g., and type of symmetric maneuver. Alignment angles of zero and ± 0.4 degrees were used at the beginning of the maneuver. Store c.g. locations of nominal and 0.5 inches forward and aft of nominal were used. The alignment time histories were computed for symmetric pullup and symmetric pushover maneuvers.

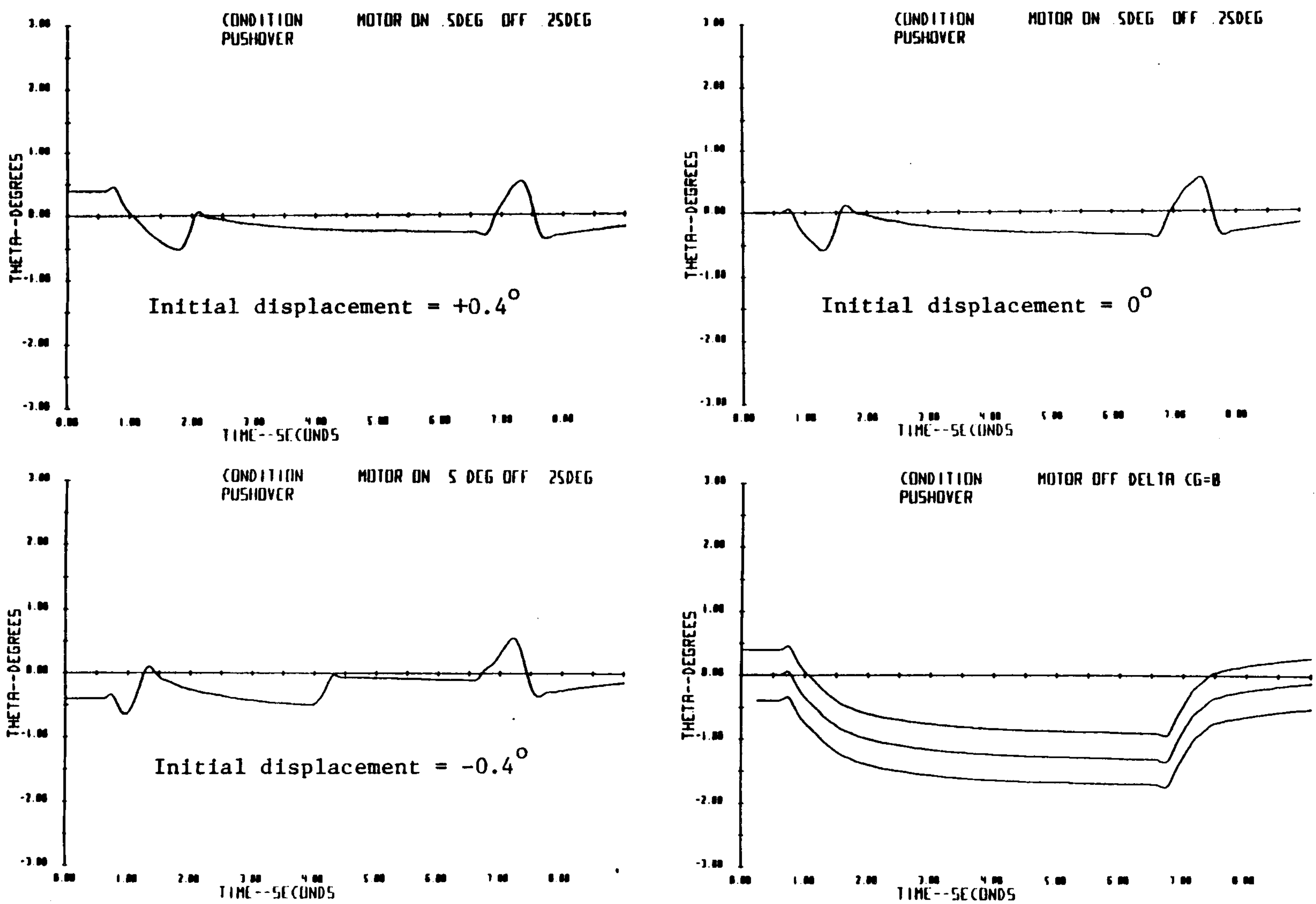

Figure C1.- Predicted Store Alignment System Performance for Symmetrical Pushover Maneuver, Neutral Store C.G.

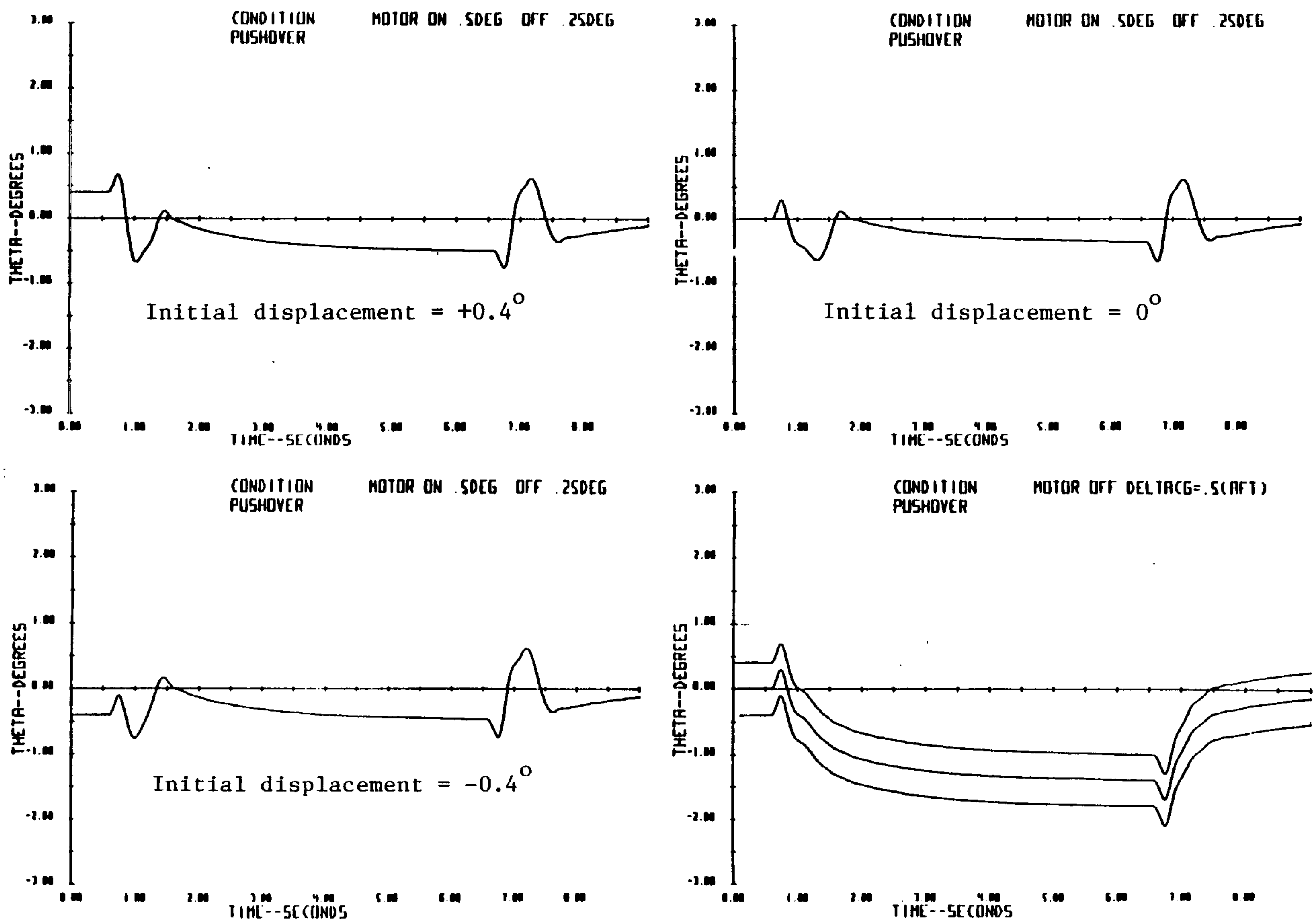

Figure C2.- Predicted Store Alignment System Performance for Symmetrical Pushover Maneuver, Aft Store C.G.

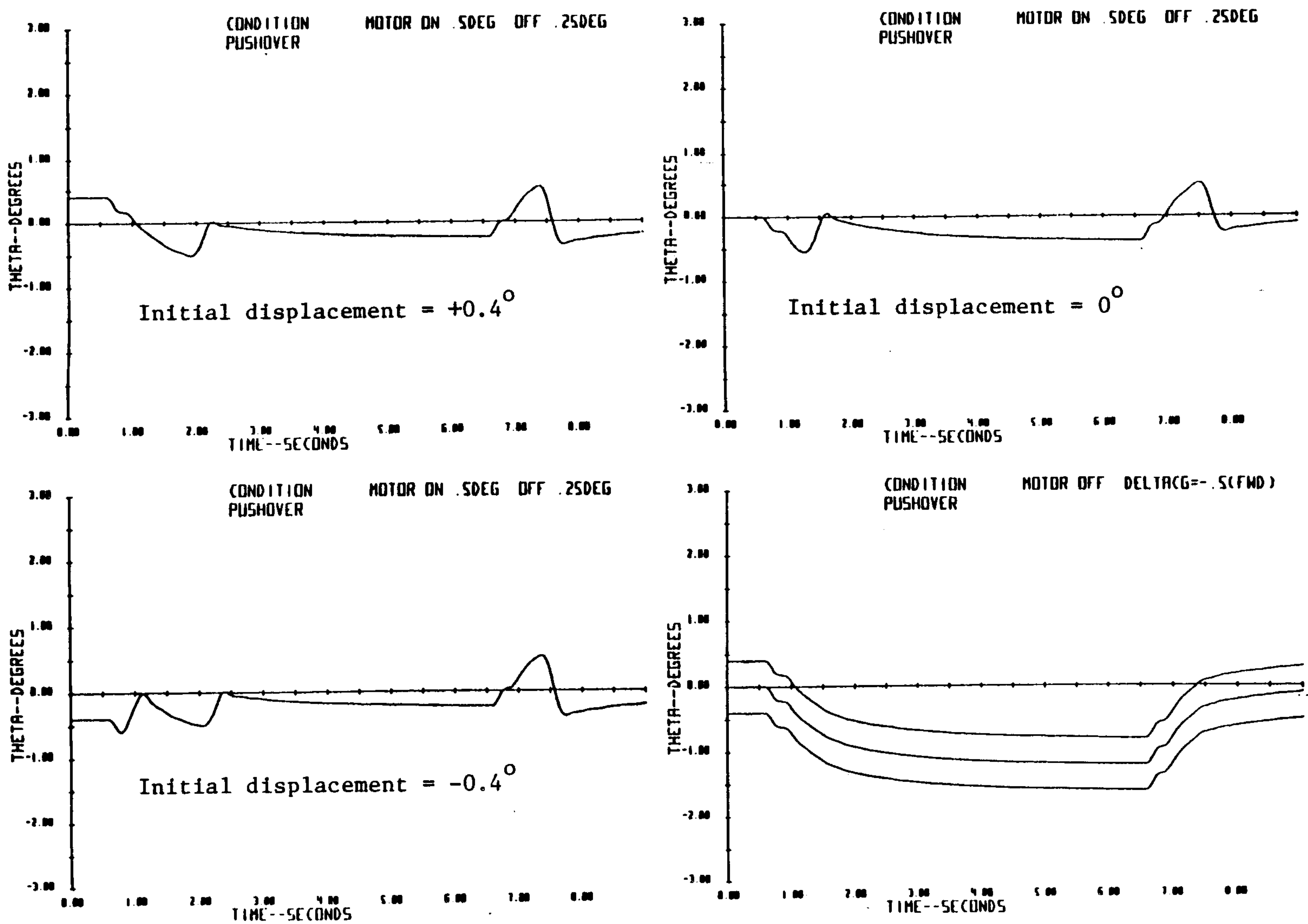

Figure C3.- Predicted Store Alignment System Performance for Symmetrical Pushover Maneuver, Forward Store C.G.

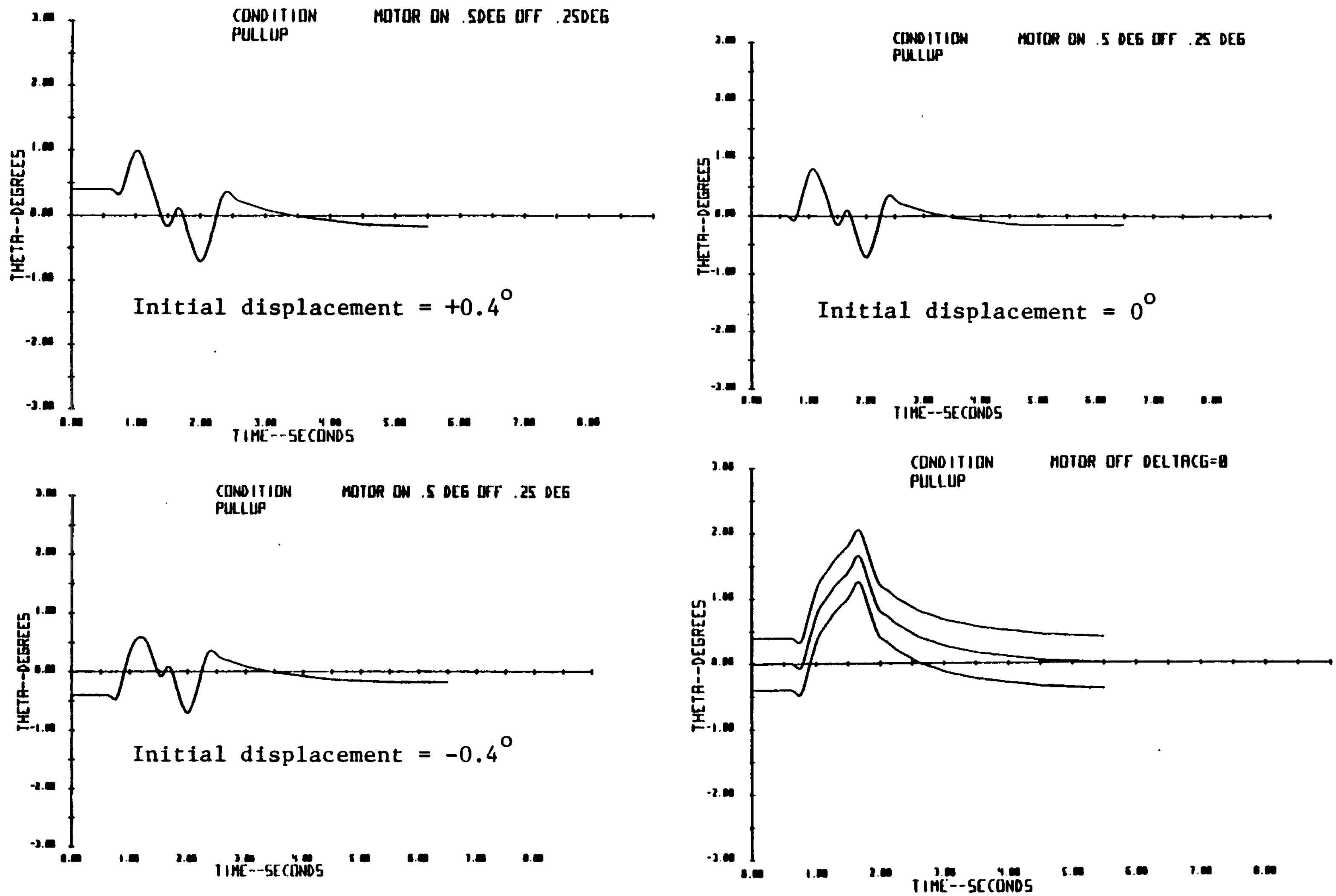

Figure C4.- Predicted Store Alignment System Performance for Symmetrical Pullup Maneuver, Neutral Store C.G.

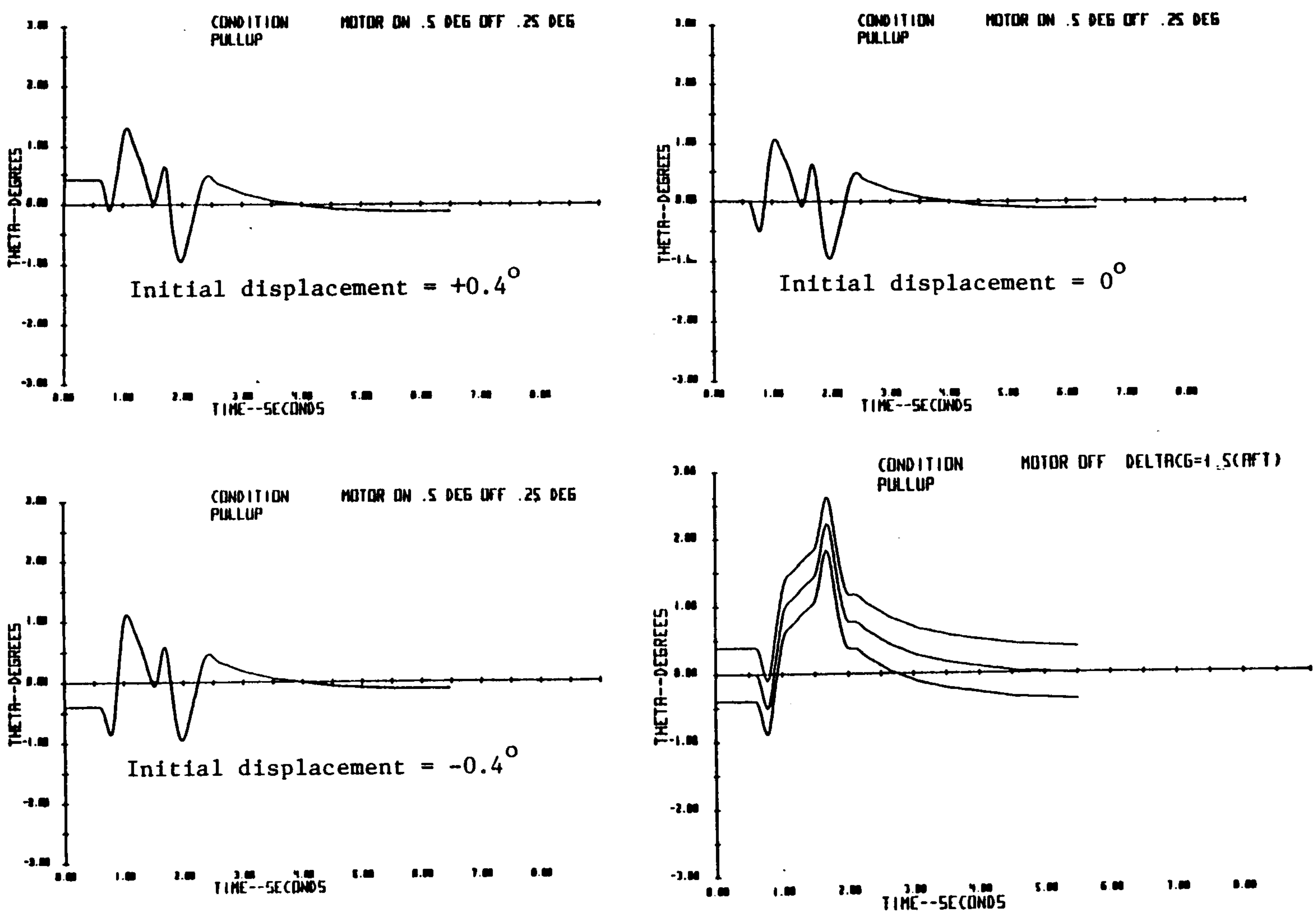

Figure C5.- Predicted Store Alignment System Performance for Symmetrical Pullup Maneuver, Aft Store C.G.

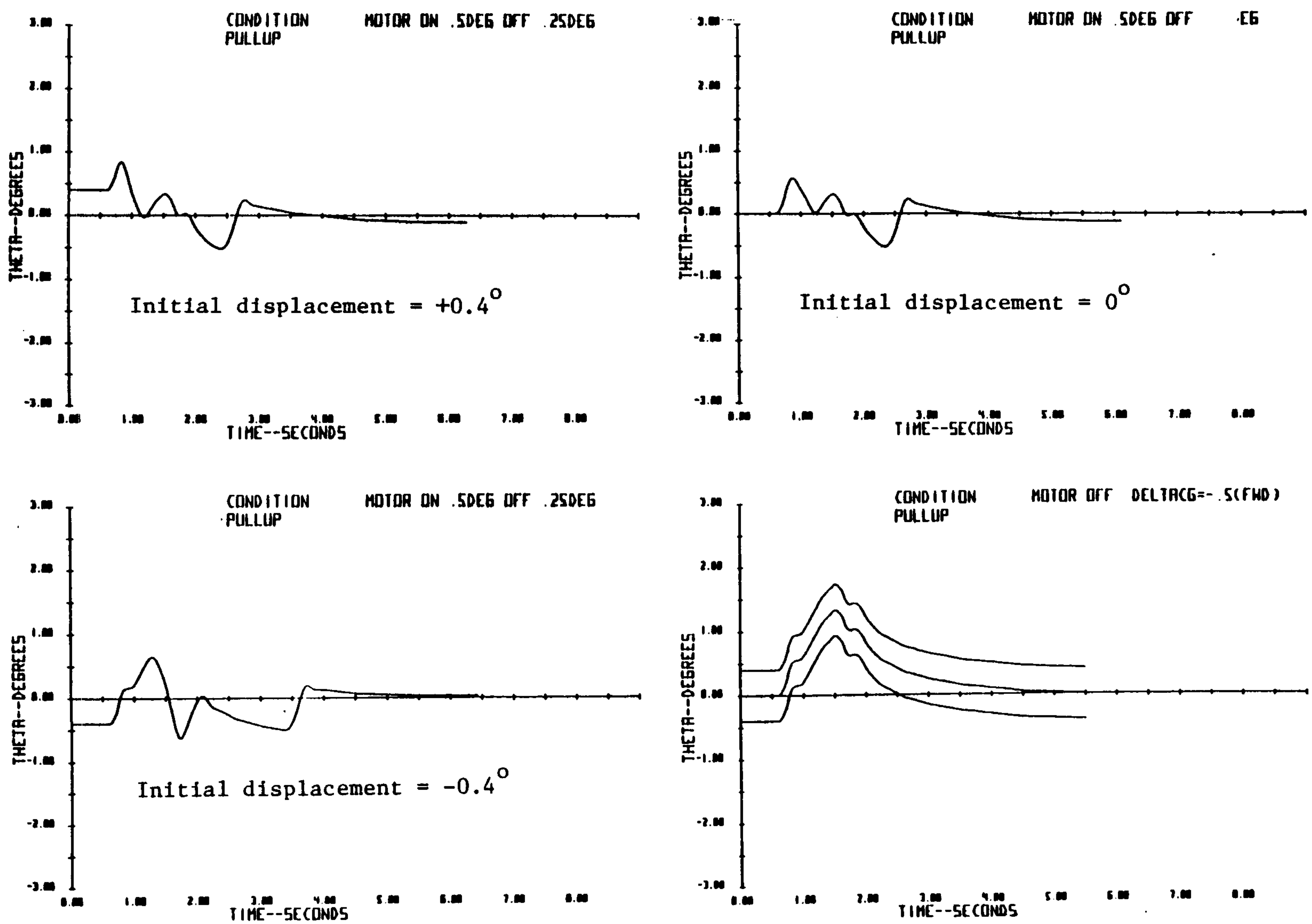

Figure C6.- Predicted Store Alignment System Performance for Symmetrical Pullup Maneuver, Forward Store C.G.

APPENDIX D

Predicted Alignment System Performance to Rudder Kicks

Time history store pitch misalignment angles were computed and are shown for variations in starting misalignment angle and store c.g. Misalignment angles of zero and ±0.4 degrees were used at the beginning of the maneuver. Store c.g. locations of nominal and 0.5 inches forward and aft of nominal were used.

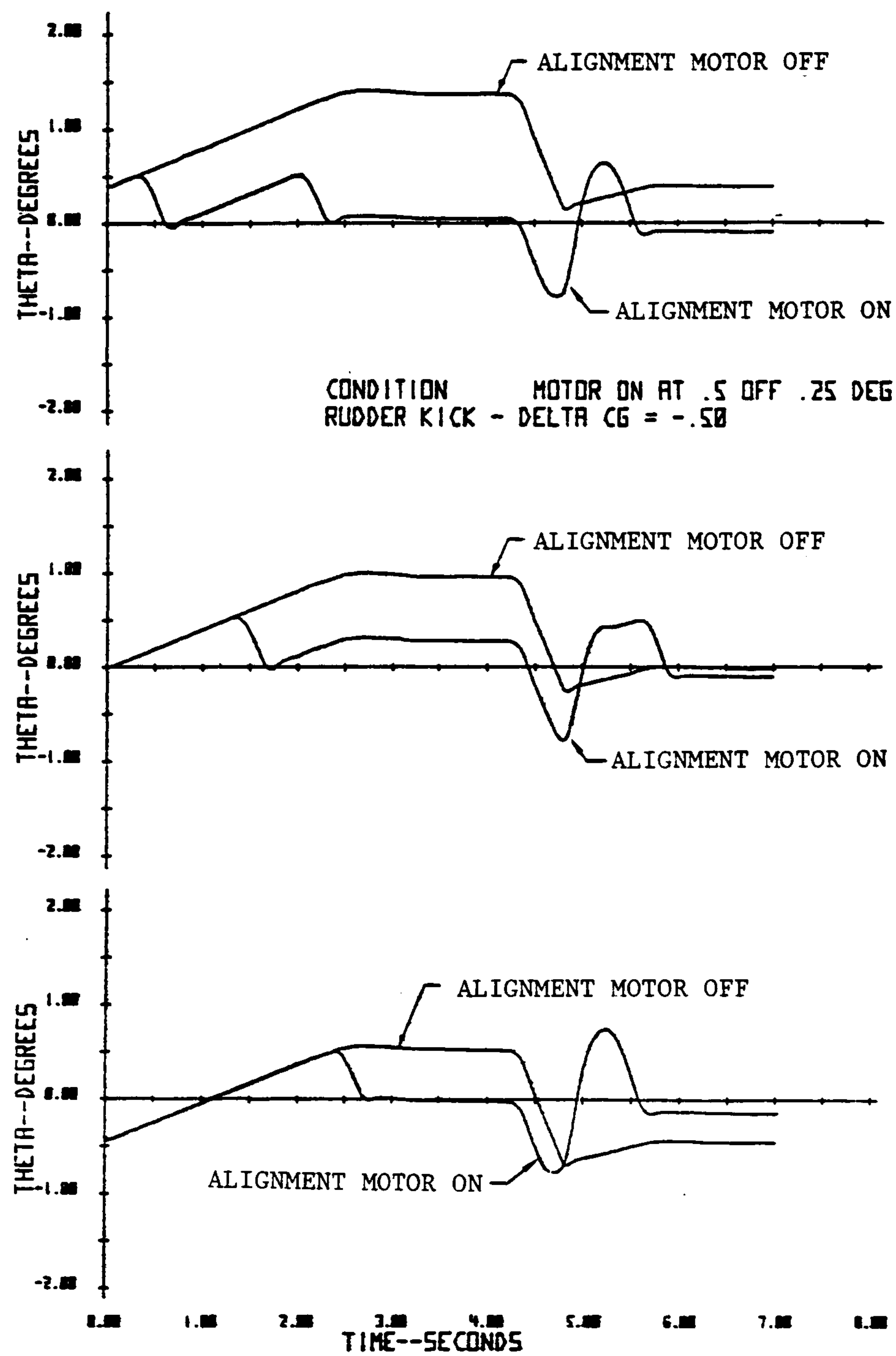

Figure D1.- Store misalignment angle for the rudder kick maneuver, forward store C.G.

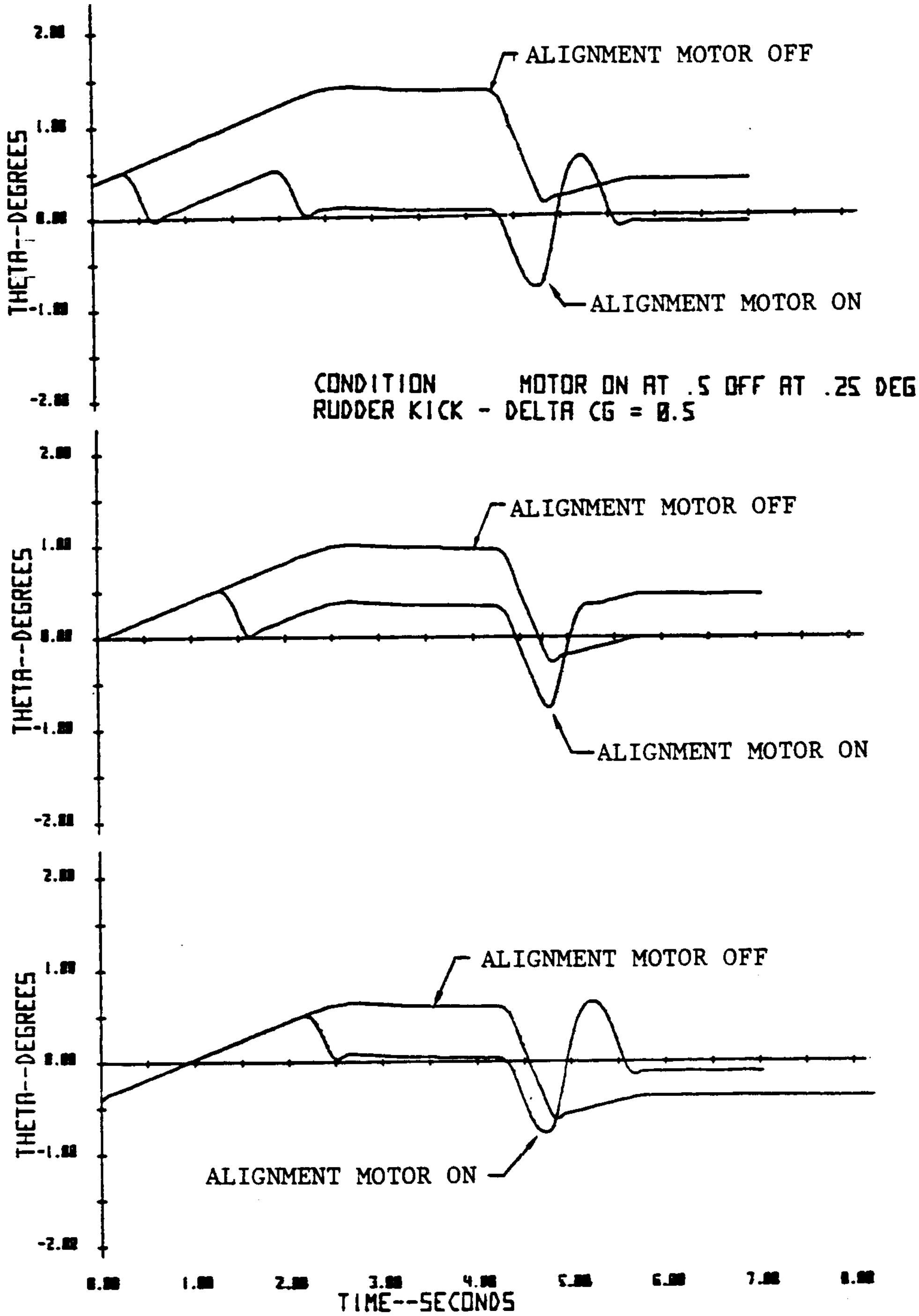

Figure D2.- Store misalignment angle for the rudder kick maneuver, aft store C.G.

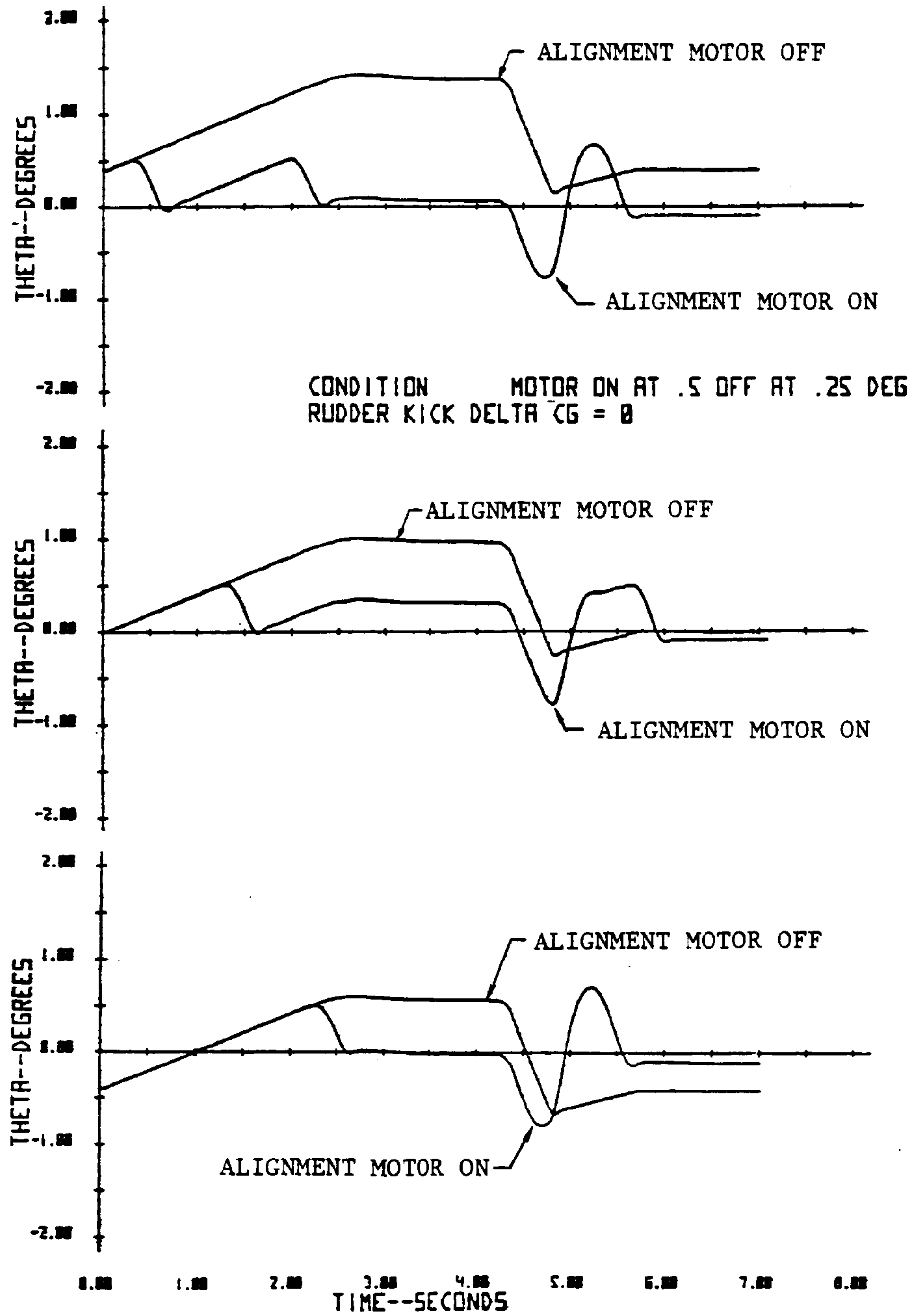

Figure D3.- Store misalignment angle for the rudder kick maneuver, neutral store C.G.

APPENDIX E

Alignment System Performance in the Test Fixture

Time history misalignment angles were measured for a time dependent pitching moment. The pitching moment was selected as one that is close to a realistic F-16 load condition. The pitching moment was applied with and without a non time-dependent yawing moment and side force. Pylon 1 test results are given in Figures E1 through E5 followed by Pylon 2 test results in Figures E6 through E10. The test conditions AL1 through AL5 are given in Table 22.

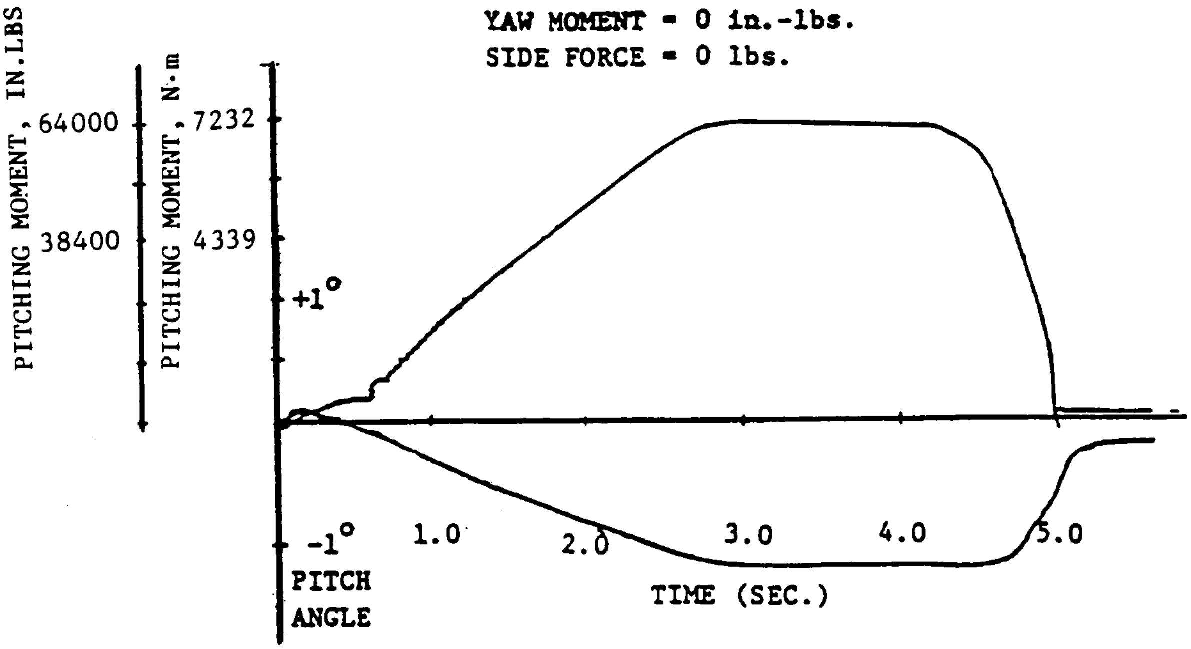

Figure E1.- Operational Test AL1, Pylon No. 1

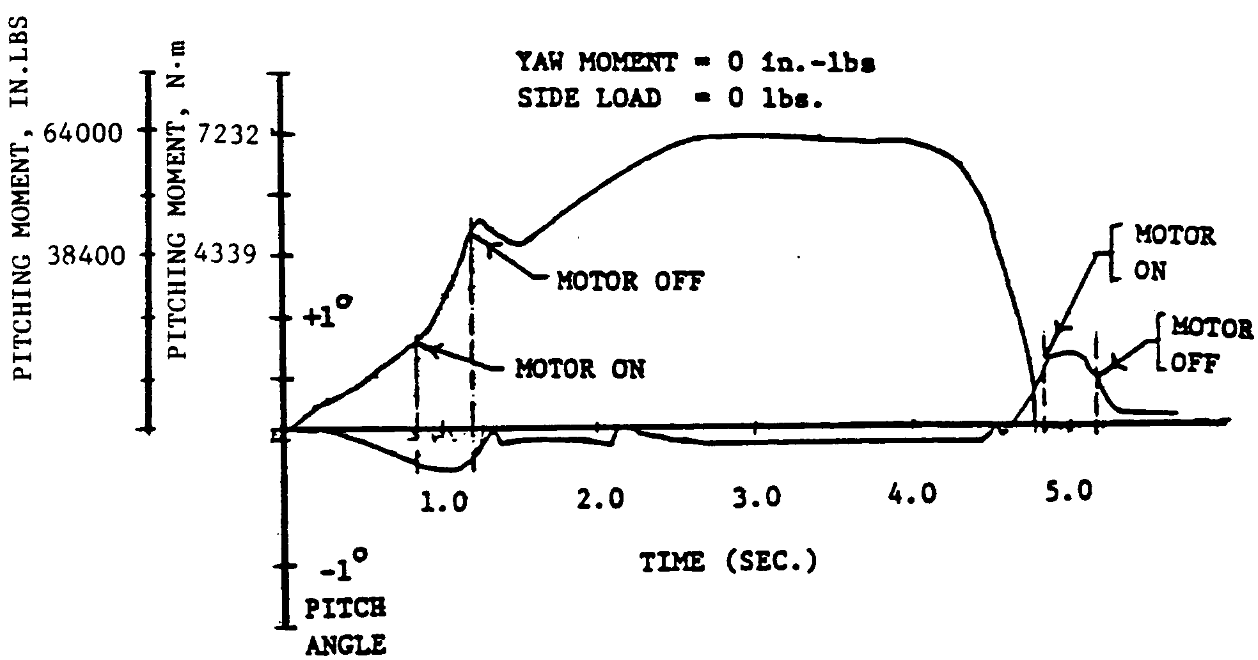

Figure E2.- Operational Test AL2, Pylon No. 1

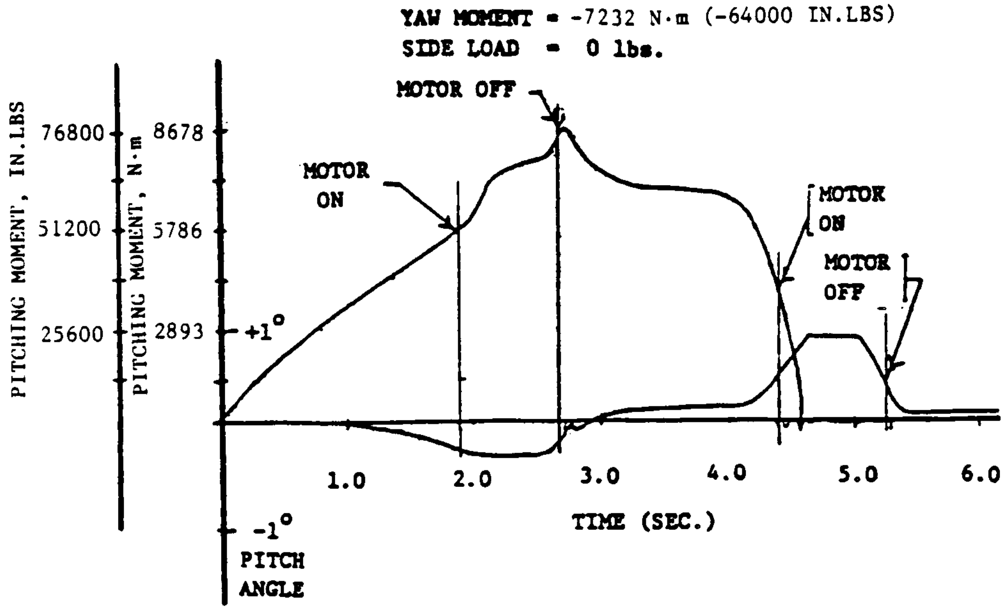

Figure E3.- Operational Test AL3, Pylon No. 1

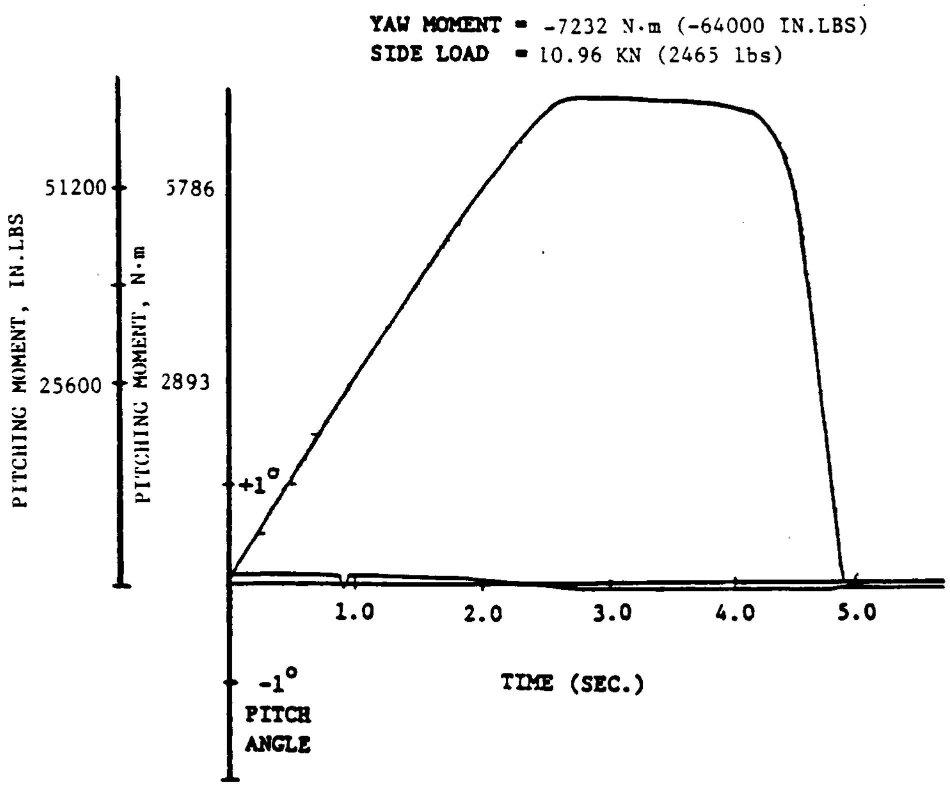

Figure E4.- Operational Test AL4, Pylon No. 1

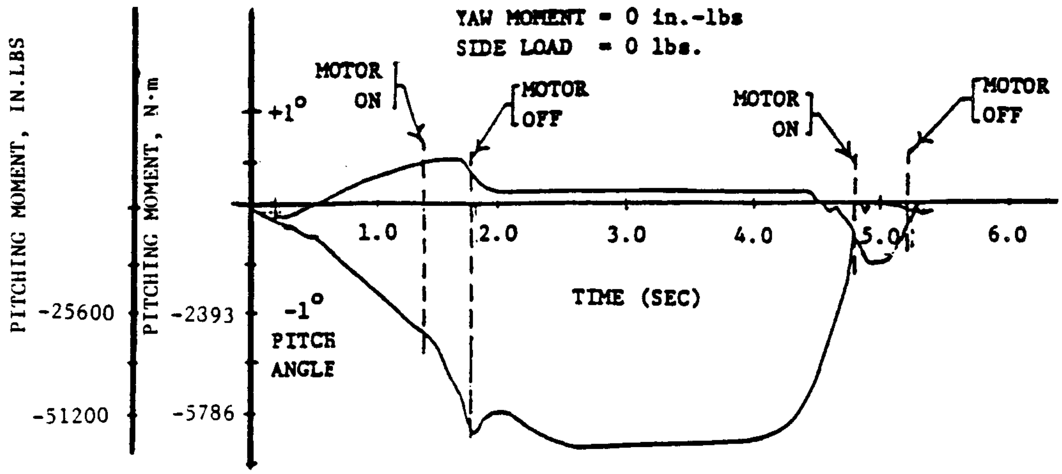

Figure E5.- Operational Test AL5, Pylon No. 1

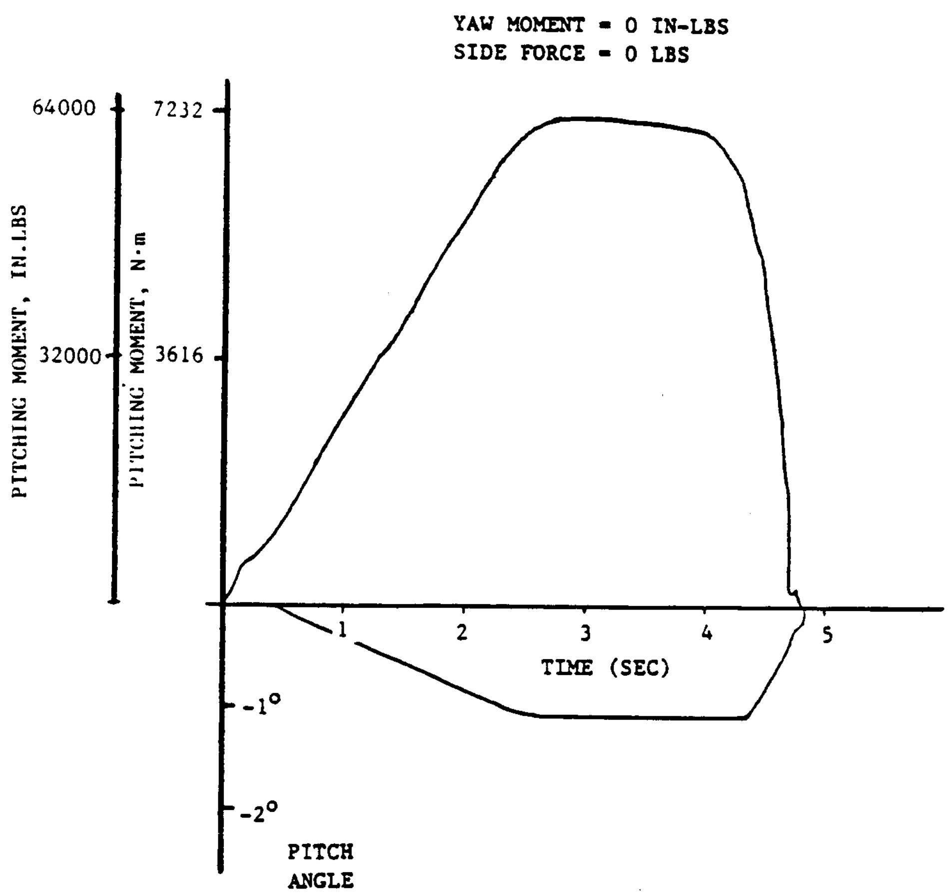

Figure E6.- Operational Test AL1, Pylon No. 2

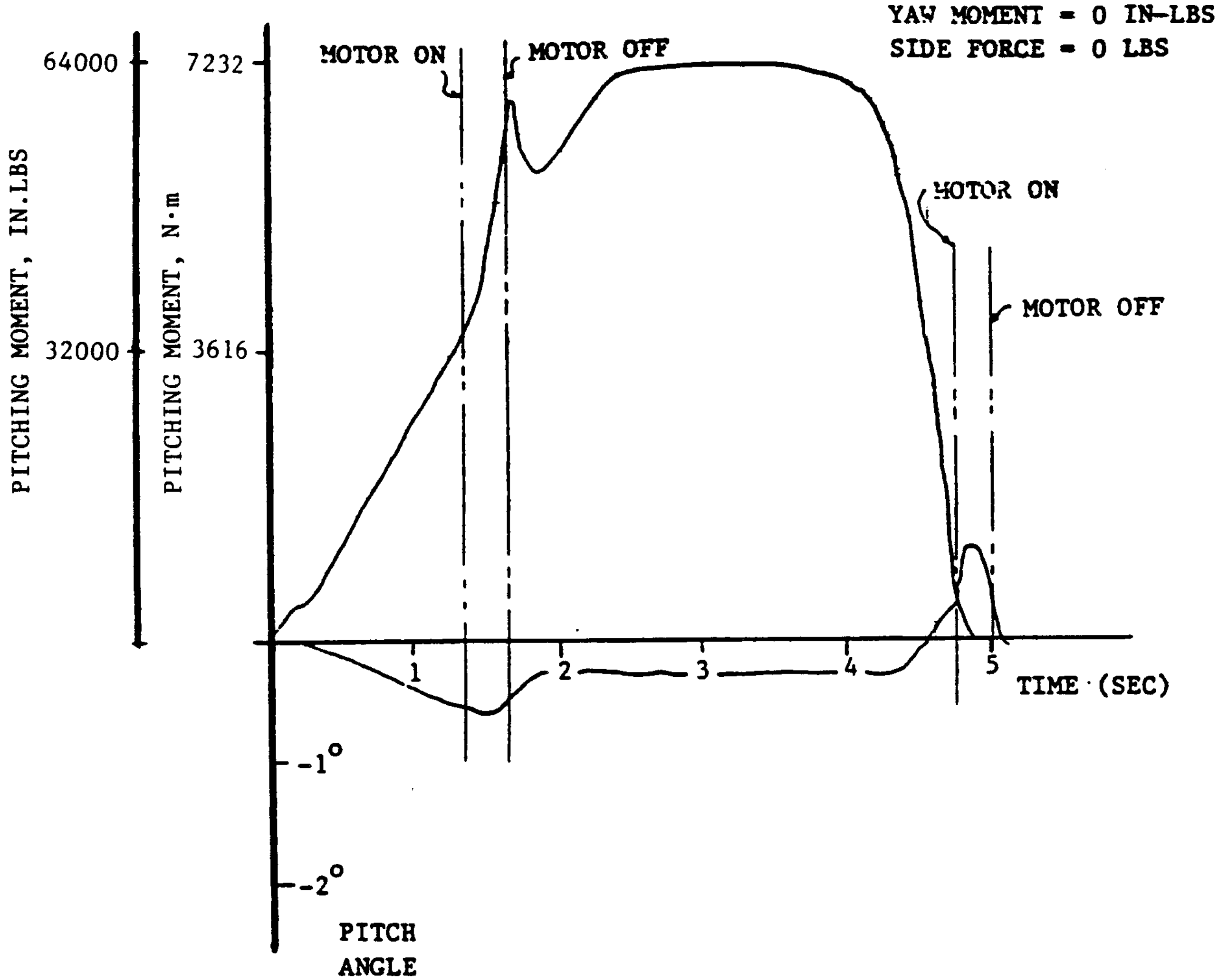

Figure E7.- Operational Test AL2, Pylon No. 2

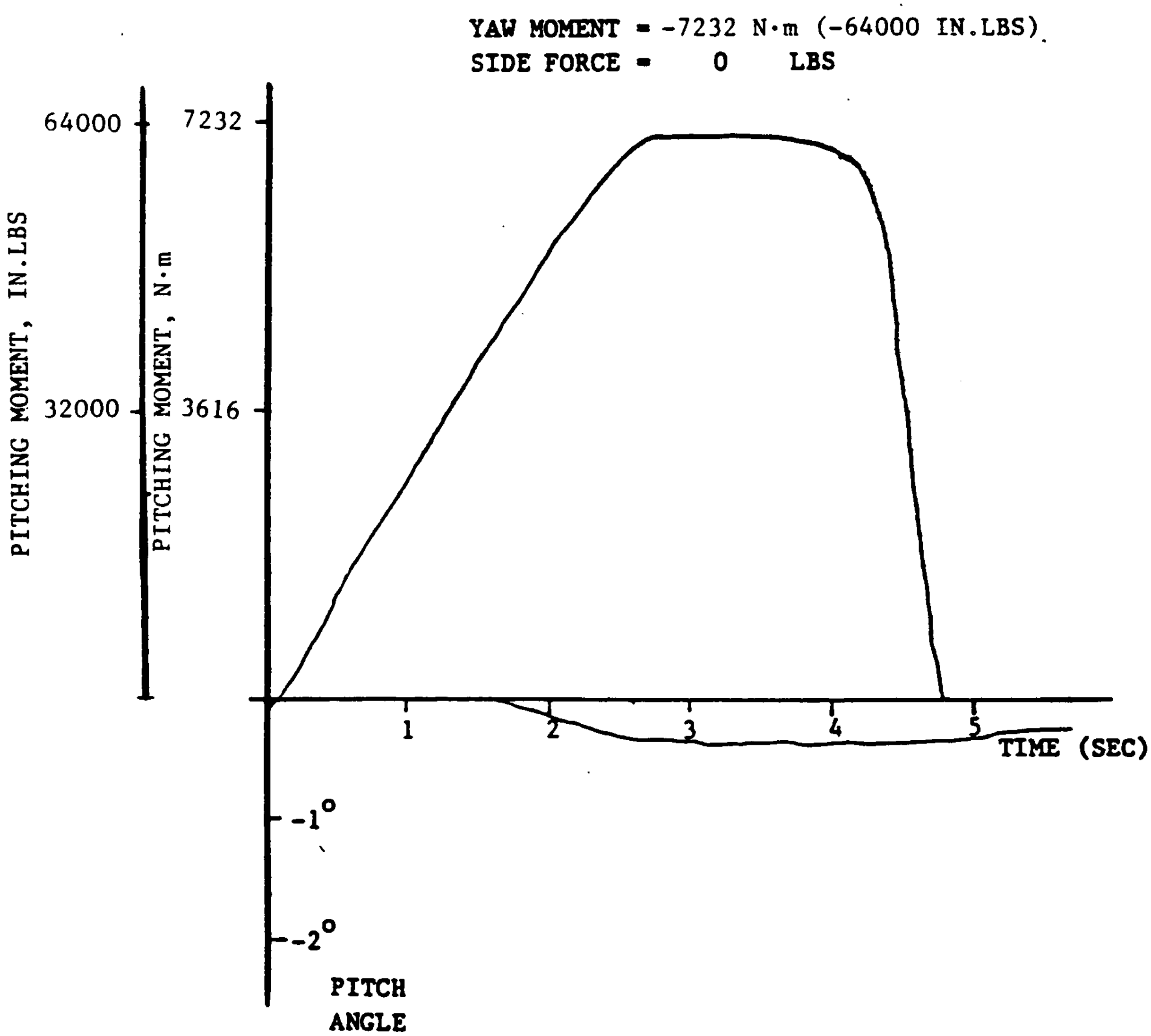

Figure E8.- Operational Test AL3, Pylon No. 2

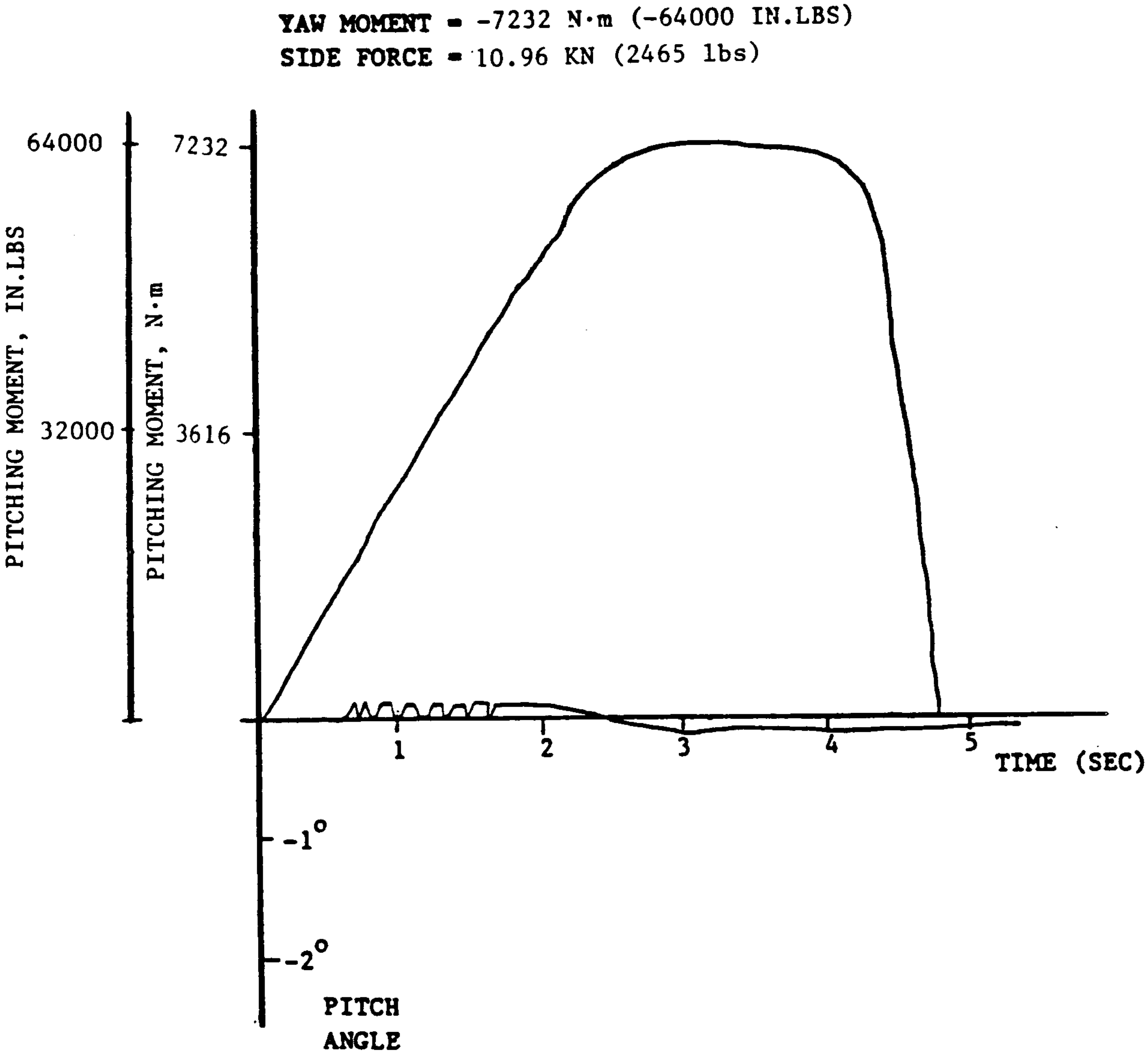

Figure E9.- Operational Test AL4, Pylon No. 2

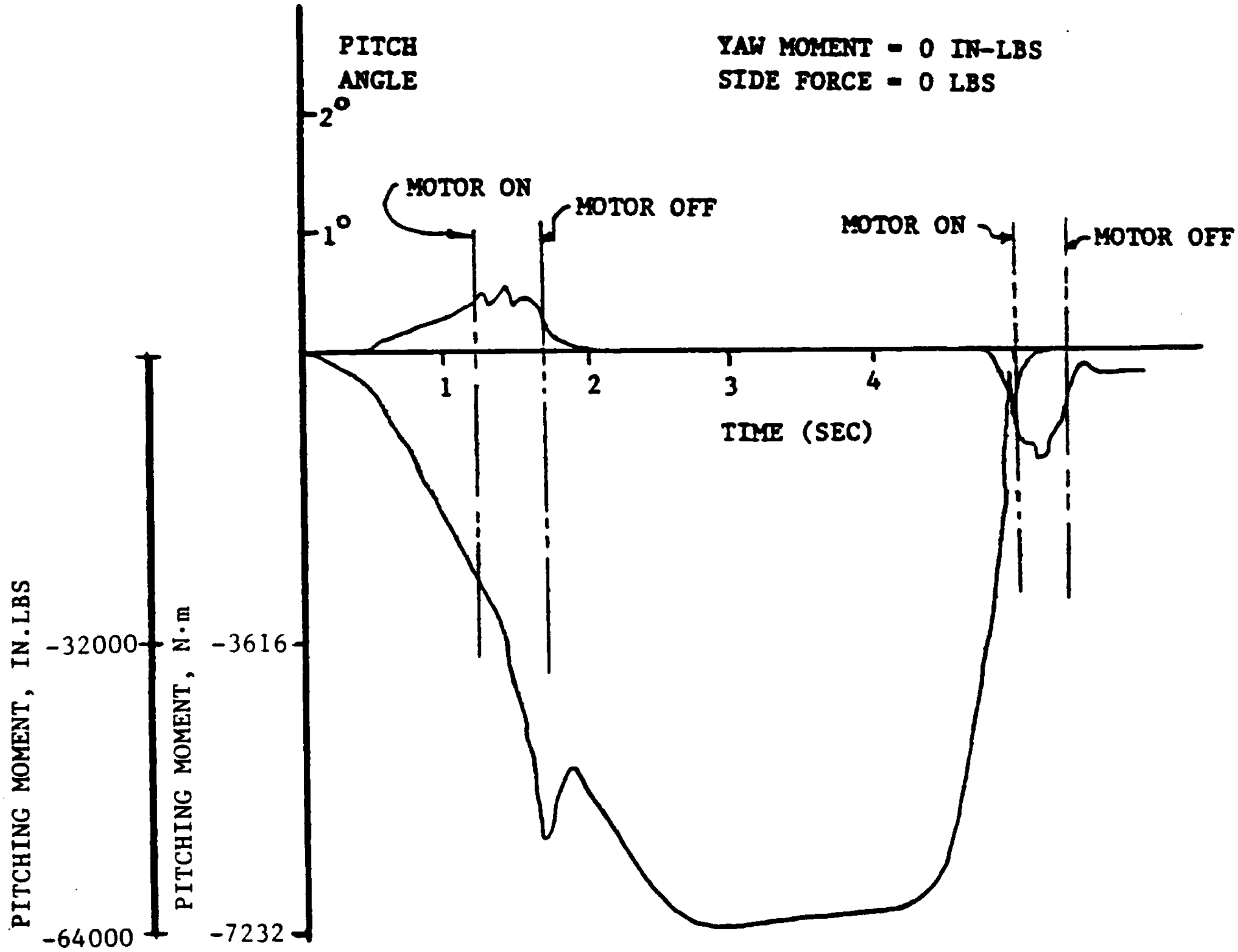

Figure E10.- Operational Test AL5, Pylon No. 2

APPENDIX F

Preliminary Hazard Analysis

This appendix contains the detailed results of the preliminary hazard analysis. All potential hazards have been identified and recommended action has been stated.

The tabular analysis sheets of Figure F1 contain the hazards identified by the PHA. Twenty-three (23) hazards were identified. Of these, three (3) were categorized as catastrophic, ten (10) critical and ten (10) marginal. All identified hazards can or have been controlled by design or procedure.

The tabular analysis sheets of Figure F2 contain the hazards identified by the O&SHA. Fourteen hazards relating to the operation and support of the pylon were identified. Of these, three (3) were categorized as catastrophic, seven (7) critical and three (3) marginal. Twelve (12) of these hazards have been recommended to remain open for resolution during flight test and follow-on publication of formal instructions.

The hazard classifications and hazard probabilities shown in the tabular analysis sheets are defined in Figures F3 and F4 respectively.

ORIGINAL PAGE IS
OF POOR QUALITY

Revised: June 1983

SYSTEM Decoupler Pylon PROCEDURE ENGINEER Hoffman/Perry DATE April 1983

NO	OPERATIONAL PHASE	HAZARD: DESCRIPTION	HAZARD: EFFECT CLASSIFICATION RISK	RECOMMENDED ACTION: CONTROL	RECOMMENDED ACTION: EFFECT CLASSIFICATION RISK	REMARKS	STATUS
1	Ground & Flight	Inadvertent release of store due to improper configuration.	Aircraft equipment damage IIC	The decoupler pylon is designed structurally to carry all stores currently certified for the F-16 weapons pylon (16S500) with at least a zero safety margin. To support the flight test program for the decoupler pylons, a minimum structural margin of safety of +.25 will be maintained for the GBU-8 loads.	Aircraft/equipment damage IIE	A warning decal "For GBU-8, BDU-38/-61 only" is recommended for the flight test program.	Closed
2	Flight & Landing	Fins on store strike flaps.	Flaps damage IIC	The GBU-8 fins will be trimmed to reduce the probability of interference between the fins and the aircraft flaps. The alignment sensing and correction system designed for this pylon will also control this hazard.	Flaps damage IIE	Flap strikes may occur during full flap deflection (20^{o}C) under the following conditions: (a) Sudden pull-up during landing approach. High Nz with gust loads (b) Very hard landing, gear completely retracted. High Nz with gust loads. (c) Wing low due to single wheel landing with gust loads.	Closed to O&SHA
3	Flight	Weapon store fails to align.	Aircraft/equipment damage IIC	Design misalignment limits ($\pm$ 3^{o} pitch) will only slightly increase aircraft drag with negligible degradation of aircraft handling qualities. If some currently unknown fault allowed misalignment to exceed design limits, jettison of the stores may be necessary.	Aircraft/equipment damage IIE	Store misalignment may occur under the following conditions: (a) Loss of sensing device between upper and lower parts of pylong. (b) Loss of alignment motor. (c) Failure of the spring assembly.	Closed to O&SHA
4	Flight	Store strikes aircraft during separation.	Aircraft/equipment damage IIC	Ground testing has been done to determine optimum amount of charge in fwd and aft attach points to insure safe separation.	Aircraft/equipment damage IID	Flight testing will be monitored to insure repetitive safe launches.	Closed to O&SHA.
5	Flight	Loss of damper.	Gain on alignment changes IIID	Ground testing with orifice removed from damper revealed that no damage to system would occur.	Gain on alignment changes IIIE		Closed
6	Flight & Landing	Pilot unaware of faulty store alignment.	Aircraft/equipment damage IID	A light indicator has been designed for installation in the aircraft crew station to advise the pilot when store misalignment reaches the design limits.	Aircraft/equipment damage IIE		Closed

MIL STD 882A PARAGRAPH 5.5.1.1
DI-H 7048 PARAGRAPH 10.2.1

Figure F1.- Preliminary hazard analysis.

PRELIMINARY HAZARD ANALYSIS

Revised: June 1983
April 1983

SYSTEM Decoupler Pylon **PROCEDURE** ______ **ENGINEER** Hoffman/Perry **DATE** ______

NO.	OPERATIONAL PHASE	HAZARD DESCRIPTION	HAZARD EFFECT CLASSIFICATION RISK	RECOMMENDED ACTION CONTROL	RECOMMENDED ACTION EFFECT CLASSIFICATION RISK	REMARKS	STATUS
7	a. Ground	Fire and/or explosion due to ignition of inadvertently released fuel.	Death or loss of aircraft IC	Decoupler pylon ignition sources have been minimized through design of electrical system in accordance with MIL-W-81381 wiring spec and MIL-W-5088E wiring installation. The switches are sealed to eliminate any source of ignition. The alignment motor was designed for aircraft use (L-1011/747) minimizing ignition sources.	Death or loss of aircraft. ID	Review of F-16 system safety mishap fault tree analysis indicates that from an electrical event the probability of a fire is 0.20 x 10^{-11} per flying hour, and from hot brakes, 0.58 x 10^{-6} per flying hour. (Reference Appendix A	Closed
	b. Flight	Fire and/or explosion due to ignition of inadvertently released fuel.	Death and/or loss of aircraft IC	The decoupler pylons will be installed at wing stations 3 & 7 (BL120) which are outboard of fuel tanks and plumbing. The probability of fuel from in-flight leaks reaching this area would be extremely remote. Also, the same pylon attach points and techniques used for other proven pylon attachments will be used.	Death and/or loss of aircraft ID	Fuel leaking into pylon from wing would be extremely remote necessitating multiple failures.	Closed
8	Ground	Sharp edges and corners.	Personnel injury IIIB	The upper skin fairing angle extends from the leading to the trailing edge of the outer skin panel and is required for panel stiffness. To reduce the sharp edge/corner effect, both the leading and trailing edges will be tapered and all exposed edges and corners will be rounded.	Personnel injury IIIC	Metal working DWGS; e.g. 676S001 32, 33, 34, 36, 40, 676 E001, 676M04 contain note for metal removal per FPS-3017. This is IAW MIL-STD-1472 which requires all exposed edges be rounded to .04R min. and corners to 0.5S min.	Closed
9	Flight	Wing flutter with decoupler pylon at maximum misalignment.	Injury and/or system damage IIIB	The flight profile for this configuration is similar to that for a fixed pylon, 0.9m at all altitudes. Pilot should reduce speed as necessary to control flutter.	Injury and/or system damage IIID	Wing flutter conditions with the decoupler pylon bottomed out will be similar to that experienced with the F-16 weapons pylon (16S500). This flutter amplitude will not cause structural damage to the aircraft or systems.	Closed
10	Flight	Loss of alignment motor brake.	Injury and/or system damage IIIC	Design will incorporate a "momentary" switch for ground check-out of the alignment system. (GD DWG 676D003 calls out spring loaded toggle switch P/N MS 27782-26F). Motor brake is released only while switch is properly held which precludes inadvertently leaving switch in this position.	Injury and/or system damage IIID	Removal of fairing at aft end of pylon will be required to gain access to the motor brake switch.	Closed
11	Flight	Decoupler pylon inoperative due to ice formation.	Injury and/or system damage IIIB	Ice buildup which would deactivate the alignment device would still allow the decoupling effect of the pylon due to spring/damper operation.	Injury and/or system damage IIID	Sufficient ice buildup to immobilize the decoupling effect is extremely improbable.	Closed

MIL-STD-882A PARAGRAPH 5.5.1.1
DI-H-7048 PARAGRAPH 10.2.1

Figure F1.- (continued)

C-3

PRELIMINARY HAZARD ANALYSIS

SYSTEM Decoupler Pylon PROCEDURE ENGINEER Hoffman/Perry DATE April 1983

NO.	OPERATIONAL PHASE	HAZARD: DESCRIPTION	HAZARD: EFFECT CLASSIFICATION RISK	RECOMMENDED ACTION: CONTROL	RECOMMENDED ACTION: EFFECT CLASSIFICATION RISK	REMARKS	STATUS
12	Flight	Unable to electrically de-energize the decoupler in emergency conditions.	Injury and/or system damage IIIB	An alignment system power/stop indicator switch will be located in the crew station. This switch will have three positions (1) total power off, (2) power off to alignment motor while retaining up/down limit stop indication, and (3) total power on.	Injury and/or system damage IIID		Closed
13	Flight	Alignment spring failure.	Severe injury and/or major system damage IIC	Spring under load only during flight with store attached. The spring is designed for a maximum load of 14,000 lbs. to accommodate non-GBU-8 stores. Maximum load attributed to the GBU-8 store is 5,000 lbs.	Severe injury and/or major system damage IID	A spring failure, which is highly improbable, will allow the alignment to bottom out which will require flying to handbook limits (see PHA Item 9).	Closed
14	Flight	Critical component failure.	Severe injury and/or major system damage IIC	Identified critical components have been determined to have safety margins ranging from +.49 to +1.80 for the GBU-8 store. Safety margins for the DBU-38 and -61 stores are even greater due to their lighter weight.	Severe injury and/or major system damage IID	Critical components identified to date include: (1) Fwd links (P/N 676S032) (2) Aft Links (P/N 676S034) (3) Link Pins (P/N 676S033) (4) Spring (P/N 676S036)	Closed
15	Flight & Ground	Overheated damper.	Injury and/or system damage IIIC	275°F is considered an overheat condition for hydraulic components on the F-16 aircraft. The energy dissipation requirement for the damper is presently unknown. Some cooling will occur during flight. Additional cooling incorporated without cause could contribute to problems of cold soaking.	Injury and/or system damage IIID	Hazard to be evaluated during flight test.	Closed to O&SHA
16	Flight	Bearing lockup.	Injury and/or system damage IIIB	Should bearing lockup occur, the decoupler pylon would perform like a fixed pylon and aircraft flown accordingly.	Injury and/or system damage IIIC		Closed to O&SHA
17	Flight	Decoupler bottoming out at limit positions.	Injury and/or system damage IIIB	Should the decoupler pylon become misaligned to the maximum limits it will bump against the damper stops which will cushion the impact. Although aircraft drag will be increased slightly, degradation of aircraft handling qualities will be negligible. Flutter speed will revert to that similar to the production pylon.	Injury and/or system damage IIID	See PHA Hazard No. 9.	Closed

MIL STD 882A PARAGRAPH 5.5.1.1
DI H 7048 PARAGRAPH 10.2.1

Figure F1.- (continued)

PRELIMINARY HAZARD ANALYSIS

Revised: June 1983

SYSTEM Decoupler Pylon PROCEDURE ENGINEER Hoffman/Perry DATE April 1983

NO.	OPERATIONAL PHASE	HAZARD: DESCRIPTION	HAZARD: EFFECT CLASSIFICATION RISK	RECOMMENDED ACTION: CONTROL	RECOMMENDED ACTION: EFFECT CLASSIFICATION RISK	REMARKS	STATUS
18	Flight	Store fins impailed on flaps.	Flap damage IIC	The GBU-8 fins will be trimmed to eliminate this situation in all normal flight regions.	Flap damage IID	Conditions in PHA Item No. 2 should be considered.	Closed to O&SHA
19	Ground	28 volt DC and 115 volt 3 phase AC power levels are present.	Death or severe injury to personnel IB	Voltage points shall be marked to indicate highest voltage present and barriers located to minimize accidental contact by maintenance personnel.	Death or severe injury to personnel ID		Closed to O&SHA
20	Ground or Flight	Pylon wiring damage.	Injury or system damage IIIC	Designed to MIL-W-81381 wiring spec and MIL-W-5088E wiring installation spec to prevent fraying and chafing. Wires are kept away from structure and free of sharp bends by using cushion clamps to secure wires. Strain reliefs are used by all connectors. The wire has a 200°C temperature range and can operate continuously at this temperature without insulation damage.	Injury or system damage IIID		Closed
21	Ground or Flight	Safe[illegible] factors.	Death or system loss IC	Safety factor for flight test is 1.875. This includes a 1.5 system factor plus a 25% margin of safety for the flight test.	Death or system loss ID	A review of the stress analysis indicates safety margins of +.49 to +1.80 for decoupler components when using the GBU-8 store.	Closed
22	Ground or Flight	Corrosion	Severe injury or major system damage IIC	In accordance with the F-16 finish spec FPS-3001 the decoupler pylon material of different electrical composition will be separated by being installed with wet zinc chromate primer.	Severe injury or major system damage IID	GD DWG 676S001 requires decoupler pylon assy. be installed with wet prime in accordance with element 206 of FPS -3001.	Closed
23	Flight	Cabin depressurization due to pressure hull leakage.	Severe injury or major system damage IID	This hazard considers the possibility of cabin penetration by: (a) In-flight mishap - This hazard considers a mishap whereby portions of the decoupler pylon penetrate the cabin. This is not considered a possibility since the pylon is mounted on the wing aft of the cabin and any portion of the decoupler pylon that may break lose will be directed aft by the air flow around the wing. (b) Aircraft modification - This hazard considers penetration of the cabin to route additional electrical lines to the decoupler pylon master switch and limit warning lights. Also, failure to properly seal the added holes causing cabin depressurization. This is not considered a possibility since the design uses existing internal cabin wiring for its power source.	Severe injury or major system damage IID		Closed

MIL STD 882A PARAGRAPH 5.5.1.1
DI H 7048 PARAGRAPH 10.2.1

Figure F1.- (concluded)

ORIGINAL PAGE IS
OF POOR QUALITY

OPERATING AND SUPPORT HAZARD ANALYSIS

SYSTEM NASA Decoupler Pylon   PROCEDURE Flight Test   ENGINEER Perry   DATE April 1983

NO.	OPERATIONAL PHASE	SYSTEM DESCRIPTION	HAZARD			RECOMMENDED ACTION		REMARKS	STATUS	CAUTION AND WARNING NOTES
			DESCRIPTION	IDENTIFICATION	EFFECT CLASSIFICATION RISK	CONTROL	EFFECT CLASSIFICATION RISK			
1	Flight	Decoupler pylon test	Weapons store fails to align	Flight test procedures	Aircraft and equipment damage IIC	Design misalignment limits ($\pm 3^{\circ}$ pitch) will only slightly increase aircraft drag with negligible degradation of aircraft handling qualities. Pilot will fly to store misalignment procedures.	Aircraft and equipment damage IID	Aircraft handling qualities with misaligned stores to be determined during flight testing.	Open	Ref. PHA Item No. 3
2	Flight	Decoupler pylon test	Store strikes aircraft during separation.	Flight test procedures	Aircraft and equipment damage IIC	Ground testing has been completed to determine optimum charge in fwd and aft attach points to insure safe separation.	Aircraft and equipment damage IID	Flight testing will be monitored to insure repetitive safe separations.	Open	Ref. PHA Item No. 4
3	Flight & Ground	Decoupler pylon	Overheated damper		Injury and/or system damage IIIC	275°F is considered an overheat condition for hydraulic components on the F-16 aircraft. The energy dissipation requirement for the damper is presently unknown. Some cooling will occur during flight.	Injury and/or system damage IIID	Potential hazard to be evaluated during flight test.	Open	Ref. PHA Item No. 15
4	Flight	Decoupler pylon	Bearing lockup		Injury and/or system damage IIIB	Should bearing lockup occur, the decoupler pylon would perform like a fixed pylon and aircraft flown accordingly.	Injury and/or system damage IIIC	Hazard to be evaluated during flight test.	Open	Ref. PHA Item No. 16
5	Mainten-ance	Decoupler pylon	28 volt DC and 115 volt 3 phase AC power levels are present.		Serious injury or death to personnel IB	Voltage points shall be marked to indicate highest voltage present and barriers located to minimize accidental contact by maintenance personnel.	Serious injury or death to personnel ID	Recommend warning note be included in applicable tech order/AEI instructions for follow-on production and operations.	Open	Contact with electrical circuits may cause electrical shock. Use properly insulated tools and keep electrical source turned off when not required. Do not contact electrical equipment while in vicinity of wet area. Failure to comply may result in serious injury or death. Ref. PHA Item No. 19

MIL STD 882A PARAGRAPH 5.5.1.4
DI H 7048 PARAGRAPH 10.2.4

Figure F2.- Operating and support hazard analysis

OPERATING AND SUPPORT HAZARD ANALYSIS

SYSTEM NASA Decoupler Pylon PROCEDURE Drawing No. 676S100 ENGINEER Perry DATE April 1983

NO.	OPERATIONAL PHASE	SYSTEM DESCRIPTION	HAZARD: DESCRIPTION	HAZARD: IDENTIFICATION	HAZARD: EFFECT CLASSIFICATION RISK	RECOMMENDED ACTION: CONTROL	RECOMMENDED ACTION: EFFECT CLASSIFICATION RISK	REMARKS	STATUS	CAUTION AND WARNING NOTES
1	Mainten-ance	Decoupler pylon installation/removal	Hit switch on MAU-12 rack.	Reference 16AEI-75-1006 para. 8.1c.	Damage to equipment IVC	AEI cautions to observe protruding switch from the MAU-12 rack to preclude equipment damage.	Damage to equipment IVD	Aerospace equipment instructions, 16AEI-75-1006, for production pylon (16S500) used for decoupler pylon installation.	Closed	
2	Mainten-ance	Decoupler pylon installation/removal	Electrical shock	Reference 16AEI-75-1006 para. 8.1d and 8.2j.	Serious injury or death to personnel and equipment damage 1C	Add warning note to insure electrical power is off prior to connecting/disconnecting electrical connectors.	Serious injury or death to personnel and equipment damage 1D	Recommend warning note be included in applicable tech order/AEI instructions for follow-on production and operations.	Open	Connecting/disconnecting electrical components when power is applied may cause electrical shock. Turn off source of power to system prior to connecting/disconnecting electrical connectors. Failure to comply may result in serious injury or death.
3	Mainten-ance	Decoupler pylon installation/removal	Handling heavy equipment	Reference 16AEI-75-1006 para. 8.1c and 8.2e.	Serious injury or death to personnel and equipment damage 1C	Add warning note to advise maintenance personnel of inherent dangers in handling this equipment.	Serious injury or death to personnel and equipment damage 1D	Recommend warning note be included in applicable tech order/AEI instructions for follow-on production and operations.	Open	Mishandling heavy equipment may be hazardous to personnel and equipment. Complete all procedures prior to installation/removal of pylon. Failure to comply may cause serious injury or death.

MIL STD 882A PARAGRAPH 5.5.1.4
DI H 7048 PARAGRAPH 10.2.4

Figure F2.- (continued)

ORIGINAL PAGE IS
OF POOR QUALITY

OPERATING AND SUPPORT HAZARD ANALYSIS

SYSTEM NASA Decoupler Pylon PROCEDURE Drawing No. 676M010 ENGINEER Perry DATE April 1983

NO.	OPERATIONAL PHASE	SYSTEM DESCRIPTION	HAZARD			RECOMMENDED ACTION		REMARKS	STATUS	CAUTION AND WARNING NOTES
			DESCRIPTION	IDENTIFICATION	EFFECT CLASSIFICATION RISK	CONTROL	EFFECT CLASSIFICATION RISK			
1	Maintenance	Damper assy.	Pressure fill damper with hydraulic fluid.	Drawing Note 4.	Injury to personnel IIC	Warning note is needed to advise maintenance personnel of inherent danger.	IID	Recommend warning note be included in applicable tech order/AEI instructions for follow-on production and operations.	Open	Hydraulic fluid under pressure may spray personnel and damage eyes. Wear protective face-shield or industrial safety goggles to avoid contact with eyes. Insure line pressure is reduced to zero prior to disconnecting hoses. Failure to comply may result in serious injury.
2	Maintenance	Damper assy.	Scratching sliding surfaces while pushing diaphragm into piston.	Drawing Note 6.	Damage to equipment IIIC	Note contains caution. NOTE: Push down cautiously to avoid scratching sliding surfaces.	Damage to equipment IIID	Recommend warning note be included in applicable tech order/ AEI instructions for follow-on production and operation.	Closed	
3	Maintenance	Damper assy.	Pressure fill with hydraulic fluid through removed bleeder-plug.	Drawing Note 7.	Injury to personnel IIC	Warning note added to drawing note 4 (O&SHA Item 1) would also cover this item.	Injury to personnel IID	Recommend warning note be included in applicable tech order/ AEI instructions for follow-on production and operation.	Open	See O&SHA Item 1.
4	Maintenance	Damper assy.	Disconnect air valve.	Drawing Note 9.	Injury to personnel IIC	Warning note is needed to advise maintenance personnel of inherent danger.	Injury to personnel IIC	Recommend warning note be included in applicable tech order/ AEI instructions for follow-on production and operation.	Open	High pneumatic pressure may propel particles or damage eyes with direct pressure. Wear protective faceshield or industrial goggles to avoid contact with eyes. Insure line pressure is reduced to zero prior to disconnecting hoses. Failure to comply may result in serious injury or death.

MIL-STD-882A PARAGRAPH 5.5.1.4
DI-H-7048 PARAGRAPH 10.2.4

Figure F2.- (continued)

OPERATING AND SUPPORT HAZARD ANALYSIS

SYSTEM NASA Decoupler Pylon PROCEDURE Drawing No. 676M010 ENGINEER Perry DATE April 1983

NO.	OPERATIONAL PHASE	SYSTEM DESCRIPTION	HAZARD			RECOMMENDED ACTION		REMARKS	STATUS	CAUTION AND WARNING NOTES
			DESCRIPTION	IDENTIFICATION	EFFECT CLASSIFICATION RISK	CONTROL	EFFECT CLASSIFICATION RISK			
5	Mainten-ance	Damper assy.	Charge accumulator with air or nitrogen to 100 10 psi	Drawing Note 11	Injury to personnel IIC	Warning note added to drawing note 9 (O&SHA Item 4) would also cover this item.	Injury to personnel IID	Recommend warning note be included in applicable tech order/AEI instructions for follow-on production and operations.	Open	See O&SHA Item 4.
6	Mainten-ance	Damper assy.	Pressures up to 1000 psi applied to air valve.	Drawing note 17	Injury to personnel IIC	Warning note added to drawing note 9 (O&SHA Item 4) would also cover this item.	Injury to personnel IID	Recommend warning note be included in applicable tech order/AEI instructions for follow-on production and operations.	Open	See O&SHA Item 4.

MIL STD-882A PARAGRAPH 5.5.1.4
DI-H-7048 PARAGRAPH 10.2.4

Figure F2.- (concluded)

The hazards found in this report are classified in accordance with paragraph 5.4.3.1 of MIL-STD-882A as follows:

a. Category I - Catastrophic (CAT)
Any hazard that may cause death or system loss.

b. Category II - Critical (CRIT)
Any hazard that may cause severe injury, severe occupational illness, or major system damage.

c. Category III - Marginal (MARG)
Any hazard that may cause minor injury, minor occupational illness, or minor system damage.

d. Category IV - Negligible (NEG)
Any hazard that will not result in injury, occupational illness, or system damage.

Figure F3.- Hazard classification.

DESCRIPTIVE WORD	FLEET OR INVENTORY	LEVEL
Frequent	Continuously experienced	A
Reasonably probable	Will occur frequently	B
Occasional	Will occur several times	C
Remote	Unlikely to occur, but possible	D
Extremely improbable	So unlikely, it can be assumed that this hazard will not be experienced	E
Impossible	Physically impossible to occur	F

Figure F4.- Hazard probability.

1. Report No.
NASA CR - 172354

2. Government Accession No.

3. Recipient's Catalog No.

4. Title and Subtitle
DESIGN AND FABRICATION OF THE NASA DECOUPLER PYLON FOR THE F-16 AIRCRAFT

5. Report Date
January 1985

6. Performing Organization Code

7. Author(s)
J. D. Clayton, R. L. Haller, J. M. Hassler, Jr.

8. Performing Organization Report No.

9. Performing Organization Name and Address
General Dynamics - Fort Worth Division
P. O. Box 748
Fort Worth, Texas 76101

10. Work Unit No.

11. Contract or Grant No.
NAS1-16879

13. Type of Report and Period Covered
Contractor Report
Jan 1982 - Aug 1983

12. Sponsoring Agency Name and Address
National Aeronautics and Space Administration
Washington, D.C. 20546

14. Sponsoring Agency Code
505-33-43-07

15. Supplementary Notes
Langley Technical Monitor: F. W. Cazier, Jr.
Final Report

16. Abstract

The NASA Decoupler Pylon is a passive means of suppressing wing-store flutter. The feasibility of demonstrating this concept on the F-16 airplane was established through model wind tunnel tests and analyses. As a result of these tests and studies a ship set of Decoupler Pylons was designed and fabricated for a flight test demonstration on the F-16 aircraft. Basic design criteria were developed during the analysis study pertaining to pylon pitch stiffness, alignment system requirements, and damping requirements. A design was developed which utilized an electrical motor for the pylon alignment system. The design uses a four pin, two link pivot design which results in a remote pivot located at the center of gravity of the store when the store is in the aligned position. The pitch spring was fabricated from a tapered constant stress cantilevered beam. The pylon has the same external lines as the existing production pylon and is designed to use a MAU-12 ejection rack which is the same as the one used with the production pylon. The detailed design and fabrication was supported with a complete ground test of the pylons prior to shipment to NASA.

17. Key Words (Suggested by Author(s))
Flutter
Flutter Suppression
Decoupler Pylon
Wing-Store Flutter
Aeroelasticity

18. Distribution Statement
[redacted]

[redacted]

19. Security Classif. (of this report)	20. Security Classif. (of this page)	21. No. of Pages	22. Price
Unclassified	Unclassified	204	